

**GEOLOGICAL SURVEY OF WESTERN AUSTRALIA**

**BULLETIN 139**

**GEOLOGY OF THE  
ASHBURTON BASIN  
WESTERN AUSTRALIA**

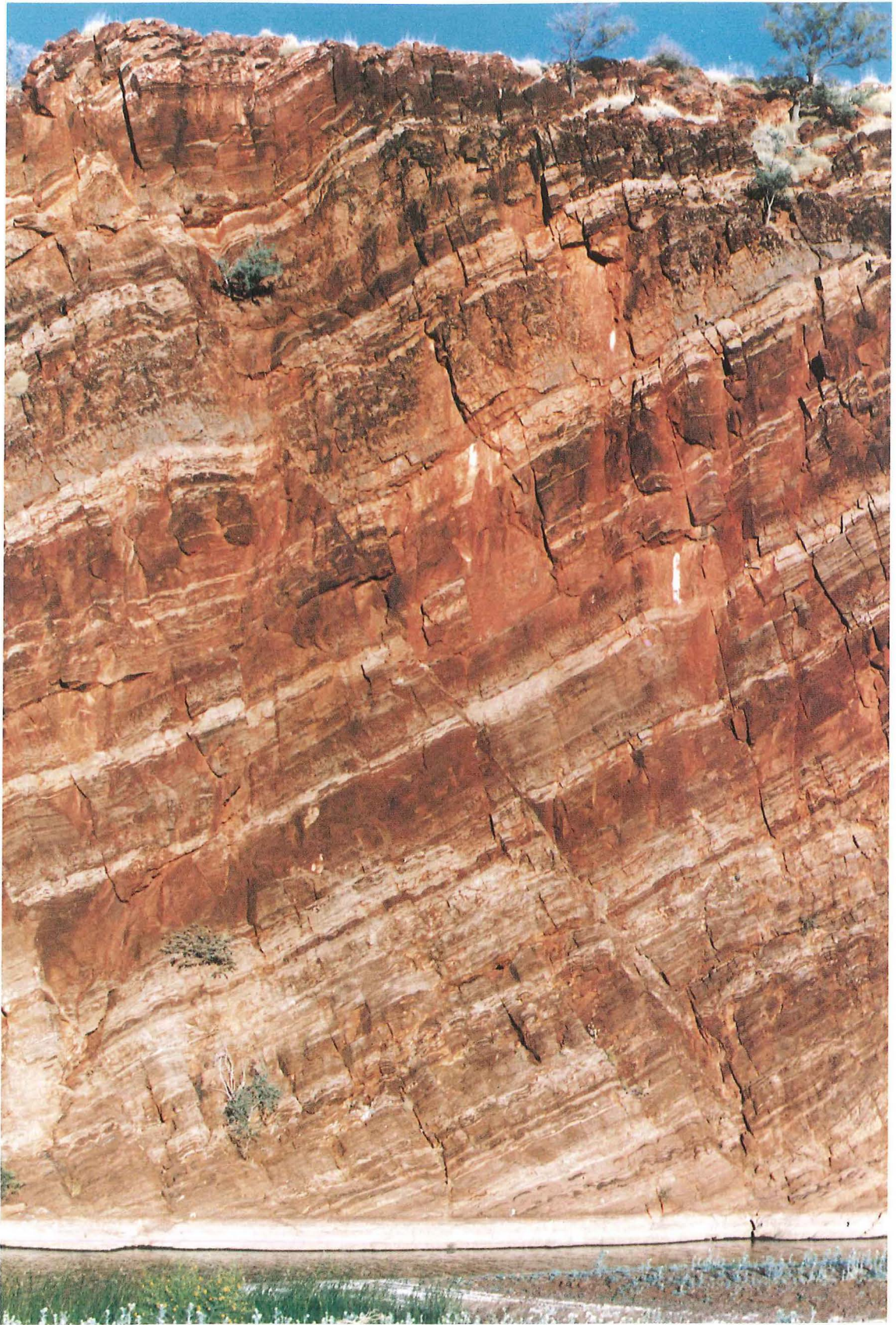
**BY  
A.M. THORNE AND D.B. SEYMOUR**



**DEPARTMENT OF MINES  
WESTERN AUSTRALIA**

**GEOLOGY OF THE  
ASHBURTON BASIN  
WESTERN AUSTRALIA**





GSWA 21566

### FRONTISPIECE

Upward-shallowing sequences in the Duck Creek Dolomite, Duck Creek Gorge. Alternating beds of stromatolitic and non-stromatolitic dolomite (dark and light coloured units respectively) are cut by a normal fault whose trace extends from top left to bottom right of the photograph; downthrow is about 2.5m.



**GEOLOGICAL SURVEY OF WESTERN AUSTRALIA**

**BULLETIN 139**

**GEOLOGY OF THE  
ASHBURTON BASIN  
WESTERN AUSTRALIA**

**BY  
A. M. THORNE AND D.B. SEYMOUR**

**Perth 1991**



**MINISTER FOR MINES  
THE HONOURABLE JEFF CARR M.L.A.**

**DIRECTOR GENERAL OF MINES  
D.R. KELLY**

**DIRECTOR, GEOLOGICAL SURVEY OF WESTERN AUSTRALIA  
PHILLIP E. PLAYFORD**

**National Library of Australia  
Cataloguing-in-publication entry**

Thorne, A.M.  
Geology of the Ashburton Basin, Western Australia.

*Bibliography*  
ISBN 0 7309 1099 7.

1. Geology — Western Australia — Ashburton Basin. I  
Seymour, D.B. II. Geological Survey of Western  
Australia. III. Title. (Series: Bulletin (Geological  
Survey of Western Australia); 139).  
559.413

ISSN 0085 8137

Typeset by Typestyle, East Perth.  
Printed by Lamb Print, Perth. Western Australia

**Copies available from:  
The Director  
Geological Survey of Western Australia  
100 Plain Street  
East Perth, Western Australia 6004  
Ph. (09) 222 3168**

# CONTENTS

	Page
Chapter summaries. ....	xiv

## CHAPTER 1 INTRODUCTION

Communication and settlement. ....	1
Climate and vegetation. ....	1
Physiography. ....	2
Previous investigations. ....	3
Terminology. ....	5
Pre-Wyloo Group rocks. ....	5
Granite-greenstone. ....	5
Hamersley Basin. ....	6
Limits of the Ashburton Basin. ....	7
Stratigraphy of the Ashburton Basin. ....	7
Previous stratigraphic subdivision. ....	7
Stratigraphy used in this bulletin. ....	8
Age of the Ashburton Basin. ....	9
Regional correlation of the Wyloo Group. ....	9
Blair, Mount Minnie, and Bresnahan Basins. ....	9
Cainozoic Deposits. ....	10

## CHAPTER 2 BEASLEY RIVER QUARTZITE

Mid-fan facies association. ....	11
Mid-fan lobe facies. ....	11
Description. ....	11
Interpretation. ....	11
Interlobe facies. ....	12
Description. ....	12
Interpretation. ....	12
Outer-fan facies association. ....	12
Braided stream facies. ....	13
Description. ....	13
Interpretation. ....	13
Sheetflood-sandstone facies. ....	13
Description. ....	13
Interpretation. ....	13
Delta-plain facies association. ....	15
Description. ....	15
Interpretation. ....	15
Tidal-channel and tidal sand-bar facies association. ....	16
Tidal-channel facies. ....	16
Description. ....	16
Tidal sand-bar facies. ....	16
Description. ....	16
Interpretation. ....	17
Tidal channels. ....	19
Tidal sand-bars. ....	19
Offshore facies association. ....	20
Description. ....	20
Interpretation. ....	20
Distribution of facies associations. ....	20
Depositional model and palaeogeographic reconstruction. ....	22
Discussion. ....	24



## CHAPTER 3 CHEELA SPRINGS BASALT AND WOOLY DOLOMITE

	Page
Cheela Springs Basalt .....	27
Description .....	27
Interpretation .....	27
Volcanic centres .....	28
Wooly Dolomite .....	29

## CHAPTER 4 MOUNT McGRATH FORMATION

Delta-plain facies association .....	31
Distributary-channel facies .....	31
Description .....	31
Interpretation .....	31
Interdistributary-bay facies .....	34
Description .....	34
Interpretation .....	36
Delta-front facies association .....	36
Distributary-mouth bar facies .....	36
Description .....	36
Interpretation .....	37
Beach facies .....	38
Description .....	38
Interpretation .....	38
Shoreface and offshore-shelf facies .....	38
Description .....	38
Interpretation .....	40
Distribution of facies associations .....	40
Depositional model and palaeogeographic reconstruction .....	42
Summary of depositional history .....	42
Discussion .....	42

## CHAPTER 5 DUCK CREEK DOLOMITE AND JUNE HILL VOLCANICS

Duck Creek Dolomite .....	45
Inner shelf facies association .....	45
Description .....	45
Offshore-barrier facies .....	45
Subtidal-lagoon facies .....	45
Intertidal-shelf facies .....	45
Supratidal-shelf facies .....	46
Facies sequences .....	48
Interpretation .....	48
Holocene analogue .....	48
Upward-shallowing sequences in the Duck Creek Dolomite .....	49
Relic evaporite textures in the Duck Creek Dolomite .....	52
Outer shelf and slope-and-basin facies association .....	53
Description .....	53
Interpretation .....	53
Distribution of facies associations .....	55
Depositional model and palaeogeographic reconstruction .....	55
Discussion .....	56
June Hill Volcanics .....	58

## CHAPTER 6 ASHBURTON FORMATION

Lithofacies .....	59
Mudstone and siltstone .....	59
Description .....	59
Interpretation .....	59
Sandstone .....	59
Description .....	59

	Page
Lithofacies	
Sandstone	
Interpretation .....	60
Conglomerate .....	62
Description .....	62
Interpretation .....	62
Banded iron-formation and chert .....	62
Description .....	62
Interpretation .....	62
Volcanic rocks .....	64
Description .....	64
Interpretation .....	64
Carbonate rocks .....	64
Description .....	64
Interpretation .....	65
Lithofacies Associations .....	65
Description .....	65
Conglomerate–massive sandstone–mudstone association .....	65
Massive sandstone–thin- to medium-bedded sandstone–mudstone association .....	65
Mudstone–thin-bedded sandstone–BIF and chert association .....	67
Interpretation .....	67
Distribution of lithofacies associations and palaeocurrent data .....	70
Southeastern region .....	70
Palaeocurrent data .....	72
Central region .....	72
Palaeocurrent data .....	72
Northwestern region .....	72
Palaeocurrent data .....	72
Summary of Ashburton Formation stratigraphy .....	73
Sandstone composition .....	73
Southeast and central Ashburton Basin .....	73
Results .....	73
Interpretation .....	75
Southeasterly derived sandstones .....	75
Southwesterly derived sandstones .....	77
Northwestern region .....	77
Results .....	77
Interpretation .....	77
Depositional model and palaeogeographic reconstruction .....	77
Discussion .....	78

## **CHAPTER 7 LARGE ALLOCHTHONOUS BLOCKS AND OLISTOSTROMES WITHIN THE ASHBURTON FORMATION**

Northwestern region .....	83
Mount Amy .....	83
Mount Stuart .....	83
Hardey Junction and the western closure of Wyloo Dome .....	83
Southeastern region .....	85
Radio Hill Fault .....	85
Mount Elephant .....	85
Mount Boggola .....	85
Discussion .....	87
Northwestern region .....	87
Southeastern region .....	89
Emplacement mechanisms .....	89

## **CHAPTER 8 CAPRICORN FORMATION, MOUNT MINNIE GROUP AND BRESNAHAN GROUP**

Capricorn Formation .....	91
Braided-fluvial facies association .....	91
Description .....	91



	Page
Capricorn Formation	
Braided-fluvial facies association	
Interpretation .....	91
Shallow-marine or lacustrine facies association .....	91
Description .....	91
Interpretation .....	92
Fan-delta facies association .....	94
Description .....	94
Interpretation .....	94
Distribution of facies associations .....	96
Depositional model .....	96
Discussion .....	96
Mount Minnie Group .....	98
Brodagee Sandstone .....	98
Description .....	98
Interpretation .....	99
Wabco Shale .....	99
Description .....	99
Interpretation .....	99
Warramboe Sandstone .....	99
Description .....	99
Interpretation .....	99
Lithofacies distribution .....	99
Depositional model .....	99
Discussion .....	99
Bresnahan Group .....	99
Valley-fill facies association .....	100
Description .....	100
Interpretation .....	100
Alluvial-fan channel facies association .....	101
Description .....	101
Interpretation .....	103
Lacustrine facies association .....	103
Description .....	103
Interpretation .....	103
Distribution of facies associations .....	103
Depositional model and palaeogeographic reconstruction .....	104
Discussion .....	105

## CHAPTER 9 STRUCTURE AND METAMORPHISM

Structure .....	107
Capricorn Orogen structures .....	107
Ophthalmia Fold Belt .....	107
Pre-Wyloo Group structures .....	107
Syn-Wyloo Group structures .....	107
Interpretation of Ophthalmia Fold Belt structures .....	108
Ashburton Fold Belt structures .....	109
D <sub>1</sub> structures .....	109
D <sub>2</sub> structures .....	109
Zone A .....	109
Zone B .....	110
Zone C .....	110
Interpretation of Ashburton Fold Belt structures .....	112
Late D <sub>2</sub> structures in the Mount Minnie Basin .....	113
Post-Capricorn Orogen structures .....	113
Metamorphism .....	113
Regional metamorphism .....	114
Contact metamorphism .....	114

## CHAPTER 10 ECONOMIC GEOLOGY

Gold .....	115
Post-Wyloo Group quartz veins in the Wyloo Dome .....	115
Paulsen (Melrose Group) .....	115

Gold	
Post-Wyloo Group quartz veins in the Wyloo Dome	
Belvedere Group .....	115
Monster Lode .....	115
Quartz veins in Ashburton Formation .....	116
Top Camp .....	116
Soldiers Secret .....	116
Dead Finish .....	116
Star of the West .....	116
Star of the East .....	116
Hearns Find (O'Gradys) .....	116
Northwest of Dead Finish .....	116
The Gorge .....	116
Mount Mortimer .....	117
Cainozoic alluvial and colluvial deposits .....	117
Syngenetic mineralization in the Ashburton Formation .....	117
Main Prospect .....	117
Eastern Prospect .....	118
Discussion .....	118
Copper .....	118
Post-Wyloo Group quartz veins in the Wyloo Dome .....	118
Quartz veins in Duck Creek Dolomite .....	118
Quartz veins and shears in Ashburton Formation and Capricorn Formation .....	119
Red Hill district .....	119
Ashburton Downs district .....	119
Volcanogenic deposits in Ashburton Formation .....	120
Lead and Silver .....	120
Post-Wyloo Group quartz veins in the Wyloo Dome .....	121
Quartz veins in the Duck Creek Dolomite .....	121
Silent Sisters Mine .....	121
Aerial Mine .....	121
Quartz veins and shears in Ashburton Formation and Capricorn Formation .....	121
Kooline centre .....	121
Ashburton Downs district .....	121
Gorge Creek .....	121
Wyloo occurrences .....	121
Iron .....	122
Mount McGrath Formation .....	122
Ashburton Formation .....	122
Uranium .....	122
Marble .....	122
Amethyst .....	123
Discussion .....	123
Age and distribution of mineralization .....	123
Exploration targets in the Ashburton Basin .....	123
Formation of iron ore in the Hamersley Basin .....	124

## CHAPTER 11 TECTONIC EVOLUTION

Introduction .....	125
Pilbara Craton rifting .....	126
Passive continental margin phase .....	126
Active continental margin phase .....	127
Continental crustal collision .....	127
Post- Cheela Springs Basalt to Duck Creek Dolomite .....	127
Ashburton Formation - D <sub>1</sub> Deformation - Capricorn Formation .....	130
D <sub>2</sub> Deformation-Mount Minnie Group .....	130
Post-collision sedimentation .....	130
Discussion .....	131
Precambrian plate tectonics .....	131
Comparisons between the Pilbara and Yilgarn Cratons .....	131
Subduction related volcanism .....	131
Ophiolites and glaucophane schists .....	131
Palaeomagnetic data .....	131
Geochronological data .....	131



Discussion	
Active margin and foreland basin volcanism .....	132
References .....	133

## ILLUSTRATIONS

### PLATES

(in wallet)

1	Stratigraphy and structure of the Ashburton Basin
2	Structural interpretation map of the Ashburton Basin

### FIGURES

	Page	
1	Main tectonic units of Western Australia .....	2
2	Ashburton Basin: access and key to 1:250 000 map sheets .....	3
3	Geological map of northwest Western Australia .....	4
4	Explanation of graphic log symbols used in this bulletin .....	5
5	Stratigraphic subdivision of the Mount Bruce Supergroup (based upon Trendall, 1979; 1990) .....	6
6	Stratigraphic subdivision of the southwestern Pilbara .....	8
7	Beasley River Quartzite outcrop and location of measure sections .....	12
8	Mid-fan facies association of Beasley River Quartzite showing variations in thickness, grain-size, and internal structure between lobe and interlobe deposits .....	13
9A	Very thick-bedded, massive mid-fan lobe conglomerate Beasley River Quartzite, locality 1 .....	14
9B	Internal structure of part of mid-fan lobe facies association, Beasley River Quartzite, locality 1 .....	14
9C	Small-scale trough cross-stratification in outer-fan braided stream facies, Beasley River Quartzite, locality 2 .....	14
9D	Parallel-laminated and ripple cross-laminated sheetflood facies sandstone overlying massive braided stream facies pebbly sandstone, Beasley River Quartzite, locality 1 .....	14
10	Schematic summary of rock-types present in the outer-fan facies association of the Beasley River Quartzite .....	15
11	Palaeocurrent data from the braided stream facies (outer fan), Beasley River Quartzite, localities 1 and 2 .....	16
12	Schematic summary of rock-types present in the delta plain facies association of the Beasley River Quartzite .....	16
13	Lenticular - bedded sets of trough cross-stratified, medium- to coarse-grained quartz sandstone; delta plain facies association, Beasley River Quartzite, locality 6 .....	17
14	Palaeocurrent data from the delta plain facies association, Beasley River Quartzite, locality 6 .....	17
15A	Major scour surface in tidal-channel facies, Beasley River Quartzite, locality 2 ....	18
15B	Internal structure of tidal channel facies showing superposed sets of medium-scale trough cross strata, Beasley River Quartzite, locality 1 .....	18
16	Palaeocurrent data from the tidal channel facies, Beasley River Quartzite, localities 2 and 3 .....	19
17	Schematic profile showing internal structure of the tidal sand-bar facies, Beasley River Quartzite .....	19
18A	Fine- to medium-grained quartz sandstone showing details of internal structure, Tidal sand-bar facies, Beasley River Quartzite, locality 2 .....	20
18B	Symmetrical and asymmetrical wave ripples in Tidal sand-bar facies, Beasley River Quartzite, locality 1 .....	20
19	Palaeocurrent data from tidal sand-bar facies, Beasley River Quartzite, localities 1, 2 and 6 .....	21
20	Generalized stratigraphic profiles through the Beasley River Quartzite showing interrelation of facies associations .....	22
21	Model showing the principal depositional environments of the Beasley River Quartzite in the vicinity of the southeastern Wyloo Dome .....	23
22	Palaeogeography of the southwestern Pilbara during deposition of the Beasley River Quartzite .....	23
23	Summary of the depositional history of the Beasley River Quartzite in the eastern Wyloo Dome .....	24
24	Stratigraphy of the lower part of the Cheela Springs Basalt on the northeastern flank of Wyloo Dome .....	28

	Page
25	Irregular vesicles in a fine-grained basalt flow top, Cheela Springs Basalt, northeastern Wyloo Dome ..... 29
26	Part of the contact between the Woolly Dolomite and the overlying Mount McGrath Formation, southern Wyloo Dome ..... 29
27	Mount McGrath Formation outcrop and location of measured sections ..... 32
28A	Conglomerate and massive sandstone, distributary channel facies, Mount McGrath Formation, locality 3 ..... 33
28B	Parallel stratification and low-angle scour surfaces in distributary channel facies, Mount McGrath Formation, locality 3 ..... 33
28C	Siltstone, sandstone, and conglomerate Interdistributary bay facies, Mount McGrath Formation, locality 3 ..... 33
29	Distributary channel facies palaeocurrent data, Mount McGrath Formation, localities 3 and 4 ..... 34
30A	Conglomeratic distributary-channel facies, Mount McGrath Formation, locality 4 ..... 35
30B	Distributary-channel and interdistributary-bay facies, Mount McGrath Formation, locality 3 ..... 35
31	Interdistributary-bay facies, Mount McGrath Formation, locality 4 ..... 36
32	Ripple cross-lamination in distributary-mouth bar sandstone, Mount McGrath Formation, locality 3 ..... 37
33	Distributary-mouth bar facies sequence, Mount McGrath Formation, locality 3 ..... 38
34	Beach and offshore shelf facies sequence, Mount McGrath Formation, locality 2 ..... 39
35	Shelf-facies sandstone, Mount McGrath Formation ..... 39
36	Generalized stratigraphic profiles through the Mount McGrath Formation ..... 41
37	Model showing principal depositional environments of the Mount McGrath Formation ..... 43
38	Palaeogeography of the southwestern Pilbara during deposition of the lower Mount McGrath Formation ..... 44
39	Simplified outcrop map of the Duck Creek Dolomite ..... 46
40A	Erosively based intraclast grainstone overlying intertidal and supratidal dolomite, Duck Creek Dolomite, Duck Creek Gorge ..... 47
40B	Domical stromatolites, intraclast grainstone, and laminated dolomite, Duck Creek Dolomite, Duck Creek Gorge ..... 47
41A	<i>Pilbaria perplexa</i> , showing niche development and detail of internal lamination, Duck Creek Dolomite, Duck Creek Gorge ..... 48
41B	Large branching-columnar stromatolites ( <i>Pilbaria cf perplexa</i> ), Duck Creek Dolomite, Duck Creek Gorge ..... 48
42	Tepee structure, supratidal facies, Duck Creek Dolomite, Duck Creek Gorge ..... 49
43	Silicified crested pseudocolumnar stromatolites, supratidal facies, Duck Creek Dolomite, Duck Creek Gorge ..... 49
44	Disrupted domical stromatolite, supratidal facies, Duck Creek Dolomite, Duck Creek Gorge ..... 50
45	Low-domical stromatolite comprising the tiny digitate form <i>Asperia ashburtonia</i> High intertidal to supratidal facies, Duck Creek Dolomite, Duck Creek Gorge ..... 50
46	Vertical profiles showing shelf - facies-association sequences, Duck Creek Dolomite ..... 51
47	Stratigraphic record of a complete upward-shallowing sabkha sequence from the Holocene of the Arabian Gulf ..... 51
48	A comparison between an ideal Holocene sabkha sequence and Sequences 1 and 2 from the Duck Creek Dolomite ..... 52
49	Fenestrate texture, a possible replacement after former anhydrite, supratidal facies, Duck Creek Dolomite, Duck Creek Gorge ..... 53
50A	Thin-bedded slope and basin facies dolomite, Duck Creek Dolomite, 50 km west of Paraburdoo ..... 54
50B	Nodular dolomite, slope and basin facies, Duck Creek Dolomite, northern Wyloo Dome ..... 54
50C	Clast-supported dolomitic conglomerate, slope and basin facies, Duck Creek Dolomite, northern Wyloo Dome ..... 54
50D	Dolomitic conglomerate, slope-and-basin facies, Duck Creek Dolomite, southern Wyloo Dome ..... 54
51	Generalized vertical profiles showing the stratigraphy of the Duck Creek Dolomite in the northwest and southeast Ashburton Basin ..... 55
52	Depositional model for the Duck Creek Dolomite during the shelf progradation phase ..... 56



	Page
53	Palaeogeography of the southwestern Pilbara during deposition of the middle Duck Creek Dolomite ..... 57
54	Basaltic breccia, June Hill Volcanics, 5 km north of June Hill ..... 58
55	Principal outcrop areas of the Ashburton Formation and location of regions 1, 2, and 3 ..... 60
56A	Interbedded siltstone and mudstone, Ashburton Formation, 10km north of Mount Dawson ..... 61
56B	Sandstone turbidites interlayered with cleaved mudstone and siltstone, Ashburton Formation, 15 km west of Ashburton Downs Homestead ..... 61
56C	Sandstone and siltstone turbidites, Ashburton Formation, 5 km east of Mount Amy ..... 61
56D	Climbing-ripple cross-lamination in fine-grained sandstone, Ashburton Formation, 10 km north of Mount Dawson ..... 61
57	Divisions of the Bouma sequence ..... 62
58A	Massive sandstone and conglomerate, Ashburton Formation, 8 km northeast of Mount Stuart Station ..... 63
58B	Parallel stratified pebble-conglomerate overlying massive sandstone Ashburton Formation, 7 km east of Mount Amy ..... 63
59A	Creep-fold in interlayered BIF and chert, Ashburton Formation, Mount Stuart ..... 64
59B	Sparsely vesicular pillow lava, Ashburton Formation, Mount Boggola ..... 64
60A	Type 1 conglomerate and massive sandstone sequence, Ashburton Formation ..... 66
60B	Type 1 conglomerate and mudstone sequence, Ashburton Formation ..... 67
61	Type 2 conglomerate, massive sandstone and mudstone sequence, Ashburton Formation ..... 68
62A	Upward-coarsening and thickening sandstone sequence, Ashburton Formation ..... 69
62B	Upward-thinning and fining sandstone sequence, Ashburton Formation ..... 69
63	Outcrop areas, palaeocurrent trends, and sampling areas in southeastern Ashburton Basin ..... 71
64A	Palaeocurrent data from the southeastern Ashburton Basin ..... 72
64B	Palaeocurrent data from the central Ashburton Basin ..... 72
65	Generalized stratigraphy for the Ashburton Formation ..... 73
66	Composition diagrams for Ashburton Formation sandstones ..... 74
67	Mean compositions and standard deviations of Ashburton Formation sandstones from areas 1 - 6 in the southeastern and central Ashburton Basin ..... 75
68	Mean compositions and standard deviations of Ashburton Formation sandstones from source areas in the Sylvania Inlier, western Hamersley Basin, and southwest of the Ashburton Basin ..... 78
69	Palaeogeographic reconstruction of the southwestern Pilbara during deposition of the lower Ashburton Formation ..... 79
70	Palaeogeographic reconstruction of the southwestern Pilbara during deposition of the upper Ashburton Formation ..... 80
71	Geological map of the northwestern Ashburton Basin, showing localities mentioned in the text ..... 84
72	Geological map of the Hardey Junction area ..... 85
73	Geological map of the southeastern Ashburton Basin, showing localities mentioned in the text ..... 86
74	Geological map of the Mount Elephant area ..... 87
75	The northeastern slopes of Mount Elephant, viewed from the north ..... 87
76	Geological map of the Mount Boggola area ..... 88
77	Geological map of the south and southwestern Pilbara showing principal outcrops of Capricorn Formation, Mount Minnie Group, and Bresnahan Group .... 92
78A	Lenticular coarse-grained sandstone, interbedded with cleaved siltstone and fine-grained sandstone, Capricorn Formation, locality 3 ..... 93
78B	Small, laterally linked columnar stromatolites, Capricorn Formation, locality 3 ... 93
79A	Palaeocurrent data, braided-fluvial facies association, Capricorn Formation ..... 94
79B	Palaeocurrent data, fan-delta facies association, Capricorn Formation ..... 94
80A	Ball-and-pillow structures, shallow-marine facies association, Capricorn Formation, locality 3 ..... 95
80B	Trough-cross stratified pebbly sandstone, fan-delta facies association, Capricorn Formation, locality 3 ..... 95
81	Generalized stratigraphic profiles summarizing the vertical and lateral distribution of facies within the Capricorn Formation ..... 97
82	Depositional model for the lower Capricorn Formation ..... 98
83	Depositional model for the Mount Minnie Group during the transition from Brodagee Sandstone to Wabco Shale ..... 100
84	Palaeocurrent data from the alluvial-fan channel facies association, Bresnahan Group ..... 101

	Page
85	Unconformable contact between the Capricorn Formation and the Bresnahan Group, Mount Bresnahan ..... 101
86A	Lenticular bedding and large-scale trough cross-stratification in alluvial-fan channel facies association, Bresnahan Group, Mount Bresnahan ..... 102
86B	Trough cross-stratification in alluvial-fan channel pebbly sandstone, Bresnahan Group, south of Horrigan Pool ..... 102
86C	Sandstone, siltstone, and mudstone, lacustrine facies association, Bresnahan Group, central Kunderong Range ..... 103
87	Depositional model for the Bresnahan Group ..... 105
88	Cross-section showing the evolution of the Bresnahan Basin by repeated back-stepping of its western margin ..... 105
89	Geological map showing the principal structural divisions of the southwest Pilbara ..... 108
90A	Open, F <sub>2</sub> folds in Ashburton Formation sandstone, Ashburton River, east of Mount Dawson ..... 111
90B	F <sub>2</sub> folds in Ashburton Formation metapelites, west of Glen Florrie Homestead ..... 111
91	Comparative stratigraphies of the Ashburton Basin and Glengarry Sub-Basin ..... 126
92A	Evolution of the southern Pilbara–Pilbara Craton rifting and deposition of the Fortescue Group ..... 128
92B	Evolution of the southern Pilbara–Passive margin stage (Hamersley Group) ..... 128
92C	Evolution of the southern Pilbara–active margin stage (Beasley River Quartzite) .. 128
92D	Evolution of the southern Pilbara–continental crustal collision (Mount McGrath Formation) ..... 129
92E	Evolution of the southern Pilbara–crustal loading and foreland basin subsidence (Duck Creek Dolomite) ..... 129
92F	Evolution of the southern Pilbara–foreland basin infill (Ashburton Formation) ..... 129
92G	Evolution of the southern Pilbara–deposition of the Capricorn Formation during the interval between D <sub>1</sub> and D <sub>2</sub> ..... 129

## TABLES

1	Stratigraphy of Woolly Dolomite ..... 30
2	Composition of Ashburton Formation sandstones from the southeast and central Ashburton Basin ..... 76
3	Composition of Ashburton Formation sandstones from the northwestern Ashburton Basin ..... 79
4	Gold production from the Ashburton Basin to 31 December 1986 ..... 115
5	Copper production from the Ashburton Basin to 31 December 1986 ..... 118
6	Lead and silver production from the Ashburton Basin to 31 December 1986 ..... 120

## Summary

### Chapter 1

The bulletin presents the results of a six-year study of the Ashburton Basin, an arcuate belt of Proterozoic low-grade meta-sedimentary and meta-volcanic rocks flanking the southern and western margins of the Pilbara Craton. The Ashburton Basin forms the northern part of the Capricorn Orogen, and corresponds to the present-day outcrop of the 2000 Ma Wyloo Group. Pre-Wyloo Group units comprise Pilbara Craton granite–greenstone and overlying volcanic and sedimentary rocks of the Mount Bruce Supergroup. The Wyloo Group is subdivided, in ascending order, into: Beasley River Quartzite, Cheela Springs Basalt and Wooly Dolomite, Mount McGrath Formation, Duck Creek Dolomite, June Hill Volcanics, and Ashburton Formation. The Wyloo Group is unconformably overlain by pre-Bangemall Group rocks of the Blair, Mount Minnie, and Bresnahan Basins. Cainozoic deposits comprise Robe Pisolite; valley-fill calcrete and silcrete; partly consolidated or unconsolidated colluvium and river gravel; eolian sand dunes, and sheetwash deposits.

The elevation of the Ashburton valley floor increases from 50–100 m in the northwest to 300–500 m in the southeast. Local relief approaches 200 m. Drainage is ephemeral and follows major structural trends. Climate is arid to semi-arid tropical. Vegetation is dominated by *Acacia* and *Cassia*; *Triodia* (spinifex) is common in the northwest, and eucalypts occur along drainage lines throughout the area.

The region is traversed by the sealed North West Coastal Highway, the partly sealed Tom Price–Nanutarra Road, and graded gravel roads (Mount Vernon–Nanutarra and Prairie Downs–Turee Creek). A network of tracks links the pastoral stations and major roads.

### Chapter 2

The Beasley River Quartzite (360 m) is the lowermost formation of the Wyloo Group; it rests with angular unconformity, or disconformity, upon the Mount Bruce Supergroup. Five major facies associations are recognized:

- (a) Mid-fan facies association, comprising immature clast- and matrix-supported conglomerate, pebbly sandstone, and minor siltstone and mudstone.
- (b) Outer-fan facies association, consisting of trough cross-stratified sandstone and pebbly sandstone, and parallel-laminated sandstone.
- (c) Delta-plain facies association comprising, cross-stratified quartz sandstone.
- (d) Tidal-channel and sand-bar facies association, consisting of quartz sandstone showing a complex organization of sedimentary structures.
- (e) Offshore-facies association comprising mudstone, siltstone and thin-bedded sandstone.

These facies associations record the former presence of a tide-influenced fan-delta system near the eastern closure of Wyloo Dome; shallow-marine, tidal sedimentation prevailed over other parts of the southwestern Pilbara, and deeper marine water occurred to the south and west. Much of the siliciclastic material deposited in the eastern part of the shelf was derived from a braided-delta complex, located along the northeastern margin of the basin.

Around the southeastern Wyloo Dome, Beasley River Quartzite stratigraphy records two phases of tectonically induced sedimentation. Each began with source-area uplift and fan-delta progradation. The periods of shelf subsidence which followed each phase of uplift were characterized by tidal shoreline and offshore sedimentation. In the northeastern part of the basin, uplift and later subsidence resulted in a single phase of delta progradation and abandonment.

### Chapter 3

The Cheela Springs Basalt (2 km) conformably overlies the Beasley River Quartzite. It comprises basalt flows with subordinate fine- to coarse-grained tuff, immature sandstone, siltstone, and mudstone. Dolerite sills are abundant. The nature of sedimentary rocks interbedded with the volcanics suggests the formation was deposited in a gently sloping coastal environment. A small outlier of coarse basaltic agglomerate, gabbro, and basalt, northeast of Duck Creek Homestead in the southwestern Hamersley Basin, may represent a feeder conduit of the Cheela Springs Basalt.

The Woolly Dolomite (325 m) is confined to the southern margin of the Wyloo Dome, where it conformably overlies the Cheela Springs Basalt. The formation comprises shoreline and offshore-shelf carbonate deposits.

### Chapter 4

The Mount McGrath Formation rests disconformably, or with local angular unconformity, upon lower units of the Wyloo Group and Mount Bruce Supergroup. Five major sedimentary facies, are recognized:

- (a) Distributary-channel facies, comprising clast-supported conglomerate, pebbly sandstone and fine- to coarse-grained sandstone.
- (b) Interdistributary-bay facies, consisting of mudstone and siltstone, with thin-bedded sandstone and conglomerate.
- (c) Distributary-mouth bar facies, comprising ripple-laminated and cross-stratified sandstone.
- (d) Beach facies, composed of parallel-stratified, or low-angle cross-stratified sandstone.
- (e) Shoreface and offshore-shelf facies, consisting of sandstone, mudstone, siltstone and carbonate.

Deposition of the Mount McGrath Formation occurred in response to post-Cheela Springs Basalt uplift and erosion in the southern Hamersley Basin. Coarse-grained siliciclastic detritus was laid down on gravelly, braided deltas which fringed the northeastern margin of the Ashburton Basin. Mud, silt and carbonate were deposited in open shelf waters further to the south and west. Maximum development of the deltaic complex occurred during deposition of the lower Mount McGrath Formation. Middle and upper parts of the formation record a gradual waning of siliciclastic supply; this was accompanied by a deepening of shelf waters throughout the basin.

### Chapter 5

The Duck Creek Dolomite (1000 m) rests conformably upon the Mount McGrath Formation, except around the western part of the Wyloo Dome where it unconformably overlies the Fortescue and Hamersley Groups. Two important facies associations are recognized:

- (a) Inner-shelf facies association, comprising repeated shallowing-upward sequences of offshore-barrier intraclast grainstone; subtidal lagoon stromatolitic (domical and

columnar) dolomite; intertidal laminated dolomite; and supratidal dolomite containing a mixed assemblage of biogenic and diagenetic structures.

- (b) Outer-shelf, slope, and basin facies association, comprising thin-bedded, fine-grained dolomite and medium- to very thick-bedded dolomitic conglomerate.

Deposition of the lower Duck Creek Dolomite took place in a relatively deep-water, shelf, slope and basin environment which existed along the northeastern margin of the Ashburton Basin. To the north and east, a belt of shallow, marine, inner-shelf carbonate deposition fringed the low-relief Pilbara Craton. The carbonate shelf underwent one major episode of progradation during deposition of the middle Duck Creek Dolomite. Upper parts of the formation were laid down in a gradually deepening basin, which received increasing amounts of fine-grained siliciclastic detritus.

The June Hill Volcanics (120 m) conformably overlie the Duck Creek Dolomite in the northwestern Ashburton Basin. The formation comprises mafic lava, tuff and agglomerate, interbedded with felsic volcanic and sedimentary rocks.

## Chapter 6

The Ashburton Formation (5–12 km) conformably overlies the Duck Creek Dolomite, except in the northwestern part of the Ashburton Basin where it is disconformable upon the June Hill Volcanics. Principal lithofacies are: mudstone; siltstone; thin- to thick-bedded sandstone; conglomerate; banded iron-formation (BIF) and chert; and local mafic and felsic volcanic rock. Three major lithofacies associations are recognized:

- (a) Conglomerate, massive sandstone, mudstone.
- (b) Massive sandstone, thin- to medium-bedded sandstone, mudstone.
- (c) Mudstone, thin-bedded sandstone, BIF and chert.

The lithofacies associations were laid down in a deep-sea submarine-fan complex. The principal areas of sediment accumulation were: major channels (conglomerate, massive sandstone, mudstone); channel levees and basin plain (mudstone, thin-bedded sandstone, BIF and chert); and depositional lobes and distributary channels (massive sandstone, thin- to thick-bedded sandstone, mudstone).

Palaeocurrent and sandstone composition data suggest three sources for the Ashburton Formation. Most sediment deposited in the southeastern and central Ashburton Basin was derived from granites and greenstones of the Sylvania Inlier. Detritus from a second granite–greenstone terrane, in the region of the present-day Gascoyne Complex, was laid down in the central Ashburton Basin. Volcanic and sedimentary rock fragments from the Mount Bruce Supergroup and low to middle Wyloo Group were deposited in a third submarine fan complex located northwest of Wyloo Dome.

## Chapter 7

Field relationships suggest that most reported occurrences of allochthonous rocks and olistostromes within the Ashburton Formation are either unrelated to Ashburton Formation sedimentation, or are autochthonous parts of the stratigraphy. Only at three localities, all in the northwestern part of the Ashburton Basin, is there strong evidence to support an allochthonous interpretation.

## Chapter 8

The Capricorn Formation, Mount Minnie Group, and Bresnahan Group are localized



pre-Bangemall Group rock units which unconformably overlie the Wyloo Group. The Capricorn Formation (800 m) overlies the central and southeastern part of the Ashburton Basin. It is the oldest post-Wyloo Group unit, and was deposited after  $D_1$  deformation but prior to  $D_2$ . The formation comprises sandstone, siltstone, mudstone, conglomerate, and subordinate dolomite and felsic volcanic rock. Three major facies associations are recognized: braided-fluvial, shallow-marine (or lacustrine) and fan-delta. Lower and middle levels of the Capricorn Formation record braided-fluvial sedimentation in eastern and western parts of the basin; and shallow-marine (or lacustrine) and fan-delta sedimentation in central areas. Upper levels of the formation were deposited in response to a marked increase in sediment supply which caused progradation of the fluvial and fan-delta complex.

The Mount Minnie Group (1600–2400 m) was deposited during the  $D_2$  episode of post-Wyloo Group deformation and is confined to the northwestern part of the Ashburton Valley. Three formations are recognized: Brodagee Sandstone (conglomerate, medium- to coarse-grained sandstone); Wabco Shale (mudstone, siltstone, thin-bedded sandstone); and Warramboe Sandstone (thin- to thick-bedded sandstone, mudstone, and siltstone). The Mount Minnie Group is interpreted as a fan-delta deposit laid down in a small, fault-bounded basin.

The Bresnahan Group post-dates  $D_2$  structures in the eastern Ashburton Basin. It has a maximum measured thickness of 4000 m and comprises conglomerate, sandstone pebbly sandstone, and minor siltstone and mudstone. Three facies associations are recognized: valley fill, alluvial-fan channel, and lacustrine. Palaeocurrent and provenance data indicate that the principal source lay to the west. Bresnahan Group deposition took place in a fault-bounded basin which evolved by back-stepping of its western margin.

## Chapter 9

The Ashburton Basin forms the northern part of the Capricorn Orogen. Two generations of structures related to the orogen are recognized: an early set belonging to the Ophthalmia Fold Belt, in the northern Ashburton Basin and southern Hamersley Basin; and a later set of Ashburton Fold Belt structures, occurring throughout the Ashburton and southern Hamersley Basins.

Two sets of Ophthalmia Fold Belt structures are recognized: large-scale, open, pre-Wyloo Group folds in the southwestern Hamersley Basin; and small-scale, isoclinal and large-scale north-facing folds of post-Cheela Springs Basalt to pre-Mount McGrath Formation age, in the northeastern Ashburton Basin. Ophthalmia Fold Belt structures are thought to result from reverse movements on basement faults during north-south crustal shortening.

Ashburton Fold Belt structures affect the Mount Bruce Supergroup, Wyloo Group, Capricorn Formation, and Mount Minnie Group. Two deformation events ( $D_1$  and  $D_2$ ) are recognized. The  $D_1$  event pre-dated the Capricorn Formation and gave rise to a widespread  $S_1$  foliation. In the southeastern part of the Ashburton Basin,  $S_1$  is associated with large-scale, tight, southwest- or northeast-facing folds. The most prominent structures were formed during the  $D_2$  deformation, which post-dates the Capricorn Formation and pre-dates the Bresnahan Group. Large-scale, open to tight folds and dextral wrench faults characterize the northeastern margin of the Ashburton Fold Belt. Tight to isoclinal, non-cylindrical folds and steep reverse faults occur in the northeastern part of the Ashburton Formation outcrop on TUREE CREEK, EDMUND and southeast WYLOO. Large-scale, open to tight, non-cylindrical folds, interference folds, and dextral wrench faults occur in southern and southwestern parts of the fold belt.  $D_1$  structures are interpreted as a response to thrusting in the basement and cover;  $D_2$  structures were formed by dextral wrench faulting during the late stages of Capricorn Orogen evolution.

Post- $D_2$  to pre-Bangemall Group deformation produced open, southeast-trending folds and northeast-trending normal faults in the Bresnahan Basin. Post-Bangemall Group structures comprise open to tight, northwest- to north-trending folds in the Mount Minnie and western Ashburton Basins.

During  $D_1$ , rocks of the Ashburton Basin were subject to generally low-grade regional metamorphism. Localized contact metamorphism accompanied intrusion of the Boolaloo Granodiorite during the interval between  $D_1$  and  $D_2$ .

## Chapter 10

The principal gold, silver, copper, iron, lead, and uranium occurrences in the Ashburton Basin are described. Most known deposits are small, and are associated with  $D_2$  wrench faults and shears in the Wyloo Group (chiefly in Duck Creek Dolomite and Ashburton Formation), Capricorn Formation, and Mount Bruce Supergroup. Significant uranium mineralization is associated with post-Bresnahan Group normal faulting in the eastern Ashburton Basin. The Mount Clement gold–silver prospect is interpreted as a submarine hot-spring deposit in the Ashburton Formation. The Yarraloola copper deposit probably formed in a distal volcanogenic setting.

Dextral wrench faults, and associated synthetic and antithetic faults, which cut Mount McGrath Formation, Duck Creek Dolomite and Ashburton Formation represent exploration targets for gold mineralization. Orebody size may be limited by the generally shallow depth of supergene enrichment. Pre-Wyloo Group Ophthalmian folds in the western Hamersley Basin are possible targets for large-scale hematite mineralization.

## Chapter 11

Major differences, now recognized, between the Pilbara and Yilgarn Cratons invalidate previous rift models for tectonic evolution of the Capricorn Orogen. An alternative model, based upon plate tectonic theory, is proposed; five major stages are recognized:

- (a) Continental rifting and breakup of the Pilbara Craton during deposition of the low to middle Fortescue Group (about 2.8–2.7 Ga).
- (b) Passive margin sedimentation (upper Fortescue Group and Hamersley Group, about 2.7–2.4 Ga).
- (c) Active margin sedimentation and deformation (Turee Creek Group to lower Wyloo Group - sometime between 2.4–2.0 Ga).
- (d) Continental crustal collision (middle Wyloo Group to  $D_2$  dextral wrenching—some-time between 2.0–1.7 Ga).
- (e) Post-Capricorn Orogen deformation and sedimentation (sometime between 1.7–1.5 Ga).

The principal objections to a plate tectonic model are discussed. Most are either unsubstantiated by available data, or can be rejected as geologically unreasonable.

# Introduction

The Ashburton Basin is an arcuate belt of Proterozoic sedimentary and volcanic rocks which forms the northern margin of the Capricorn Orogen, a major orogenic zone between the Pilbara and Yilgarn Cratons (Fig. 1). It flanks the southern and western margins of the Pilbara Craton between latitudes 21° 30'S and 24° 00'S and longitudes 115° 30'E and 119° 25'E, and crops out in the area covered by GSWA 1:250 000 geological maps: \*EDMUND, MOUNT BRUCE, NEWMAN, TUREE CREEK, WYLOO, and YARRALOOA (Fig. 2). This bulletin describes the stratigraphy, sedimentology, structure, and economic geology of the Ashburton Basin. It summarizes also the geology of the Blair, Mount Minnie, and Bresnahan Basins. Their locations are shown in Fig. 3. Chapters 1–8, 10 and 11 were written by A. M. Thorne; Chapter 9 was co-written by A. M. Thorne and D. B. Seymour.

## Communication and settlement

The western part of the Ashburton Basin is traversed by the sealed North West Coastal Highway and the partly sealed Tom Price–Nanutarra road. The Mount Vernon–Nanutarra gravel road crosses the central part of the region, joining the Tom Price–Nanutarra road on the southeastern part of MOUNT BRUCE. On NEWMAN, a graded gravel road links Prairie Downs and Turee Creek Stations. Main highways and pastoral stations are linked by a network of tracks which provide reasonable access to much of the area.

Most of the sparse population of the area live at the following pastoral stations (from northwest to southeast): Yarraloola, Red Hill, Cane River, Duck Creek, Mount Stuart, Wyloo, Kooline, Glen Florrie, Ashburton Downs, Mininer, Turee Creek, and Prairie Downs. The mining centres of Newman, Pannawonica, Paraburdoo, and Tom Price, and the port of Onslow, are the closest towns; their populations are about 5500, 1200, 2400, 3500, and 600 respectively.

## Climate and vegetation

The climate is semi-arid to arid: annual rainfall is between 200 and 300 mm (Bartlett, 1986). Most rain falls from January to June. Summers are very hot: January

maxima range from 36 to 41°C; minima from 24 to 26°C. Winters are mild: July maxima range from 21 to 25°C; minima from 6 to 11°C. Evaporation from a free-water surface is between 3200 and 3600 mm per year.

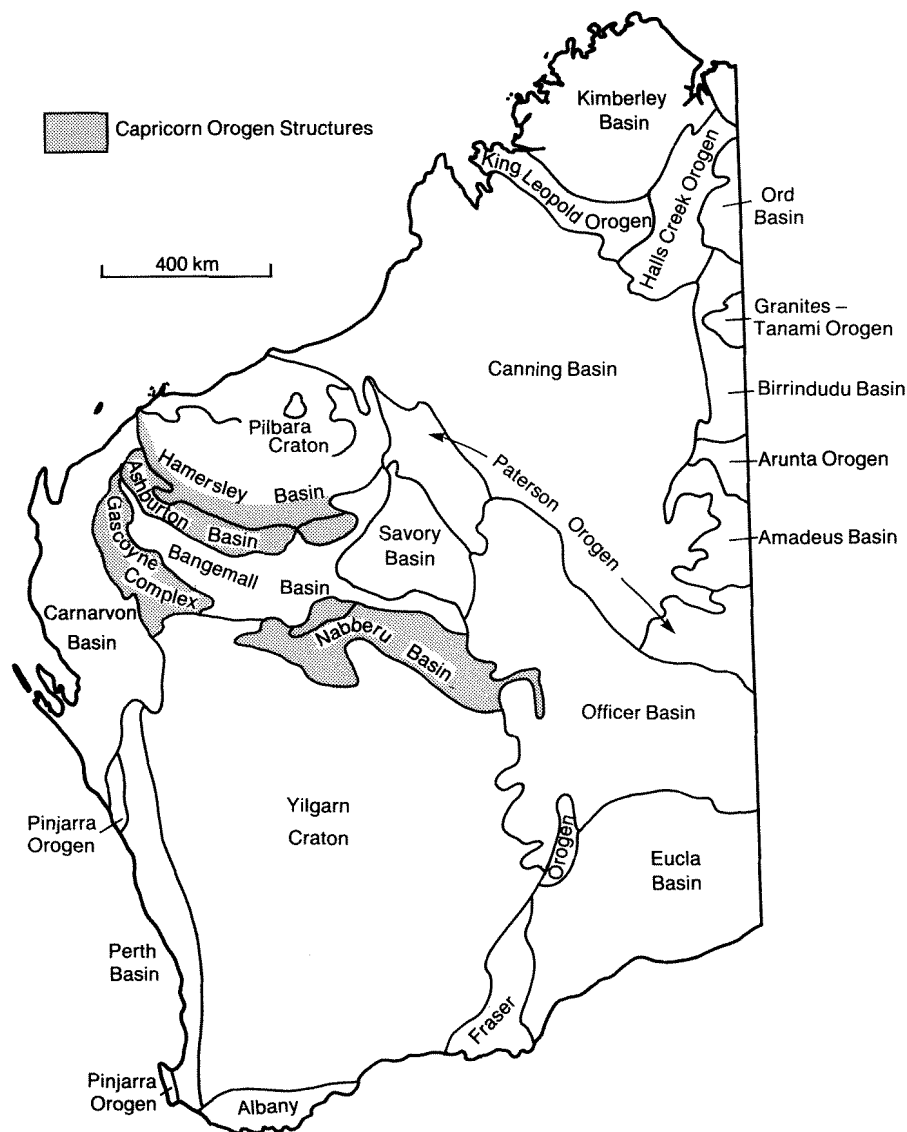
The country north of a line from Glen Florrie Station (22° 56' 00"S, 115° 58' 50"E) to Cheela Springs Outcamp (22° 57' 30"S, 116° 50' 20"E) forms part of the Fortescue Botanical District (Beard, 1975). In the extreme north-west there is a general cover of buck spinifex (*Triodia basedowii*, *T. wiseana*), and a sparse population of shrubs, of which *Acacia elliptica* and other unidentified *Acacia* are the most common. *Eucalyptus dichromophloia* and *E. sp. aff. aspera* are found along drainage lines; they are associated with the shrubs *Cassia pruinosa* and *C. oligophylla*, and the ephemerals *Goodenia ?microptera*, *Ptilotus calostachyus*, *P. exaltatus*, and *Trachymene glaucifolium*.

From Mount Amy (22° 15'S, 115° 53'E) southwards to Glen Florrie, vegetation is more plentiful. On outcrops, the cover consists of buck spinifex (*Triodia wiseana*), scattered snakewood (*Acacia xiphophylla*), *A. pyrifolia*, *A. victoriae*, *Cassia* spp., and the ephemeral *Angianthus* sp. Sandplains and patches of sandy soil on granitoid outcrop are characterized by *Acacia pyrifolia*, soft spinifex (*Triodia pungens*), *Acacia pachycarpa* and *Grevillea pyramidalis*. *Eucalyptus setosa* is locally present on deep sand.

The southeastern Ashburton Basin forms part of the Ashburton Botanical District (Beard, 1975). Mudstone and sandstone of the Ashburton Formation are colonized by species of *Cassia* and *Eremophila*, which often root in bedding and cleavage planes; these shrubs are generally 0.6–1.0 m tall. Stunted *Acacia* are present locally. Mulga (*Acacia aneura*), snakewood (*A. xiphophylla*) and *A. victoriae* grow on colluvium and Cainozoic gravel; they may be associated with the groundcover *Lepidium leptopetalum*, and with small shrubs such as *Eremophila cuneifolia*, *Bassia divaricata*, and *Atriplex inflata*. Vegetation is much thicker on drainage lines, and includes *Acacia aneura*, *A. citrinoviridis*, *A. grasbyi*, *A. wanyu*, and *A. bivenosa*.

Main river channels throughout the Ashburton Basin are lined with *Eucalyptus camaldulensis*, up to 20 m in height, and with smaller *Melaleuca leucodendron*. Alluvial flats adjacent to the large channels may contain abundant *Eucalyptus microtheca*, *Acacia citrinoviridis*, and *A. coriacea*; and a ground cover of *Cenchrus ciliaris* and *Calotis multicaulis*.

\* To avoid confusion with place names, 1:250 000 sheet names are written in full capitals throughout the bulletin.



GSWA 25167

Figure 1 Main tectonic units of Western Australia.

## Physiography

The floor of the Ashburton valley rises from 80 m in the northwest to 300 m in the southeast. Local relief reaches 380 m. The highest point is an unnamed hill of 740 m (on TUREE CREEK) 10 km southwest of Snowy Mountain (23° 24' 10"S, 118° 04' 00"E).

Gently dipping, resistant sandstone and dolomite form cuestas. Where these rocks are sub-horizontal they form rounded hills (e.g. Mount Amy, Mount Boggola); and where steeply dipping, ranges (e.g. Capricorn and Parry Ranges). Areas of tightly folded mudstone and sandstone of the Ashburton Formation are characterized by rugged ridges of low to moderate relief. Gently undulating hills of low relief occur where folds are open and the proportion of mudstone high.

Rivers and creeks flow only after heavy rain, but there are permanent water holes — such as Horrigan, Koonong, and Kooline Pools — on many of the larger drainage lines. The Ashburton River flows from southeast to northwest, parallel to the principal structural trend in underlying bedrock. Although confined to a single large channel for much of its length, the river locally splits into an anastomosed network in its middle and lower reaches. In the southeast, northeast-trending faults determine the orientation of many Ashburton River tributaries, e.g. Tunnel Creek, Turee Creek, and lower reaches of the Angelo River. Superimposed drainage patterns occur near the headwaters of Cherrybooka Creek and Kennedy Creek, close to the Bresnahan Group–Ashburton Formation unconformity.

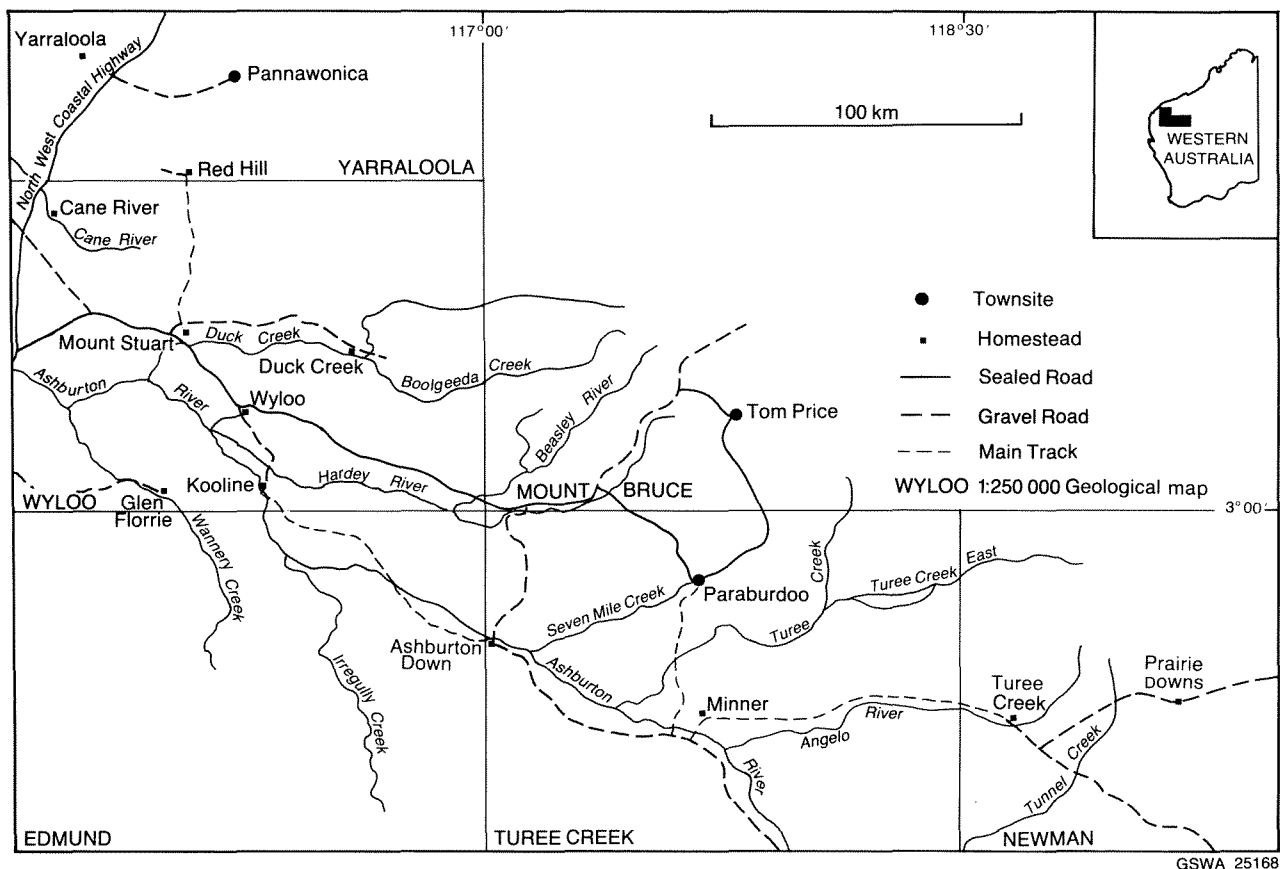


Figure 2 Ashburton Basin: access and key to 1:250 000 map sheets.

## Previous investigations

The earliest descriptions of the Ashburton region were made by the explorer Frank Gregory, who visited the area in 1861 (Gregory and Gregory, 1884; Favenc, 1888). The first geological account, a description of the Top Camp gold-mining centre, was given by H.P. Woodward (1891). He recognized a major unconformity between steeply dipping slates, which he thought were Silurian in age, and an overlying succession of gently dipping dolomite and sandstone, which he correlated with Devonian and Carboniferous strata elsewhere in the State. Additional summaries of Ashburton region geology were given by Woodward (1910, 1912).

A. G. Maitland made geological traverses through the area in 1907. He named the Ashburton Beds (Ashburton and Capricorn Formations in later terminology) and correlated them with similar rocks, the Mosquito Creek Series, of the eastern Pilbara (Maitland, 1909, 1919). His reports refer also to dolomite and conglomerate units associated with the Ashburton Beds, and to the unconformity at the base of the Bangemall Beds (Bangemall Group).

H. W. B. Talbot visited the Ashburton region during the 1920s and gave further accounts of the unconformity between the Ashburton Beds and overlying units (Talbot, 1926). These upper beds (Capricorn Formation, Bresnahan,

and Bangemall Groups, in present-day nomenclature) were grouped together and correlated with the Nullagine Series of the northeastern Pilbara.

Maitland and Talbot's stratigraphic framework provided the basis for geological description until the early 1960s. During this time attention was focussed mainly on mining activity. Simpson (1926) gave a summary of the geology of principal mining centres in the Ashburton Valley. More detailed accounts of selected gold, copper, and lead occurrences were given by Forman (1938), Finucane (1939), Jones and Telford (1939), Ellis (1951), Simpson (1951), and Low (1963).

Results of geological mapping in the south and west Pilbara during the early 1960s were presented by MacLeod et al. (1963), Halligan and Daniels (1964), de la Hunty (1965), Daniels and MacLeod (1965), and Daniels (1968, 1969). These workers recognized five major stratigraphic units overlying the Archaean granite-greenstone terrain; they are, in ascending order: Fortescue Group, Hamersley Group, Wyloo Group, Bresnahan Group, and Bangemall Group. The three lowermost divisions were thought to be part of a conformable succession (The Mount Bruce Supergroup), which was separated from the Bresnahan and Bangemall Groups by angular unconformities. Subsequently, a third post-Wyloo Group unit, the Mount Minnie Group, was recognized in the northwestern Ashburton Basin (Williams, 1968; Daniels, 1970).



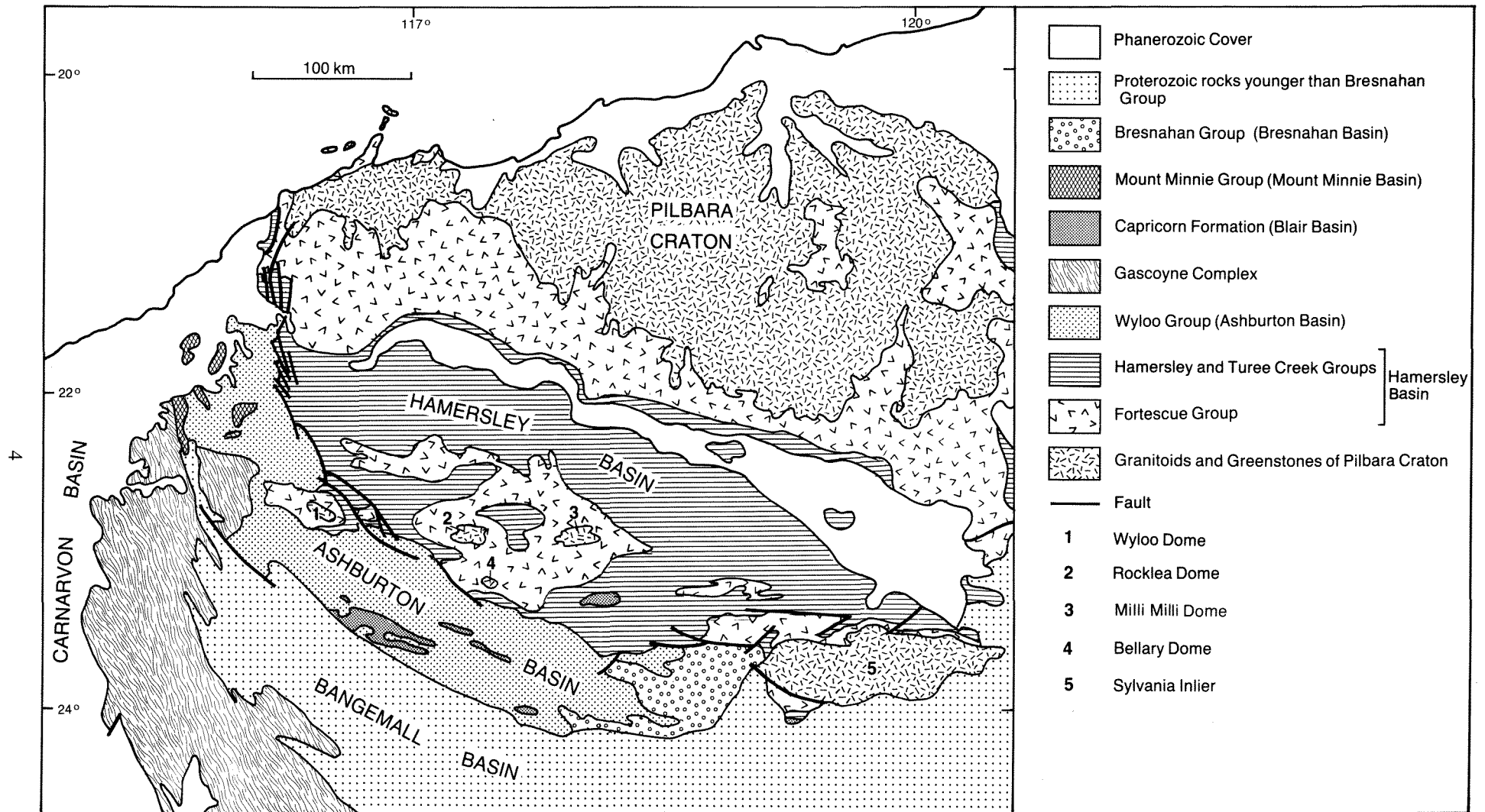
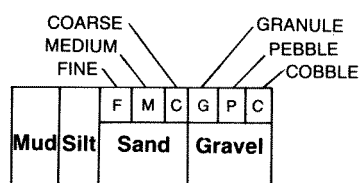
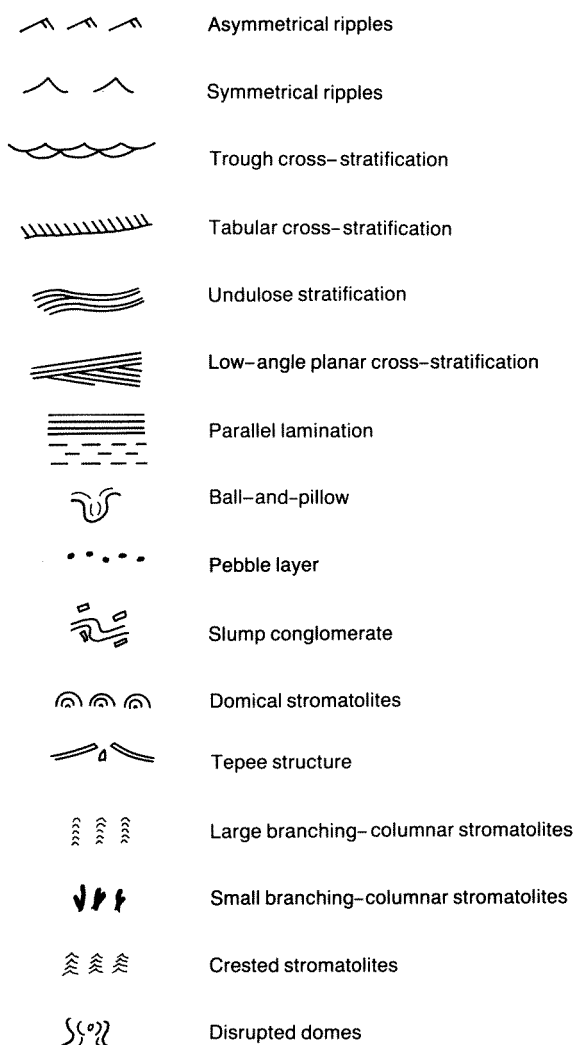


Figure 3 Geological map of northwest Western Australia.



GSWA 25170

**Figure 4** Explanation of graphic log symbols used in this bulletin.

Geochronological studies carried out during the 1960s suggested an age of 2000–1720 Ma for the Wyloo Group (Leggo, 1965; Compston and Arriens, 1968).

Trendall and Blockley (1970), Trendall (1976), and Horwitz (1978) pointed out that, locally, the Wyloo Group lay disconformably upon lower levels of the Mount Bruce Supergroup. Detailed mapping in the Wyloo Dome–Hardey Syncline area confirmed the presence of a major unconformity within the Wyloo Group and led to revision of post-Hamersley Group stratigraphy (Trendall, 1979). The Fortescue and Hamersley Groups were combined with the newly defined Turee Creek Group (previously the lowermost formation in the Wyloo Group) to form the Mount Bruce Supergroup. The remainder of the Wyloo

Group was regarded as a separate stratigraphic unit which unconformably overlay the Mount Bruce Supergroup.

Further modification was made to Wyloo Group stratigraphy in the 1980s. Horwitz (1980) raised the Cheela Springs Basalt to formation status and subdivided the Ashburton Formation into three members. The latter amendment has since been shown to be invalid (Horwitz, 1982). Another change was made by Seymour et al. (1988), who recognized a new formation, the Woolly Dolomite, during remapping of WYLOO.

The stratigraphy and tectonic setting of the Ashburton Basin were discussed by Daniels (1975), Horwitz and Smith (1978), Gee (1979), Goode (1981), Horwitz (1981, 1982, 1983) and Thorne (1986). Sedimentological studies of part of the Wyloo Group were undertaken by Thorne (1985) and Thorne and Seymour (1986). These, and other relevant works, are discussed in the following text.

## Terminology

Sedimentary and volcanic rocks of the Ashburton Basin are metamorphosed in lower to upper greenschist facies, but for simplicity in description the prefix “meta” is omitted.

Grain-size terms for clastic sedimentary rocks are based on the Wentworth scheme (Folk, 1974).

The following terms are used to describe bed and cross-stratified set thickness:

<i>Descriptive term</i>	<i>Thickness range (m)</i>
<b>Bedding</b>	
Very thick	> 1.5
Thick	0.5–1.5
Medium	0.2–0.5
Thin	< 0.20
<b>Cross-stratification</b>	
Large-scale	> 0.5
Medium-scale	0.05–0.5
Small-scale	< 0.05

A key to symbols used in the graphic logs is given in Figure 4.

## Pre-Wyloo Group rocks

### Granite–greenstone

Archaean granite and greenstone are the oldest rocks exposed in the Pilbara. They outcrop over much of the Pilbara Craton and occur also within several inliers in the southern Hamersley Basin, e.g. Wyloo and Rocklea Domes, and Sylvania Inlier (Fig. 3).

The granite–greenstone terrane of the Pilbara Craton is divisible into three principal components (Hickman, 1983; Trendall, 1983):

- (a) Synclinal greenstone belts (Pilbara Supergroup), which comprise mafic, ultramafic and felsic volcanic rocks, chert, banded iron-formation (BIF), conglomerate, sandstone and shale.
- (b) “Older granitoid” which consists of migmatite, gneiss, foliated granodiorite, monzogranite, and tonalite. This forms the bulk of the intervening batholiths and corresponds to, categories 1 and 2 of Hickman (1983, p.25).
- (c) “Younger granitoid”, which is represented by small, discrete plutons of weakly foliated and non-foliated granite and monzogranite that occur within the older granitoid. This includes the “tin granites” of Blockley (1980), and forms the category 3 of Hickman (1983).

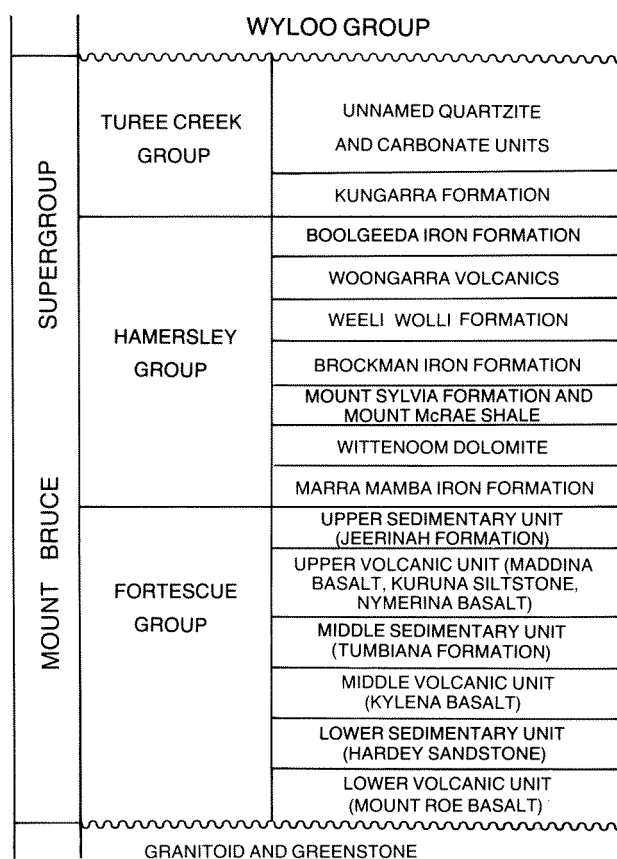
The Pilbara Supergroup has yielded Sm–Nd, galena model, and U–Pb zircon ages, of between 3450 and 3550 Ma (Trendall, 1983). “Older granitoid” has an intrusive relationship to the greenstone belts; and, consistent with this relationship, gives ages mostly within the range 2800 to 3300 Ma. In contrast, most ages for the “younger granitoid” lies between 2500 and 2700 Ma (Trendall, 1983).

The Sylvania Inlier is the largest of five granite–greenstone inliers that occur near the southern margin of the Hamersley Basin. It is characterized by a three-fold subdivision of rock- types, similar to that occurring in the northern Pilbara Craton (Tyler, in press a). Greenstones (comparable to the Gorge Creek and Whim Creek Groups of the Pilbara Supergroup) and banded granitoid make up the lower part of the stratigraphy, although their mutual relationship is unknown. Both units have been intruded by granite and monzogranite (adamellite), thought to be equivalent to the “younger granitoid” of the Pilbara Craton (Tyler, in press a).

Granite–greenstone basement rocks are also exposed in the Bellary, Milli Milli, Rocklea, and Wyloo Domes (de la Hunty, 1965; Daniels, 1970; Horwitz, 1978; Blight, 1985; Seymour et al. (1988)). In the Rocklea and Wyloo Domes, homogeneous monzogranite, with a heterogeneous gneissic marginal phase, intrudes the greenstone (Blight, 1985; Seymour et al. (1988) and may be equivalent to the Pilbara Supergroup–“older granitoid” association of the Pilbara Craton

## Hamersley Basin

Rocks of the Hamersley Basin unconformably overlie the Pilbara granite–greenstone. They comprise, in ascending order (Fig. 5), the Fortescue, Hamersley, and Turee Creek Groups, which are collectively referred to as the Mount Bruce Supergroup (Trendall, 1979, 1983). The Fortescue and Hamersley Groups have given Pb model, Rb–Sr whole-rock and model, and U–Pb zircon ages of 2750 to 2470 Ma (Trendall, 1983).



GSWA 25171

**Figure 5** Stratigraphic subdivision of the Mount Bruce Supergroup (based upon Trendall, 1979; 1990).

The Fortescue Group (3.5–6 km thick) crops out in a long, irregular strip at the northern margin of the Hamersley Basin, and within outliers on the Pilbara Block. It is also exposed in several inliers within the southern and central Hamersley Basin (Fig. 3). The succession comprises mafic lavas and subordinate mafic to felsic tuff, intrusive igneous rocks, and siliciclastic and carbonate sedimentary rocks (Hickman, 1983; Trendall, 1983 and 1990, Blake, 1984a). Over much of the Pilbara, a six-fold subdivision into lower, middle, and upper volcanic and sedimentary rock units can be recognized (Trendall, 1990).

The Hamersley Group (MacLeod et al., 1963; Trendall and Blockley, 1970) forms the middle part of the Mount Bruce Supergroup and crops out over much of the central and southern Hamersley Basin. It conformably overlies the upper sedimentary unit (Jeerinah Formation) of the Fortescue Group and comprises five major units of banded iron-formation interbedded with mudstone, carbonate and fine-grained tuff. About 1 km of the group’s total thickness of 2.5 km consists of mafic sills and acid igneous rocks of uncertain status (Trendall, 1990).

The Turee Creek Group conformably overlies the uppermost (Boolgeeda) iron-formation of the Hamersley Group. Although formerly considered to be the lowermost formation of the Wyloo Group (MacLeod et al., 1963),

the unit was raised to group status and included within the Mount Bruce Supergroup by Trendall (1979). It crops out in scattered localities in the southern part of the Hamersley Basin and has a maximum thickness of about 4 km. Beneath the basal unconformity of the Wyloo Group in the Hardey Syncline–Wyloo Dome area, the group thins from 4.0 km to zero, over a distance of 30 km. The lower and middle parts of the succession consist largely of mudstone, siltstone, and immature sandstone. Upper levels may also contain mature sandstone, conglomerate, sedimentary carbonate, and basalt.

## Limits of the Ashburton Basin

The Ashburton Basin corresponds to the present day outcrop of the Wyloo Group (Fig. 3). It is exposed over an area of approximately 30 000 km<sup>2</sup>, and comprises a 12 km thick sequence of sedimentary and volcanic rocks. The southern and western boundary of the basin is marked by younger Precambrian and Phanerozoic rocks of the Bangemall and Carnarvon Basins. To the east, scattered outcrops of Wyloo Group lie immediately west and southwest of the Sylvania Inlier; to the north and northeast there are unconformable or faulted contacts with rocks of the Hamersley Basin. A small outlier of Wyloo Group (Beasley River Quartzite and Cheela Springs Basalt) occurs within the Turee Creek Syncline, and marks the northeastern limit of Ashburton Basin in this area.

In southwest WYLOO, rocks of the Ashburton Basin merge — with increased metamorphic grade and granitoid plutonism — into the Gascoyne Complex. Northeast of the Bangemall Group unconformity, it can be seen clearly that many metapsammities and metapelites represent metamorphosed Wyloo Group; whereas to the southwest of this line, higher metamorphic grade and lack of stratigraphic continuity make the origin of many schists, gneisses and migmatites uncertain. For this reason, Gascoyne Complex rocks occurring southwest of the Bangemall Group are excluded from the Ashburton Basin.

The Ashburton Basin forms the northern part of the Capricorn Orogen, a major zone of deformed, low- to high-grade metamorphic rocks and granitoid intrusions lying between the Yilgarn and the Pilbara Cratons (Gee, 1979a). It corresponds broadly to the Ashburton Trough and Ashburton Fold Belt of Gee (1979 a, b). Neither term is considered suitable for describing the outcrop area of the Wyloo Group. “Ashburton Trough” suggests an elongate depression that existed at the time of Wyloo Group deposition (Bates and Jackson, 1980). Use of this name should be confined to descriptions of palaeogeography (see Chapter 6); as such, it would be broadly equivalent to the Ashburton Geosyncline of Daniels (1975). Gee (1979a) used the term Ashburton Fold Belt to describe rocks of the Ashburton Basin which were folded during the Capricorn Orogeny. The effects of tectonism were not, however, confined to the Wyloo Group; Archaean granitoid, Mount Bruce Supergroup, Capricorn Formation, and Mount Minnie Group were also deformed during this event (Seymour et al., 1988; Tyler and Thorne, in press). For this reason the Ashburton Fold Belt is regarded as a

structural unit, and use of the term is confined to discussion of post-Wyloo Group deformation (Chapter 9).

## Stratigraphy of the Ashburton Basin

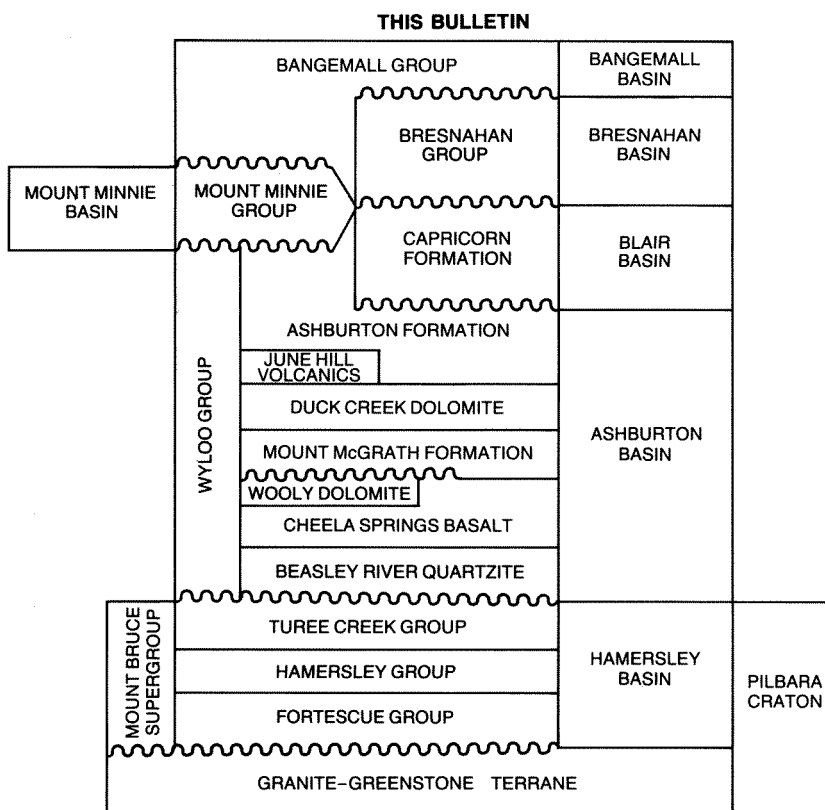
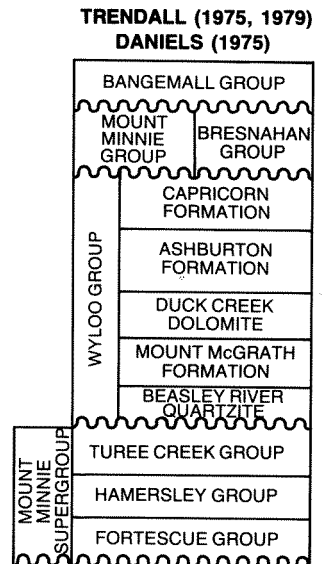
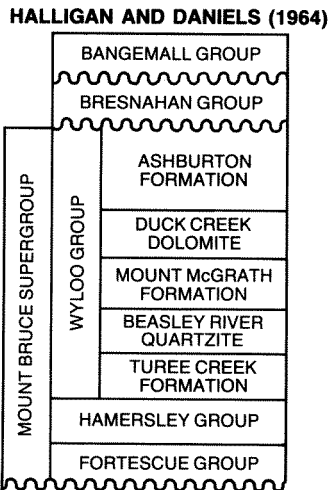
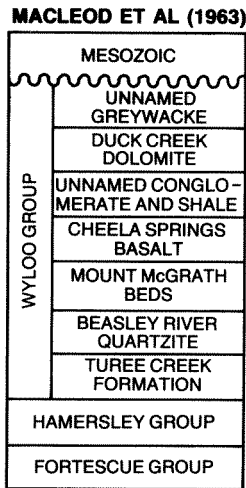
### Previous stratigraphic subdivision

The Wyloo Group unconformably overlies the Mount Bruce Supergroup, and is itself unconformably overlain by the Capricorn Formation; the Mount Minnie, Bresnahan, and Bangemall Groups; and by Phanerozoic deposits. It was named and subdivided by MacLeod et al. (1963), and later incorporated within the Mount Bruce Supergroup of the Hamersley Basin (Halligan and Daniels, 1964). Trendall (1975, 1979) pointed out that the group had not been properly established in accordance with the Australian Code of Stratigraphic Nomenclature. Specifically, there were no descriptions of type sections or type localities for any constituent formations or members. The name “Wyloo Group” and names of principal formations have, nevertheless, been widely applied during 1:250 000 geological mapping of the southern Pilbara (de la Hunty, 1965; Daniels and MacLeod, 1965; Daniels, 1968, 1969, 1970; Williams, 1968). Largely as a result of this usage, the informal nomenclature became generally accepted, although it has been amended (Fig. 6).

The recognition of a major unconformity within the lower part of the Wyloo Group prompted significant revision of the Mount Bruce Supergroup (Trendall, 1979). The Turee Creek Formation (the lower formation in the Wyloo Group), and part of the Beasley River Quartzite (the next to lowest unit), were combined to form a new stratigraphic unit — the Turee Creek Group. As a consequence, the Mount Bruce Supergroup was restructured to include the Fortescue, Hamersley and Turee Creek Groups. The Wyloo Group was regarded as a separate lithological entity whose lowermost formation, the redefined Beasley River Quartzite, unconformably overlies the Mount Bruce Supergroup.

Following remarks by Trendall (1979, p.70), Horwitz (1980) elevated the Cheela Springs Basalt Member of the Mount McGrath Formation to formation status. He also proposed a three-fold subdivision of the Ashburton Formation into, in ascending order: Wandarray Shale, Capricorn Member, and Mininer Turbidite Member. This second amendment must now be regarded as invalid, for it has since been recognized that the Capricorn Member (equivalent to the Capricorn Formation of Halligan and Daniels, 1964) unconformably overlies the Ashburton Formation (Horwitz, 1982, p. 198).

Further modifications to Wyloo Group stratigraphy have been proposed by Seymour et al. (1988). They named and assigned formation status to the Woolly Dolomite, a distinctive carbonate unit that occurs above the Cheela Springs Basalt, on southern WYLOO. The same rank was given also to the June Hill Volcanics; Williams (1968) and Daniels (1970) had previously included this unit as part of the Duck Creek Dolomite and Ashburton Forma-



GSWA 25172

**Figure 6** Stratigraphic subdivision of the southwestern Pilbara used in this bulletin. Previous stratigraphic schemes are shown for comparison.

tion. A third modification affected the status of the Mudong Member — an assemblage of quartzite, schist, marble and amphibolite that had formerly been considered a part of the Ashburton Formation (Daniels, 1970). Its component lithologies are not, in general, characteristic of the Ashburton Formation, or its metamorphosed equivalents. This fact, coupled with structural complexity and lack of stratigraphic continuity in the outcrop area, makes correlation with the Ashburton Formation doubtful. In recognition of this the Mudong Member was excluded

from the Ashburton Formation, and was renamed the Mudong Metamorphics, and incorporated in the Morrissey Metamorphic Suite of the Gascoyne Complex.

### Stratigraphy used in this bulletin

The stratigraphic subdivision of the Wyloo Group used in this bulletin (Fig. 6) is based on that of MacLeod et al. (1963), Halligan and Daniels (1964), Trendall (1979),



Horwitz (1980) and Seymour et al. (1988). In contrast to these earlier schemes, however, the Capricorn Formation is no longer included within the Wyloo Group. Halligan and Daniels (1964) included these rocks as an unnamed unit within the Ashburton Formation. They were subsequently named, and placed at the top of the Wyloo Group by Daniels (1968). He considered the Capricorn Formation to be generally conformable upon the Ashburton Formation, although it was recognized that disconformable contacts exist locally. Fieldwork for the present study has shown that a major angular unconformity separates the two formations. The contact is exposed at several places in the Capricorn Range, and at Mount Boggola (Chapter 8). In all, it can be shown that the Ashburton Formation was folded and eroded prior to deposition of the Capricorn Formation. Talbot (1926, p.34) recognized this relationship at Mount Boggola, but his stratigraphic nomenclature has since been superseded.

The Ashburton and Capricorn Formations are separated by a basin-wide unconformity, and there are marked lithological differences between them. The Ashburton Formation comprises "deeper water" chloritic mudstone with subordinate turbidite sandstone and siltstone. In contrast, the Capricorn Formation consists principally of shallow-marine and subaerial facies (rippled and cross-stratified sandstone, stromatolitic carbonate and ferruginous and micaceous siltstone, and mudstone). These important differences were recognized by Daniels (1969).

On the basis of these arguments the Capricorn Formation is excluded from the Wyloo Group. It is regarded as a separate lithological unit which unconformably overlies the Wyloo Group and is itself unconformably overlain by the Bresnahan and Bangemall Groups. As a corollary, the Ashburton Formation is now the uppermost formation of the Wyloo Group.

No type section for the Capricorn Formation has previously been established. To conform with normal stratigraphic procedure (Staines, 1985) it is proposed that the section of Capricorn Formation exposed along the northward draining creek at 23° 23' 30"S, 116° 55' 00"E be given this status. A lithological description of this locality is given in Chapter 8.

No attempt is made to raise the Capricorn Formation to group status. The Australian Code of Stratigraphic Nomenclature recommends that a group be established only where the stratigraphy can be subdivided into at least two units of formation rank (Staines, 1985). Lateral and vertical facies variations within the Capricorn Formation make this type of formal stratigraphic subdivision impracticable.

## Age of the Ashburton Basin

The age of the Wyloo Group is poorly known. Clasts of Woongarra Volcanics (Hamersley Group) occur in conglomerate at the base of the Wyloo Group and provide an older age limit of  $2470 \pm 30$  Ma (U–Pb zircon, Compston et al., 1981). The Ashburton Formation, the

uppermost stratigraphic unit of the Wyloo Group, is intruded by the Boolaloo Granodiorite for which Leggo and others (1965) obtained a Rb–Sr<sup>+</sup> mineral isochron of 1680 Ma. Data from the June Hill Volcanics give Rb–Sr<sup>+</sup> rock model ages of  $1977 \pm 165$  Ma (Compston and Arriens, 1968) and 1811 Ma (Leggo et al., 1965). Samples of galena from the Yarraloola copper prospect (a volcanogenic copper–galena deposit occurring within the Ashburton Formation) give a Pb model age of about 2000 Ma (J.R. Richards, written communication, 1987). On present information therefore, the Wyloo Group has a probable age of approximately 2000 Ma (Gee, 1980).

## Regional correlation of the Wyloo Group

Several workers (Horwitz and Smith, 1978; Gee, 1979a; Doust, 1984; and Bunting, 1986) have correlated the Wyloo Group with parts of the Nabberu Basin stratigraphy (principally the Glengarry Group). The Ashburton and Nabberu Basins are today separated by cover rocks of the Bangemall Basin and by high-grade metamorphic rocks and granitoid intrusions of the Gascoyne Complex. This lack of lithologic continuity, coupled with major differences in the stratigraphy of the respective basins (see Chapter 11), and inadequate geochronological controls, makes regional correlations of this type speculative.

## Blair, Mount Minnie, and Bresnahan Basins

The Ashburton Basin is locally overlain by three small basins which pre-date the Bangemall Group (Fig. 3). The Blair Basin (named after Mount Blair, 23° 26'40"S, 117° 08' 30"E) corresponds to the present-day outcrop of the Capricorn Formation. It forms the main part of the Capricorn Range, and is also exposed in several small outliers within the central and eastern Ashburton Basin, e.g. Mount Dawson and Mount Boggola. The Mount Minnie Basin is delineated by scattered outliers of Mount Minnie Group in the northwestern Ashburton Basin. The Bresnahan Basin is located between longitudes 117° 50'E and 119° 22'E, and corresponds to the present day outcrop of the Bresnahan Group.

The ages of these post-Wyloo Group units are poorly known. The Capricorn Formation was deposited in the interval between two episodes (D<sub>1</sub> and D<sub>2</sub>) of post-Wyloo Group–pre-Bresnahan Group deformation. The Boolaloo Granodiorite intruded the Wyloo Group during this break. However, the timing of this event relative to deposition of the Capricorn Formation is uncertain. On such evidence, this Capricorn Formation has a maximum age of about 2000 Ma (the likely age of the Wyloo Group) and a minimum age of about 1680 Ma the Rb–Sr age of the Boolaloo Granodiorite–(Leggo et al., 1965).

---

\* Recalculated using <sup>87</sup>Rb decay constant =  $1.42 \times 10^{-11} \text{ a}^{-1}$  (Steiger and Jager, 1977)

The Mount Minnie Group post-dates early  $D_2$  folds in the Ashburton Basin but is cut by late  $D_2$  wrench faults. These relationships indicate that the Mount Minnie Group is younger than Boolaloo Granodiorite (1680 Ma) and the Capricorn Formation. The minimum age of about 1100 Ma is set by the inferred age of the overlying Bangemall Group (Muhling and Brakel, 1985)

The Bresnahan Group is the youngest of the three post-Wyloo Group–pre-Bangemall Group rock units, having been deposited after the second post-Wyloo Group deformation event. As with the Mount Minnie Group, its maximum age is set by the Rb–Sr mineral isochron of 1680 Ma, obtained from the Boolaloo Granodiorite (Leggo et al., 1965). Its minimum age, based on data from the Bangemall Group, is about 1100 Ma (Muhling and Brakel, 1985).

## Cainozoic deposits

Older Cainozoic deposits of the Ashburton Basin are subdivided into: Robe Pisolite; valley-fill calcrete and silcrete; and partially consolidated colluvium and river gravel. They are generally considered to be of Tertiary age (Daniels, 1968; Daniels and Macleod, 1965); however, much of the evidence is indirect and some deposits could be older, or younger.

The Robe Pisolite (15–45 m) forms elevated terraces and mesas along ancestral drainage lines in northwest WYLOO. It consists of limonite and hematite pisoliths, with small amounts of terrigenous detritus, and scattered

fragments of fossil wood. Samples of clay from beneath the pisolite on Hamersley Station yielded spores and pollen; these give an older age limit of late Eocene for the Robe Pisolite (J. Backhouse, quoted in Twidale et al., 1985).

Dissected valley-fill calcretes, locally silicified, border the major drainage lines on TUREE CREEK and NEWMAN and form prominent mesas. Their calcrete cappings are about 30 m above the present valley floor. Most calcretes are 5–10 m thick; internal structure is varied, and may be planar-laminated, nodular, or cellular. Many calcretes contain cavernous voids, and the crude bedding may define domes up to several metres across and 0.5 m amplitude. Carnotite ( $K_2[UO_2]_2 V_2 O_8 \cdot 3H_2 O$ ), and manganese, in the form of cryptomelane ( $KMn_8 O_{16}$ ), and pyrolusite ( $MnO_2$ ), occur in some voids and cracks. The calcretes rest on Precambrian bedrock, kaolinitic clay, or sand and gravel. They are interpreted as groundwater deposits of a former valley floor (Mann and Horwitz, 1979).

Partly consolidated colluvium consists of poorly sorted, angular to rounded rock fragments in a mud, silt, and sand matrix. It is most extensive in the east, forming aprons around many larger outcrops. The gravels are generally less than 15 m thick.

Younger Cainozoic (probably Quarternary) deposits include: unconsolidated river alluvium in and adjacent to major drainage lines; unconsolidated colluvium deposited around margins of outcrops; eolian sand dunes and sand sheets; and sandy or clay-rich sheetwash sediments which cover extensive areas in the eastern Ashburton Basin.

## Chapter Two

# Beasley River Quartzite

The Beasley River Quartzite is the lowermost formation of the Wyloo Group and rests with angular unconformity or disconformity upon the Mount Bruce Supergroup. Over much of the Ashburton Basin the formation is 220–360 m thick, but it thins to zero around the western margin of Wyloo Dome. Brief descriptions of the formation were given by Daniels (1968, 1970, 1975), de la Hunty (1965) and Horwitz (1981, 1982). More detailed descriptions were given by Trendall (1979) and Thorne and Seymour (1986).

This chapter describes and interprets the major facies associations of the Beasley River Quartzite; most of the information was obtained from six measured sections (Fig. 7) and 1:40 000-scale mapping of adjacent outcrops.

The formation consists mainly of cream- or white-weathering, silicified quartz-sandstone; but conglomerate derived from BIF, mudstone, and carbonate occur locally. Five major facies associations are recognized: mid-fan; outer-fan; delta-plain; tidal-channel and sandbar; and offshore. The mid- and outer-fan facies associations broadly correspond to the Three Corner Conglomerate Member of Trendall (1979).

### Mid-fan facies association

The mid-fan facies association comprises mid-fan lobe and interlobe facies (Figs. 8,9). Principal rock-types are conglomerate and coarse-grained sandstone that were derived from the Hamersley Group. Clasts are predominantly angular or sub-angular fragments of BIF and chert (mainly Weeli Wolli Formation), and lesser amounts of rounded rhyodacite and dolerite; the latter often exhibit a bleached outer rind.

#### Mid-fan lobe facies

##### Description

This facies can be divided into very thick-bedded conglomerate and inversely-graded conglomerate. The lobes are usually composed of one of these lithotypes, either as a single unit or in a stacked sequence. Lobe units have sharp bases, but there is little evidence of erosion into underlying beds.

Very thick-bedded conglomerate occurs in laterally continuous (>75 m) beds, 4–17 m thick. Clast diameters are up to 0.45 m, but most lie in the range 0.02–0.15 m. The conglomerate is predominantly clast-supported, and rarely exhibits stratification other than localized, bedding-parallel, orientation of the tabular clasts. Many beds display a mixture of clast and matrix support, and bedding-parallel or random fabric. Locally, thicker conglomerate beds contain lenses of stratified, coarse-grained sandstone that have been slightly modified by soft-sediment deformation. The matrix of the conglomerate consists of sand-sized (medium to coarse) fragments of BIF, quartz, feldspar, and hematite.

Inversely graded, thick-bedded (3–4 m) conglomerate crops out in laterally continuous beds with sharp, non-erosive bases. Grain-size coarsens upwards, from a granule or, rarely, a sandy conglomerate, to cobble conglomerate with an average maximum clast size of 0.1 m. Clast support is predominant in all but the sandy conglomerate horizons. Inversely graded conglomerate usually exhibits a random fabric. The matrix is as described for very thick-bedded conglomerate.

##### Interpretation

Very thick-bedded conglomerate is interpreted as a debris-flow deposit on the basis of the following evidence: sharp, non-erosive bases; occurrence in thick, well-defined units; lack of sorting and clast abrasion; and a mixture of clast and matrix support. Lowe (1982) places deposits of this type into a broad category of cohesive debris-flow sediments; but he notes that they were deposited in a flow in which clasts were lubricated but not fully supported or suspended by the generally sandy matrix. Lewis (1981) prefers the terms “non-cohesive or low-viscosity debris flows” to describe such deposits, and suggests that intergranular support mechanisms (e.g. dispersive grain pressure) dominated.

Inversely graded conglomerate is also assigned a debris-flow origin. This type of fabric is common in highly concentrated flows and possibly results from dispersive pressure, caused by clast collision, which forces smaller clasts downwards between the larger ones (Walker, 1975). Lowe (1982) points out that inverse grading is widespread in beds of cobble conglomerate greater than 0.4 m thick; he refers to such deposits as density-modified grain flows. Here the inverse grading reflects high dispersive pressure between large (cobble-sized) clasts.

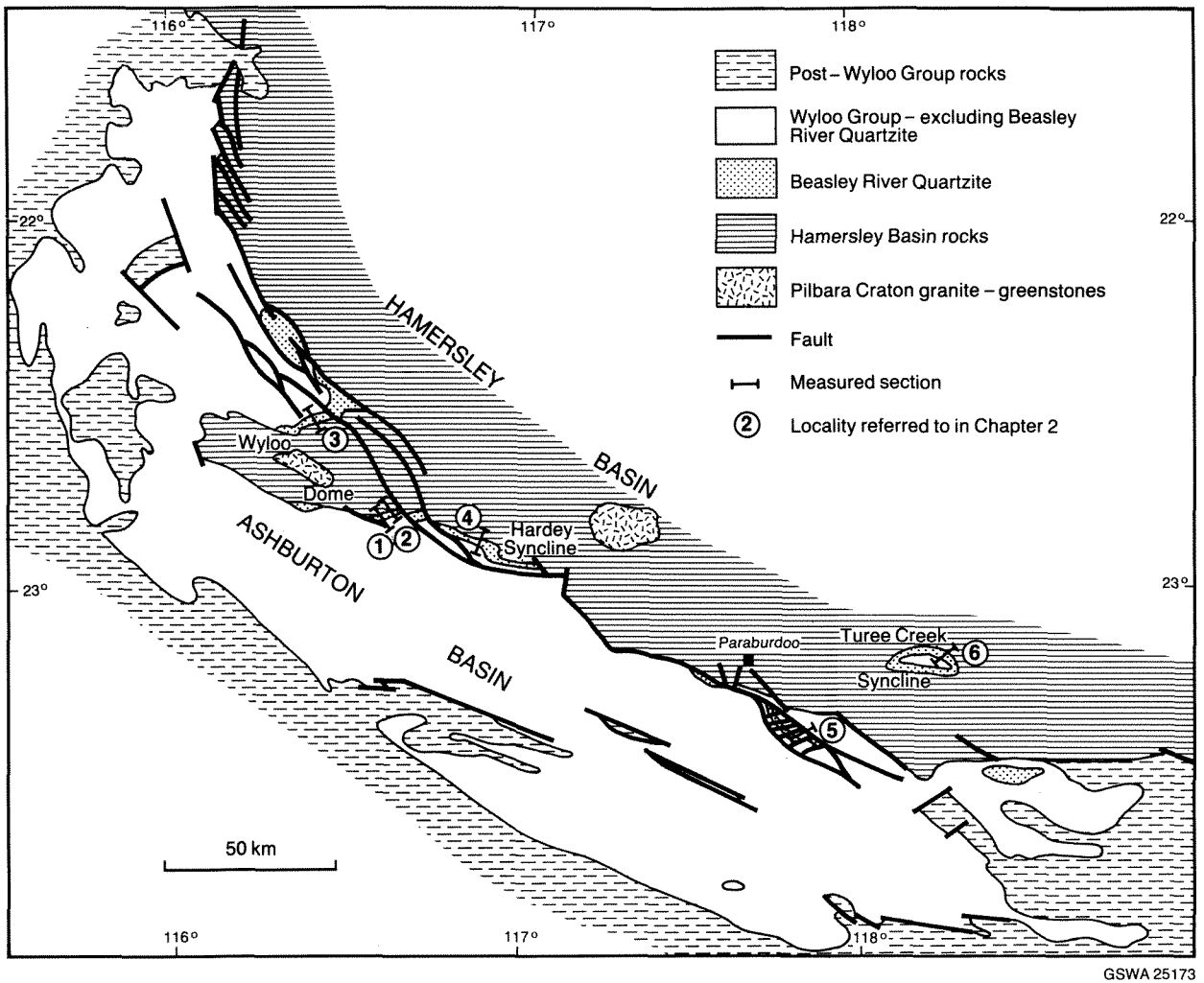


Figure 7 Beasley River Quartzite outcrop and location of measured sections.

The fabric of many thick-bedded and inversely graded conglomerate units suggests that they may have been deposited from a single flow. However, the less homogeneous beds, especially those that incorporate lenses of stratified sandstone, indicate that periods of streamflow sedimentation were intimately associated with the debris-flow events.

The thickness and coarse grain-size of the debris-flow deposits suggests that they were deposited on proximal parts of the fan. The planar boundaries and lateral extent of these bodies indicate that they were not confined to discrete channels but instead accumulated as lobes on the fan surface (Heward, 1978a).

## Interlobe facies

### Description

Upward-fining pebbly sandstone, fine- to coarse-grained sandstone, siltstone, and mudstone, occur in 0.3–4 m thick units between the lobe conglomerate. Individual beds are 0.05–0.6 m thick, and are either lenticular or laterally continuous over tens of metres. Pebbly and

medium- to coarse-grained sandstone generally exhibits parallel stratification or trough cross-stratification, the latter as sets 30–100 mm thick. Fine-grained sandstone and siltstone are parallel-laminated or ripple cross-laminated. No internal structure is visible in the mudstone.

### Interpretation

Sandstone, siltstone, and mudstone, are interpreted as streamflow sediments laid down in intervals between lobe-forming events. Cross-stratified sandstone and pebbly sandstone represent minor braided-channel deposits, whereas parallel- or ripple-laminated siltstone and sandstone are interpreted as sheetflood deposits (Bull, 1972). Structureless mudstone is considered to represent the suspended load of streams and sheetfloods, though it is recognized that it usually accumulates on more distal parts of the fan (Wasson, 1977).

## Outer-fan facies association

This association consists of braided-stream and sheetflood facies (Figs. 9C,D,10,11).

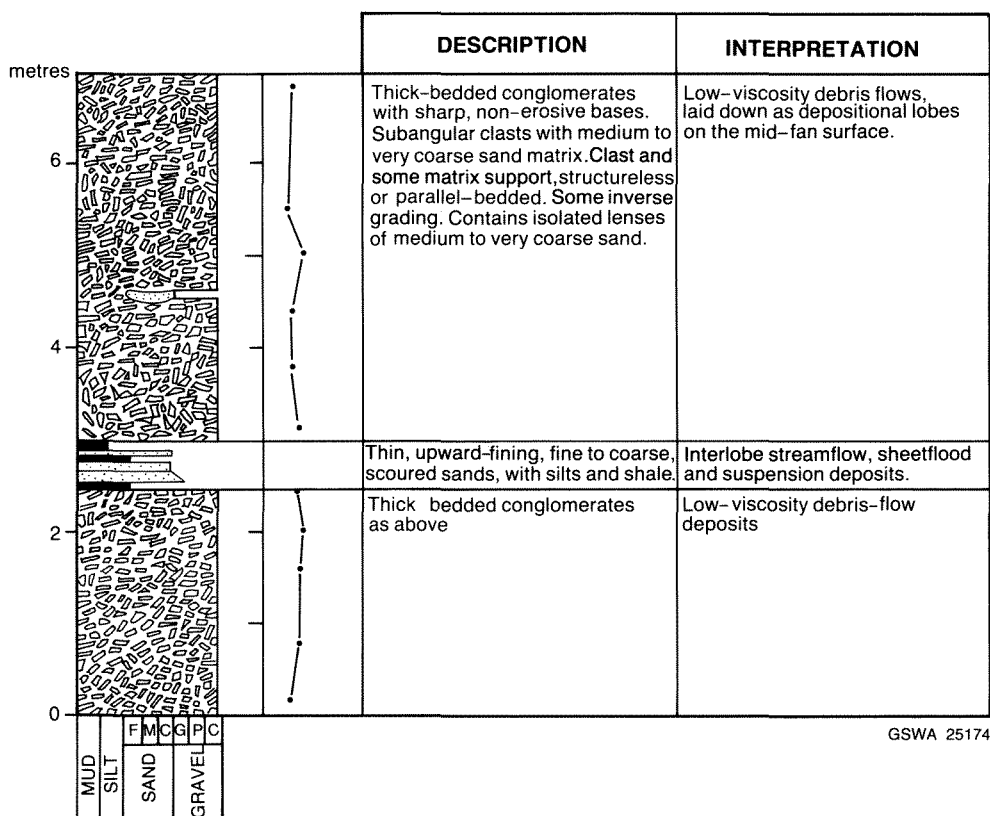


**Figure 8** Mid-fan facies association showing variations in thickness, grain-size, and internal structure between lobe and interlobe deposits.

## Braided-stream facies

### Description

The braided-stream facies consists of thin- to thick-bedded (0.1–1.0 m), trough cross-stratified, medium- to very coarse-grained sandstone and pebbly sandstone. These rocks incorporate fragments of BIF, chert, hematite, feldspar, and quartz. Sand-sized hematite, together with pebbles of BIF and chert, occur as lags in many coarse-grained beds, whereas quartz is more abundant in finer grained ones.

Generally, this facies consists of multiple intersecting troughs, 0.05–0.20 m high and up to 1.5 m wide, which together form tabular cosets 0.3–1.5 m thick. Cosets are often separated by a few centimetres of erosively based, parallel-laminated, medium- to coarse-grained sandstone. Trough cross-stratified medium- to coarse-grained sandstone and pebbly sandstone locally grade upwards into ripple-laminated fine-grained sandstone; symmetrical ripples are preserved on the tops of some beds. Palaeocurrent data from this facies (Fig. 11) are unidirectional at any stratigraphic level for a given locality and indicate that sediment transport took place towards the south and east at localities 1 and 2 (Fig. 7).

### Interpretation

Both single and multiple sets of trough cross-strata are attributed to downcurrent migration of dunes in a braided

fluvial system (Harms et al., 1982). Trough cross-stratified beds which fine upwards to a ripple-laminated top were probably deposited from relatively short-lived waning flows; their symmetrical ripples suggest local reworking by waves in standing water.

## Sheetflood-sandstone facies

### Description

The sheetflood-sandstone facies consists of horizontally laminated fine- to coarse-grained sandstone, composed of alternating light-coloured and dark ferruginous layers. The light-coloured component consists of angular, fine- to medium-grained quartz with lesser amounts of plagioclase and K-feldspar. Ferruginous layers consist of medium- to coarse-grained fragments of BIF, chert, hematite, and quartz.

Sheetflood sandstone crops out in tabular units up to 3 m thick. Many beds exhibit low-angle scours; locally, current lineations are seen. In addition, 1–3 cm thick layers of current- or wave-rippled, fine-grained quartz sandstone occur interbedded within the facies.

### Interpretation

The presence of low-angle scours and current lineations in association with widespread parallel lamination suggests that this facies was deposited in upper regime flows





**Figure 9A** Very thick-bedded, massive mid-fan lobe conglomerate. Beds are laterally continuous and separated by sharp, planar boundaries which show little evidence of erosion, locality 1.



**Figure 9B** Internal structure of part of mid-fan lobe facies association. Pebble- to cobble-sized clasts of Hamersley Group (chiefly Weeli Weeli Formation). BIF and chert form a clast-supported framework with a weak fabric parallel to bedding. Interstices are filled with sand-sized detritus, locality 1.

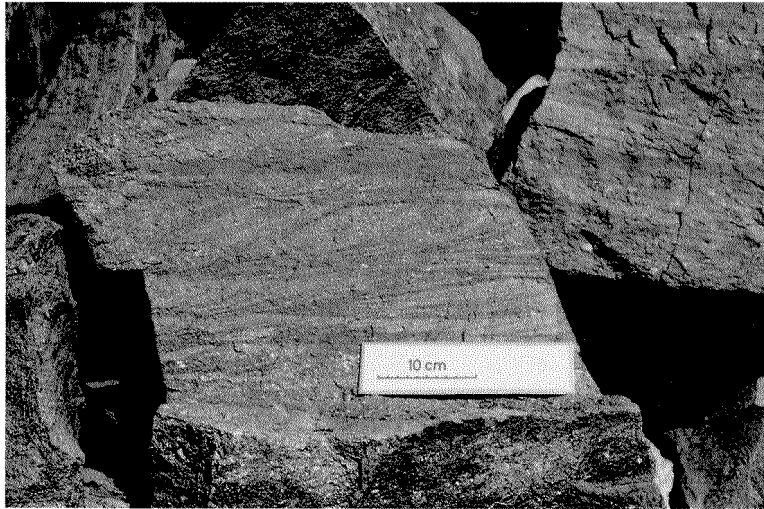


**Figure 9C** Small-scale trough cross-stratification in outer-fan braided-stream facies. Dark-coloured forsets mark concentrations of sand-sized detrital hematite, locality 2.



**Figure 9D** Parallel-laminated and ripple cross-laminated sheetflood facies sandstone overlying massive braided-stream facies pebbly sandstone (bottom right). These facies form part of the outer-fan

GSWA 25175

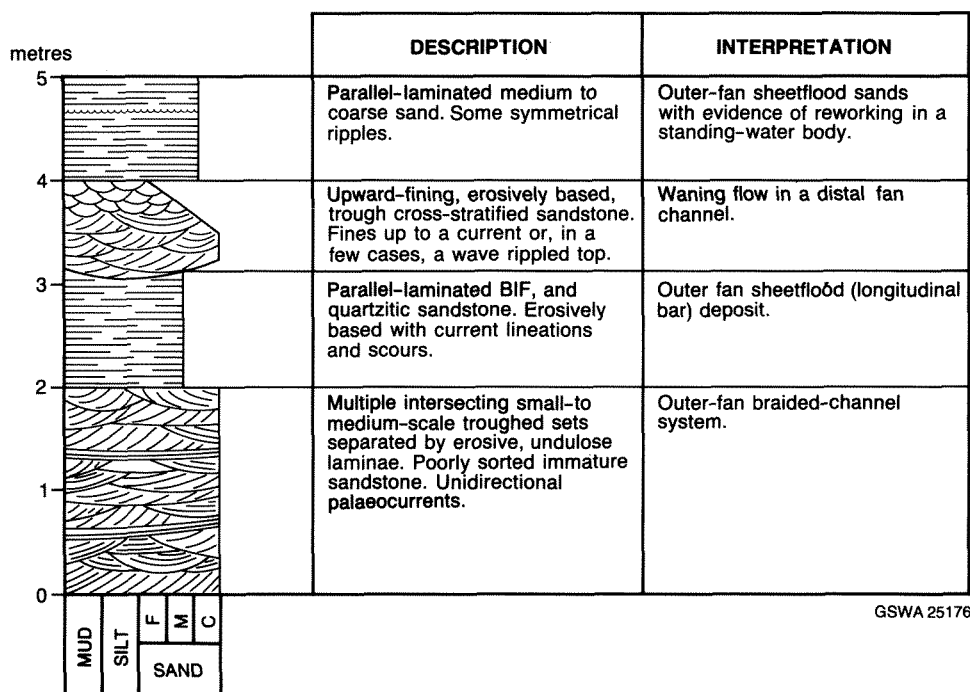


Figure 10 Schematic summary of rock types present in the outer-fan facies association.

(Harms and et al., 1982). Thin interbeds of current- and wave-rippled sandstone mark periods during which residual reworking by lower flow-regime and oscillatory currents took place.

Parallel-laminated sand bodies, similar to those described in this work, were reported from the Gum Hollow fan delta at Nueces Bay, Texas (McGowen, 1970). Study of this Holocene fan delta showed that, whereas sediment dispersal takes place along braided channels for much of the year, most of the fan growth occurs during periods of storm-induced sheetflooding. The sheetflood deposits typically comprise parallel-laminated, fine-grained sands, laid down as extensive longitudinal bars over much of the fan surface.

## Delta-plain facies association

### Description

The delta-plain facies association (Figs. 12, 13, 14) ranges in thickness from 8–70 m and consists of fine- to coarse-grained (mostly medium-grained) quartz sandstone with a little coarse-grained ferruginous sandstone and granule conglomerate. Internal structure is dominated by medium- to large-scale trough cross-stratification with subordinate parallel- or ripple-lamination. These stratification types occur in stacked lenticular cosets, 1–3 m thick and 10–40 m wide (Fig. 12). Cosets generally consist of 0.1–1.5 m thick sets of trough cross-strata, deformed into ball-and-pillow structures where local marked

differences in grain-size occur between superimposed sets. Thicker cosets show upward decrease in grain-size and scale of cross-stratification, and may incorporate 0.1–0.5 m thick intervals of parallel-laminated or gently inclined, planar-laminated fine-grained sandstone. Coset boundaries are sometimes marked by a few centimetres of mudstone or ripple-laminated siltstone. Palaeocurrent data are strongly unimodal (Fig. 14), and directed towards 260° at localities 5 and 6 (Fig. 7).

### Interpretation

Trough cross-stratification is formed by the downstream migration of lunate to sinuous dunes during moderate to high flow velocities (Harms et al., 1982). The intervals of parallel-laminated fine-grained sandstone are interpreted as upper flow regime deposits (Harms et al., 1982).

The scale and lenticular geometry of the cosets, coupled with the unidirectional palaeocurrent data, suggests that the dunes were formed in braided channels of low sinuosity. The sequence of structures in the thicker cosets preserve an almost complete record of channel infill. Large troughs, low in the sequence, represent the lower channel-bar deposits, but the overlying small-scale troughed and parallel-laminated division probably formed on emerging bars as water levels fell. Vos (1977) records a similar transition in Palaeozoic delta-plain sandstones from the Moroccan Tindouf Basin. The scale of sequences described here suggests that channels had a maximum depth of at least 3 m.

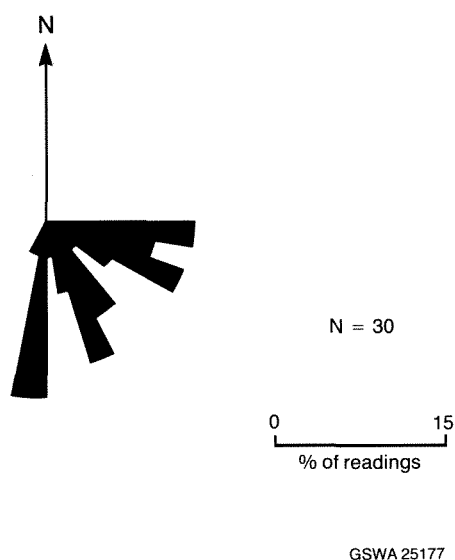


Figure 11 Palaeocurrent data from the braided-stream facies (outer fan) at localities 1 and 2.

## Tidal-channel and tidal sand-bar facies association

### Tidal-channel facies

#### Description

The tidal-channel facies (Figs. 15, 16) crops out in erosively based units 1–30 m thick. Individual channels range in width from a few metres to 120 m, with scouring between 0.25 m and 8 m into underlying beds. Channels are usually composed of medium- to very coarse-grained quartz sandstone with local pebble-cobble lags of Woongarra Volcanics detritus in larger channels. Some channels are filled with siltstone and mudstone.

Internal structure of the tidal-channel sandstone is dominated by stacked sets of trough cross-stratification;

individual sets are 0.1–1.0 m thick. Palaeocurrent data (Fig. 16) from localities 1 and 2 (Fig. 7) show south- and southeast-directed transport, but a minor component is directed towards the northwest. Measurements from locality 3 show a north-westerly directed mode, but a further broad component is directed southwards.

### Tidal sand-bar facies

#### Description

Tidal sand-bar deposits (Figs. 17, 18, 19) comprise fine- to medium-grained quartz sandstone, and occur in sharp-based tabular units 1–5 m thick (average 2 m). Individual units typically consist of a lower assemblage of trough and tabular cross-stratified sandstone which passes upwards into a ripple-laminated division 0.01–1.5 m thick.

Much of the lower portion of the sand-bar facies is dominated by 3–15 cm thick sets of trough cross-stratification. These exhibit high- or low-angle foresets with a generally low angle of climb. Many contain reactivation surfaces and pass laterally and vertically into lithotypes characterized by small-scale, planar-tabular cross-stratification or undulatory lamination. Palaeocurrent data from this division show a bipolar distribution (Fig. 19). At localities 1 and 2 (Wyloo Dome), troughed sets indicate transport towards the northwest and southeast, while tabular sets record a broad northward- or southward-directed flow (Figs 19 A, B). In the Turee Creek Syncline (locality 6) palaeocurrents are directed towards the west and east-northeast (Fig. 19E).

The upper ripple-laminated division is typically 0.05–0.2 m thick and is often capped by current-ripple or wave-ripple bedforms. Palaeocurrent directions from the current ripples differ from those in the underlying cross-stratified portion of the bar by 60–120° (Fig. 19C). Less commonly this upper division is up to 1.5 m thick and composed of sets of symmetric and asymmetric, ripple-laminated fine-grained sandstone, intercalated with 5–20

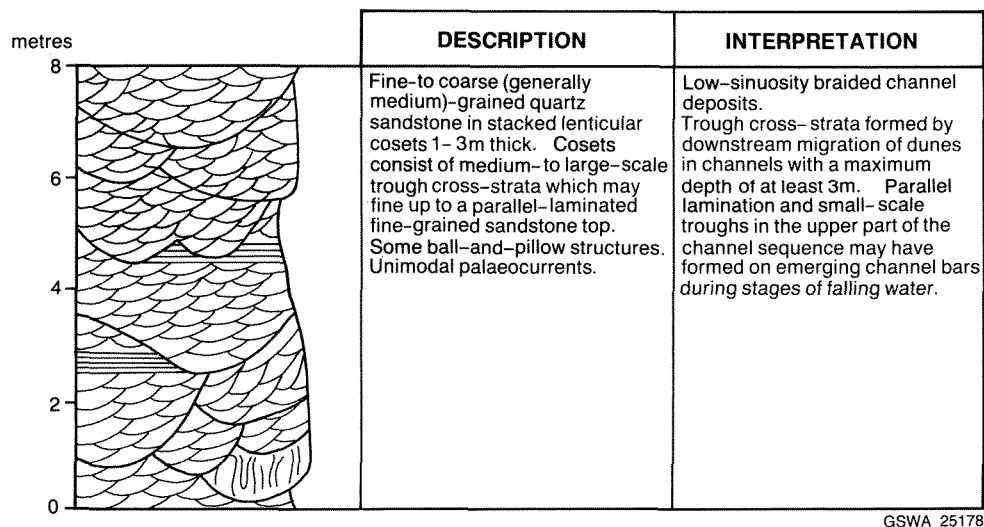


Figure 12 Schematic summary of rock types present in the delta-plain facies association.



GSWA 25179

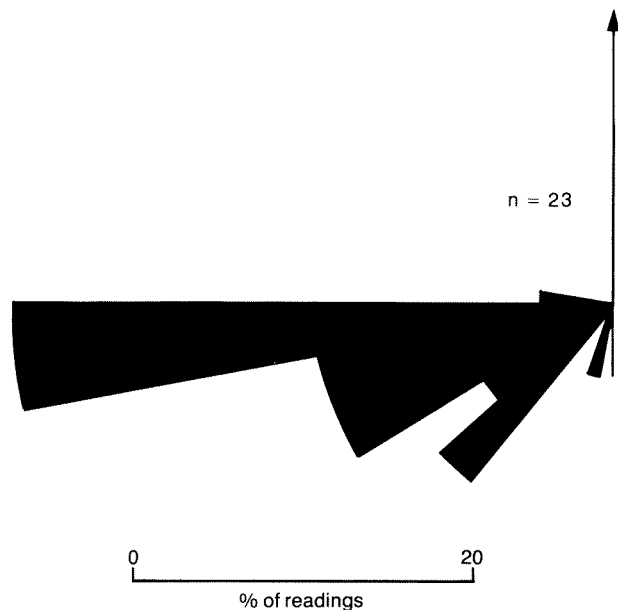
**Figure 13** Lenticular-bedded sets of trough cross-stratified, medium- to coarse-grained quartz sandstone; delta-plain facies association, locality 6.

mm thick mudstone layers and 50–100 mm thick beds of parallel-laminated sandstone. The latter are erosively based, and their upper surfaces may show evidence of wave and current reworking. Wave-ripple crests are oriented east-west near the Wyloo Dome (Fig. 19D).

## Interpretation

Sedimentary structures and palaeocurrent data, combined with the compositional maturity of the sandstone, suggest tidally influenced, shallow-marine sedimentation. Johnson (1975), summarizing the work of de Raaf and Boersma (1971), noted that the single most important criterion for recognition of tidal deposits is directional bimodality in both large-scale and small-scale cross-stratified units — a feature which characterizes this part of the Beasley River Quartzite. Other features, not diagnostic alone; nevertheless, abundant in tidal deposits, include:

- (a) Coupled arrangement of large-scale and small-scale bedded units.
- (b) Presence of fining-upward sequences in which the basal large-scale unit is generally channelled.
- (c) Discontinuity (reactivation) surfaces within unidirectional cross-stratified sets.
- (d) Various types of sand–mud alternations, e.g. lenticular or flaser bedding.



GSWA 25180

**Figure 14** Palaeocurrent data from the delta-plain facies association, locality 6.





GSWA 25181A

**Figure 15A** Major scour surface (arrowed) with downcut of about 3 m in tidal-channel facies. Channel units comprise lenticular-bedded medium- to coarse-grained quartz sandstone. Thin pebble lags are locally present above the basal scour, locality 2.



GSWA 25181B

**Figure 15B** Internal structure of tidal-channel facies showing superposed sets of medium-scale trough cross-strata, locality 1.

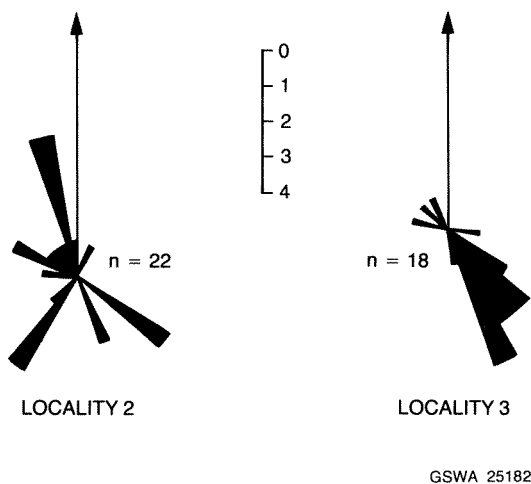


**Figure 16** Palaeocurrent data from the tidal-channel facies, localities 2 and 3.

All the above features occur in the tidal channel and tidal sand-bar facies association of the Beasley River Quartzite.

### Tidal channels

The following features are consistent with deposition in tidal channels: lenticular units with erosional lower boundaries; medium- to large-scale cross-stratification; rounding and compositional maturity of clasts; and presence of pebble lags. Palaeocurrent data indicate that the larger channels were principally ebb-dominated (by comparison with the transport direction on the subaerial fan). Smaller channels show a mixture of ebb- and flood-domi-

nated structures, and scattered palaeocurrent directions, typical of a migrating tidal channel system (Weimer et al., 1982).

### Tidal sand-bars

Trough and tabular cross-stratified sets are interpreted as the depositional record of dunes and small sand waves that formed in lower flow regime conditions, on tidal sand-bars. The complex internal organization of this facies reflects deposition in response to the velocity asymmetry of tidal currents (Klein, 1970a). Rounded upper set boundaries and reactivation surfaces formed as a result of the destructional phase of tidal-cycle reworking, whereas the bipolar palaeocurrent distribution suggests that deposition took place during both ebb and flood stages. Thin cappings of current-rippled sandstone overlying the complex cross-stratification show a quadrimodal palaeocurrent distribution, and were formed by late-stage run off, when flow directions were controlled by sand-bar topography (Klein, 1970a).

Thick cappings of wave- and current-rippled sandstone with interbedded mudstone and parallel-laminated sandstone are interpreted as tidal-flat deposits. Rippled sandstone records deposition during ebb and flood periods, whereas mudstone was deposited from suspension during periods of slack water. There is no conclusive evidence that the fine-grained sandstone-mudstone alternations were formed during a single tidal cycle (Klein, 1970b). Erosively based, parallel-laminated sandstones are interpreted as storm deposits. Similar lithotypes were described by Johnson (1975) from the Precambrian of northern Norway.

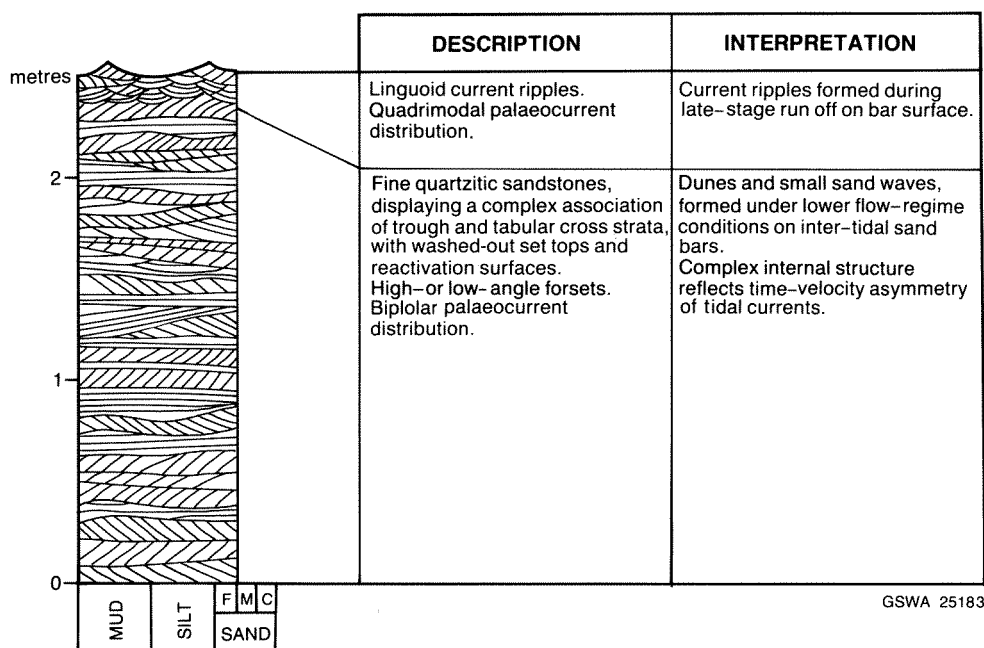


**Figure 17** Schematic profile showing internal structure of the tidal sand-bar facies, locality 2.



GSWA 25184A

**Figure 18A** Fine- to medium-grained quartz sandstone showing interlayered sets of planar-tabular cross-stratification, trough cross-stratification, and undulatory lamination. Tidal sand-bar facies, locality 2.

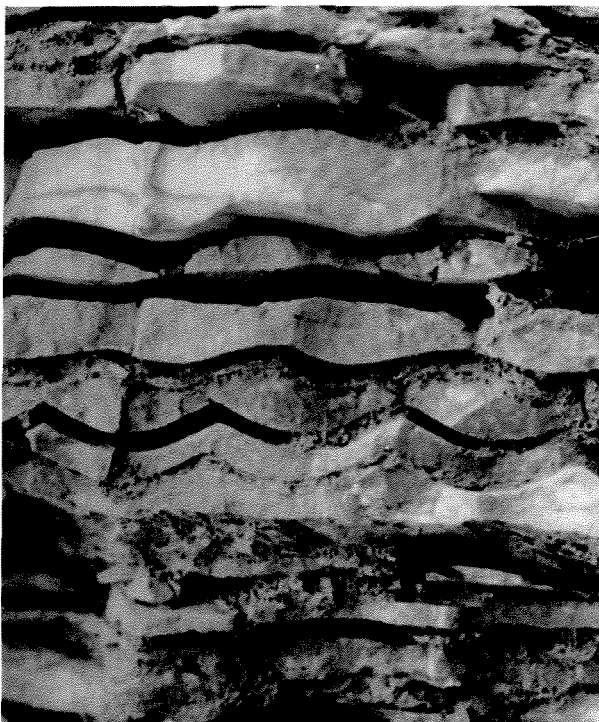
## Offshore-facies association

### Description

The offshore facies association consists of parallel-laminated mudstone and siltstone, intercalated with subordinate thin-bedded, parallel- or ripple-laminated fine-grained sandstone. North of the Wyloo Dome, this association includes dolomitic mudstone and dolomite; the latter is generally thin-bedded and parallel-laminated. Stromatolitic dolomite and quartz-bearing, cross-stratified dolomite were recorded 3–5 km east of Urandy Creek Outcamp (22° 116' 30''S, 116° 17' 00''E).

### Interpretation

Parallel-laminated mudstone and siltstone are interpreted as suspension deposits laid down in an offshore or prodelta setting (Elliott, 1986). Thin sandstones were probably deposited from turbidity currents during periods of increased terrigenous supply. Dolomitic mudstone and parallel-laminated dolomite were deposited under tranquil conditions during periods of limited terrigenous input. Cross-stratified, quartz-bearing dolomite formed during intervals when both current velocities and rates of siliciclastic supply were moderate to high.



GSWA 25184B

**Figure 18B** Symmetrical- and asymmetrical-wave ripples in interlayered (linsen-bedded) quartz sandstone, siltstone and mudstone. The finer grained lithologies have been partially removed by weathering. Tidal sand-bar facies, locality 1.

## Distribution of facies associations

The distribution of facies associations within the Beasley River Quartzite is summarized in Figure 20.



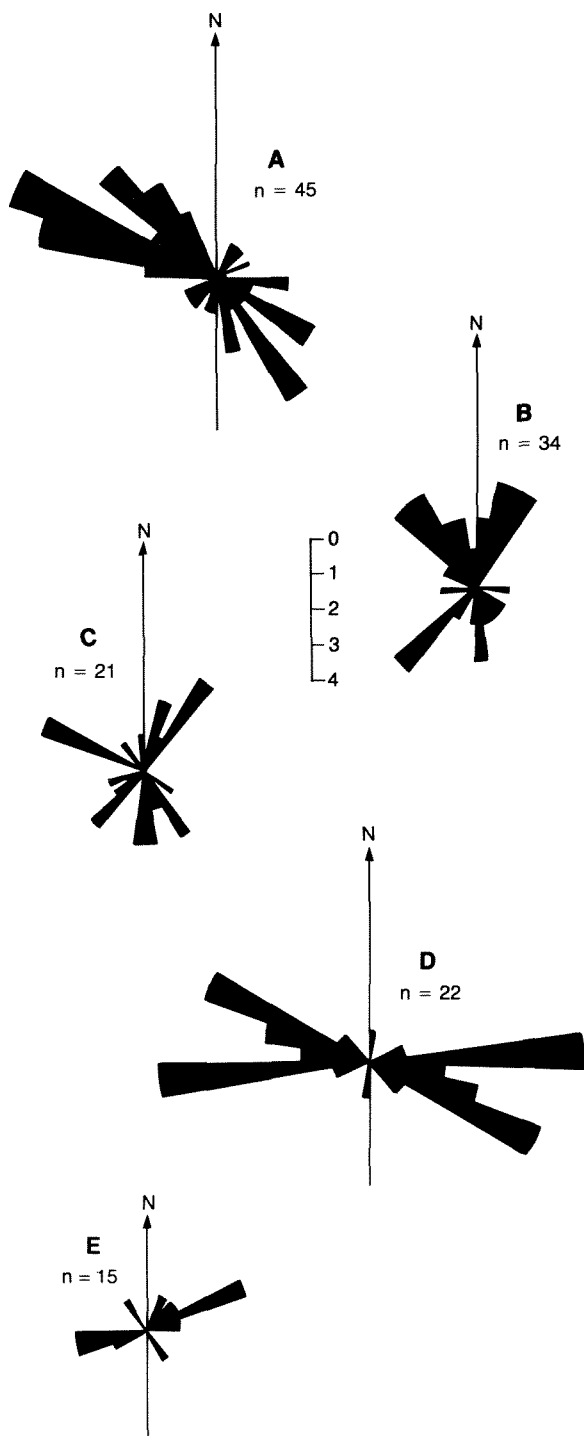


**Figure 19** Palaeocurrent data from the tidal sand-bar facies at localities 1, 2, and 6. A — Trough cross-strata. B — Tabular cross-strata. C — Current ripples. D — Wave ripple crests. E — Sand-bar facies trough cross-strata, locality 6.

Ten kilometres southwest of Deadman Hill ( $23^{\circ} 48' 00''\text{S}$ ,  $119^{\circ} 25' 00''\text{E}$ ), in the eastern Ashburton Basin, the Beasley River Quartzite is faulted against Weeli Wolli Formation (Hamersley Group). The Beasley River Quartzite has an estimated thickness of 300 m and comprises thin- to medium-bedded silicified quartz sandstone

(generally fine- to medium-grained). Internal structure consists of small- to medium-scale trough cross-stratification and undulatory lamination. The succession is assigned to the tidal-channel and sand-bar facies association.

Five kilometres southeast of Divide Well ( $23^{\circ} 28' 30''\text{S}$ ,  $118^{\circ} 28' 30''\text{E}$ ), on TUREE CREEK, the Beasley River Quartzite overlies Woongarra Volcanics and comprises 5–150 m of silicified, cross-stratified quartz-sandstone (delta-plain, and tidal-channel and sand-bar facies associations).

In the Turee Creek Syncline (Fig. 7, locality 6), the Beasley River Quartzite rests disconformably upon upper levels of the Turee Creek Group. At  $23^{\circ} 12' 30''\text{S}$ ,  $118^{\circ} 17' 00''\text{E}$ , the top of the Turee Creek Group consists of cross-stratified and ripple-laminated medium- to coarse-grained sandstone, interbedded with siltstone and mudstone. This succession, which is intruded by a 30 m thick dolerite sill near the unconformity, is interpreted as a shallow-marine shelf deposit.

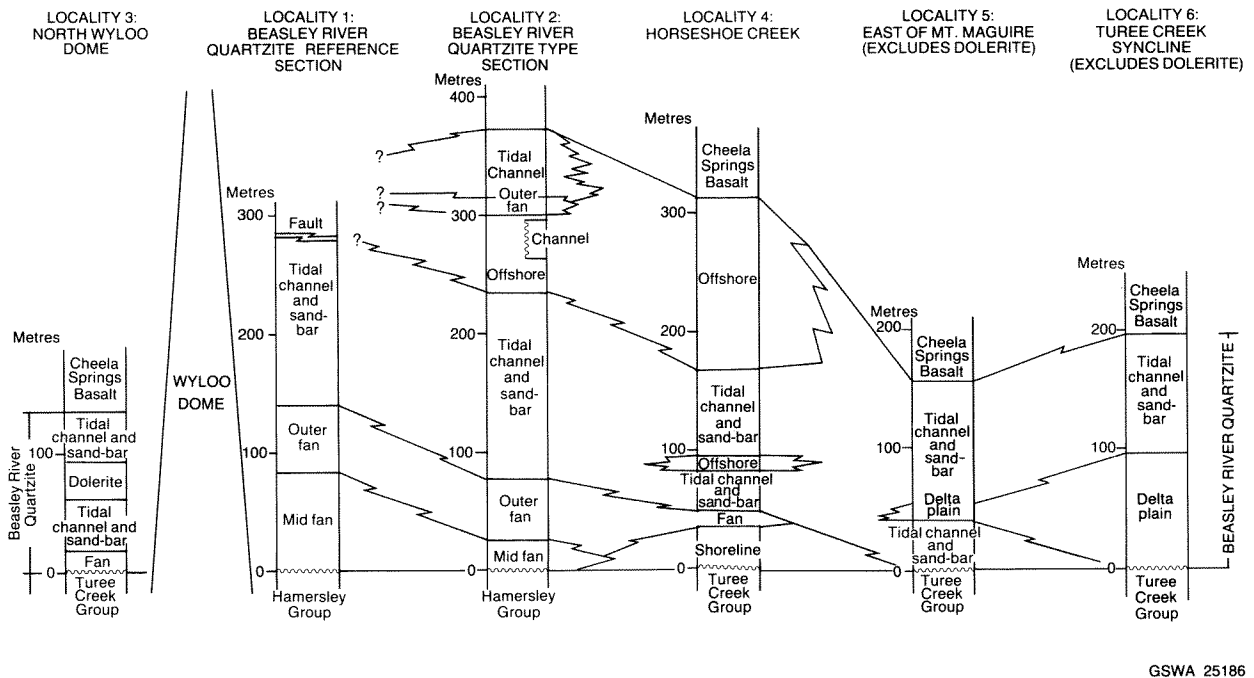
The overlying Beasley River Quartzite consists of 90 m of medium- to large-scale trough cross-stratified quartz sandstone (delta-plain facies association). The upper part of this unit is coarse grained (locally pebbly) and ferruginous. It is succeeded by a 40 m thick dolerite sill, which is in turn overlain by 100 m of thin- to thick-bedded silicified quartz sandstone. The internal structure of this quartz sandstone is dominated by small- to medium-scale trough cross-stratification, planar tabular cross-stratification, and undulatory lamination; it is assigned to the tidal-channel and sand-bar facies association. The Beasley River Quartzite is conformably overlain by Cheela Springs Basalt.

A fault-repeated Beasley River Quartzite succession is exposed for a strike length of 20 km to the southeast of Mount Maguire ( $23^{\circ} 20'\text{S}$ ,  $117^{\circ} 45'\text{E}$ ). At locality 5, the formation disconformably overlies 10–50 m of Turee Creek Group mudstone, siltstone and thin-bedded sandstone, and is conformably overlain by the Cheela Springs Basalt. It is 200 m thick, and comprises cross-stratified and undulatory-laminated quartz sandstone (tidal-channel and sand-bar facies association), with minor delta-plain deposits in the middle of the succession.

West of the Paraburdoo minesite, the Beasley River Quartzite is either unconformable upon, or faulted against, the Brockman Iron Formation and Weeli Wolli Formation of the Hamersley Group. The succession, which is generally less than 20 m thick, consists of silicified cross-stratified sandstone (tidal-channel and sand-bar facies association). It is disconformably overlain by the Mount McGrath Formation.

At Horseshoe Creek (locality 4), on the northern limb of the Hardey Syncline, the Beasley River Quartzite lies with angular unconformity upon the Turee Creek Group. The lower part of the formation comprises 25 m of parallel-stratified and cross-stratified quartz sandstone (tidal-channel and sand-bar facies association), overlain by 5–

GSWA 25185



GSWA 25186

**Figure 20** Generalized stratigraphic profiles through the Beasley River Quartzite showing interrelation of facies associations.

15 m of coarse-grained sandstone and BIF-derived conglomerate (outer-fan facies association). The conglomeratic unit is succeeded by two tidal-channel and sand-bar sandstone units that are separated by offshore siltstone and mudstone. Offshore deposits make up most of the upper 100 m of the formation. They are conformably overlain by the Cheela Springs Basalt.

In the vicinity of Wyloo Dome, the Beasley River Quartzite rests with angular unconformity upon the Fortescue, Hamersley, and Turee Creek Groups. The formation is thickest between localities 1 and 2, on the southeastern flank of the dome. Here, the lowermost 75–135 m of strata consists of BIF-derived, medium- to very thick-bedded conglomerate and sandstone (mid- and outer-fan facies associations). These are succeeded by up to 160 m of cross-stratified and ripple-laminated quartz sandstone (tidal-channel and sand-bar facies association), which are in turn overlain by 70 m of offshore facies. The remainder of the succession consists of 10 m of conglomerate and sandstone (outer-fan facies association), overlain by 30 m of trough cross-stratified quartz sandstone (tidal-channel and sand-bar facies association).

On the northeastern limb of Wyloo Dome (locality 3), the Beasley River Quartzite is 0–150 m thick and comprises 25 m of BIF-derived conglomerate (mid- and outer-fan facies association) overlain by 80–125 m of tidal-channel and sand-bar deposits. The upper part of the succession is transitional with the overlying Cheela Springs Basalt.

Widespread strike faulting in the area north of the Wyloo Dome makes it difficult to establish a reliable stratigraphy for the Beasley River Quartzite in this area. The formation apparently comprises an alternation of cross-stratified quartz sandstone and pebbly sandstone,

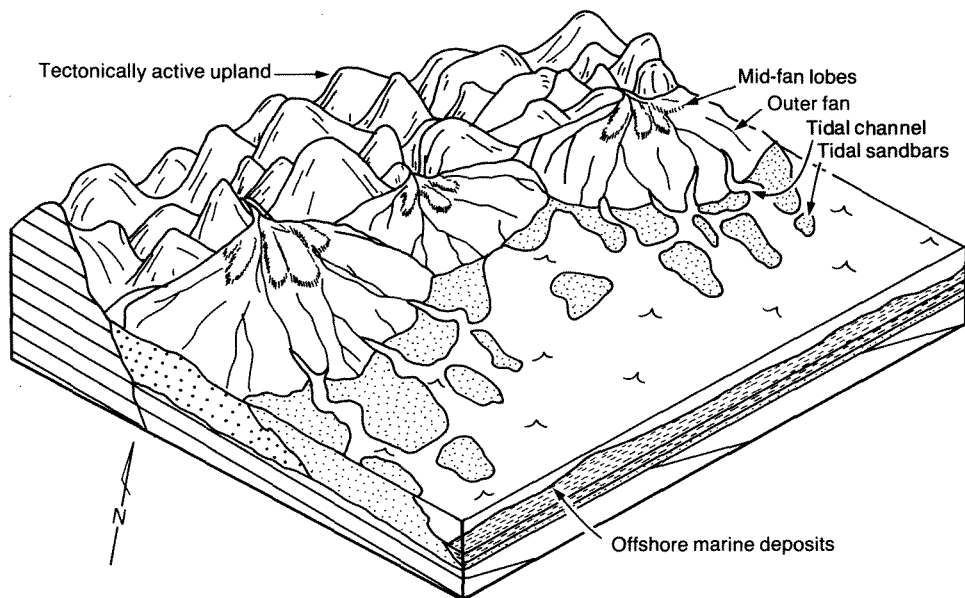
dolomite (locally cross-stratified and quartz bearing), siltstone, and mudstone. These lithologies are assigned to the outer-fan, tidal-channel and sand-bar, and offshore facies associations.

## Depositional model and palaeogeographic reconstruction

In the Wyloo Dome–Hardey Syncline, area deposition of the Beasley River Quartzite began after deformation and uplift of the Mount Bruce Supergroup. In this area the major controls on sedimentation were:

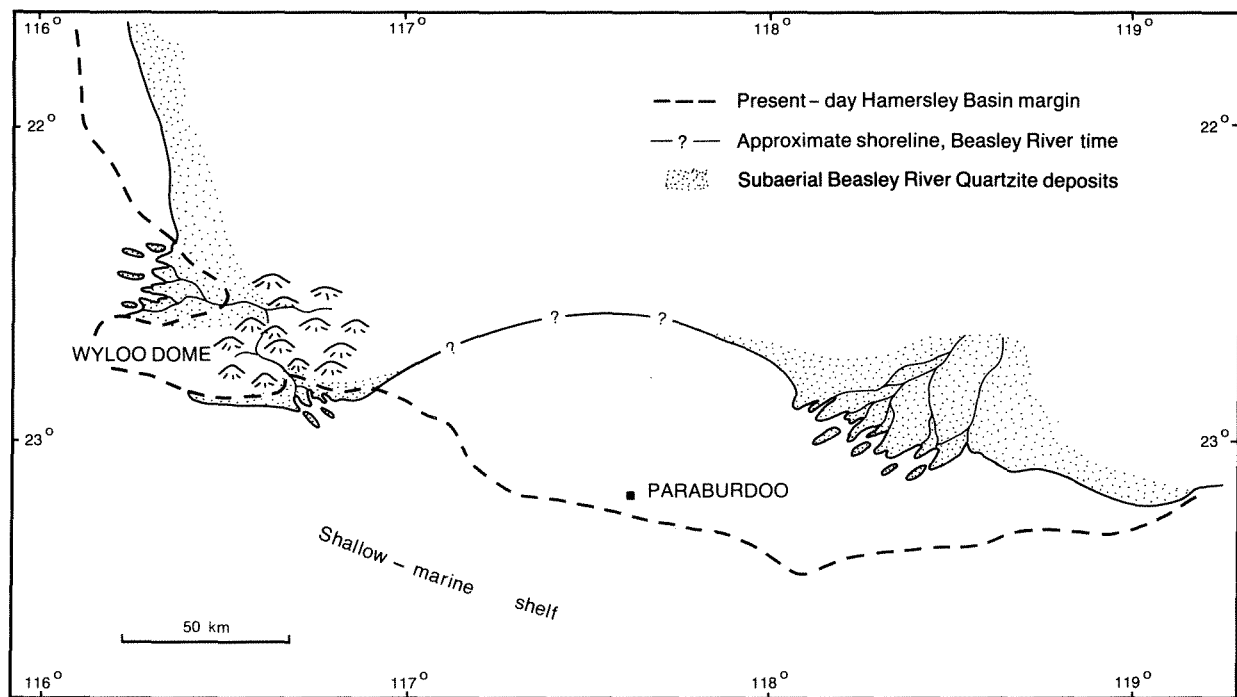
- A tectonically active upland of Hamersley and Turee Creek Group rocks adjacent to the eastern closure of Wyloo Dome (Fig. 21).
- A narrow coastal plain to the north and southeast of Wyloo Dome. The absence of extensive fluvial deposits in this area, coupled with a comparison of the dimensions of most modern alluvial fans suggests a 1–5 km wide coastal plain.
- A low wave-energy, tidally influenced marine shelf adjacent to the coastal plain.

Ephemeral streams emerging from the upland area built a complex of coalesced alluvial fans onto the coastal plain. Fan deposits were thickest southeast of Wyloo Dome, near locality 1. Here, debris flows were deposited close to the fan apex, whereas braided-stream sediments characterized mid to outer parts of the fan. More distal parts of the subaerial fan experienced longitudinal-bar formation during periods of storm-induced sheetflooding; some reworking of these deposits by coastal processes took place locally. Further still from the upland area, the coastline



GSWA 25187

**Figure 21** Model showing the principal depositional environments of the Beasley River Quartzite in the vicinity of the southeastern Wyloo Dome. Initial uplift in the source area resulted in rapid seaward progradation of the subaerial fan-delta. The period of shelf subsidence which followed was characterized by shoreline retreat and reworking of the subaerial fan by tidal marine processes.



GSWA 25188

**Figure 22** Palaeogeography of the southwestern Pilbara during deposition of the Beasley River Quartzite. The present-day positions of Wyloo Dome, Paraburadoo, and the southwestern margin of the Hamersley Basin are shown for reference. Tidal shallow-marine sedimentation prevailed over most of the northern Ashburton Basin. Quartz sand was introduced to the shelf by means of a tide-influenced delta system located near the present-day Turee Creek Syncline. Tectonic uplift and erosion in the extreme southwestern Hamersley Basin was responsible for coarse-grained fan-delta sedimentation in the Wyloo area.

was dominated by tidal channels and sand-bars, with deeper waters offshore.

Following the initial phase of coarse clastic input and fan growth, rates of coastal plain subsidence exceeded those of deposition, resulting in the advance of shoreline and offshore facies over the subaerial fan. This period of coastal retreat was terminated abruptly by a second phase of source-area uplift, fan growth, and shoreline migration, which controlled facies distributions until the close of Beasley River Quartzite deposition.

North of Wyloo Dome, a distal alluvial-fan complex built out onto a shallow-marine carbonate shelf. Here, fan-lobe switching resulted in a laterally variable stratigraphy of offshore dolomite and mudstone, interbedded with coastal and outer-fan sandstone and conglomerate.

Southeast of the Hardey Syncline, the disconformable contact between the Beasley River Quartzite and underlying rocks implies that pre-Wyloo Group tectonism was not as intense as in the Wyloo Dome–Hardey Syncline

area. In this area, quartzitic sediment was introduced from the northeast by streams of a braided-delta system (Fig. 22). At its maximum development, this complex extended to the southwest as far as Mount Maguire, where the sediment was reworked by tidal-marine processes. A subsequent waning of clastic supply resulted in the abandonment of the delta system, and a northeastward advance of coastal facies. During the height of this transgression, marine sedimentation extended at least as far northeast as the Turee Creek Syncline.

### Discussion

Near Wyloo Dome the distribution of facies points to the former presence of an alluvial fan system which built out directly into a marine environment. As a result, there was no development of extensive fluvial facies in this area.

Alluvial fans that prograde into a standing body of water are termed fan-deltas (McGowen, 1970). Rust (1979) has criticized the term fan-delta on the basis that these sediment bodies are allegedly dominated by terrestrial

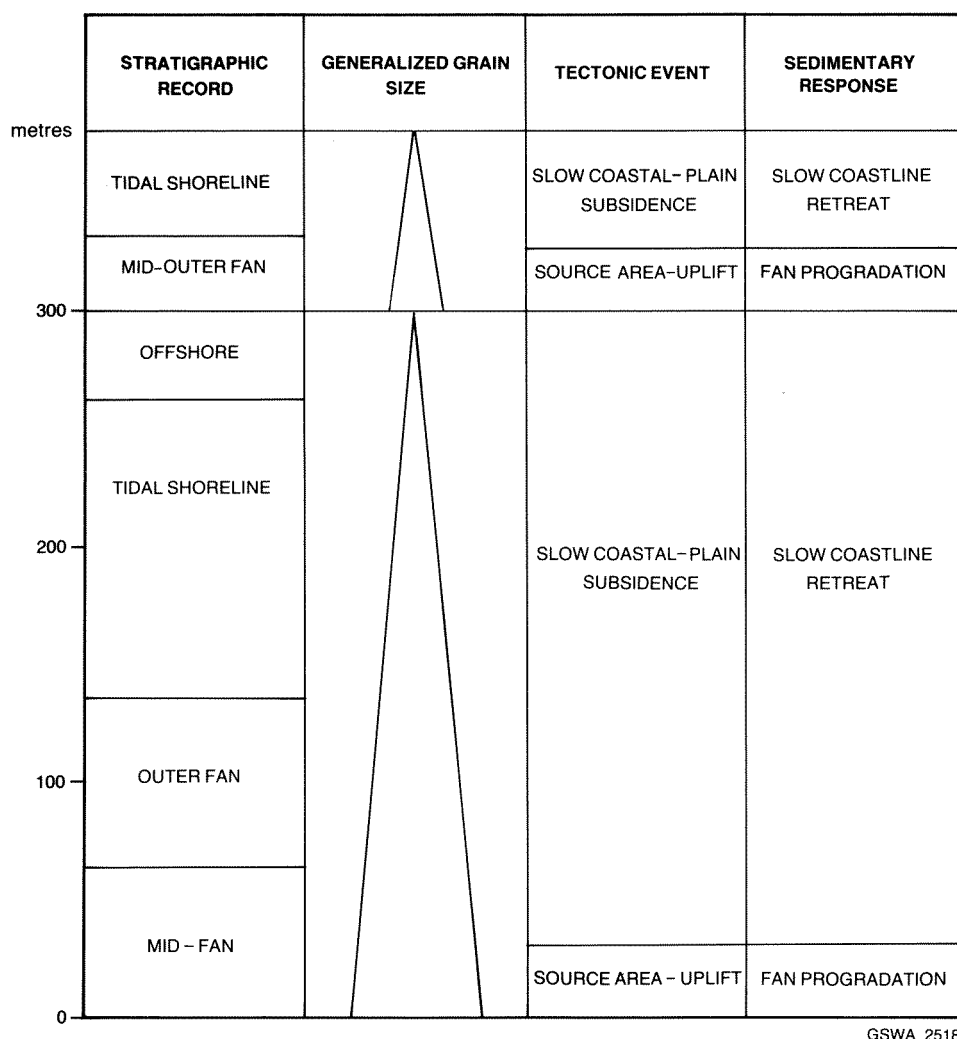


Figure 23 Summary of the depositional history of the Beasley River Quartzite in the eastern Wyloo Dome showing the relation between sedimentary facies and tectonism.

processes, and do not show a distinct separation at sea level between subaerial and subaqueous processes. This criticism could be directed at fans that prograde directly onto a steeply sloping shoreline. However, fans that build out onto a gently inclined marine shelf are characterized by distinct zones of alluvial and coastal sedimentation (Wescott and Ethridge, 1980). The Beasley River Quartzite fan-delta system is of this second type. The subaerial portion of the fan was dominated by streamflow, debris flow, and sheetflood processes, which resulted in deposition of texturally and mineralogically immature sediments composed of BIF, chert, feldspar, and quartz detritus. These alluvial lithotypes contrast with the fine quartzitic deposits of the shoreline fan, whose maturity reflects prolonged reworking by tidal and, to a lesser extent, wave processes.

Modern lobate fan-deltas, similar to those envisaged for the Beasley River Quartzite, are described from Lower Cook Inlet, Alaska (Hayes and Michel, 1982). These Holocene fan-deltas form in protected areas of low wave energy, and as a result show little beach or shoreface development. The paucity of beach and shoreface deposits in the Beasley River Quartzite suggests that the fan-delta system immediately north and east of Wyloo Dome also developed in a setting that was at least partly protected from wave action. It is likely that some shelter could have been provided by an upland area now occupied by the Wyloo Dome. When the effects of post-Wyloo Group strike-slip faulting are taken into account, this structure would have been located 11 km southeast of its present position (Chapter 9).

The central role played by tectonism in development

of Holocene fan-deltas is widely recognized (Wescott and Ethridge, 1980). Synsedimentary tectonism near Wyloo Dome was also a major influence on the depositional history of the Beasley River Quartzite. Here, the succession (summarized in Fig. 23) records two periods of tectonically induced sedimentation. Each incorporates a phase of source-area uplift and fan growth, followed by a longer interval of tectonic quiescence (characterized by tidal-shoreline sedimentation). Fan-delta lobe switching, which could have produced a similar sedimentary record locally, is not considered a likely mechanism to explain the observed facies relationships, since the entire fan system was affected by the same pulses in sedimentation.

Palaeocurrent data and facies distribution indicate that the eastern Wyloo Dome and adjacent part of the Hamersley Basin were tectonically active, and were the major source of detritus for the southwestern part of the Ashburton Basin. This view contrasts with the interpretation of Horwitz (1981, 1982) who invoked a source area to the south of the present-day outcrop.

Tidal-channel and tidal sand-bar deposits form an important part of the Beasley River Quartzite succession. Klein (1971) has shown how the thickness of a prograding tidal-flat sequence can be used to determine palaeotidal range. The possible sources of error in this method were, however, noted by Klein (1971), and relate to the effects of subsidence, erosion, and compaction. When these limitations are combined with the fact that it is difficult to distinguish low tidal-flat deposits from those of migrating tidal channels, it becomes impossible to provide a reliable estimate of palaeotidal range during Beasley River Quartzite deposition.



## Chapter Three

# Cheela Springs Basalt and Woolly Dolomite

## Cheela Springs Basalt

The Cheela Springs Basalt, previously regarded as a member within the Mount McGrath Formation (MacLeod et al., 1963), was elevated to formation status by Horwitz (1980). Throughout most of the Ashburton Basin, the Cheela Springs Basalt conformably overlies the Beasley River Quartzite, except on the southern margin of Wyloo Dome where it rests disconformably upon the Mount Bruce Supergroup.

### Description

The formation has a maximum thickness of 2 km and comprises basalt flows with subordinate fine- to coarse-grained tuff, immature sandstone, siltstone, and mudstone. Dolerite sills are abundant.

Basalt flows are generally vesicular and range from 0.5 m to 35 m thick. Two examples of thick (25 m and 35 m) flows are well exposed on the northern limb of Wyloo Dome at 22° 31' 30"S, 116° 46' 00"E. The lowermost of these (Fig. 24) immediately overlies the top of the Beasley River Quartzite, although the lowest 4 m of the flow is not exposed. The flow is medium grained in the middle, but grain size decreases, and vesicularity increases in the uppermost 8 m of section (Fig. 25). The top of the flow is irregular and pitted; the hollows are filled with fine-grained, ripple-laminated tuff. Straight-crested, symmetrical ripples — interpreted as wave ripples — are preserved on the upper surface of the tuff.

Twenty metres of mudstone and ripple-laminated siltstone and fine-grained sandstone separate the lower basalt from the thicker, overlying flow. The lower part of this flow is medium grained, but it grades upwards into a fine-grained vesicular top. It is overlain by 20 m of trough cross-stratified, fine- to very coarse-grained, ferruginous sandstone and thin basalt.

Most basalt has undergone pervasive prehnite–pumpellyite to lower greenschist facies metamorphism. In areas of low metamorphic grade, such as north of Wyloo Dome, these rocks comprise phenocrysts of andesine and clinopyroxene (partly replaced by actinolite and chlorite) set in a groundmass of andesine, actinolite, chlorite, sphene, epidote, pumpellyite, and iron oxide. At higher metamorphic grades, the clinopyroxene is completely replaced by actinolite and chlorite.

There are many dolerite sills up to 50 m thick within the formation; they consist of andesine, actinolite, chlorite, epidote, iron oxide and quartz, and show an intergranular or subophitic texture.

Sedimentary rocks — mainly immature sandstone, siltstone, and mudstone — are locally abundant, especially in the lower part of the formation. Above the lowermost basalts, west of the Hardey Syncline, (22° 47' 10"S, 116° 43' 00"E) there is a 50 m thick, upward-coarsening sequence of mudstone and siltstone, overlain by ripple-laminated fine-grained sandstone, and trough cross-stratified, ferruginous sandstone. Southeast of Wyloo Dome, 22° 50' S, 116° 43'E) upper beds of the Cheela Springs Basalt, composed of basalt, basaltic tuff, and chert, are interbedded with dolomitic mudstone. The latter become dominant upwards and there is a transitional contact with the overlying Woolly Dolomite.

### Interpretation

It has not been possible to deduce the depositional environment of the Cheela Springs Basalt on the basis of basalt flow morphology alone. Markedly vesicular basalt flows form in subaerial conditions, and in water less than 200 m deep (Williams and McBirney, 1979; Hughes, 1982). Pahoehoe flows, similar to those occurring in the Cheela Springs Basalt, are often erupted on land, but may also form in water deeper than 3–4 km, provided that the depositional slope is not so great that it leads to pillow formation (Williams and McBirney, 1979).

The most reliable indicators of the depositional environment of the Cheela Springs Basalt are sedimentary rocks interbedded with the volcanics, and the nature of the underlying and overlying formations.

North of Wyloo Dome, (22° 31' 30"S, 116° 26' 30"E) a 25 m thick basalt flow overlies tidal shoreline deposits of the Beasley River Quartzite (Fig. 25). Taking into account the probable gentle gradient of the coast (*see* discussion, Chapter 2) and the thickness of the flow, it is likely that the top of the basalt, at least, would have been exposed subaerially at the time of extrusion. The local stratigraphy indicates that a relative rise in sea level resulted in the flow top being eroded in the surf zone and subsequently buried by low-energy offshore sediments. The succeeding 35 m thick basalt is capped by immature fluvial sandstones, indicating that maximum water depths in this area were probably less than 35 m during deposition of the lower Cheela Springs Basalt.



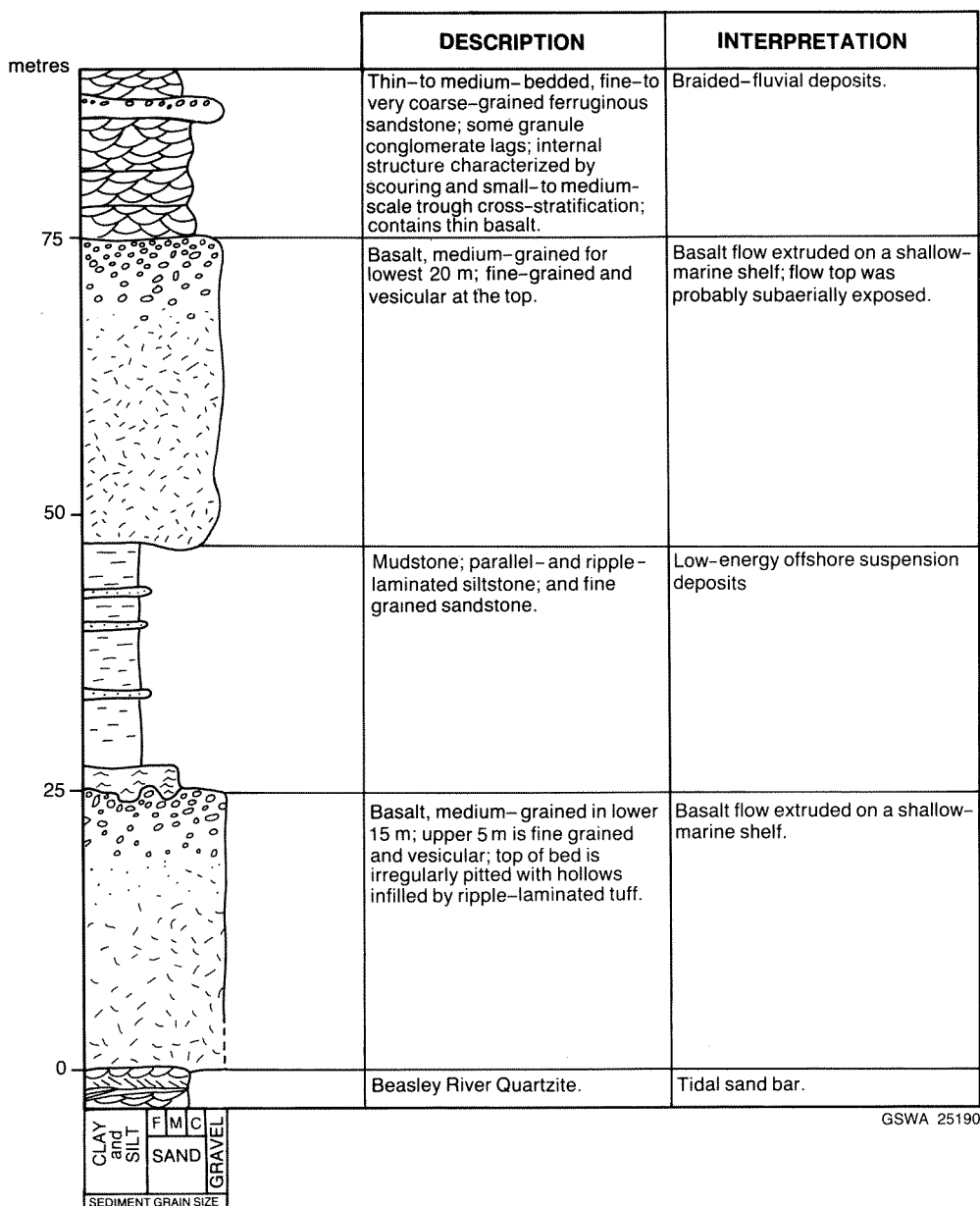


**Figure 24 Stratigraphy of the lower part of the Cheela Springs Basalt on the northeastern flank of Wyloo Dome.**

A similar depositional setting is proposed for the lower part of the formation west of the Hardey syncline. Basalts between the Beasley River Quartzite and the overlying upward-coarsening sedimentary sequence (interpreted as deltaic) probably flowed into marine water with a maximum depth of about 50 m. Flows immediately above the fluvial facies at the top of this sequence are also likely to have formed in a subaerial environment.

On the southern limb of Wyloo Dome, the uppermost beds of the Cheela Springs Basalt are transitional with shallow-marine shelf carbonates of the Woolly Dolomite. North of Wyloo Dome, the volcanic succession is conformably overlain by deltaic and shallow-marine siliciclastic deposits of the Mount McGrath Formation. This evidence suggests that, at least in the northwestern part of the Ashburton Basin, the upper beds of the Cheela

Springs Basalt were also laid down in a coastal to shallow-marine setting.

It may, therefore, be concluded that the Cheela Springs Basalt was probably laid down in a coastal to shallow-marine setting. The predominance of pahoehoe, flows as opposed to pillow lava, suggests a marine shelf of low gradient.

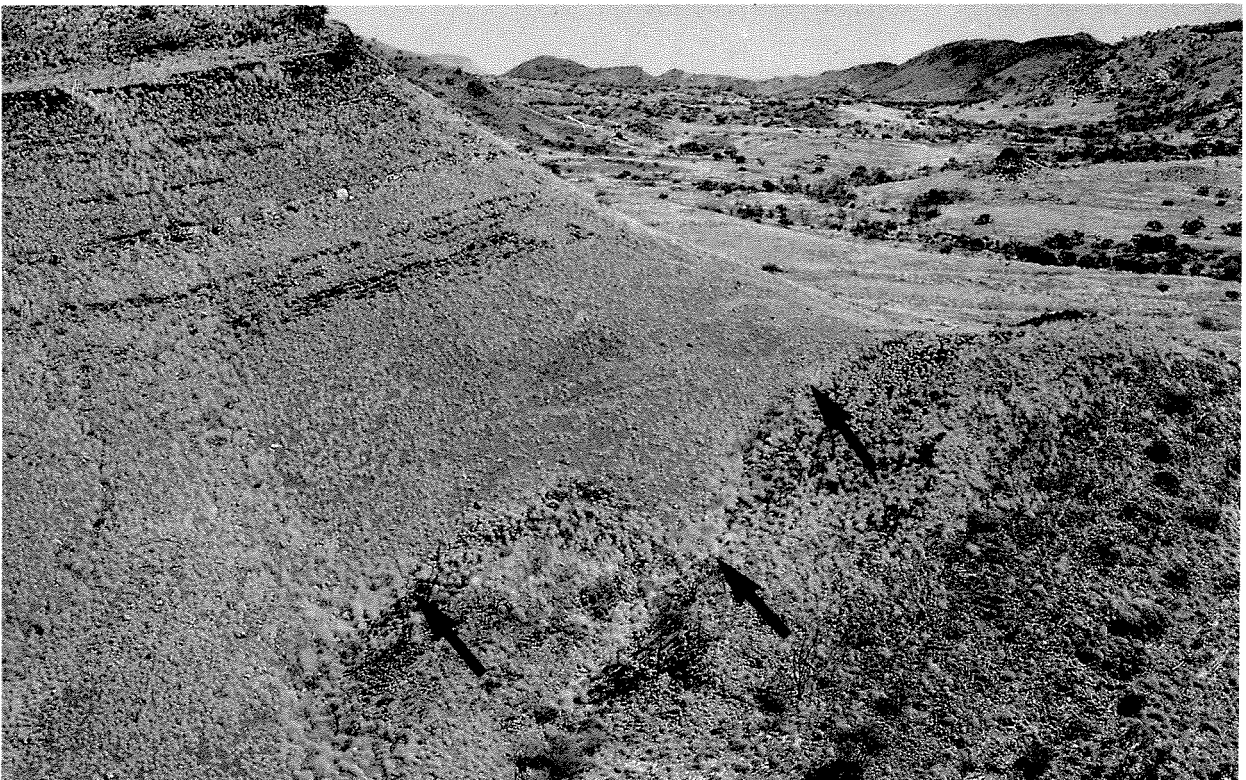
### Volcanic centres

Neither feeder pipes nor volcanic centres have been recognized within the Cheela Springs Basalt. However, a possible feeder conduit, now isolated from the main body of the formation, occurs northeast of Wyloo Dome (22° 23' 30"S, 116° 30' 00E). Here, coarse basaltic agglomerate, basalt and a gabbro dyke occur in a 5 km by 1 km fault-bounded outlier within the Brockman Iron Forma-



GSWA 25191

**Figure 25** Irregular vesicles in a fine-grained basalt flow top, Cheela Springs Basalt, northeastern Wyloo Dome.



GSWA 25192

**Figure 26** Part of the contact between the Woolly Dolomite and the overlying Mount McGrath Formation, southern Wyloo Dome. The upper surface of the dolomite (arrowed) is ferruginous and irregular, with a local relief of up to 10 m. Delta-front mudstone, siltstone and sandstone form a large-scale upward thickening and coarsening sequence in the lower part of the Mount McGrath Formation.

**TABLE 1 STRATIGRAPHY OF WOOLY DOLOMITE**  
(Between 22°47'00"S, 116°25'00"E and 22°47'50"S, 116°28'21"E)

Height above base (m)	Lithology	Interpretation
<b>MOUNT McGRATH FORMATION</b>		
325	----- Unconformity ----- Medium- to thick-bedded, finely to coarsely crystalline dolomite, locally stromatolitic, with asymmetric columnar forms. A few quartzitic, starved current-ripples in the thin-bedded, parallel-laminated horizons. Thick-bedded, parallel-laminated horizons. Thick-bedded, structureless or low-angle intraclastic dolomites occur at the top	Predominantly high-energy shallow marine deposits that received little terrigenous clastic input
125	Very thin-bedded, parallel-laminated, finely crystalline dolomites and dolomitic mudstones, interbedded with a few thin chert beds	Shelf sediments deposited below storm wave base in an area of low terrigenous clastic input
70	Thick, erosively based lenticular 5-50 cm beds of trough cross-stratified, quartzitic, sandy-pebbly dolomite, thin current-ripple-laminated quartzitic dolomite, and stromatolitic dolomite. The latter beds are up to 20 m thick and contain large domical stromatolites and some columnar forms.  The lowermost cross-stratified pebbly dolomite includes fragments of red chert derived from the underlying Cheela Springs Basalt	Moderate to high-energy shoreline deposits laid down in an area that received an intermittent terrigenous clastic supply
0	----- Conformable contact -----	
<b>CHEELA SPRINGS BASALT</b>		

tion (Hamersley Group). These mafic rocks were mapped as Fortescue Group by Daniels (1970). As the enclosing iron-formation dips steeply towards the basaltic complex, it is unlikely to be a faulted inlier of Fortescue Group. It is also difficult to envisage it being a 3 km high ridge of Fortescue Group volcanics that acted as a topographic high throughout most of Hamersley Group deposition, cf. Daniels (1970). Apart from the Cheela Springs Basalt, the only other mafic volcanic unit in this part of the Ashburton Basin is the June Hill Volcanics, whose eruptive centre lies 30 km to the west of the outlier (Chapter 5). From this, largely negative evidence, it seems possible that the outlier represents a feeder conduit for the Cheela Springs Basalt.

### Wooly Dolomite

The Wooly Dolomite is confined to the southern margin of Wyloo Dome, where it crops out over a strike

length of 30 km. This unit attains a maximum thickness of 325 m; it was mapped, though not named, by Daniels (1970) as part of the Turee Creek Formation (now obsolete). Seymour et al. (1988) raised the dolomite to formation status because it forms a distinct lithological unit conformably overlying the Cheela Springs Basalt, and is unconformably overlain by the Mount McGrath Formation.

The lowermost 70 m of the formation (Table 1), comprises small- to medium-scale cross-stratified dolomite and stromatolitic dolomite, and is interpreted as a moderate- to high-energy shoreline sequence. It is overlain by 55 m of quiet-water shelf carbonates, which are succeeded by 200 m of moderate-to high- energy shelf dolomites. The top of the Wooly Dolomite is well exposed at 22° 48' 07"S, 116° 28' 21"E. At this locality (Fig. 26), a patchy ferruginous horizon caps the irregular upper surface of the dolomite.

## Chapter Four

# Mount McGrath Formation

The Mount McGrath Formation was subdivided by de la Hunty (1965) and later redefined by Horwitz (1980) as “the essentially clastic rocks that overlie unconformably the Cheela Springs Basalt and overlap unconformably onto older formations. It is overlain conformably by the Duck Creek Dolomite, which itself overlaps onto older units.” This definition is followed, with the qualification that along the southeastern margin of Wyloo Dome, the Mount McGrath Formation unconformably overlies the Woolly Dolomite. The formation has a maximum thickness of at least 1200 m but thins to zero around the western margin of Wyloo Dome.

This chapter describes and interprets the major facies associations of the Mount McGrath Formation. Most of the information was obtained from four measured sections (located on Fig. 27), and from 1:40 000-scale mapping of adjacent outcrops.

The formation comprises ferruginous conglomerate and sandstone, quartz sandstone, siltstone, mudstone, and locally developed carbonate. Two major facies associations are recognized: delta-plain and delta-front (including offshore shelf).

### Delta-plain facies association

The delta-plain facies association comprises distributary channel and interdistributary-bay facies. Much of this association is composed of ferruginous conglomerate and sandstone, derived principally from the Mount Bruce Supergroup, with a smaller contribution from the lower Wyloo Group (generally the Beasley River Quartzite). The clasts are mainly of BIF (with hematite ore locally), vein-quartz, chert, quartz amygdals, and felsic igneous rock.

### Distributary-channel facies

#### Description

The distributary-channel facies (Figs. 28, 29) consists of thin- to very thick-bedded (0.05–4 m), clast-supported conglomerate, pebbly sandstone, fine- to coarse-grained sandstone, and minor siltstone and mudstone. These lithotypes are grouped into vertical sequences 4–30 m thick, which may extend laterally for several kilometres.

Sequences are characterized by sharp, erosive bases and sharp or transitional upper contacts.

Clast-supported conglomerate occurs in lenticular or tabular beds up to 4 m thick. Most exhibits parallel or very gently inclined stratification, with inverse or, less commonly, normal grading. Some thick-bedded conglomerates are structureless. Clasts are generally poorly sorted (4–60 mm), equant to bladed, and angular to well-rounded.

Pebbly sandstone crops out in lenticular units up to 8 m thick. Beds are either massive, parallel-stratified, or trough cross-stratified (sets 0.1–0.3 m thick). Pebbles are generally equant, 4–20 mm in diameter, and consist chiefly of vein-quartz, chert, and quartz amygdals. The poorly sorted matrix is ferruginous lithic arenite or wacke.

Trough cross-stratified and parallel-stratified, medium- to very coarse-grained sandstones occur in units up to 20 m thick. Trough cross-stratified sandstones are the most abundant lithotype. They occur as isolated sets, or are stacked to form thick cosets up to 40 m wide and with a maximum downcut of 3 m. Individual sets are 0.05–0.5 m (generally 0.1–0.25 m) thick. Both set and coset boundaries may be marked by a gravel lag. Palaeocurrent data (Fig. 29) indicate that sediment transport was towards the south and southwest at localities 2, 3, 5, and 6; and towards the west and southeast at locality 4.

Ferruginous siltstones and mudstones outcrop in lenticular or tabular beds up to 2.5 m thick. Siltstones are parallel-laminated or ripple cross-laminated.

Examples of distributary channel sequences are shown in Figure 30. Conglomeratic channel profiles (Fig. 30A) show little systematic variation in grain size or bed thickness. They consist generally of thin- to thick-bedded conglomerate alternating with minor sandstone and pebbly sandstone. Channel sequences which contain a high proportion (20–90%) of sandstone in addition to conglomerate are usually more structured (Fig. 30B). These units, which are often characterized by an overall upward-coarsening grain-size trend, incorporate small, upward-fining sequences of conglomerate or pebbly sandstone overlain by sandstone, siltstone, and mudstone.

#### Interpretation

The conglomerate and sandstone are interpreted as braided-fluvial deposits on the basis of the following

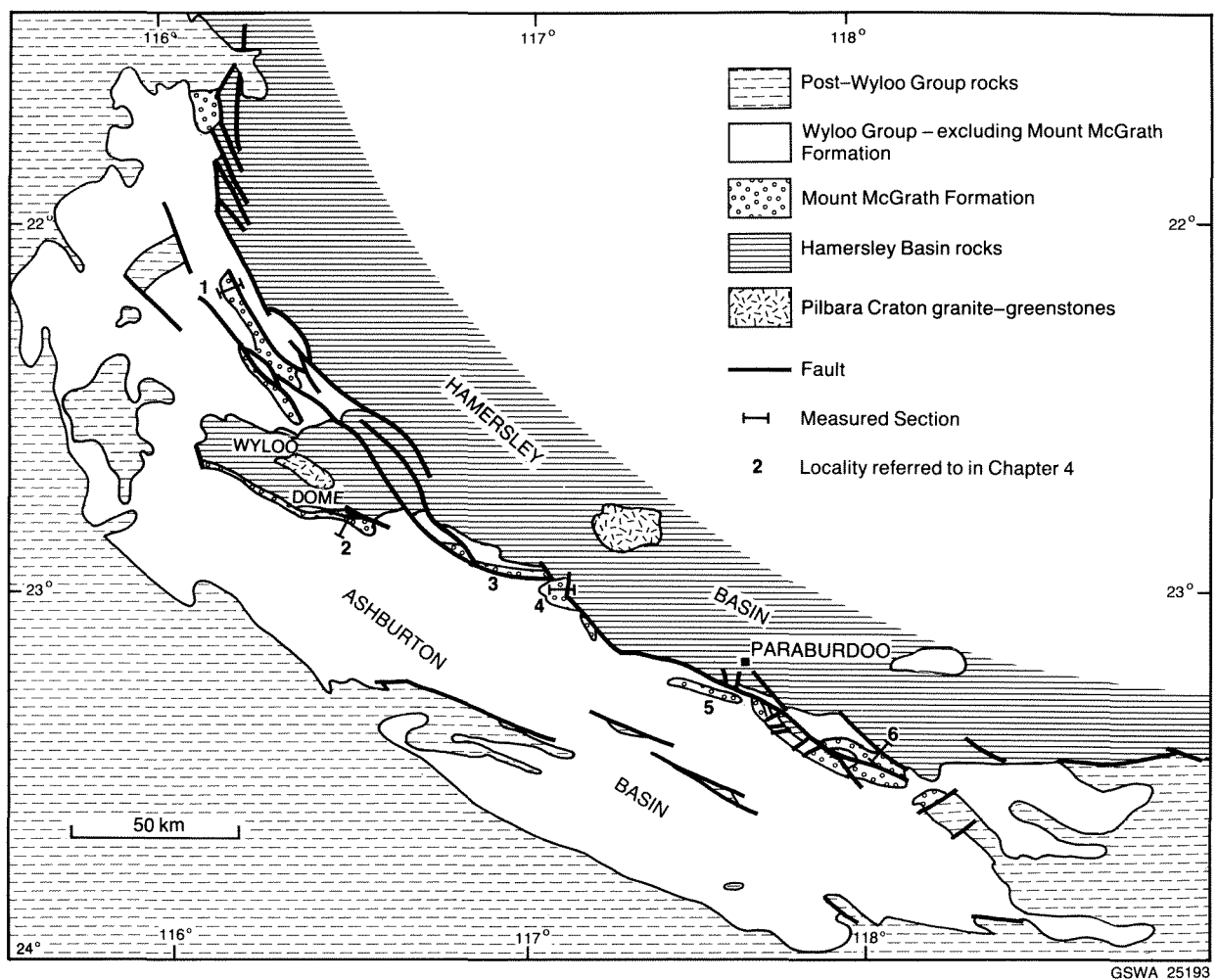


Figure 27 Mount McGrath Formation, outcrop and location of measured sections.

characteristics: occurrence in lenticular or tabular units with sharp, erosive bases; nature of internal structure; unidirectional palaeocurrent data; compositional and textural immaturity; and sequence organization.

The conglomerate units within the Mount McGrath Formation are closely similar to deposits of modern proximal braided rivers (reviewed by Miall, 1977, 1978; Collinson, 1978 a,b; Cant, 1982;). In this environment, the principal sites of sediment accumulation are diffuse gravel sheets and complex braid bars within channels; both settings are characterized by horizontally stratified, clast-supported gravel. Hein and Walker (1977) note that diffuse gravel sheets predominate in the upstream reaches of the Kicking Horse River, British Columbia; whereas various braid bars (e.g. longitudinal, diagonal and transverse) are better developed downstream. Within the gravel sheets, horizontal stratification reflects the mechanism of bed-load transport by which the coarsest gravel moves as layers, one or two pebble diameters in thickness at times of peak discharge. Hein and Walker (1977) postulate that longitudinal and transverse bars evolve from a gravel-sheet core, and that the development of horizontal stratification results from the downstream growth of the bar under conditions of high fluid and sediment discharge.

The small (0.5–4 m thick), upward-coarsening conglomerate units in the Mount McGrath Formation are thought to result from downstream migration of coarse bar-head gravel over finer bar-tail detritus. Such a mechanism has been used to explain inverse grading in Triassic braided stream conglomerates of Staffordshire, United Kingdom (Steel and Thompson, 1983). Rare, upward-fining conglomerate beds probably represent bar deposits which developed from a coarse gravel sheet and grew upwards by the addition of finer grained material as discharge waned.

Trough cross-stratified sandstone and pebbly sandstone are attributed to downstream migration of small-to medium-sized dunes (Harms and others, 1982) in a braided-fluvial channel. Parallel-stratified sandstones, interbedded with the trough sets, were probably deposited during the falling-water stage, when transitional to upper flow regime conditions prevailed (Miall, 1977).

Small upward-fining sequences of conglomerate and sandstone reflect the development of bars within the braided channels. Horizontally bedded conglomerate at the base of the sequence represents the lower part of the channel fill, while the overlying troughed, or horizontally





**Figure 28A** Lenticular-bedded, conglomerate and massive sandstone (dark- and light-coloured rock types respectively in lower half of photograph) overlain by parallel-stratified sandstone. Distributary-channel facies, Mount McGrath Formation, locality 3.

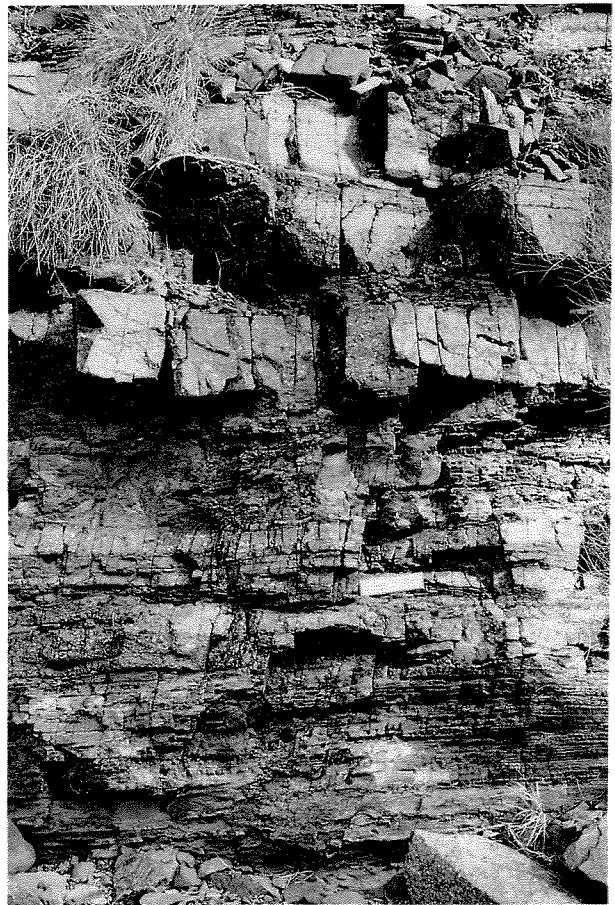


**Figure 28B** Parallel-laminated siltstone and sandstone interlayered with tabular-bedded conglomerate. Interdistributary-bay facies, Mount McGrath Formation, locality 3.



**Figure 28C** Parallel stratification and low-angle scour surfaces in pebbly sandstone. Light-coloured clasts, chiefly vein quartz, chert, and quartz amygdalae, are set in a matrix of coarse-grained ferruginous sandstone. Distributary-channel facies, Mount McGrath Formation, locality 3.

GSWA 25194

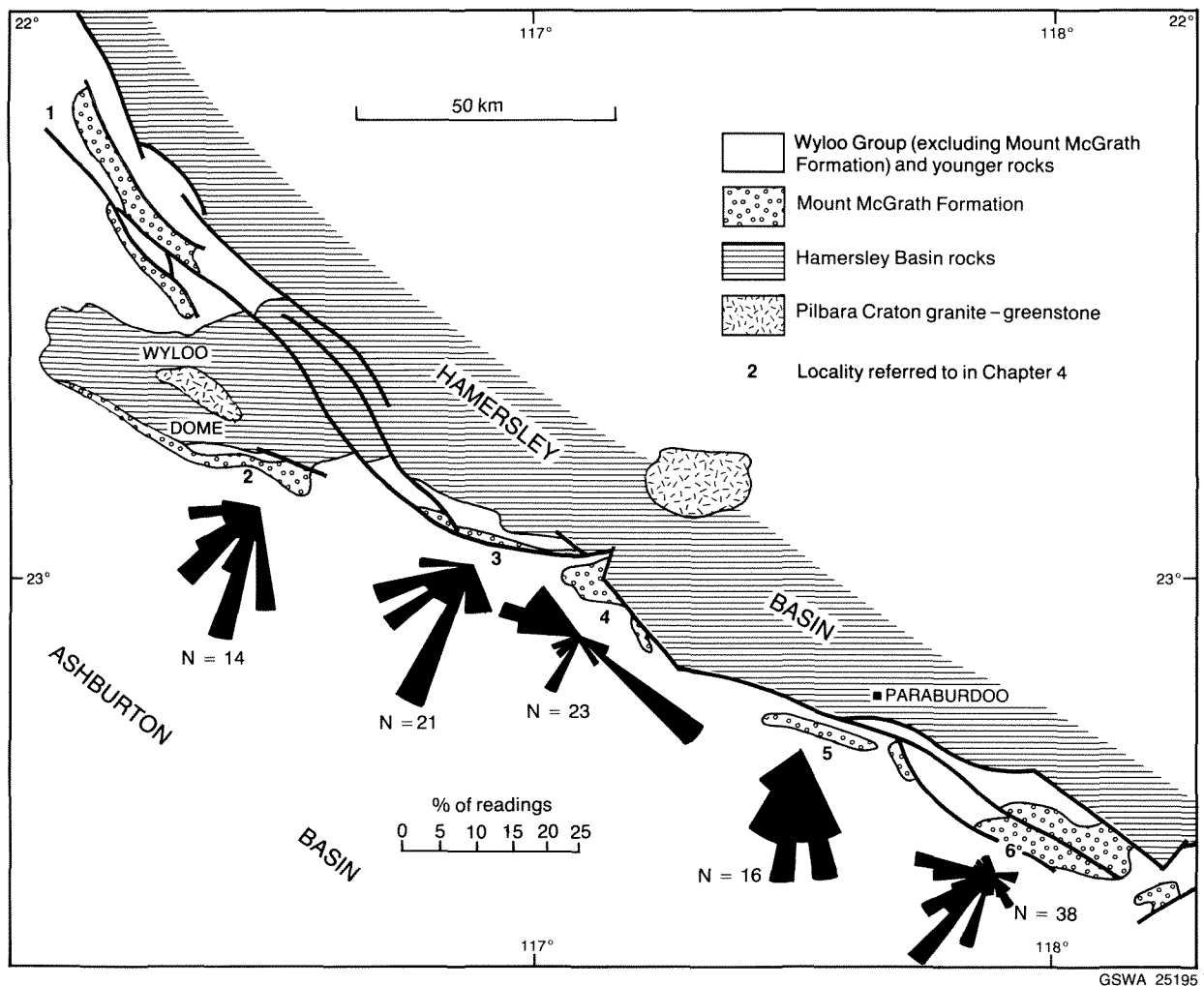


**Figure 29** Distributary-channel facies palaeocurrent data (from trough cross-strata), Mount McGrath Formation, localities 3 and 4.

stratified sandstones are interpreted as upper channel and bar-top deposits (Cant, 1982). Thin siltstones and mudstones, which occur locally at the top of these sequences, were probably deposited on inactive parts of the bar top during the falling-water stage.

Miall (1978) recognized six main types of braided-fluvial deposit. The Scott model was erected for non-cyclic, proximal braided-stream deposits in which the predominant lithotype is horizontally stratified gravel with only minor sand. The conglomeratic channel sequences in the Mount McGrath Formation are similar to this model in terms of sediment type, bed structure, and over-all sequence organization. The most notable difference occurs with respect to sediment grain-size: the conglomerate units described here are generally finer grained (pebble sized) than the cobble gravels which characterize Scott-type rivers. While this may result partly from differences in the size of the source material, it is thought more likely that the smaller clasts reflect deposition in a slightly more distal setting than is normally equated with the Scott model.

Mixed sandstone and conglomerate sequences (Fig. 30B) compare with Miall's (1978) Donjek model for

braided-fluvial deposits. Here, the crude vertical repetition of lithotypes is due to repeated stacking of channel and bar deposits, whereas incomplete sequences result from a combination of erosion and non-deposition. Possible causes of this cyclicity, e.g. channel switching, are discussed by Miall (1977).

Miall (1978) suggested that transition from Scott to Donjek style of deposition may reflect a downstream decrease in the ratio of gravel to sand. On this basis, the 10–30 m thick upward-coarsening and upward-thickening sequences noted in this study are thought to record a change from relatively distal (Donjek) to proximal (Scott) style of sedimentation with time.

## Interdistributary-bay facies

### Description

The interdistributary-bay facies (Figs. 28B, 30B, 31) consists of ferruginous siltstone and mudstone interbedded with thin sandstone, pebbly sandstone and conglomerate. These rocks generally occur in 5–20 m thick sequences (60 m maximum) which are interbedded with distributary-



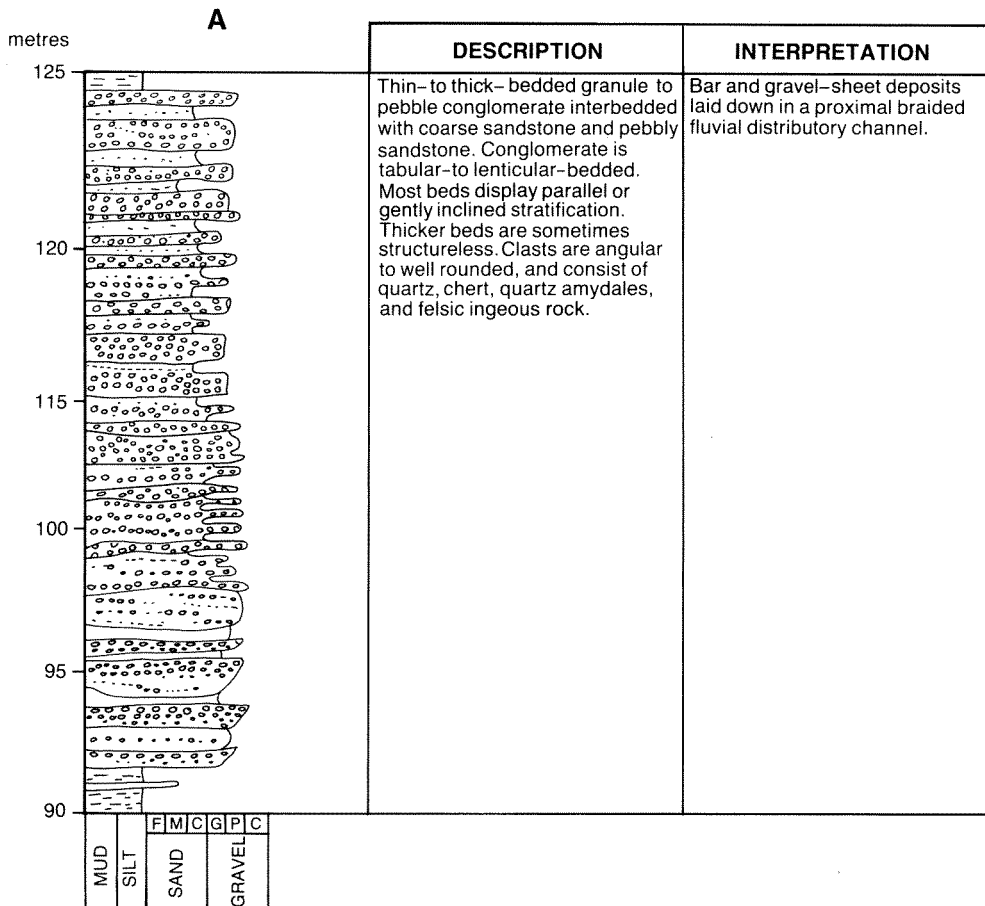


**Figure 30A** Vertical profile through conglomeratic distributory-channel facies, summarizing major rock types and internal structure. Mount McGrath Formation, locality 4.

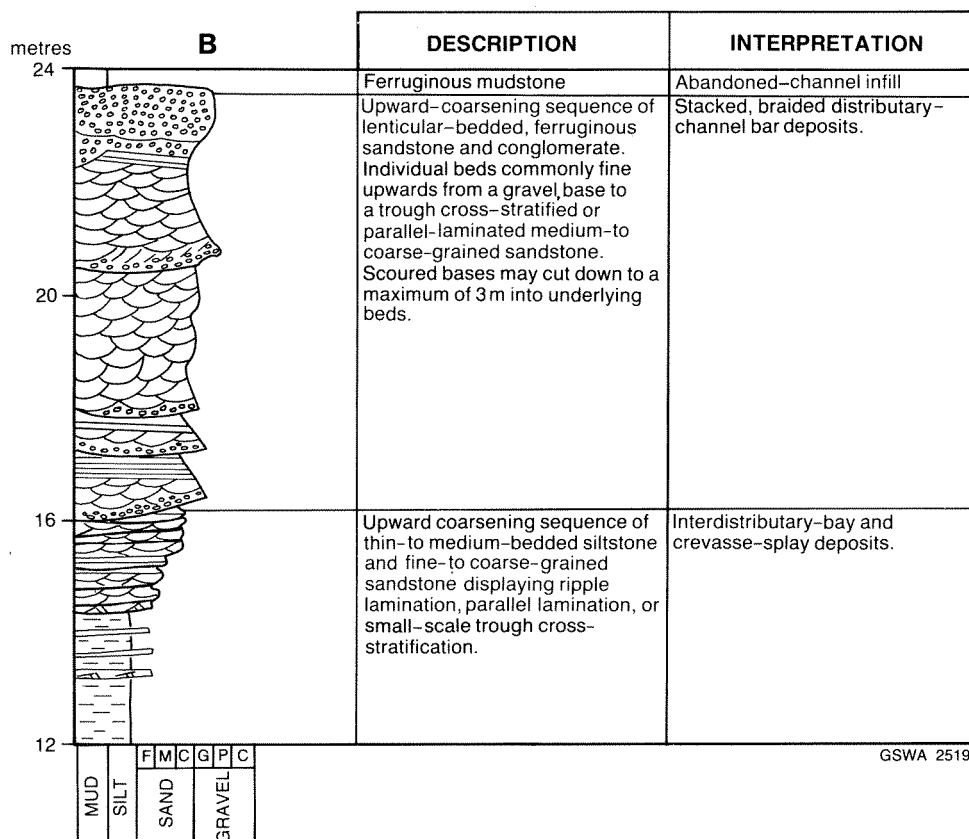


**Figure 30B** Vertical profile showing mixed sandstone and conglomeratic distributory-channel facies overlying interdistributory-bay facies. Mount McGrath Formation, locality 3.

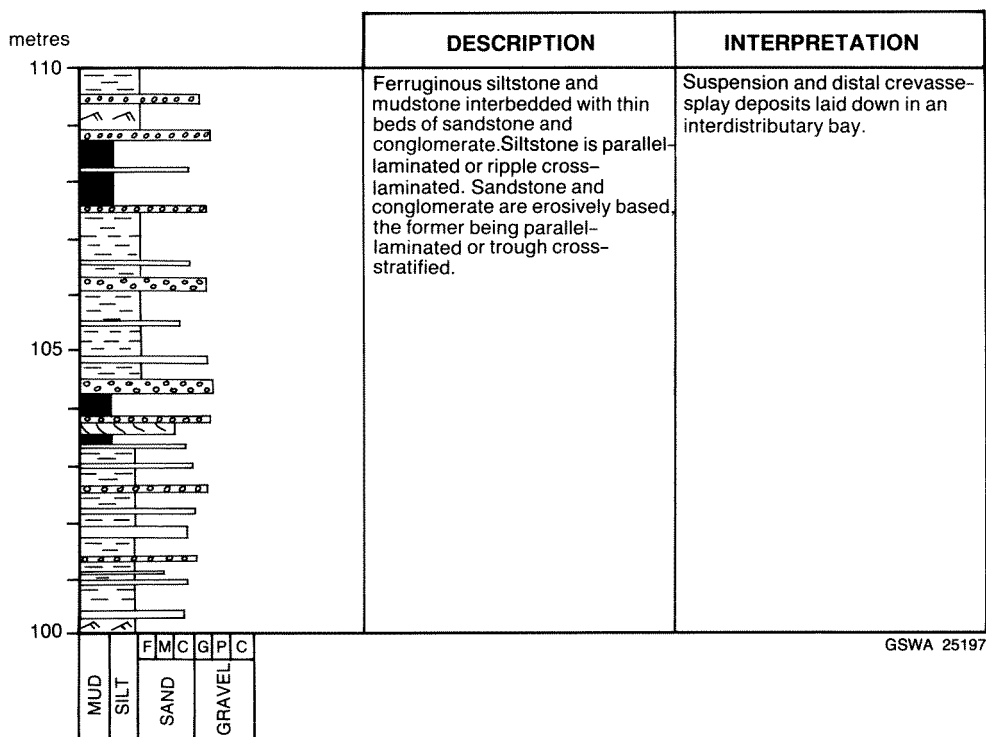


**Figure 31** Vertical profile through interdistributary-bay facies, summarizing major rock types and internal structure. Mount McGrath Formation, locality 4.

channel facies. Interdistributary-bay sequences are bounded by transitional (lower) and erosional (upper) boundaries.

Ferruginous siltstone and mudstone occur in tabular to gently lenticular beds 0.01–4 m thick. The former are parallel-laminated or ripple cross-laminated; the latter are structureless or parallel-laminated.

Sandstone, pebbly sandstone, and conglomerate beds, are thin (0.01–0.2 m), tabular or lenticular; they display erosive bases and sharp or transitional tops. Sandstones and pebbly sandstones are generally parallel-stratified or trough cross-stratified (sets 0.05–0.15 m thick). Some are structureless apart from rare scour surfaces. Clast- and matrix-supported conglomerates are composed of granule to fine-pebble sized clasts, and may fine upwards to a medium- to coarse-grained sandstone.

Examples of interdistributary-bay sequences from the Mount McGrath Formation are shown in Figures 30B and 31. Most consist of a simple alternation of mudstone or siltstone and sandstone, pebbly sandstone, and conglomerate. Locally, coarser grained lithologies form small, upward-coarsening sequences, separated by mudstone and siltstone.

### Interpretation

These rocks were laid down in an environment where deposition of mud and silt from suspension and weak currents was interrupted by periods of higher energy sand and gravel sedimentation. The close association of these deposits with fluvial distributary-channel facies suggests that they were laid down in interdistributary bays.

Modern interdistributary bays are bodies of shallow water, generally less than 8 m deep, either open to the sea or surrounded by marsh and distributary channels. Their deposits are described by Elliott (1974) and Coleman and Prior (1982).

The mudstone and siltstone are interpreted as low-energy bay-floor sediments. Thin, erosively based sandstone and conglomerate beds probably represent distal crevasse-splay deposits laid down during times of flood when distributary channels were breached and channel flow was diverted into the bay. Small upward-coarsening sequences of sandstone and conglomerate (Fig. 30B) probably represent crevasse-channel and bar deposits formed closer to the site of the distributary-channel breach.

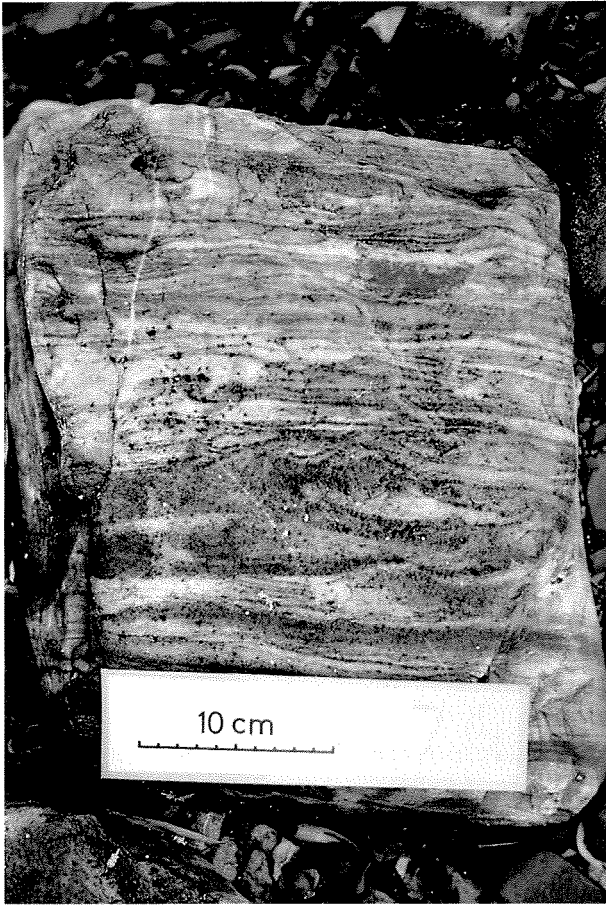
## Delta-front facies association

The delta-front facies association comprises distributary-mouth bar, beach, and shoreface to offshore facies.

### Distributary-mouth bar facies

#### Description

The distributary-mouth bar facies (Figs. 32, 33) consists of ripple cross-laminated or trough cross-stratified quartz sandstone with minor siltstone and mudstone. Bar sequences range from 2–13 m thick, and occur interbedded with distributary-channel, shoreface, and offshore facies. Contacts with the former are gradational; those with the latter are either erosional or gradational.



GSWA 25198

**Figure 32** Ripple cross-lamination and undulatory lamination in distributary-mouth bar sandstone. Primary sedimentary structures have been partly deformed by sediment loading and fluid escape. Mount McGrath Formation, locality 3.

Ripple cross-laminated, fine- to medium-grained sandstones occur in tabular units 0.2–8 m thick. A variety of ripple types are recognized; in most, the laminae are of alternating quartz- and iron-rich layers. Subcritical to supercritical climbing ripple profiles (Allen, 1984) are abundant. Symmetrical and asymmetrical straight-crested forms exhibit complex internal structure characterized by chevron upbuilding, form-discordant and draped laminae, and bidirectional cross-laminae. Ripple profiles are often overlain by irregular undulating laminae which may constitute most of the thickness of the bed.

Trough cross-stratified quartz sandstone forms tabular to lenticular units 0.02–4.5 m thick. Troughed sets are 0.05–0.3 m thick and may contain lags of small mudstone clasts.

Beds of quartzitic and ferruginous siltstone are 0.01–0.3 m thick. They exhibit parallel lamination or ripple cross-lamination, and are often interbedded with thin mudstone.

Examples of distributary-mouth bar sequences are shown in Figure 33. Most common are those in which siltstone and mudstone are overlain by ripple-laminated

sandstone, which in turn is succeeded by either trough cross-stratified sandstone or more siltstone and mudstone.

## Interpretation

The internal structure and compositional maturity of the sandstones indicate that deposition took place in an environment characterized by sustained current and wave activity. Climbing ripple cross-lamination forms in response to ripple migration under lower flow-regime conditions, where there is moderate to high sediment fallout from suspension (Harms et al., 1982). Subcritical cross-lamination results where moderate rates of sediment fallout cause the angle of climb to be less than the slope of the ripple stoss. Supercritical cross-lamination forms when high sediment fallout, coupled with slow migration of the ripple allows it to climb at an angle greater than the ripple stoss (Allen, 1984).

Straight-crested symmetrical and asymmetrical ripples with complex internal structures are interpreted as wave ripples formed under conditions of low to moderate sediment supply (de Raaf et al., 1977; Allen, 1984). Undulose lamination probably formed during periods of rapid sedimentation.

Trough cross-stratification results from downcurrent migration of dunes under lower flow-regime conditions, at current velocities greater than those required to form current ripples (Harms et al., 1982).

Mature sands and silts, which display a variety of wave- and current-formed structures, are the principal deposits of modern distributary-mouth bars, formed at the seaward termination of major distributary channels. In this setting, sediment deposition takes place close to the mouth of the distributary channel and constructs a series of discrete or coalesced bars depending on channel spacing. Bar crests aggrade rapidly during times of flood; however, the new sediment is subsequently reworked and transported to the seaward side of the bar during falling water levels. By this mechanism, distributary-mouth bars prograde seawards over the prodelta (offshore) deposits (Coleman et al., 1974). This results in a thick, upward-coarsening sequence in which the offshore muds and silts are overlain by distal-bar sands that have been reworked by waves and currents. These, in turn, are succeeded by coarser grained sand displaying current-formed structures (Elliott, 1986). As a result of marine and fluvial reworking, much of the distributary-mouth bar sequence consists of clean, well-sorted sands (Coleman and Prior, 1982).

Sequences shown in Figure 33 resemble those produced from distributary-mouth bar progradation. The lowermost ferruginous mudstones and siltstones are interpreted as offshore and distal bar deposits. The overlying current- and wave-rippled sandstones equate with sediments laid down on higher parts of the bar; trough cross-stratified sandstones represent bar crest and distributary outlet deposits. Incomplete sequences, i.e. those that do not include bar-crest sediments, were probably laid down in a setting away from the axial part of the distributary outlet.

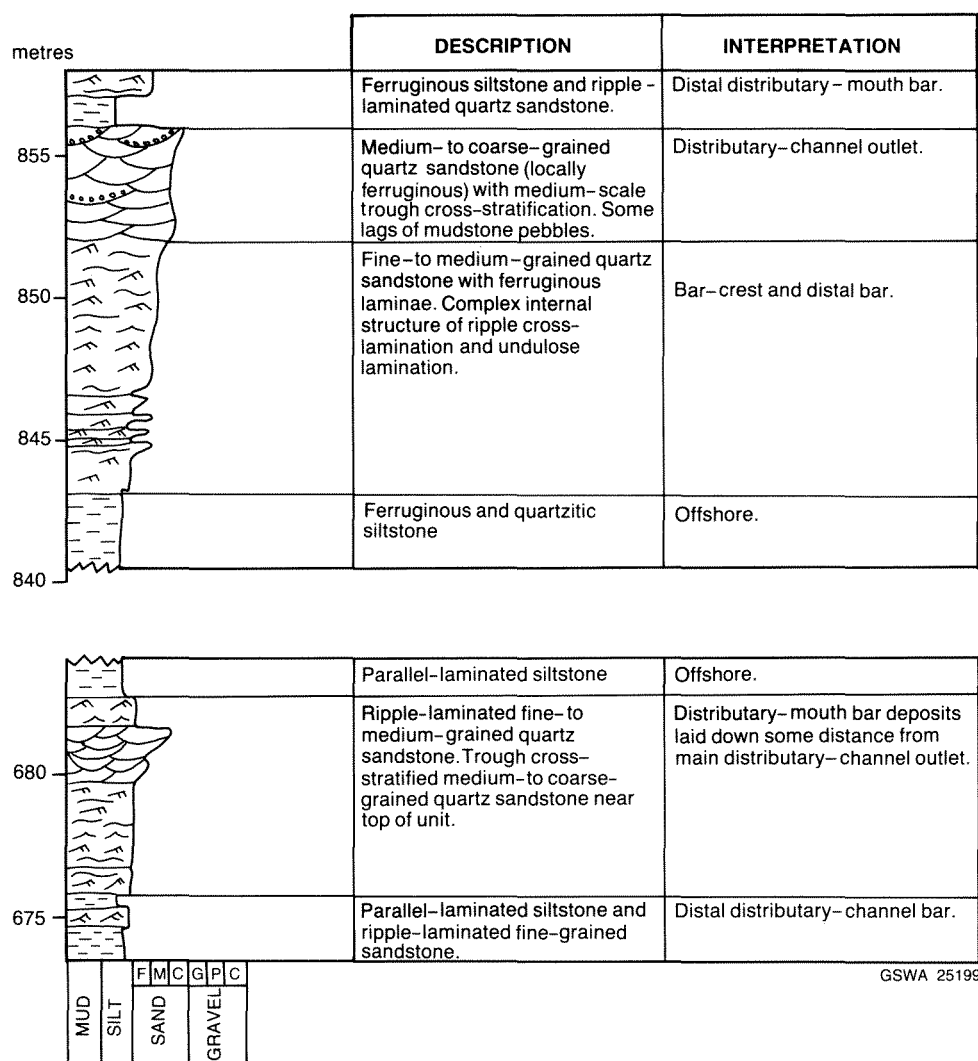


Figure 33 Vertical profile through distributary-mouth bar facies summarizing major rock-types and internal structure. Mount McGrath Formation, locality 3.

## Beach facies

### Description

The beach facies consists of fine- to medium-grained, well-sorted quartz sandstone with rare laminae of quartz granules or mud clasts. These rocks, forming tabular units, 2–10 m thick, are interbedded with shoreface and offshore, or interdistributary-bay deposits.

Internal structure is dominated by parallel stratification, or by very low-angle planar cross-stratification in which the laminae are parallel to the lower set boundary. Both types of stratification may incorporate low-angle scours.

### Interpretation

The compositional and textural maturity of the sandstone, and widespread parallel-lamination and low-angle planar cross-stratification, with associated scours, indicates that deposition took place in a moderate- to high-energy

environment. Harms et al. (1982) suggested that low-angle planar cross-stratification is the product of non-uniform, unsteady flow, and point out that it is the dominant structure formed in the swash zone of modern sandy shorelines. In these settings, the thickness of the beach sediments is generally only slightly greater than the tidal range (Harms et al., 1982). On this basis, the maximum thickness of beach deposits in the Mount McGrath Formation indicate a tidal range of approximately 10 m. No great reliance can be placed on this value, however, since it takes no account of possible basin subsidence or eustatic sea-level changes during deposition.

## Shoreface and offshore-shelf facies

### Description

The shoreface and offshore-shelf facies (Figs. 34, 35) comprises mudstone, dolomitic mudstone, dolomite, siltstone, and fine- to coarse-grained quartz sandstone that form 5–450 m thick sequences associated with beach or distributary-mouth bar deposits.

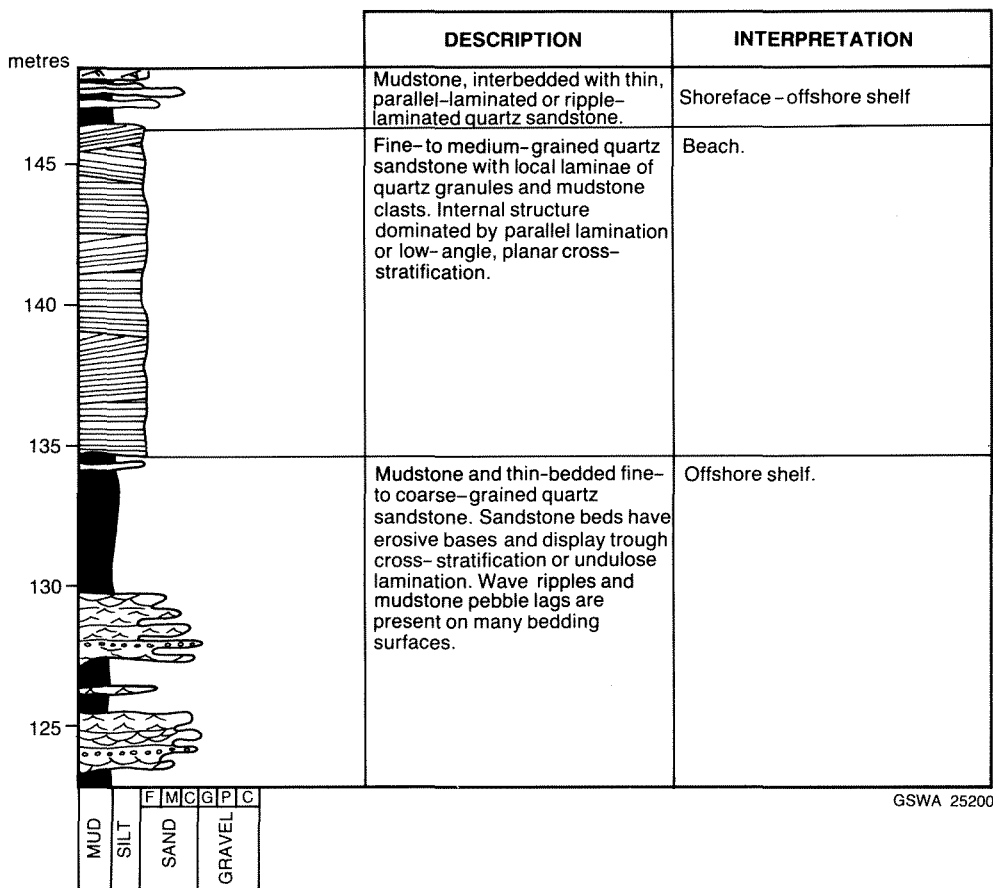


**Figure 34** Vertical profile through the beach and offshore-shelf facies summarizing major rock-types and internal structure. Mount McGrath Formation, locality 2.

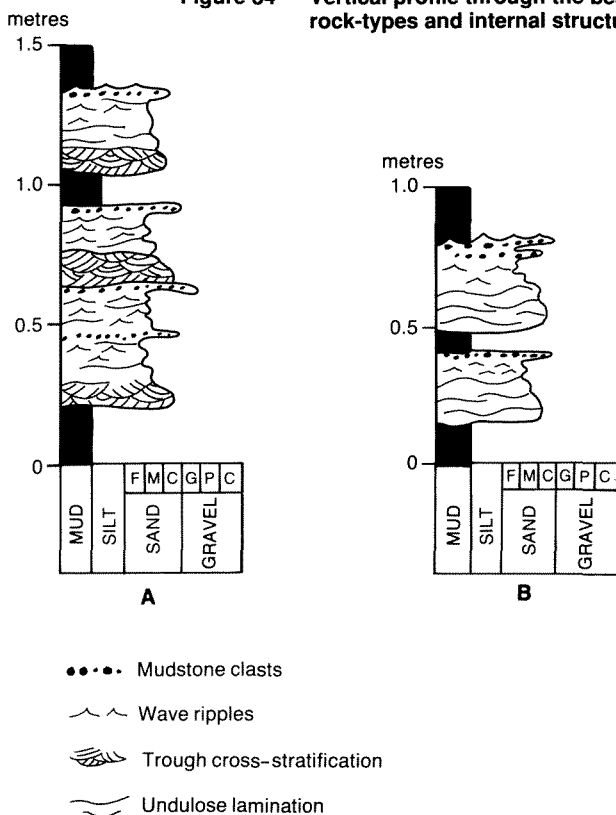


**Figure 35** Mount McGrath Formation shelf-facies sandstone beds showing detail of internal structure.

Mudstones are green to purple, structureless, or parallel-laminated, and may incorporate thin beds of siltstone or fine- to medium-grained sandstone. The latter rock types are generally parallel-laminated, or ripple cross-laminated.

Dolomitic mudstone commonly exhibits parallel, or gently undulose lamination with rare shallow scours. In addition, decimetre-scale soft-sediment folds occur locally. Dolomitic mudstone is commonly transitional into crystalline dolomite, which occurs as thin, isolated beds or as units 2–180 m thick. These carbonates are generally parallel-laminated, but may also contain small soft-sediment folds and thin beds of intraformational breccia. Domical and columnar stromatolites occur locally.

Quartz sandstone beds are 0.01–0.3 m thick; they are isolated, or grouped into thin-bedded units 0.2–10 m thick. Beds are characterized by irregularly undulose upper and lower bounding surfaces, and display varied internal structure (Fig. 35). They commonly grade upwards from cross-stratified coarse-grained sandstone to fine- to medium-grained sandstone capped by conglomerate consisting of mudstone clasts. The upper divisions typically display straight-crested or sinuous ripples with symmetric or asymmetric profiles. Each bed is overlain by a thin mudstone layer, or by another erosively based sandstone. The most common variation of this sequence (Fig. 35B) is

one in which a non-graded, undulatory, laminated division occurs in place of the cross-stratified sandstone in the lower part of the bed.

### Interpretation

By analogy with modern counterparts, the extensive mudstone sequences were probably deposited in a low-energy, marine environment; the associated beach and distributary-mouth bar facies suggests a shallow-marine shelf rather than a deep-ocean basin.

Johnson and Baldwin (1986) noted that on most modern shallow-marine shelves, deposition of mud is episodic: maximum sedimentation occurs immediately after storms; and minimum sedimentation, during long periods of fair weather. Thin beds of dolomitic mudstone and dolomite interbedded with the Mount McGrath Formation mudstone were probably formed during fair weather when rates of clastic deposition were low compared to background chemical sedimentation. Thick carbonate sequences are likely to have been laid down during long breaks in siliciclastic supply, possibly caused by nearby delta-lobe switching or delta abandonment.

Undulatory-bedded quartz sandstone is interpreted as a shelf storm deposit, formed under the influence of both unidirectional and oscillatory currents. The basal scoured surface is thought to have formed as a result of erosion at the height of the storm. The presence of trough cross-stratification in the lower part of the bed implies that this division was laid down from unidirectional, lower flow-regime currents; these were probably active shortly after the storm's peak. The overlying rippled portion is analogous to low-energy, wave-rippled sequences described by de Raaf et al. (1977) from the Carboniferous of Ireland; it represents the waning phase of the storm when deposition and reworking was largely controlled by oscillatory currents. Thin pebble layers, locally present on the top of these beds, are winnowed lag deposits which may have formed during brief storms. Similar features are described by Levell (1980) from the Late Precambrian of Finnmark, Norway. Non-graded, undulatory-stratified sandstone, which occurs in place of the cross-stratified division in some beds, is analogous to hummocky cross-stratification (Harms et al., 1982) and probably formed in response to high-energy oscillatory currents.

### Distribution of facies associations

The vertical and lateral distribution of facies within the Mount McGrath Formation is summarized in Figure 36.

In the southeastern part of the Ashburton Basin, the formation lies with marked erosional unconformity upon lower units of the Wyloo Group and the Mount Bruce Supergroup. Southeast of Snowy Mountain, (23° 28' 30"S, 118° 07' 00"E), the lowermost beds of the Mount McGrath Formation consist of distributary-channel facies (conglomerate and sandstone). These directly overlie the Weeli

Wolli Formation (Hamersley Group). A thick, though incomplete succession occurs south of Mount Channar at locality 6 (23° 30'S, 117° 58'E). Here, the lower part of the formation succeeds the Cheela Springs Basalt, and comprises at least 100 m of offshore facies (mudstone, siltstone, and local dolomite), overlain by 500 m of distributary-channel and interdistributary-bay deposits (conglomerate, sandstone, and mudstone). The remainder of the succession consists of an estimated 600 m of offshore facies, interbedded with thin distributary-mouth bar and distributary-channel deposits.

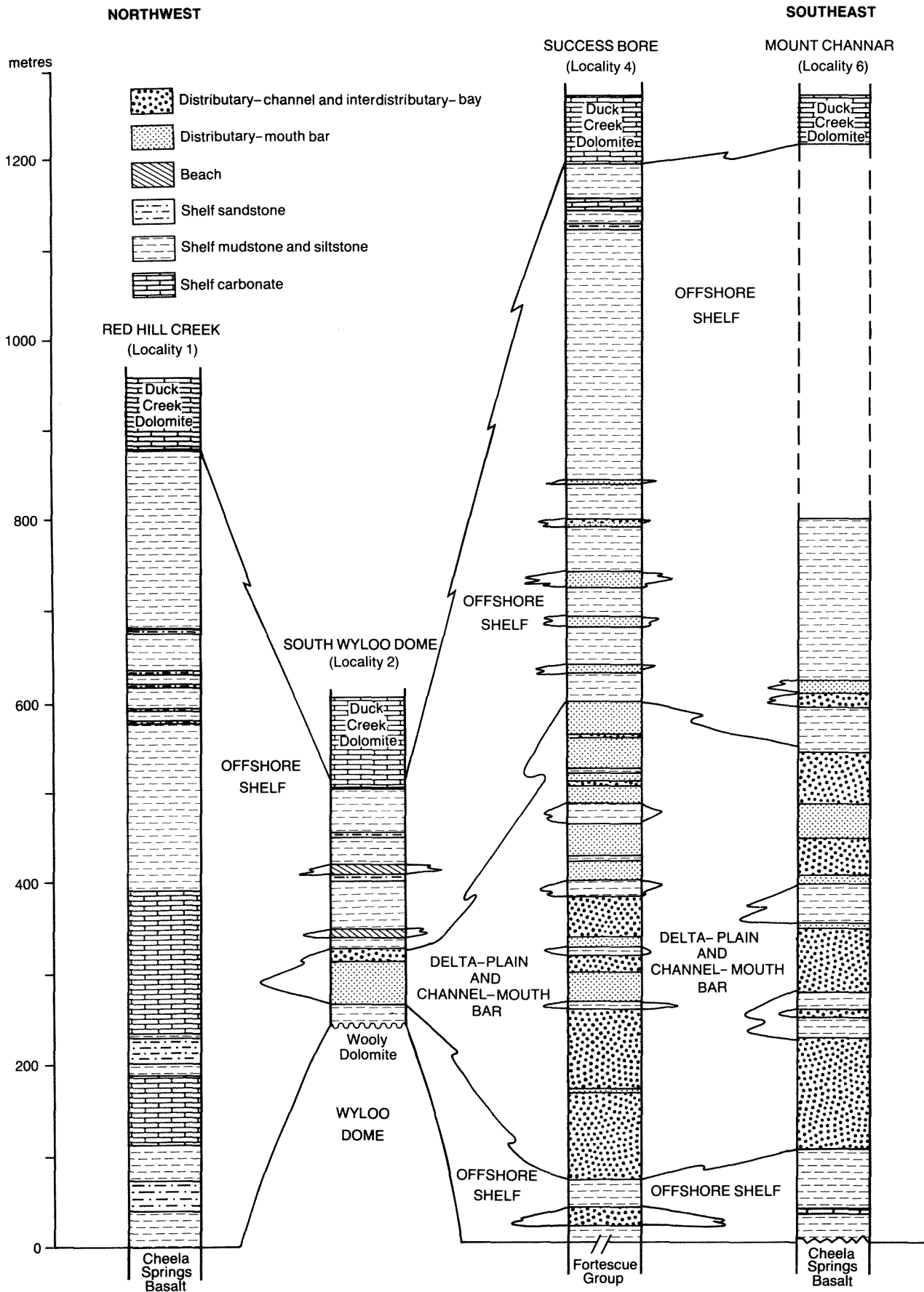
Southwest of Horrigan Pool (23° 33' 30"S, 118° 15' 00"E) the formation is faulted against the Bresnahan Group. Here the succession consists of alternating distributary-channel, interdistributary-bay, and offshore facies (sandstone, minor conglomerate and mudstone).

Immediately southwest of the Paraburdoo minesite of Hamersley Iron Pty Ltd, conglomeratic distributary-channel facies overlie thin (generally less than 10 m) quartz sandstone of the Beasley River Quartzite. Near Pirraburdu Creek (23° 14'S, 117° 34'E) these conglomerates contain rounded pebbles of mature hematite ore (Morris, 1980). Seventeen kilometres to the southeast, at Stony Creek (23° 17' 20"S, 117° 44' 00"E), conglomeratic and sandstone channel facies overlies the Weeli Wolli Formation of the Hamersley Group. These deposits also contain pebbles of hematite ore (R. Harmsworth, pers. comm. 1987).

Ten kilometres east of Success Bore (locality 5, 23° 02' 30"S, 117° 04' 00"E) the Mount McGrath Formation is faulted against the Fortescue Group. The lower part of the succession comprises 500 m of distributary-channel and interdistributary-bay facies, (sandstone, conglomerate and mudstone) and minor offshore mudstone and siltstone. These are overlain by 800 m of offshore and distributary-mouth bar facies, (mudstone, dolomite, siltstone and sandstone) interbedded with thin, channel and interdistributary-bay deposits. Carbonates, present in the upper part of the succession, were mapped as Duck Creek Dolomite by Daniels et al. (1967).

Around the Wyloo Dome, the Mount McGrath Formation rests unconformably upon underlying units. On the southern flank of the dome (locality 2, 22° 48' 09"S, 116° 28' 21"E) the succession unconformably overlies the Woolly Dolomite. The lowermost 70 m of strata consist of a single upward-coarsening sequence of offshore, beach, distributary-mouth bar, and channel facies (mudstone, quartz sandstone, and conglomerate; see Fig. 26). These deposits are overlain by 90 m of alternating beach and offshore deposits (quartz sandstone and mudstone), which are, in turn, succeeded by an estimated 150 m of offshore mudstone and dolomite.

On the northern rim of Wyloo Dome (22° 33' 30"S, 116° 19' 00"E), an estimated 50 m of offshore mudstone and siltstone unconformably overlie the Marra Mamba Iron Formation. They pass upwards into distributary-mouth bar sandstone, which is capped by conglomeratic channel facies. The upper part of the succession comprises 140 m



GSWA 25202

**Figure 36** Generalized stratigraphic profiles through the Mount McGrath Formation showing the interrelationship of facies associations.

of offshore mudstone with a little sandstone. Two and a half kilometres east of the above-mentioned grid-reference point, the conglomerate is up to 6.5 m thick and contains pebbles of hematite ore. This deposit, known as the Barrett Lennard orebody, was described by Campana (1964) and MacLeod (1966).

North of the Wyloo Dome, the Mount McGrath Formation is approximately 900 m thick, and conformably overlies the Cheela Springs Basalt. Here, the succession is largely offshore facies (mudstone and quartz sandstone) with subordinate distributary-channel and channel-mouth bar sandstone. Dolomite forms a major part of the succession in the vicinity of Red Hill Creek (22° 03'S, 116° 10'E).

## Depositional model and palaeogeographic reconstruction

The following model for Mount McGrath Formation sedimentation is based upon the nature of the facies, their vertical and spatial distribution, and their relationship to underlying rock units. The main features of the model are summarized in Figs 37 and 38.

Deposition of the Mount McGrath Formation was initiated following a major episode of uplift and erosion in the southeastern Hamersley Basin. To the southeast of the Hardey Syncline the principal controls on sedimentation were:

- (a) a tectonically active upland region of Mount Bruce Supergroup and lower Wyloo Group rocks occurring to the north and east of Paraburdoo (Fig. 37);
- (b) a coastal plain of variable width to the southwest of the upland; and
- (c) a marine shelf of low wave-energy located further to the southwest.

Braided streams, entering the marine environment from the upland area, constructed a delta complex on the eroded surface of lower Wyloo Group and Mount Bruce Supergroup rocks. On proximal parts of the delta plain (close to the present day margin of the Hamersley Basin), sedimentation took place in gravelly, braided, fluvial channels. Near the delta front, deposition of mud and immature sand and gravel occurred in shallow bays formed between the channels; cleaner sands were laid down on bars located at the mouths of major channels. Mudstone and thin dolomite layers accumulated in deeper waters further offshore.

Near Wyloo Dome, sediments from the uplifted southeastern Hamersley Basin were deposited as a distal delta complex on folded lower Wyloo Group and Mount Bruce Supergroup rocks. On the southern margin of the dome, sands were extensively reworked by coastal marine processes and deposited on delta-front beaches. North of Wyloo

Dome, pre-Mount McGrath uplift and erosion was minimal, and thin deltaic facies, together with thicker offshore shelf deposits, were laid conformably on the Cheela Springs Basalt.

## Summary of depositional history

Notwithstanding local and regional variations, the stratigraphy of the Mount McGrath Formation records a similar evolution throughout the eastern and central part of the Ashburton Basin. Much of the lower part of the succession contains a high proportion of coarse-grained rocks, and records the main period of source-area uplift, clastic input, and delta growth. In contrast, the upper part of the formation, which contains more fine-grained detritus and carbonate, was laid down during a period of waning siliciclastic supply which led to abandonment of the delta complex. The sedimentary facies in this upper part of the formation indicate that the dwindling of clastic input was accompanied by the gradual deepening of shelf waters. In the northwestern Ashburton Basin, supply of coarse-grained siliciclastic material was generally low throughout deposition of the Mount McGrath Formation. Here, the trend towards deeper water sedimentation during the latter part of Mount McGrath Formation history is also evident.

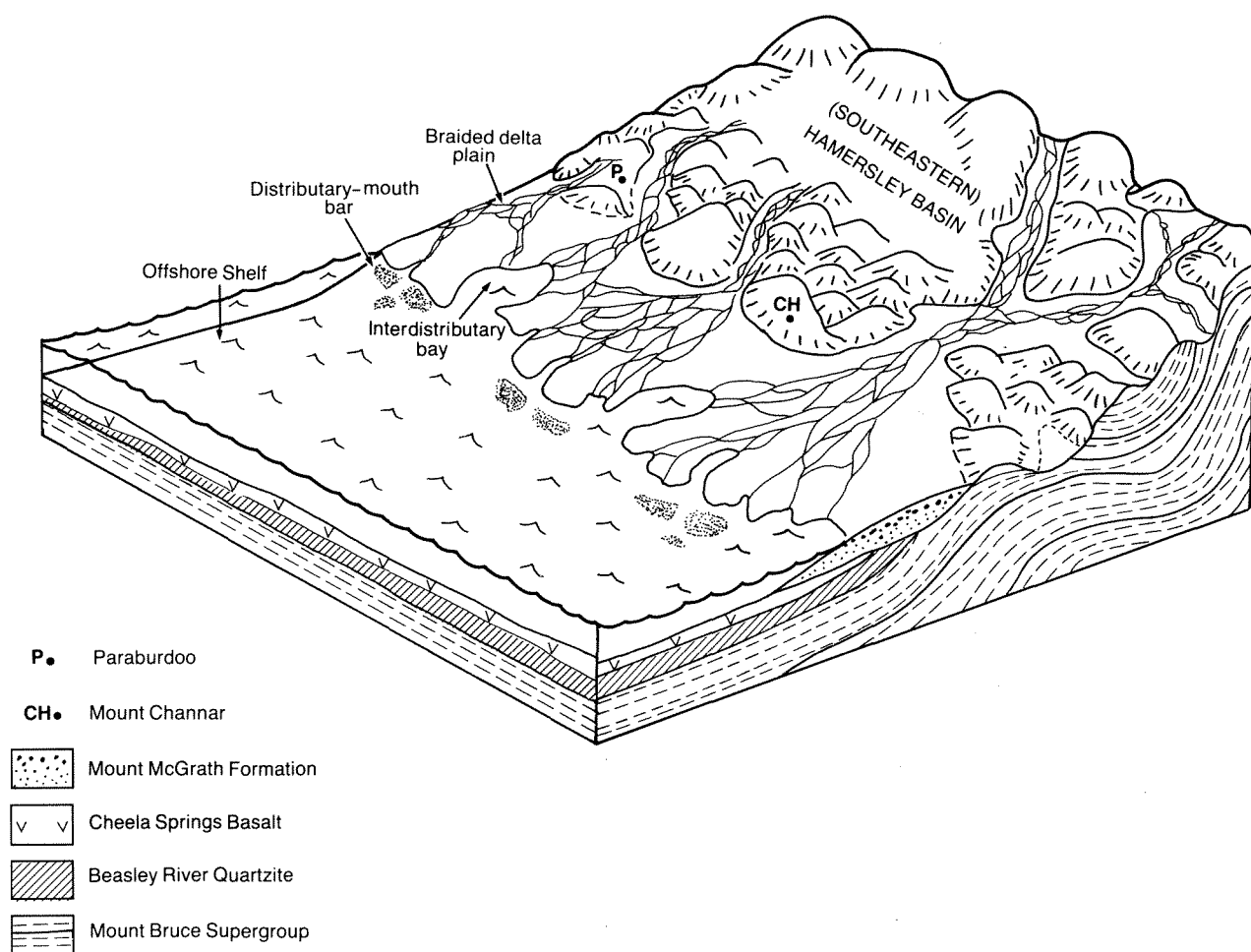
## Discussion

The unconformity at the base of the Mount McGrath Formation resulted from folding, uplift, and erosion in the southeastern Hamersley Basin following deposition of the Cheela Springs Basalt. This tectonic event also resulted in a marked increase in the volume of coarse-grained clastic detritus supplied to the northeastern part of the Ashburton Basin during deposition of the low to middle Mount McGrath Formation. Geological relationships, (Tyler, in press a; Tyler and Thorne, in press) indicate that the major phase of uplift probably followed development of large-scale, upright folds in the southeastern Hamersley Basin. This conclusion is based on the following argument:

- (a) the occurrence of Beasley River Quartzite and Cheela Springs Basalt in the core of one of these folds (the Turee Creek Syncline) provides a lower age limit for the folding;
- (a) along the southern margin of the Hamersley Basin the intra-Wyloo folds are cut by west northwest-trending mafic dykes (Tyler, in press b);
- (c) at Paraburdoo, these dykes pre-date formation of hematite ore in the Brockman Iron Formation (Morris, 1980); and
- (d) pebbles of hematite ore occur in the Mount McGrath Formation (Morris, 1980), limiting the age of ore genesis to pre-Mount McGrath Formation.

Folding must therefore have taken place after eruption of the Cheela Springs Basalt but before deposition of the Mount McGrath Formation.





GSWA 25203

**Figure 37 Model showing principal depositional environments of the Mount McGrath Formation in the northeast Ashburton Basin. Post-Cheela Springs Basalt folding and uplift in the southeastern Hamersley Basin supplied coarse-grained sediment to a braided-delta complex developed along the northeastern margin of the Ashburton Basin. Initial source-area uplift was followed by a period of rapid basin subsidence and delta abandonment.**

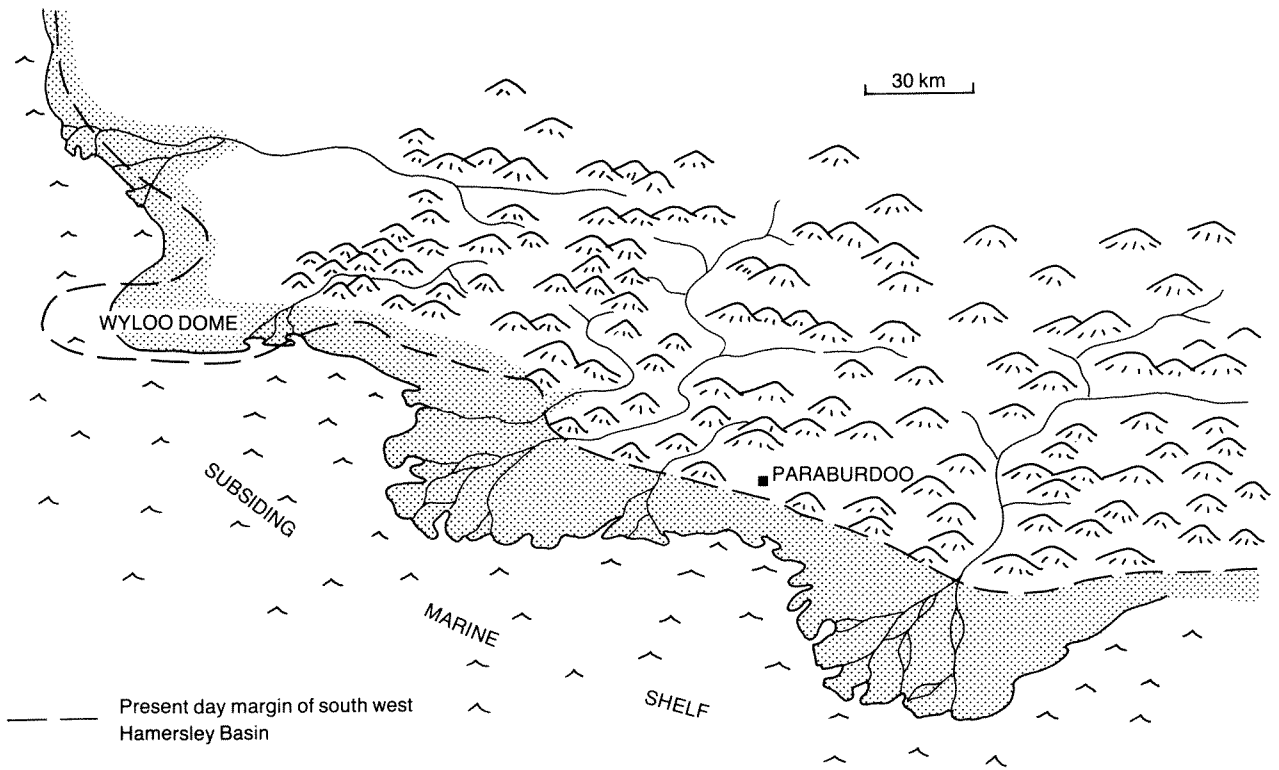
On the southern side of Wyloo Dome, the angular unconformity at the base of the Mount McGrath Formation points to the presence of intra-Wyloo Group folding in this area. The thickness and character of the formation, here and in adjacent parts of the Ashburton Basin, suggests that Wyloo Dome was not a major topographic high at this time, though it probably had some positive relief. The stratigraphy records that during deposition of the low to middle part of the Mount McGrath Formation, the area was inundated by the sea, and then buried by distal deltaic sediments derived from the southern Hamersley Basin.

There is no direct evidence for intra-Wyloo Group (pre-Mount McGrath Formation) folding in the north-western part of the Ashburton Basin or adjacent Hamersley Basin. The predominance of shallow-marine shelf deposits in the low to middle Wyloo Group (Beasley River Quartzite and Mount McGrath Formation) suggests that the area was tectonically inactive at this time, apart from the period of eruption of the Cheela Springs Basalt.

The present study does not corroborate the view that the lower Wyloo Group was deposited in a narrow trough

that developed close to the southwestern margin of the Hamersley Basin (cf. Daniels, 1975; Horwitz, 1982, 1983). Instead, the information presented in Chapters 2-4 implies that sedimentation took place on a shallow-marine shelf that evolved on and around the southwestern Hamersley Basin. Facies distributions, together with palaeocurrent and provenance data, indicate that the Hamersley Basin was also the major source of detritus for the lower Wyloo Group. This evidence does not support the work of Horwitz (1982, 1983) who suggested that much of it was from an upland area to the southwest of the present-day lower Wyloo Group outcrop.

In the southeastern Ashburton Basin, deltaic deposits of the Mount McGrath Formation show little evidence of tidal reworking. In contrast, tidally formed structures are abundant in the underlying Beasley River Quartzite. The apparent decline in tidal influence during deposition of the low-to middle Wyloo Group may have been due to a change in basin geometry which resulted in a drop in tidal range; however, it may also reflect change to a more active tectonic environment. Hayes and Michel (1982) note that in the macrotidal Lower Cook Inlet, Alaska,



GSWA 25204

**Figure 38** Palaeogeography of the southwestern Pilbara during deposition of the lower Mount McGrath Formation. The locations of Paraburadoo, Wyloo Dome, and the southwestern Hamersley Basin are shown for reference. Braided-delta deposits are thickest in the eastern Ashburton Basin, adjacent to areas of greatest source-area uplift.

tectonic setting is an important control on the style of shoreline sedimentation. There, coarse-grained sediment from a rising source area is delivered to the sea by high gradient streams which construct fan-deltas at the shoreline. The authors note that even though the tidal range

is 4–6 m, tidal currents contribute little to the reworking of sediment, particularly of coarse-grained detritus at the shoreline. As a result, wave, or fluvial dominated fan deltas are the principal sites of sedimentation.

## Chapter Five

# Duck Creek Dolomite and June Hill Volcanics

## Duck Creek Dolomite

The Duck Creek Dolomite (1000 m thick) rests conformably upon the Mount McGrath Formation except around the western part of Wyloo Dome, where it unconformably overlies the Fortescue and Hamersley Groups. Over most of the Ashburton Basin the formation is conformably overlain by the Ashburton Formation. The only exception is north of Wyloo Dome, where there is gradational contact with the locally developed June Hill Volcanics. Brief descriptions of the Duck Creek Dolomite are given by Daniels (1968, 1970, 1975), de la Hunty (1965), Horwitz (1981, 1982), Seymour et al. (1988), and Williams (1968). Most work has concerned its palaeontology (Edgell, 1964; Grey 1979, 1982, 1985; Grey and Thorne, 1985; Hofmann and Schopf, 1883; Knoll and Barghoorn, 1976; Knoll et al., 1988; Preiss, 1977; and Walter, 1972); but a sedimentological study has been made by Thorne (1985).

This chapter describes and interprets the principal facies associations present in the Duck Creek Dolomite. Most of this information was obtained by 1:40 000 scale mapping of the outcrop area (Fig. 39), supplemented by data from one measured section.

The formation consists of thin- to thick-bedded, buff- or grey-mauve-weathering dolomite. It is commonly stromatolitic; and silicification is locally intense. Two major facies associations have been recognized: inner-shelf; and outer-shelf, slope and basin.

### Inner-shelf facies association

This association comprises offshore-barrier, subtidal-lagoon, intertidal-shelf, and supratidal-shelf facies.

#### Description

##### *Offshore-barrier facies*

The offshore-barrier facies (Fig. 40A) consists of intraclast grainstone that crops out in laterally persistent, tabular beds (0.05–1.0 m thick). The upper and lower bedding surfaces are sharply defined, and the lower contact usually shows evidence of erosion. Most beds show little internal structure; however, small- to medium-scale trough cross-stratification, parallel-stratification, and low-angle

planar cross-stratification are present locally. The grainstones are generally poorly sorted and may contain fragments of stromatolitic dolomite up to 1.5 m across.

In thin section, the intraclasts are seen to be angular to well-rounded; they are derived from pre-existing stromatolitic and grainstone deposits. Clasts are cemented by an early generation of fine- to medium-grained (0.02–0.2 mm) dolomite, and by later generations of coarse-grained subhedral dolomite and large, equant to bladed, quartz crystals.

##### *Subtidal-lagoon facies*

The subtidal-lagoon facies comprises a variety of stromatolitic rock-types. Domical stromatolites (Fig. 40B) are generally nucleated on tabular oncoids or intraclasts. Usually these nuclei are found as isolated clasts, and give rise to spaced domical stromatolites whose synoptic relief decreases from about 0.1 m at the base, to zero at the top of the dome. In some beds, the nuclei, particularly the oncoids, may occur in clusters; they then form the cores of large, isolated domes up to 1.5 m across.

Small, branching-columnar stromatolites (*Pilbaria perplexa* Walter 1972) form continuous tabular biostromes 0.1–0.25 m thick. The stromatolites are 0.02–0.05 m wide, up to 0.25 m high, and display irregular branching in which individual branches do not maintain constant thickness. In addition, most stromatolitic margins have niches; and the internal laminae are steeply convex and may form distinct walls (Fig. 41). The area between the branches is dolomitic intraclast grainstone or intraclast packstone, and is generally silicified.

Large, branching-columnar stromatolites (*Pilbaria cf. perplexa* Walter 1972) occur in tabular units 0.5–2.0 m thick (Fig. 41B). Stromatolite columns are usually 0.05–0.1 m wide and sub-cylindrical in form, with niches in the walls (Grey, 1985). Some columns are coalesced or bridged. Unsilicified intercolumn areas are filled by dolomitic intraclast grainstone or intraclast packstone.

##### *Intertidal-shelf facies*

The intertidal-shelf facies (Fig. 40B) consists of planar to gently undulatory, laminated dolomite with abundant laminoid or irregular fenestrae — now filled by sparry dolomite, chalcedony, and coarsely crystalline quartz.

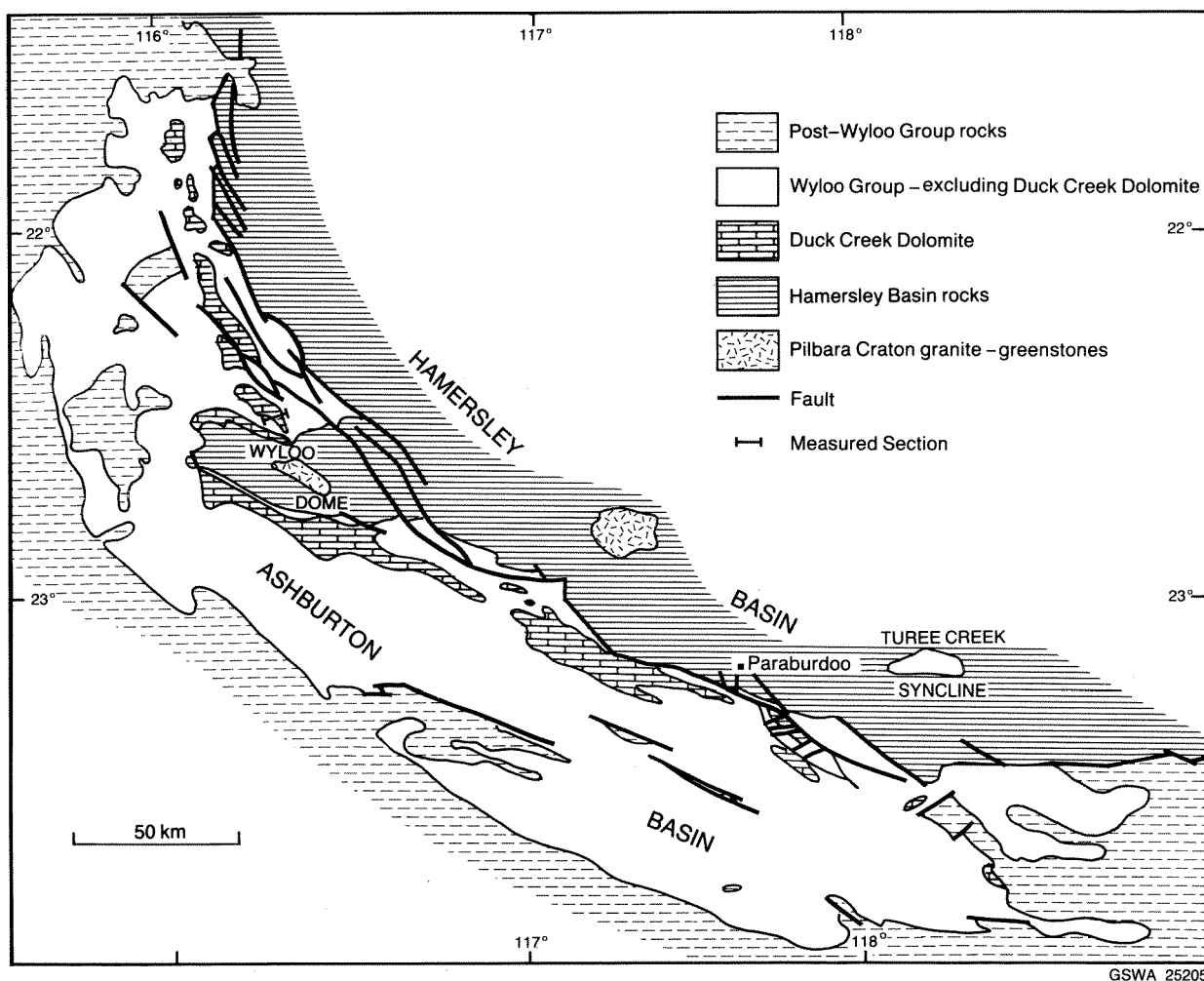


Figure 39 Simplified outcrop map of the Duck Creek Dolomite.

Some laminae are disrupted by penecontemporaneous shrinkage cracks oriented normal to the bedding. Petrographically, two distinct types of laminae can be recognized. One type is marked by variations in the average size (0.005–0.25 mm) of the dolomite crystals. The finest grained laminae, in particular, are discontinuous and irregularly undulose. The second type of lamination is formed by sand-sized intraclasts that occur as laterally continuous layers 1–50 mm thick.

#### *Supratidal-shelf facies*

The supratidal-shelf facies incorporates a range of sedimentary and organosedimentary structures including: tepees, crested pseudocolumnar stromatolites, disrupted domes, and low-domical stromatolites.

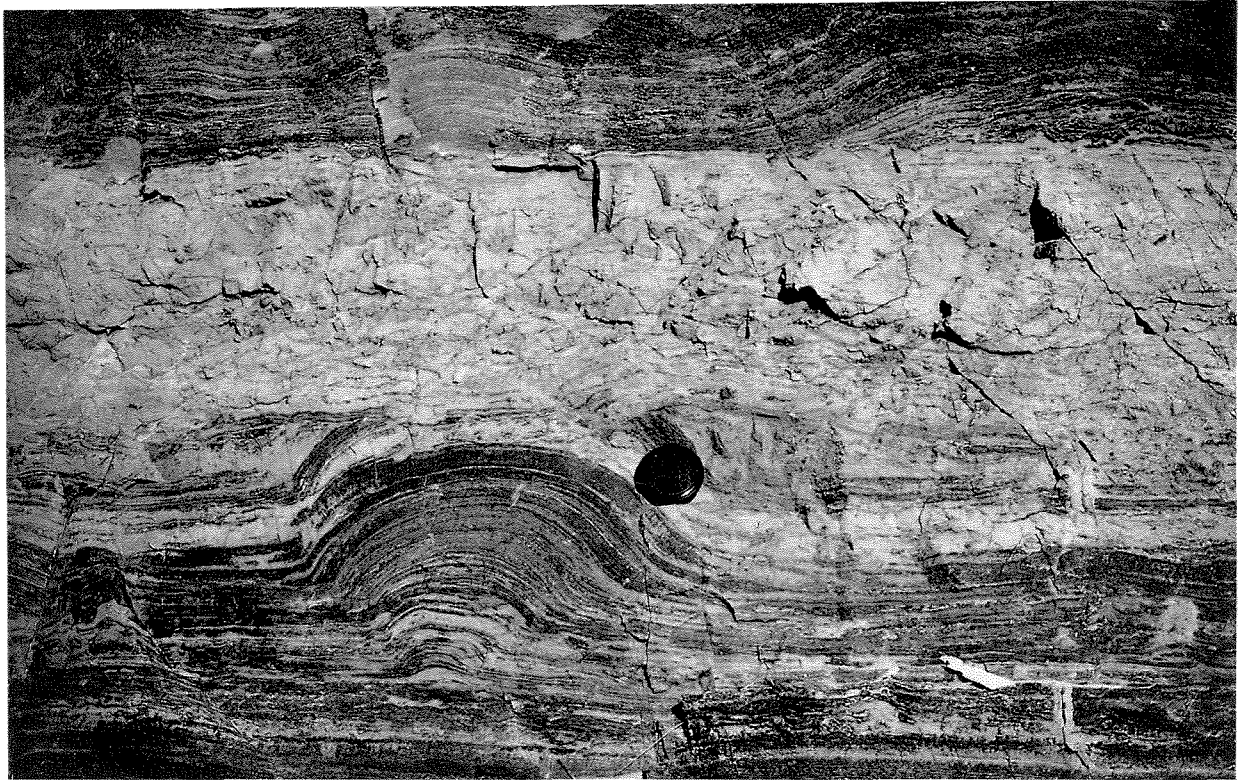
Tepees (Fig. 42) have an irregular, cusped cross-section with amplitudes of a few tens of centimetres and wavelengths up to 2.5 m. The anticlinal portions of many tepees are brecciated and filled by coarse-grained detritus. The fact that the tepees are gradually overlapped by successively younger deposits, and often show evidence of

penecontemporaneous erosion, demonstrates their syndepositional origin.

Crested pseudocolumnar stromatolites (Fig. 43) consist of stacked, low (10–30 mm synoptic relief), laterally linked peaks. Individual laminae either maintain constant thickness or vary when traced from peak to trough. The stromatolite crests may merge upwards into convex forms.

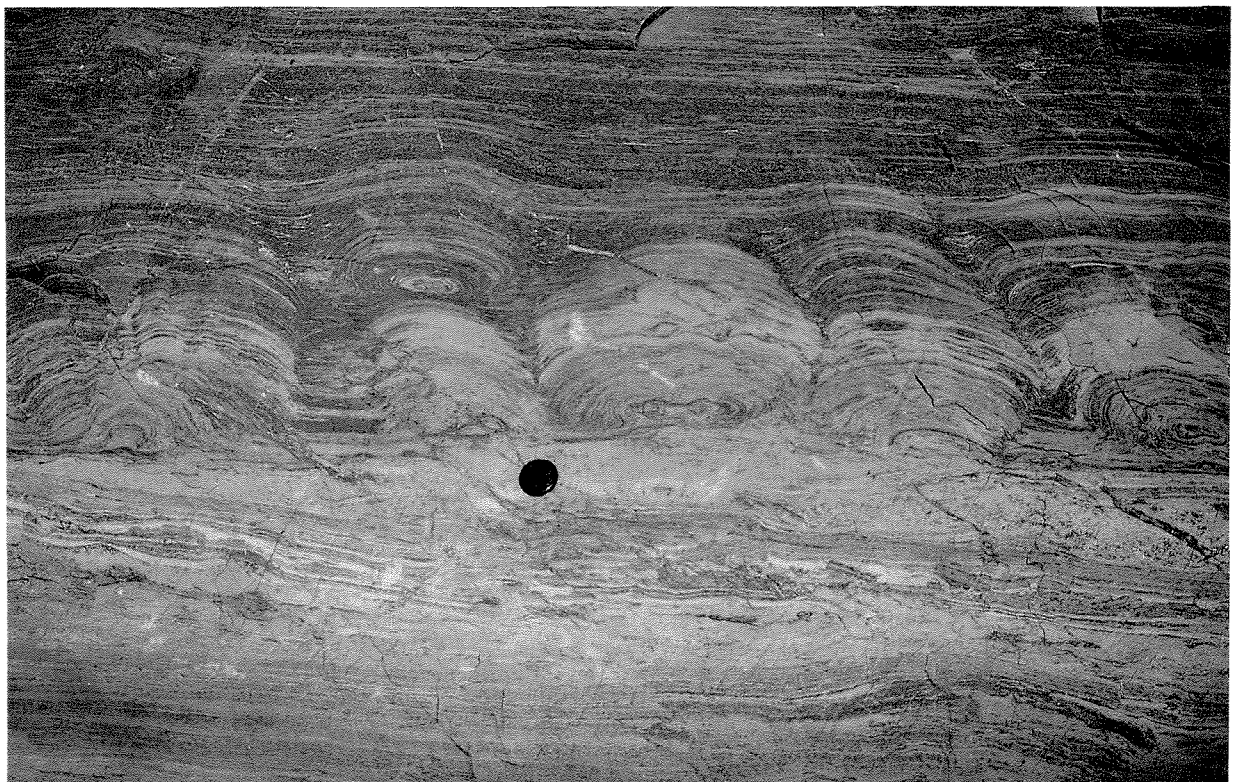
Disrupted domical stromatolites (Fig. 44) are bulbous forms with a relief up to 0.1 m. In the core of the dome, the original laminae are disrupted, and are partly or completely replaced by silica or coarsely crystalline dolomite. The tops of many domes show evidence of penecontemporaneous erosion.

Low-domical stromatolites (Fig. 45) have a gently arched cross-section (0.2–0.6 m wide) and a synoptic relief generally up to 0.1 m. Usually they have grown upon irregularities on the underlying substrate. They exhibit two distinct types of internal structure: one form is identical to the internal structure of the laminated dolomite of the intertidal shelf facies; the other comprises 10–50 mm thick layers of tiny branching columnar stromatolites (*Asperia ashburtonia* Grey 1985).



GSWA 25206A

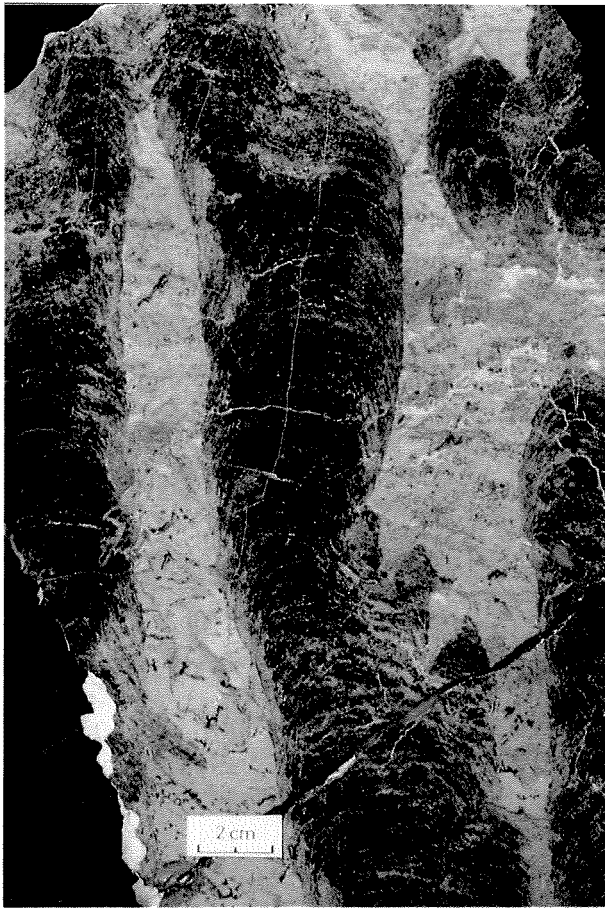
**Figure 40A** Erosively based intraclast grainstone (0.25 m thick) overlying intertidal and supratidal dolomite. The grainstone, which rarely displays any cross-stratification, is poorly sorted and may contain clasts up to 1.5 m across. This facies is interpreted as a transgressive-barrier deposit. Duck Creek Dolomite, Duck Creek Gorge.



GSWA 25206B

**Figure 40B** Lagoonal, domical stromatolites overlying an intraclast grainstone containing a large imbricate clast (dipping gently to the left). The domical stromatolites are nucleated upon pebble-sized intraclasts and oncoids, and the synoptic relief of the domes decreases upwards until they merge with the overlying intertidal laminated-dolomite facies. Duck Creek Dolomite, Duck Creek Gorge.





GSWA 252071

**Figure 41A** Polished slab of *Pilbaria perplexa*, showing niche development and detail of internal lamination. Interbranch areas are filled with dolomitic packstone and intraclast grainstone. Lagoon to lower intertidal facies of the Duck Creek Dolomite, Duck Creek Gorge.

### Facies sequences

The inner-shelf facies association consists of numerous repeated sequences of stromatolitic and non-stromatolitic facies. Using Markov Chain analysis, Thorne (1985) recognized two types of sequence. The first (Sequence 1, Fig. 46) is approximately 1.5 m thick and consists of an erosively based intraclast grainstone, which is succeeded by nucleated domical stromatolites and laminated dolomite. The sequence then passes upwards into a mixed assemblage of tepees, disrupted domes, low-domical stromatolites and pseudocolumnar stromatolites; this is overlain by the next erosively-based intraclast grainstone.

The second type (Sequence 2, Fig. 46) is generally 2–4 m thick and consists of an erosional intraclast grainstone overlain by small branching-columnar stromatolites (*P. perplexa*). These develop upwards into large branching-columnar stromatolites (*P. cf. perplexa*) which are overlain directly by laminated dolomite. This is followed by the basal intraclast grainstone of the next sequence, or by a mixed assemblage of tepees, disrupted domes or low-domical stromatolites (including *A. ashburtonia*), which is then capped by intraclast grainstone.

### Interpretation

#### *Holocene analogue*

The various facies and facies sequences outlined above can be compared with the Holocene deposits of the Trucial Coast, Arabian Gulf (described by Purser, 1973; Till, 1978). In this region, the coastal strip, up to 40 km wide near Abu Dhabi, has a complex outer barrier zone of offshore islands, channels and tidal deltas, separated from the mainland by a lagoonal system. Landward of the lagoonal complex is a zone of intertidal flats which passes imperceptibly into the dessicated supratidal plain or sabkha. The sediments associated with the outer barrier system are composed of ooids and skeletal sand with a lesser amount of coral or algal reef material; but the lagoon is characterized by muddy sand with coarser detritus in the lagoonal channels. The intertidal flats are colonized by cyanobacteria, which trap sediment and build a variety of microbial mat forms, the morphology of which controlled by the frequency of storm-driven flooding events. The sabkha surface contains carbonate sediment deposited by exceptional storms. However, the characteristic feature of these flats is the occurrence of early diagenetic anhydrite, gypsum, celestite, and ephemeral halite, within the sediment and on top of the sabkha surface.



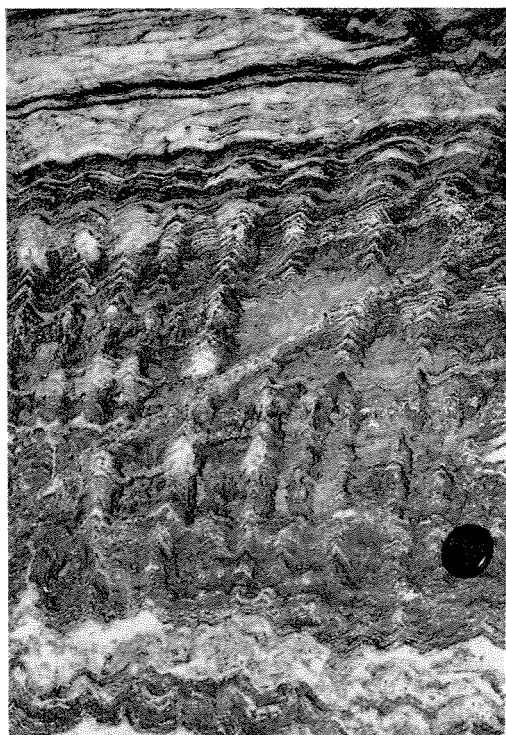
GSWA 25207B

**Figure 41B** Large branching-columnar stromatolites (*Pilbaria cf. perplexa*). Intercolumn areas have been infilled by partly silicified dolomitic grainstone. Lens cap is 6 cm diameter. Lagoon to lower intertidal facies. Duck Creek Dolomite, Duck Creek Gorge.



GSWA 25208

**Figure 42** Tepee Structure in supratidal facies of the Duck Creek Dolomite, Duck Creek Gorge. The anticlinal portion, shown in the centre of the photograph, represents the buckled margin of a broad polygonal structure formed by a complex history of sediment layer expansion, contraction and mechanical fracturing.



GSWA 25209

**Figure 43** Silicified crested pseudocolumnar stromatolites showing the change to a convex form when traced upwards. Individual laminae either maintain constant thickness or vary in thickness when traced from peak to trough. Supratidal facies, Duck Creek Dolomite, Duck Creek Gorge.

The lateral distribution of surface environments in the Abu Dhabi region is mirrored in the Holocene sediment profile of the coastal sabkha. This is the result of a marine transgression and regression which occurred during the past five thousand years. During the initial transgression, sedimentation rates were too slow to keep pace with the retreat of the shoreline, and only 0.1 m of transgressive subtidal and intertidal sediments is preserved. Subsequent regression, caused mainly by sediment offlap, together with a 1.2 m drop in sea level, has resulted in deposition of up to 4 m of regressive subtidal, intertidal, and supratidal sediments on top of the transgressive sediments. This ordered stacking of subtidal, intertidal, and supratidal deposits is known as an upward-shallowing sequence (James, 1984).

The above sequence is to some degree incomplete, because it does not record the presence of the offshore-barrier deposits. During the Holocene transgression, these sands did not advance as far as the present day sabkha zone. Had this transgression migrated far enough inland, the sabkha profile would be expected to include the complete sequence of barrier, lagoonal, intertidal, and supratidal deposits shown in Fig. 47.

*Upward-shallowing sequences in the Duck Creek Dolomite*

Figure 48 compares the complete upward-shallowing sequence from the Trucial Coast with Sequences 1 and 2



GSWA 25210

**Figure 44** Disrupted-domatic stromatolite. The lamination in the core of the small dome has been disrupted and is now replaced by coarsely crystalline dolomite and silica. The structure is closely similar to anhydrite diapirs reported from Holocene sabkha sediments of the Arabian Gulf. The planation surface truncating the dome may have resulted from penecontemporaneous wind erosion. Supratidal facies, Duck Creek Dolomite, Duck Creek Gorge.



GSWA 25211

**Figure 45** Low-domatic stromatolite comprising the tiny digitate form *Asperia ashburtonia*. High intertidal to supratidal facies, Duck Creek Dolomite, Duck Creek Gorge.

from the Duck Creek Dolomite. The erosively based grainstone at the base of Sequence 1 is equivalent to the ooid and skeletal-sand horizon of the ideal sabkha profile, and is interpreted as the remnants of a transgressive off-shore-barrier system. The largest clasts in this grainstone are derived from lithified or semi-lithified lagoonal, intertidal, and supratidal deposits. A thin transgressive record, such as occurs in the Duck Creek Dolomite and Trucial Coast sequences, points to fairly rapid rise in relative sea level.

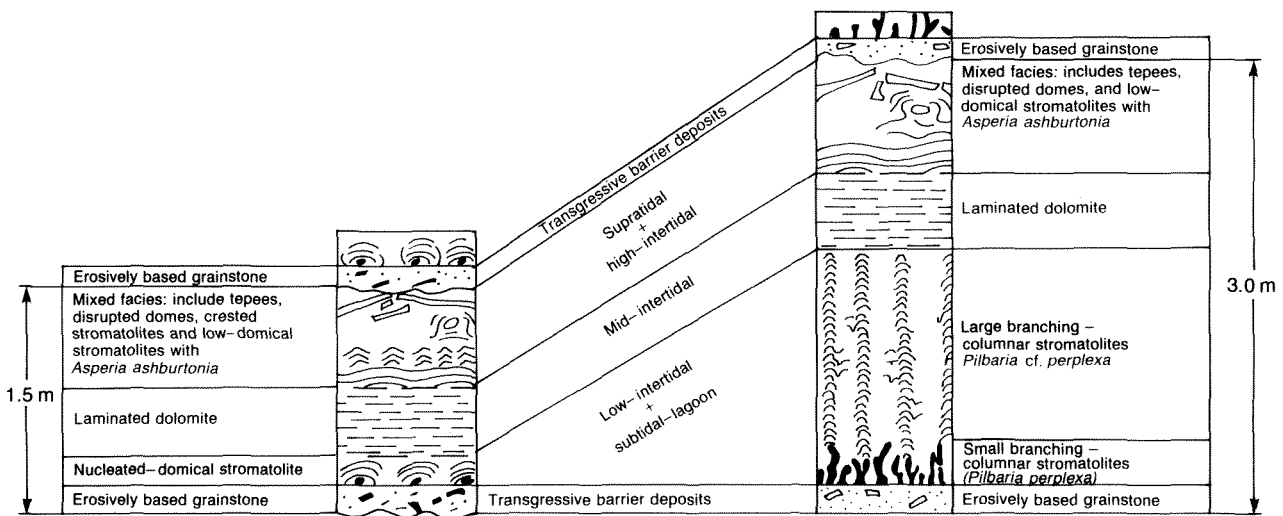
Nucleated domical stromatolites are interpreted as a subtidal lagoonal facies despite the fact that they have no exact counterpart in the Holocene of the Arabian Gulf. Kinsman and Park (1976) recorded small gelatinous stromatolitic domes associated with bioclastic muddy sands in some Trucial Coast lagoons. Those stromatolites, however, differ in detailed morphology and internal structure from domical forms in the Duck Creek Dolomite. More closely analogous to the Precambrian stromatolites are the subtidal forms reported by Gebelein (1976) from Florida, the Bahamas, and Bermuda. These domical stromatolites grow up to 0.1 m high and 0.3 m wide and, particularly in moderately agitated environments, are associated with oncoids.

The laminated dolomite which overlies the domical stromatolite horizon is analogous to the laminated middle intertidal sediments of the Holocene sabkha profile. Park



SEQUENCE 1

SEQUENCE 2



GSWA 25212

Figure 46 Vertical profiles showing the interrelationship of rock types and organo-sedimentary structures in the shelf-facies association of the Duck Creek Dolomite.

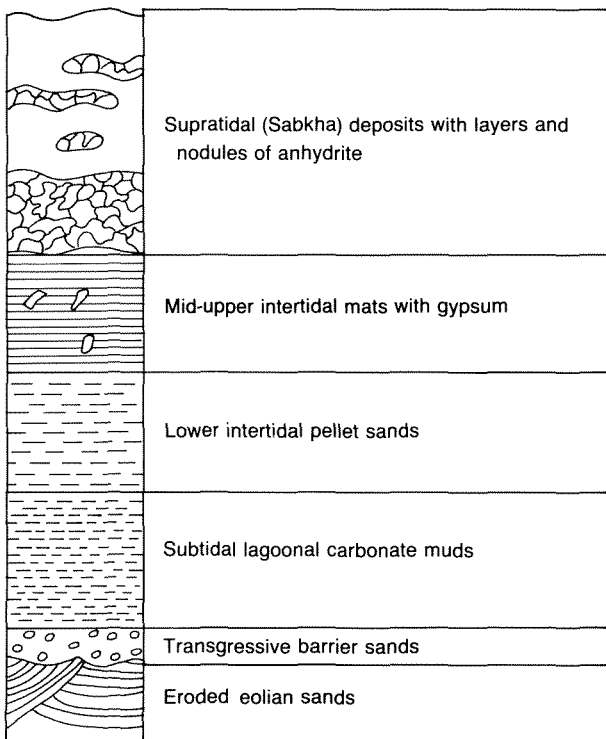
(1976) described how these Holocene laminites consist of alternations of cyanobacteria and layers of trapped sediment. Rotting of the microbial layers causes development of irregular laminoid fenestrae; however, if the decay is accompanied by dehydration, compaction, and lithification, thin layers of finely crystalline carbonate would result instead (Park, 1977). Thin layers of intraclast grainstone that form an integral part of this facies are interpreted as storm deposits. Park (1976) noted that storm sedimentation is probably the single most important depositional process in the intertidal zone of the Trucial Coast. Here, sediment layers greater than about 10 mm thick are attributed to storm activity which was sustained for several days.

Low-domical stromatolites, crested pseudocolumnar stromatolites, tepees, and disrupted domical stromatolites are grouped together as a mixed facies equivalent to the high-intertidal and supratidal portion of the Holocene sabkha sequence.

Crested pseudocolumnar stromatolites and low-domical stromatolites have no precise analogue in the Arabian Gulf. The crested pseudocolumnar stromatolites are loosely comparable with the pinnacle algal mat from high intertidal environments (Park, 1976), though these Holocene forms probably have a small chance of preservation.

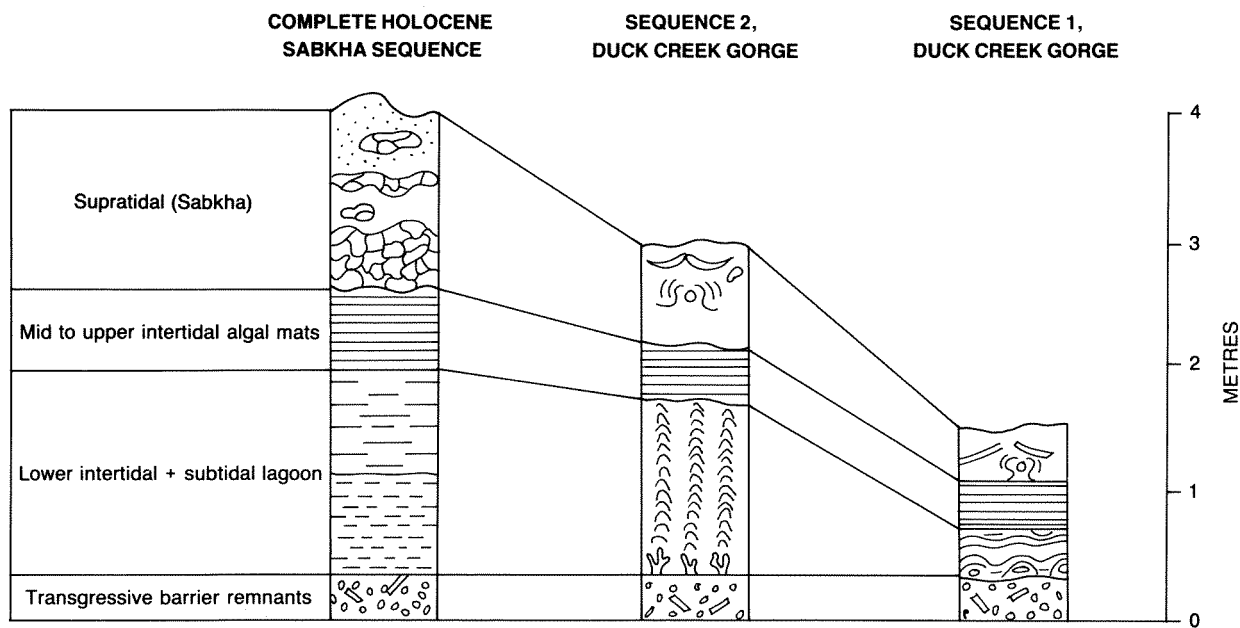
Internal structure of the low-domical stromatolites is often similar to that of intertidal laminated dolomite. These domes, which occur above the laminated dolomites in the facies sequence, are therefore interpreted as a high intertidal form. The origin of low domes, whose internal structure consists of layers of the tiny digitate stromatolite *Asperia ashburtonia*, is less clear. The stromatolites are

SABKHA SURFACE



GSWA 25213

Figure 47 Diagrammatic representation of a complete upward-shallowing sabkha sequence from the Holocene of the Arabian Gulf.



GSWA 25214

**Figure 48** A comparison of lithologies and thicknesses between an ideal Holocene sabkha sequence and the Sequences 1 and 2 from the shelf-facies association of the Duck Creek Dolomite.

comparable in morphology and fabric to Holocene stromatolites at Lake Clifton, an interdunal lake on the southwestern coast of Western Australia (Grey and Thorne, 1985). Grotzinger (1986), however, interpreted forms similar to *A. ashburtonia*, occurring in the 1890 Ma Rocknest Formation of Canada, as relic aragonite tufas, precipitated on supratidal flats.

Tepees represent buckled margins of large polygonal structures formed in the supratidal zone by desiccation, wetting, cementation, and mechanical fracturing of sediment layers (Assereto and Kendall, 1977).

Structures closely comparable with the disrupted domical stromatolites are reported to be forming just below Holocene sabkha surfaces, and result from displacive growth of anhydrite within the sediment (Shearman, 1980).

The above comparison, between Sequence 1 from the Duck Creek Dolomite and the complete sabkha sequence, shows that they have similar facies-types and internal stratigraphy. From this evidence, Sequence 1 is interpreted as an upward-shallowing sequence that formed as a result of marine transgression and regression across a sabkha-type coastline.

Sequence 2 is also interpreted as an upward-shallowing sequence. Here, a distinctive feature is the presence of layers of small branching-columnar stromatolites, and large branching-columnar stromatolites, which occur between the basal intraclast grainstone and the laminated dolomite, (i.e. in place of the nucleated domical stromatolite horizon). These branching stromatolites have no modern equivalent. Stromatolites at Lake Clifton, Western Australia, display

a niched wall structure, but have a domical morphology. Columnar stromatolites found today in subtidal settings at Shark Bay (Playford and Cockbain, 1976) are loosely comparable in form to examples described here, but differ markedly in details of internal and external texture.

In the absence of a suitable modern analogue, the depositional environment of the small branching-columnar stromatolites and the large branching-columnar stromatolites is inferred from their position in the upward-shallowing sequence. As shown in Figures 42 and 45, the stromatolitic facies in question are found above the intraclast grainstone (transgressive-barrier deposit) and below the laminated dolomite (intertidal facies). This would indicate that the small branching-columnar stromatolites grew in a subtidal lagoonal environment, whereas the large branching-columnar stromatolites occupied a subtidal lagoon to shallow intertidal setting.

#### *Relic evaporite textures in the Duck Creek Dolomite*

A characteristic feature of modern sabkha sequences is the association of evaporite minerals, notably gypsum and anhydrite, with dolomitized algal-laminated sediments. No occurrence of evaporite minerals has yet been found in the Duck Creek Dolomite; however, there is evidence in the form of relic textures which points to their former development, albeit on a small scale.

Apart from the disrupted domical stromatolites described earlier, many of the supratidal facies in the upward-shallowing sequences contain irregular fenestrae (0.01–0.2 m wide) that cut across, merge into, or disturb the sedimentary layering. The internal structure of some of

these fenestrae (Fig. 49) is similar to the chicken-wire texture which results from the growth of anhydrite in Holocene and ancient sabkha profiles (Robertson-Handford et al., 1982). In many of the Duck Creek Dolomite examples, the original evaporite minerals have been replaced by anhedral or subhedral dolomite spar. In other cases the replacement mineral is silica, either in the form of chalcidony (optically length fast or length slow), or coarsely crystalline, anhedral to subhedral quartz.

## Outer-shelf and slope-and-basin facies association

### Description

The outer-shelf and slope-and-basin facies association (Fig. 50A, B, C, D) comprises thin-bedded dolomite and thin- to very thick-bedded dolomitic conglomerate.

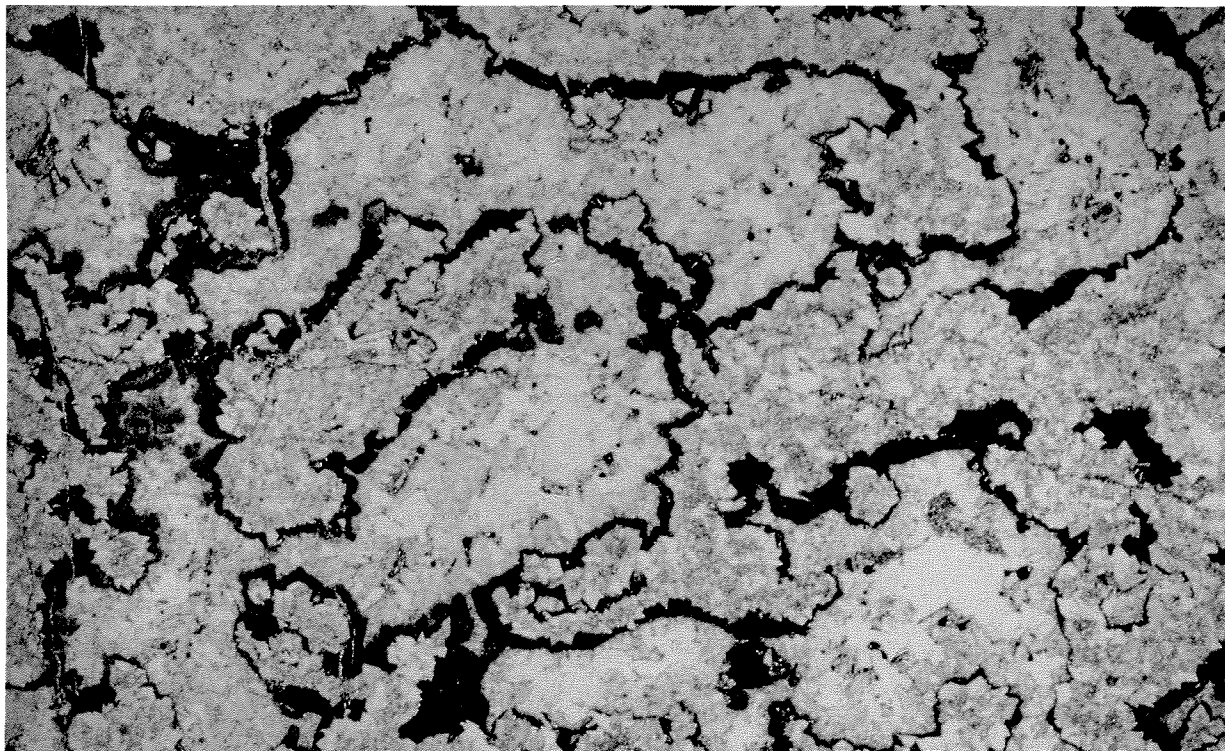
Thin-bedded dolomite (including nodular dolomite) is the most abundant rock type in this association. Beds are generally 0.01–0.15 m thick (Fig. 50A) and consist of grey-, mauve-, or buff-weathering dolomite, often with layers and nodules of black or red chert. The dolomites are planar to undulose laminated, and are generally separated by 1–100 mm of dolomitic, chloritic, or ferruginous mudstone. Small syndepositional folds and boudinaged layers may be present locally. In thin section, the dolomite is seen to consist of fine- to coarse-grained (mostly 0.05–0.2 mm) anhedral spar, with some laminae consisting of dolomitized sand-sized peloids.

Thin-bedded dolomites are transitional into nodular dolomite (Fig. 50B). Their fabric ranges from a gentle pinch-and-swell in the dolomite layers, to a complex network of interlocking nodules, which resembles a mechanical breccia.

Thin to very thick (0.05–20 m) beds of clast- and matrix-supported, very coarse-grained conglomerate, occur interlayered with the thin-bedded dolomite (Fig. 50C, D). Beds are characterized by sharp lower bounding surfaces and irregular tops, often with projecting clasts. Conglomerates consist of a chaotic mixture of dolomite fragments set in a matrix of chloritic or dolomitic mudstone, coarsely crystalline dolomite, or sparry quartz. Clasts are generally 0.01–0.5 m across, angular to rounded, and consist of thin-bedded, parallel-laminated dolomite, mudstone, and fragments of pre-existing conglomerate. Rarely, the thicker beds show an overall upward decrease in clast-size, while in others the clast fabric defines medium-scale slump folds.

### Interpretation

Laterally continuous bedding, parallel lamination, lack of scouring, and mudstone interbeds suggest that the thin-bedded dolomites were deposited in a low-energy environment which received small amounts of terrigenous detritus in suspension. Many carbonates are dolomitized and recrystallized, making it difficult to determine their origin. Most were probably fine-grained before burial, and may have been carbonate suspension sediments, derived from the shelf. Coarser grained peloidal laminae are



GSWA 25215

**Figure 49** Coarsely crystalline, subhedral to anhedral dolomite spar, interpreted as a replacement after former anhydrite. The anhydrite is believed to have grown displacively within the original sediment, forcing it aside until only vestiges remain. Traces of original sediment are now represented by the dark, finely crystalline dolomite walls. Supratidal facies, Duck Creek Dolomite, Duck Creek Gorge.



**Figure 50A** Thin-bedded slope-and-basin facies dolomite. Dolomite beds are planar to undulatory laminated and, in thin section, are seen to comprise anhedral dolomite spar with local peloid layers. Beds are separated by dolomitic, chloritic or ferruginous mudstone and chert. Duck Creek Dolomite, 50 km west of Paraburdoo.



**Figure 50B** Nodular dolomite. "clasts" comprise anhedral dolomite spar or chert. This lithology results from differential compaction and/or cementation of thin-bedded dolomite. Slope-and-basin facies, Duck Creek Dolomite, northern Wyloo Dome.

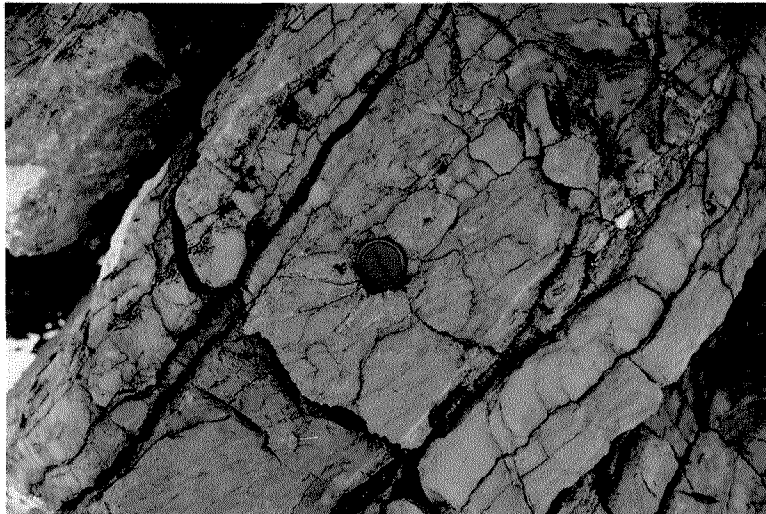


**Figure 50C** Clast-supported dolomitic conglomerate (lens cap) overlying thin-bedded dolomite. Slope-and-basin facies, Duck Creek Dolomite, northern Wyloo Dome.

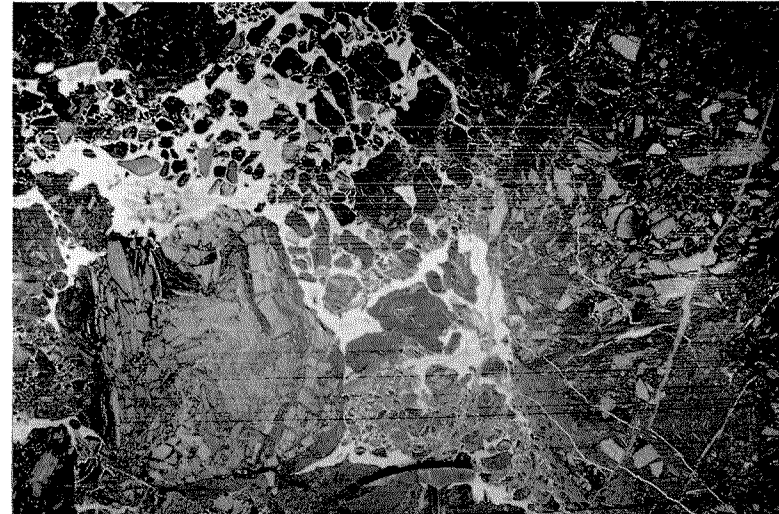


**Figure 50D** Cut surface of slope-and-basin dolomitic conglomerate. Clasts comprise laminated thin-bedded dolomite, and pre-existing dolomitic conglomerate. These are set in a matrix of chloritic mudstone, coarsely crystalline dolomite, and sparry quartz. Horizontal lines are saw marks. Duck Creek, southern Wyloo

interpreted as turbidite sediments, derived from the inner shelf.

Nodular dolomites are considered to result from differential compaction and/or cementation of thin-bedded dolomite (James, 1984); whereas boudinage structures and small- to medium-scale slump folds were formed in response to post-depositional downslope creep.

Thin to very thick beds of dolomitic conglomerate are interpreted as submarine mass-flow deposits, resulting from slumping and dislocation on the shelf slope. The predominance of thin-bedded dolomite clasts, many angular, suggests that they were derived from sediment which was at least partly lithified. Conglomerate fragments point to a history of slope failure and resedimentation.

### Distribution of facies associations

The distribution of facies associations in the Duck Creek Dolomite is summarized in Figure 51. In the south-eastern part of the Ashburton Basin the dolomite rests conformably upon the Mount McGrath Formation and can be subdivided into three stratigraphic units. For example, 5 km east of Success Bore (23° 17' 20"S, 117° 44' 00"E), the lowermost 300 m of strata consists of slope and basin deposits (thin-bedded dolomite and dolomitic conglomerate) with slumped and conglomeratic units locally forming up to 70% of the succession. These pass upwards into approximately 300 m of cyclic shelf carbonates, which are succeeded by an estimated 480 m of slope and basin deposits, consisting principally of thin-bedded and nodular dolomite.

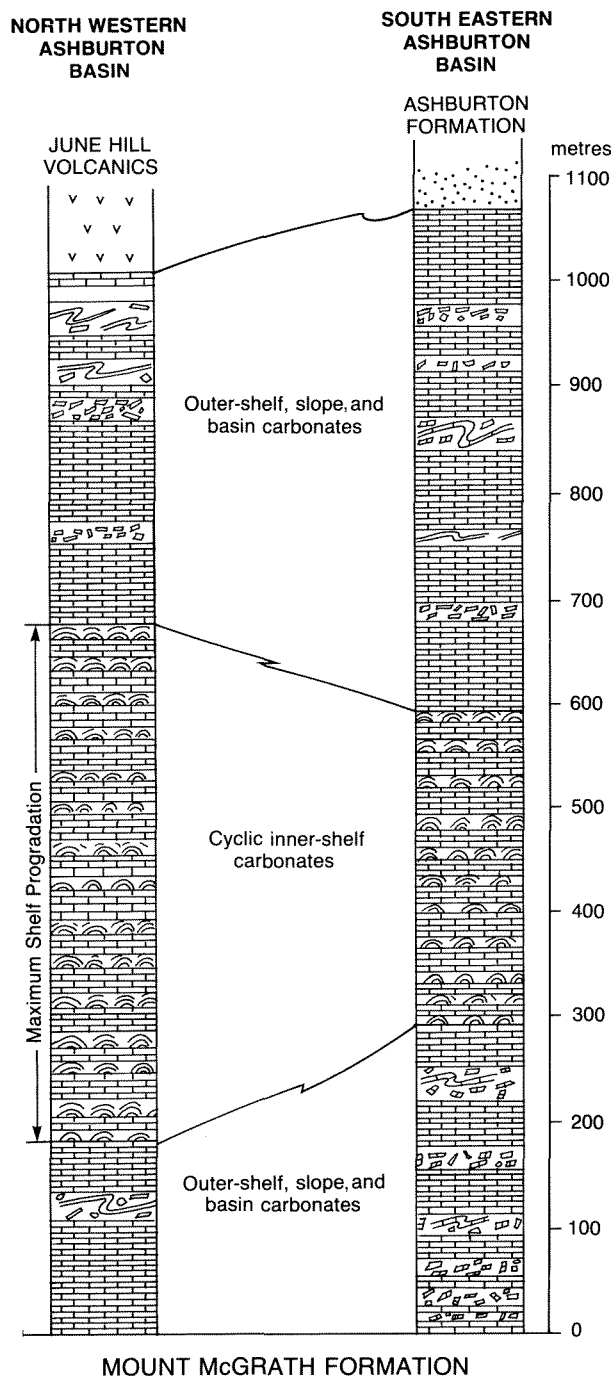
One kilometre northeast of the Aerial lead mine (22° 53' S, 116° 37' E), the middle part of the succession comprises cross-stratified and parallel-stratified barrier facies (quartzitic grainstones); these are overlain by some 500 m of slope and basin deposits. Thick-bedded conglomerates are abundant in the lower half of this unit.

In the northwestern part of the Ashburton Basin the Duck Creek Dolomite conformably overlies the Mount McGrath Formation, except around the western part of Wyloo Dome where it unconformably overlies the Mount Bruce Supergroup. Near Duck Creek Gorge (22° 28' 39"S, 116° 19' 25"E), the succession shows a threefold subdivision similar to that seen in the southeast of the region. The lowermost 180 m of strata consist of slope and basin deposits (mainly thin-bedded dolomite), succeeded by an estimated 500 m of cyclic shelf carbonates. The uppermost 300 m of the formation comprises slope and basin dolomites, with some fine-grained siliciclastic horizons, and minor shelf deposits. Thin basalt and mafic tuff layers are interbedded with the uppermost dolomites in the area immediately to the north of June Hill (22° 29' 28"S, 116° 16' 00"E).

### Depositional model and palaeogeographic reconstruction

The following model for Duck Creek Dolomite sedimentation (Figs. 52, 53) is based upon the nature of the facies, their vertical and spatial distribution, and their relationship to underlying rock units. Over the southern and western Pilbara the major controls on sedimentation were:

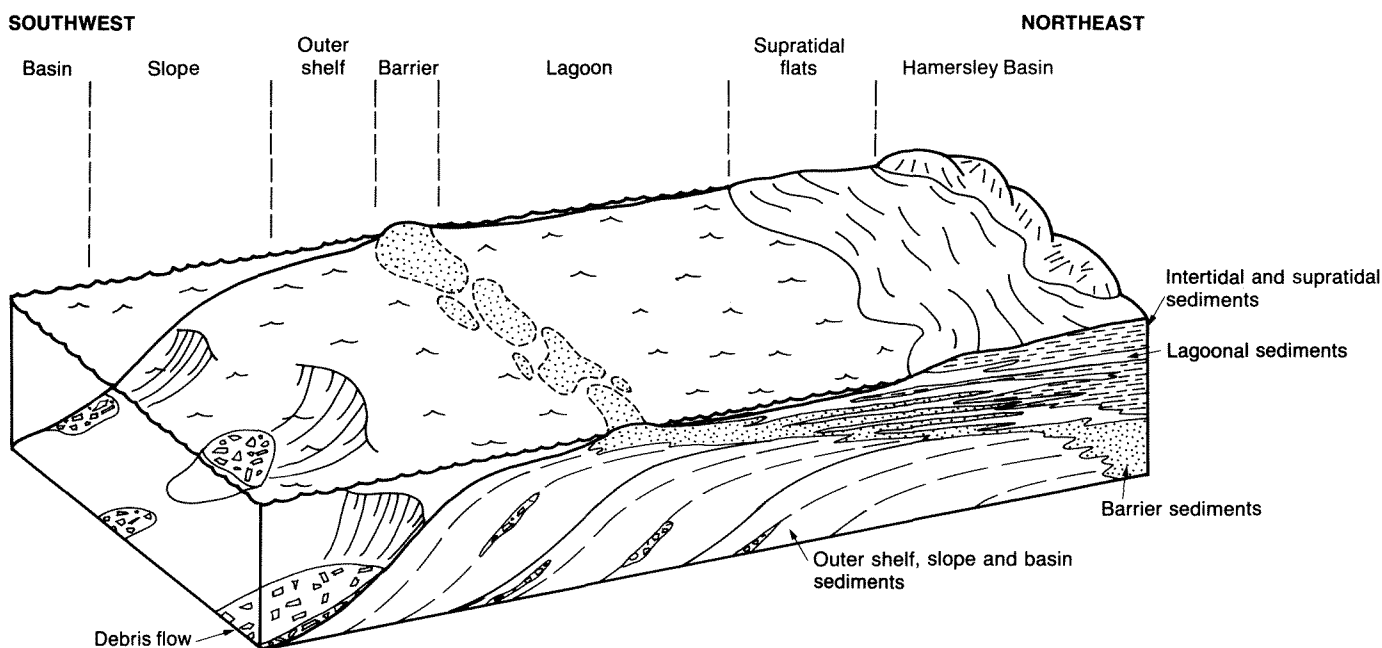
- (a) a low landmass with limited drainage lying northeast of the Ashburton Basin;



GSWA 25217

Figure 51 Generalized vertical profiles showing the stratigraphy of the Duck Creek Dolomite in the northwest and southeast Ashburton Basin.





GSWA 25218

**Figure 52** Depositional model for the Duck Creek Dolomite during the shelf progradation phase. See text for discussion.

- (b) a shallow carbonate shelf with a moderately steep outer slope, fringing the southwestern margin of the landmass; and
- (c) a deep basin located further to the south and west.

The Duck Creek Dolomite was laid down in response to gradual deepening of shelf waters, and partial drowning of the northeastern landmass, which began during the latter part of Mount McGrath Formation sedimentation. As a result of this relative rise in sea level, supply of terrigenous detritus ended and carbonate was deposited in waters fringing the land mass.

The principal sites of carbonate accumulation (Fig. 52) were:

- (a) low-lying intertidal and supratidal flats adjacent to the landmass;
- (b) a shallow lagoon, connected to the open sea;
- (c) a sandy barrier system away from the seaward margin of the shelf; and
- (d) a moderate shelf slope further offshore.

Deposition on the shelf was strongly influenced by short-term fluctuations of sea level which resulted in multiple cycles of marine transgression and regression. This history is recorded in the stratigraphy of the shelf deposits, which consist of numerous upward-shallowing sequences formed during repeated drowning, and subsequent progradation, of the tidal flats. Fine-grained carbonate sediment, carried in suspension across the barrier, was deposited below wave base on the outer shelf, shelf slope,

and basin floor. Tectonic instability was probably responsible for the development of debris flows and slump folds on the shelf slope.

The stratigraphy of the Duck Creek Dolomite is broadly uniform throughout the Ashburton Basin; it suggests that the carbonate shelf experienced one major period of progradation, which reached its maximum development while the middle part of the formation was being deposited. The facies in the upper part of the Duck Creek Dolomite indicate that the period of outbuilding was followed by drowning of the shelf and a return to slope and basin sedimentation.

## Discussion

The depositional setting envisaged for the Duck Creek Dolomite has many characteristics of a distally steepened carbonate ramp (Read, 1985). In this model, the major break in slope occurs not at the seaward margin of the offshore barrier, but many kilometres further offshore. Because the barrier facies lie well back from the break in slope, deep-water conglomerates lack clasts of shallow-shelf sands, and instead contain fragments of low-energy outer-shelf and slope facies. Read (1985) notes that carbonate shelves of this type may develop where faulting or flexuring steepens the outer part of the shelf.

Thorne (1985), commented on the two forms of upward-shallowing sequence recognized in the inner-shelf facies association, and pointed out that they differ not only in constituent lithotypes, but also in thickness and stratigraphic distribution. Sequence 1, abundant low in the shelf succession, is on average 1.5 m thick; this is approximately half the thickness of Sequence 2, which

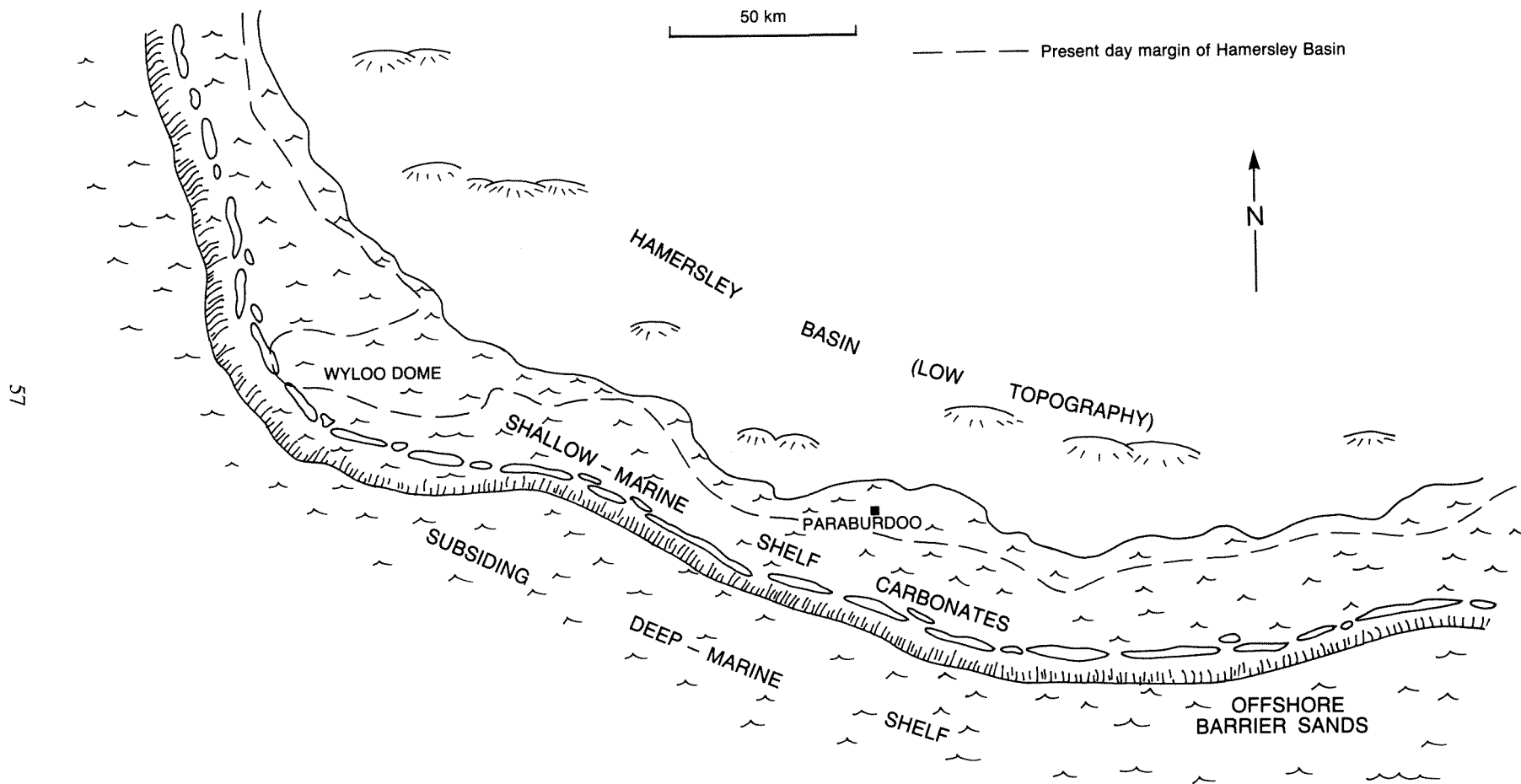


Figure 53 Palaeogeography of the southwestern Pilbara during deposition of the middle Duck Creek Dolomite. This reconstruction shows the maximum extent of shelf progradation. The locations of Paraburadoo, Wyloo Dome, and the southwestern margin of the Hamersley Basin are shown for reference.



occurs most frequently in upper levels of the shelf succession. Most of the difference is due to poor development of the lagoonal to lower intertidal facies in Sequence 1. The thickness, prior to compaction, of the lagoonal portion of the upward-shallowing sequence largely reflects the depth of the original lagoon; this indicates that the lagoon was poorly developed early in the history of the shelf, but in time became deeper and probably wider. This environment, with its higher wave energies, was apparently a favourable setting for growth of the small branching-columnar, and large branching-columnar, stromatolites of Sequence 2.

In many coastal sabkhas of the Abu Dhabi region, zones of nodular anhydrite make up at least half the thickness of supratidal deposits (Shearman, 1980). In contrast, relic evaporite textures in the Duck Creek Dolomite form less than 5% of the supratidal facies. Although some anhydrite in the Duck Creek Dolomite may have vanished without trace during erosion or diagenesis, it is unlikely that evaporites were ever as widespread in the Duck Creek Dolomite as in present-day sabkhas of the Trucial Coast. This may indicate that the southern Pilbara was cooler, and possibly more humid, than the Arabian Gulf today.

No satisfactory explanation has been found for the history of marine transgression and regression recorded in the shelf association. White (1981) and Grotzinger (1986) discussed possible mechanisms for producing repeated transgressions in carbonate environments; these include local tectonic subsidence, global tectonism, or glaciation. Any of these mechanisms, or combinations of them, could account for the repetition of upward-shallowing sequences observed in the Duck Creek Dolomite.

## June Hill Volcanics

The June Hill Volcanics comprise mafic lava (some pillowed), tuff, and agglomerate, interbedded with felsic volcanics and sedimentary rocks. The formation conformably overlies the Duck Creek Dolomite north of Wyloo Dome; it is disconformably overlain by the Ashburton Formation — a relationship recognized by Daniels (1970), who nevertheless included the volcanic rocks within the Ashburton Formation. The June Hill Volcanics are up to 120 m thick in the vicinity of June Hill (22° 29' 28"S, 116° 16' 00"E), but northwards they thin and wedge out over a distance of 45 km.

Immediately north of June Hill, the contact between the Duck Creek Dolomite and the volcanics is transitional: thin beds of tuff, containing relic shards, and basalt, are interbedded with the uppermost dolomites. These beds are succeeded by up to 75 m of crystal and lithic tuff, or coarse pillow-breccia (Fig. 54) and basalt. The uppermost



GSWA 25220

**Figure 54** Basaltic breccia composed of poorly sorted fragments of sparsely vesicular fine-grained basalt. June Hill Volcanics, 5 km north of June Hill.

basalts are interbedded with dolomite and volcanoclastic rocks. Thirty five kilometres north of June Hill, this assemblage makes up most of the formation.

Williams (1968) reports that a localized suite of strongly chloritized and carbonated, possibly acid, lava and intrusive rocks are associated with, and overlie, the Duck Creek Dolomite immediately northeast of Deepdale (21° 42' S, 116° 05' E). Ferruginous shale, tuff, and thin beds of stromatolitic dolomite are interbedded with the volcanic rocks, which are correlated with the June Hill Volcanics.

A tuffaceous siltstone from the June Hill area yielded a Rb–Sr rock model age of 1811 Ma (Leggo et al., 1965); data from an acid porphyry in the Deepdale area gave a Rb–Sr rock model age of  $1977 \pm 165$  Ma (Compston and Arriens, 1968). Both dates have been recalculated using  $^{87}\text{Rb}$  decay constant =  $1.42 \times 10^{-11} \text{ a}^{-1}$ .

## Chapter Six

# Ashburton Formation

The Ashburton Formation conformably overlies the Duck Creek Dolomite over much of the Ashburton Basin. Exceptions occur around the western closure of Wyloo Dome, where it directly overlies the Fortescue Group, and north of Wyloo Dome, where it disconformably overlies the June Hill Volcanics. The Ashburton Formation is unconformably overlain by the Capricorn Formation and by the Mount Minnie, Bresnahan, and Bangemall Groups.

Structural complexity and lack of marker horizons make it difficult to assess the thickness of the Ashburton Formation. Daniels (1968) suggested a figure of 7800 m, based on a transect in the southeastern part of TUREE CREEK. He did not, however, take full account of deformation in this area, and regarded the value as possibly suspect. Horwitz (1980) suggested a thickness of over 15 km for the formation in the southeastern part of the Ashburton Basin. Included in this figure are 6 km of Capricorn Member, a unit no longer considered part of the Ashburton Formation (Horwitz, 1982).

A summing of the thicknesses of distinctive lithological units in a transect across the formation indicates a minimum thickness of 5–6 km, whereas estimates based upon a simple unfolding of major  $D_2$  fold structures suggest a thickness of 12 km. Therefore, the thickness of the Ashburton Formation appears to be between 5 km and 12 km.

The outcrop of the Ashburton Formation is shown in Figure 55. The formation is composed of mudstone and immature sandstone, interbedded with minor amounts of conglomerate, BIF and chert, dolomite, and felsic to mafic volcanics. This chapter describes and interprets the principal lithofacies associations in the Ashburton Formation, and discusses sandstone and conglomerate provenance. Petrographic studies of the sandstones are based on the method of Dickinson (1970), and all palaeocurrent data have been corrected for effects of tectonism (Dott, 1974).

## Lithofacies

### Mudstone and siltstone

#### Description

Mudstone and siltstone (Fig. 56A, B) make up an estimated 65% of the Ashburton Formation. Chloritic,

and ferruginous, mudstone occurs as layers a few millimetres to several metres thick that are interbedded with sandstone, conglomerate, or chemical deposits; they also form units up to several hundred metres thick. Mudstones are either structureless or parallel laminated.

Chloritic siltstones generally occur as layers, 1–200 mm thick, within thick mudstone sequences, or as a capping to thin- to medium-bedded sandstones. Their internal structure consists of parallel lamination or climbing ripple cross-lamination. In many beds, primary structure is modified by soft-sediment deformation.

#### Interpretation

The fine grain-size, parallel lamination, and lack of scouring suggest that the mudstones were laid down from suspension in a low-energy environment. Parallel-laminated siltstones are also interpreted as suspension deposits, for similar reasons. Siltstones that display climbing ripple cross-lamination were formed under lower flow-regime conditions, when there was moderate to high sediment fallout from suspension (Harms et al., 1982).

### Sandstone

#### Description

Sandstone (Figs. 56, 57) makes up approximately 30% of the Ashburton Formation. Two varieties are recognized, thin- to medium-bedded sandstone; and massive sandstone.

Thin- to medium-bedded (0.01–0.30 m) sandstones have sharp bases, and planar tops which generally grade upwards into siltstone or mudstone. Beds are laterally continuous and consist of fine- to very coarse-grained sandstone. Most fine upwards and display partial, or less commonly, complete development of the Bouma sequence of sedimentary structures (Fig. 57). Most of the thickest sandstones display a well-developed graded (A) division overlain by one or more of the following: parallel-laminated sandstone (B division), ripple-laminated sandstone (C division), and parallel-laminated siltstone and mudstone (D division). In addition, a cross-stratified horizon, not present in the Bouma sequence, is occasionally recognized in some coarse-grained Ashburton Formation sandstones. It forms either the lowest part of the bed or directly overlies the A division. Very thin-bedded

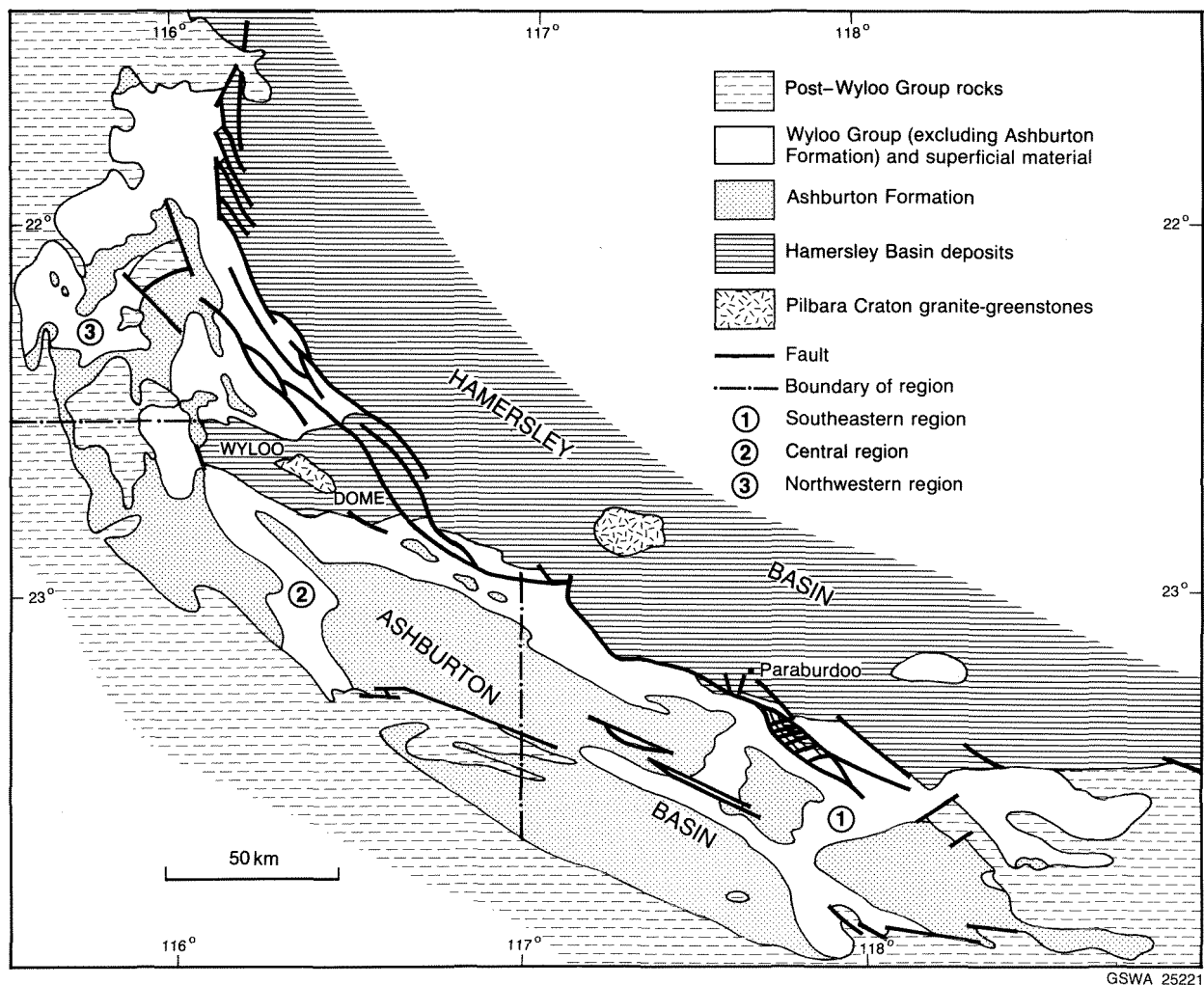


Figure 55 Principal outcrop areas of the Ashburton Formation and location of regions 1, 2, and 3.

sandstones generally display a partial or complete record of the upper part of the Bouma sequence, e.g. BC, BCD, or CD. In many of these, the ripple-laminated division also contains small slump folds and convolute lamination (Fig. 56D)

The lower bedding surfaces of thin- to medium-bedded sandstones may exhibit a variety of flute and tool markings. Many of these have been modified by loading.

Massive sandstones are generally medium- to coarse-grained (locally pebbly); they outcrop in tabular to lenticular beds 0.3 - 5 m thick. Lower bedding surfaces are often gently scoured, and beds may amalgamate to form thicker units. Some individual beds show coarse-tail grading or parallel lamination (Fig. 56A), but most are structureless.

### Interpretation

The Bouma sequence is widely believed to represent deposition from a waning turbidity current (Harms and Fahnestock, 1965; Walker, 1967). The graded (A) divi-

sion forms in response to initial very rapid settling of sediment at the base of the flow. The overlying plane-parallel (B) and ripple-laminated (C) divisions are the result of sediment traction under upper and lower flow regime conditions respectively. The laminated (D) division records deposition of fines from the tail of the current. The interbedded mudstone (E) division represents turbidity-current fines and background pelagic sedimentation. The concept of a waning flow was discussed further by Allen (1984), who showed that another sequence of sedimentary structures could be expected in coarse-grained sandstones. A major difference between the two models is the presence of a cross-stratified division (caused by dune migration under lower flow regime conditions) in the lower part of the coarse-grained sequence.

The various truncated sequences are thought to represent deposition from turbidity currents of differing flow strengths and sediment grain-sizes. Thick beds with a well-developed (A) division were deposited by powerful flows laden with coarse-grained sediment; thinner beds, preserving the BCD or CD divisions, were laid down from weaker currents which carried only fine-grained detritus.



**Figure 56A** Interbedded siltstone and mudstone. Siltstones show climbing-ripple cross-lamination, strongly modified by soft-sediment deformation. Mudstones are parallel-laminated.



**Figure 56B** A typical Ashburton Formation outcrop showing medium-bedded turbidite sandstone interlayered with cleaved mudstone and siltstone, 15 km west of Ashburton Downs Homestead.



**Figure 56C** Interbedded turbidite sandstone and siltstone. The sandstone has a coarse-grained lower (A) division, overlain by a medium-grained, parallel-laminated (B) division. Pencil is 15 cm long. Ashburton Formation, 5 km east of Mount Amy.



**Figure 56D** Climbing-ripple cross-lamination in fine-grained sandstone. The upper part of the bed shows small slump folds; their vergence is parallel to the local palaeocurrent direction (left to right in this photograph). Pencil is 15 cm long. Ashburton Formation, 10 km north of Mount Dawson.

GSWA 25222

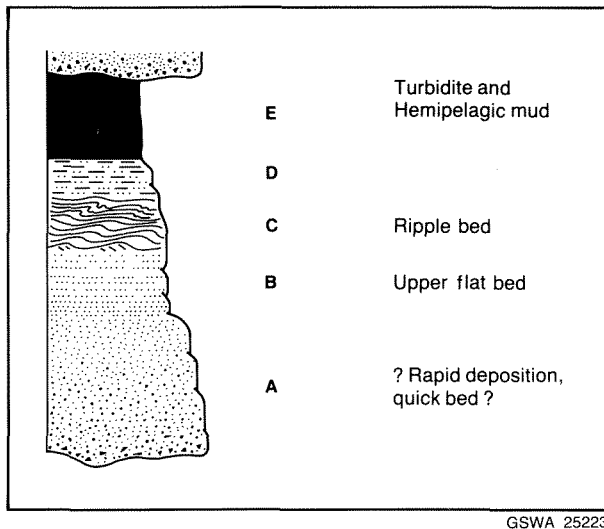


**Figure 57** Five divisions of the Bouma sequence: **A** — massive or graded; **B** — sandy parallel laminations; **C** — rippled and/or convoluted; **D** — interlaminated silt and mud; **E** — mud. Modified from Walker (1986).

The precise method of deposition of the massive sandstones is not clearly understood. Walker (1970) suggests that beds of this type are products of deposition from turbidity currents; others, reviewed by Rupke (1978), have stressed the importance, during deposition of alternative processes such as grain–grain interaction and movement of pore fluids. These processes may have operated together during deposition of the massive sandstones, with different support mechanisms varying in effectiveness as the flow evolved.

## Conglomerate

### Description

Clast- and matrix-supported conglomerates (Fig. 58A, B) constitute approximately 3% of the Ashburton Formation. They outcrop in lenticular or tabular beds 0.3–40 m thick. Lower bedding surfaces are generally sharp and may show evidence of erosion into the underlying bed (Fig. 58A). Upper contacts are sharp or transitional.

Clasts are between 2 mm and 500 mm in diameter (mostly 10–100 mm) and are generally well rounded. The matrix is sandstone. Many beds are parallel-stratified (Fig. 58B) with locally developed normal grading; inverse grading and clast imbrication are rarely observed. Many coarse-grained conglomerates are structureless. Clast types are discussed in the section describing sandstone composition.

### Interpretation

The various conglomeratic rocks are thought to be deposits of high-density, gravel-bearing turbidity currents. Lowe (1982) noted that inversely graded conglomerates are laid down early in the turbidity current’s history, when grain collision and sediment traction are important support mechanisms. Normally graded conglomerates are deposited from suspension, whereas the graded, stratified deposits are laid down in an environment where gravelly suspension sediments are reworked by remnants of the flow. Walker (1975) and Lowe (1982) argue that this spectrum of rock types commonly reflects deposition at sites successively further downcurrent.

## Banded iron-formation and chert

### Description

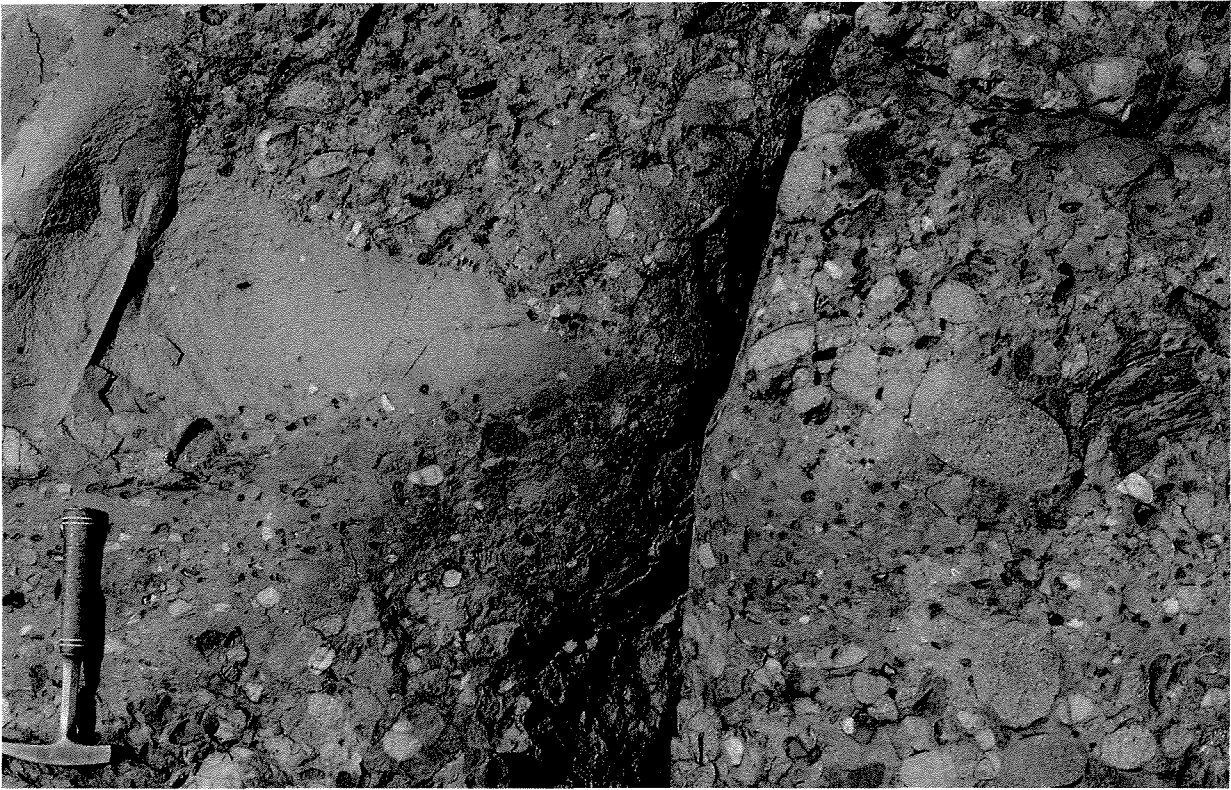
Banded iron-formation (BIF) and chert (Fig. 59A) form approximately 1% of the Ashburton Formation. BIF and chert layers occur as locally developed, 1–10 mm thick cappings on thin-bedded sandstone or mudstone; they also form thick sequences, particularly where overlying intermediate to mafic volcanic sequences. In the latter situations, BIF (commonly manganiferous) and chert are interlayered in beds 0.1–0.5 m thick. Thin BIF and chert are generally parallel-laminated; thick beds are frequently nodular, and exhibit small creep folds and boudinage structures. Small corrugations occur where creep folds intersect the bedding surface. These are similar to the “regional rippling” described by Trendall and Blockley (1970) in BIFs of the Hamersley Group.

### Interpretation

Banded iron-formation and chert are interpreted as chemical deposits that were laid down during periods of low clastic supply. Similar rocks within the Hamersley Group are widely regarded as having originated as precipitates from seawater, although there is disagreement as to the mechanism by which this occurred (Trendall and Blockley, 1970; Trendall, 1983; Ewers, 1983; McConchie, 1984; Morris and Horwitz, 1983). In the Ashburton Formation, the association of the thicker BIF units with intermediate to mafic volcanic sequences suggests that supply of iron may have been locally enhanced by seawater circulating through, and leaching, the volcanic pile.

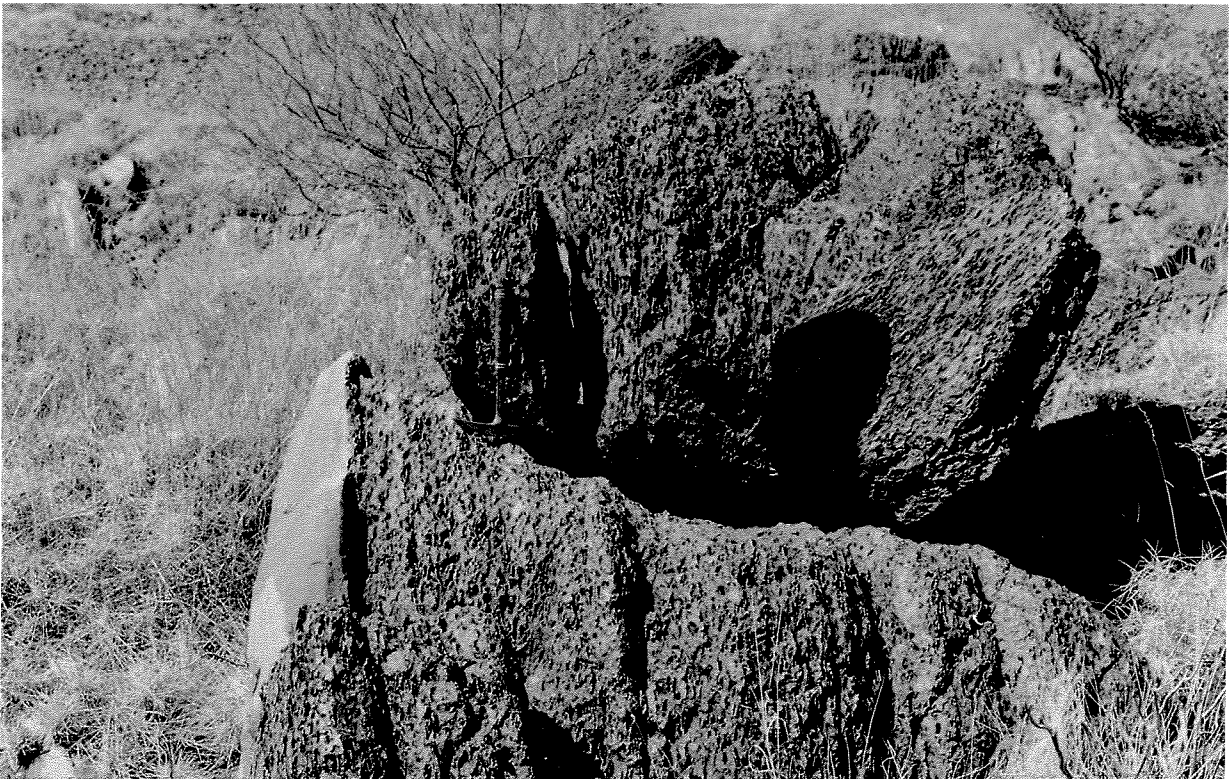
The iron- and silica-rich layers probably accumulated as gels on the sea floor (McConchie, 1984). Because of high interparticle cohesion, these precipitates do not respond to current action as do clastic sediments. Moreover, they are especially susceptible to plastic creep processes, which tend to homogenize irregularities originally present in the deposits. As a result, the most common primary structure is fine banding, thought to reflect seasonal changes in seawater chemistry (McConchie, 1984). Most other structures are of diagenetic origin. Chert nodules form because of lateral redistribution of silica by compaction; the small folds and boudinage structures are the results of downslope creep.





GSWA 25224A

**Figure 58A** A lenticular bed of massive sandstone, truncated by the overlying pebble and cobble conglomerate. Ashburton Formation, 8 km northeast of Mount Stuart Station.



GSWA 25224B

**Figure 58B** Vertical beds of parallel-stratified pebble conglomerate overlying massive sandstone. Ashburton Formation, 7 km east of Mount Amy.



GSWA 25225A

**Figure 59A** Small, soft-sedimentary creep fold in interlayered BIF and chert. Photograph is 10 cm wide. Ashburton Formation, Mount Stuart.

## Volcanic rocks

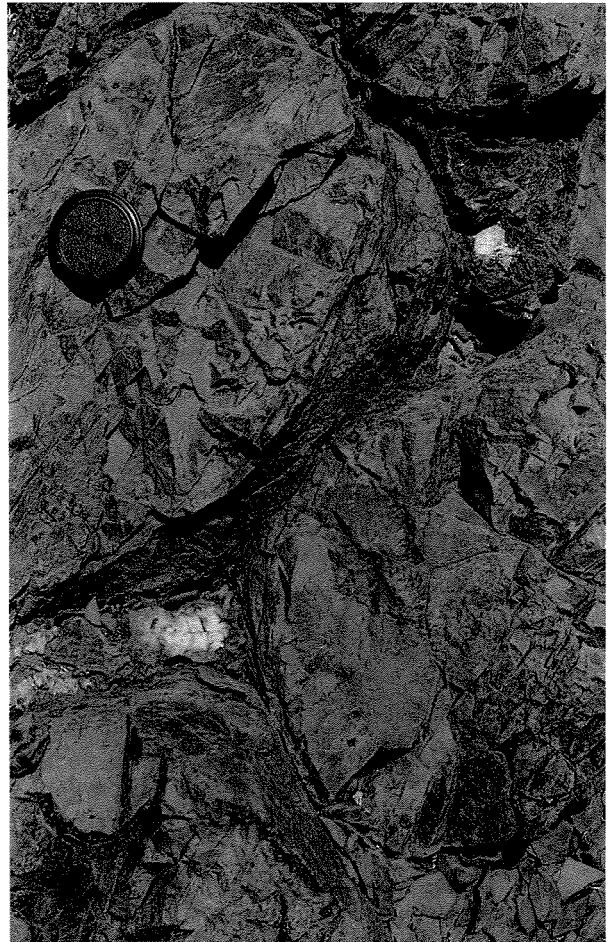
### Description

Volcanic rocks (Fig. 59B) form approximately 1% of the Ashburton Formation; they include localized occurrences of mafic to intermediate pillow lava, pillow breccia, coarse-grained volcanoclastic deposits, finely laminated tuff; and felsic lapilli-tuff.

The most extensive outcrop of intermediate to mafic volcanic rock, which was mapped as a dolerite dyke on the first edition of TUREE CREEK (Daniels et al., 1967), is near Mount Boggola (23° 45' 30"S, 117° 41' 00"E). It comprises approximately 600 m of vesicular pillow lava and pillow breccia (fragments up to 2 m across), with coarse-grained volcanoclastics and laminated tuffs (Fig. 59B). The lowermost volcanics are interbedded with Ashburton Formation mudstone, and the top of the unit is overlain by mudstone or BIF and chert.

A similar suite of rocks is interbedded with mudstone and sandstone northwest of Wyloo Dome (22° 21' 30"S, 115° 48' 00"E). Here, the volcanic sequence is approximately 450 m thick and 2 km long; it is a chaotic assemblage of basalt, which is locally vesicular, coarse-grained basaltic agglomerate, and fine-bedded basaltic tuff.

Localized beds of felsic lapilli tuff, 0.5–1.5 m thick, are interbedded with mudstone and sandstone at three localities immediately to the south of the Kooline–Ashburton Downs road (23° 03' S, 116° 34' E; and 23° 03' 40" S, 116° 37' 00" E; and 23° 02' 10" S, 116° 29' 40" E). At these localities, the flattened lapilli are up to 20 mm in



GSWA 25225A

**Figure 59B** Sparsely vesicular pillow lava, Ashburton Formation, Mount Boggola.

diameter. Several 0.2–1.0 m thick beds of felsic tuff and breccia, interbedded with mudstone occur near Mount Blair (23° 27' S, 117° 09' E). The thick quartz–feldspar porphyry that outcrops to the southeast of Mount Amy (22° 14' 30" S, 115° 57' 30" E), has been interpreted as an allochthonous block of Woongarra Volcanics (Horwitz, 1981); it is discussed further in Chapter 7.

### Interpretation

The pillow lava and pillow breccia are interpreted as being formed by submarine eruption on moderate to steep slopes (Williams and McBirney, 1979). The other deposits are not sufficiently diagnostic to identify their depositional setting.

## Carbonate rocks

### Description

Carbonate rocks form <1% of the Ashburton Formation; they include thin-bedded dolomite and stromatolitic dolomite. Principal occurrences are in the eastern part of the Ashburton Basin, immediately below the Bresnahan



Group unconformity. Much of the following description is based upon unpublished data from W.M. Hunter and K. Grey.

Thin-bedded dolomite has been observed at two localities west of Tunnel Creek (23° 53'E, 118° 31'E and 23° 54'S, 118° 41'E). Dolomite beds are 10–200 mm thick, and are interlayered with chloritic mudstone. Beds may display normal grading, slump folds, and boudinage structures; many contain irregular chert nodules.

At Yindabiddy Pool (23° 54' 00"S, 118° 42' 30"E), an inverted sequence of medium- to thick-bedded stromatolitic dolomite occurs interbedded with grey to black mudstone and siltstone. The partly silicified stromatolites have a flattened domical form, up to 0.3 m across; synoptic relief is 50–200 mm. Locally, beds of columnar stromatolite separate the domical forms.

On the the southern side of the Kunderong Range (23° 41'S, 118° 35'E) finely laminated stromatolitic dolomite crops out beneath the Bresnahan Group unconformity. The sub-parallel, undulose laminae can be traced laterally into partly silicified domical or columnar stromatolites. The columnar forms have been identified as *Pseudogymnosolen* f. indet. and *Patomia* f. indet. (Grey, 1981a; K. Grey, quoted in Tyler et al., in press).

*Patomia* f. indet. has also been recorded in domical bioherms from an area 15 km northwest of Turee Creek Homestead (23° 29'S, 118° 33'E). The bioherms are formed by tall, widely spaced columns, characterized by smooth, steeply convex laminae.

Samples of *Patomia* f. indet. have been obtained from dolomite fragments in alluvium, northeast of Kennedy Creek (23° 44' 45"S, 118° 19' 30"E). Attempts to locate the outcrop have so far been unsuccessful (Grey, 1984).

*Pseudogymnosolen* f. indet. has been described from small dolomite outcrops (23° 36'S, 118° 26'E) near the western end of the Kunderong Range (Grey, 1981b).

## Interpretation

The carbonate rocks were deposited during breaks in the supply of terrigenous detritus to the Ashburton Basin.

Thin-bedded dolomite was probably deposited in a low-energy marine environment, below the effects of wave reworking. The depositional environment of the stromatolitic dolomite is, however, more likely to be shallow-marine (K. Grey, quoted in Tyler et al., in press).

## Lithofacies associations

### Description

Three major lithofacies associations are recognized within the Ashburton Formation: (a) conglomerate–massive sandstone–mudstone; (b) massive sandstone–thin-

medium-bedded sandstone–mudstone; and (c) mudstone–thin-bedded sandstone–BIF and chert.

### Conglomerate–massive sandstone–mudstone association

The conglomerate–massive sandstone–mudstone association (Figs. 60, 61) ranges in thickness from 25–225 m, and is interlayered with the mudstone–thin-bedded sandstone–BIF and chert association. Two sequences of lithofacies are identified. The first (type 1) is of a single conglomerate and sandstone unit, 30–225 m thick; although the thinnest of these (Fig. 60B) may show overall upward-fining grain-size distribution, the thicker sequences are more variable. For example, at Mulga Bore (22° 22' 00"S, 116° 07' 20"E), most of the upper and lower parts of the sequence consist of stratified conglomerate, pebbly sandstone and massive sandstone, while the middle of the sequence consists mainly of channelized pebble and cobble conglomerate (Fig. 60A).

Type 2 sequences (Fig. 61) consist of two or three thick-bedded conglomerate and sandstone units separated by mudstone. The conglomerate and sandstone units are 10–100 m thick and show little systematic variation in grain-size. Interbedded mudstone units are 10–35 m thick; they incorporate thin beds of ripple-laminated siltstone and fine-grained sandstone, and erosively based beds of coarse-grained sandstone and conglomerate.

### Massive sandstone–thin- to medium-bedded sandstone–mudstone association

The massive sandstone–thin- to medium-bedded sandstone–mudstone association forms sequences 7–60 m (mostly 20–35 m) thick: they occur in isolation or as part of a stacked succession up to several hundred metres thick. These sequences are interlayered with the mudstone–thin-bedded sandstone–BIF and chert association. Three types of sequence are recognized:

- (a) upward-coarsening and thickening;
- (b) upward-fining and thinning; and
- (c) disorganized.

Upward-coarsening and thickening sequences (Fig. 62A) range from 7–60 m thick, and are characterized by a basal unit of mudstone and thin- to medium-bedded sandstone, which passes upwards into thicker bedded, massive sandstone with local pebbly sandstone.

Upward-fining and thinning sequences (Fig. 62B) are generally 12–25 m thick, and comprise a thick-bedded sandstone or pebbly sandstone base, overlain by successively thinner bedded sandstones. In addition, the thickness and frequency of mudstone interbeds increases upwards.

Disorganized sequences are up to several hundred metres thick; they show no systematic vertical trend in grain-size or bed thickness.

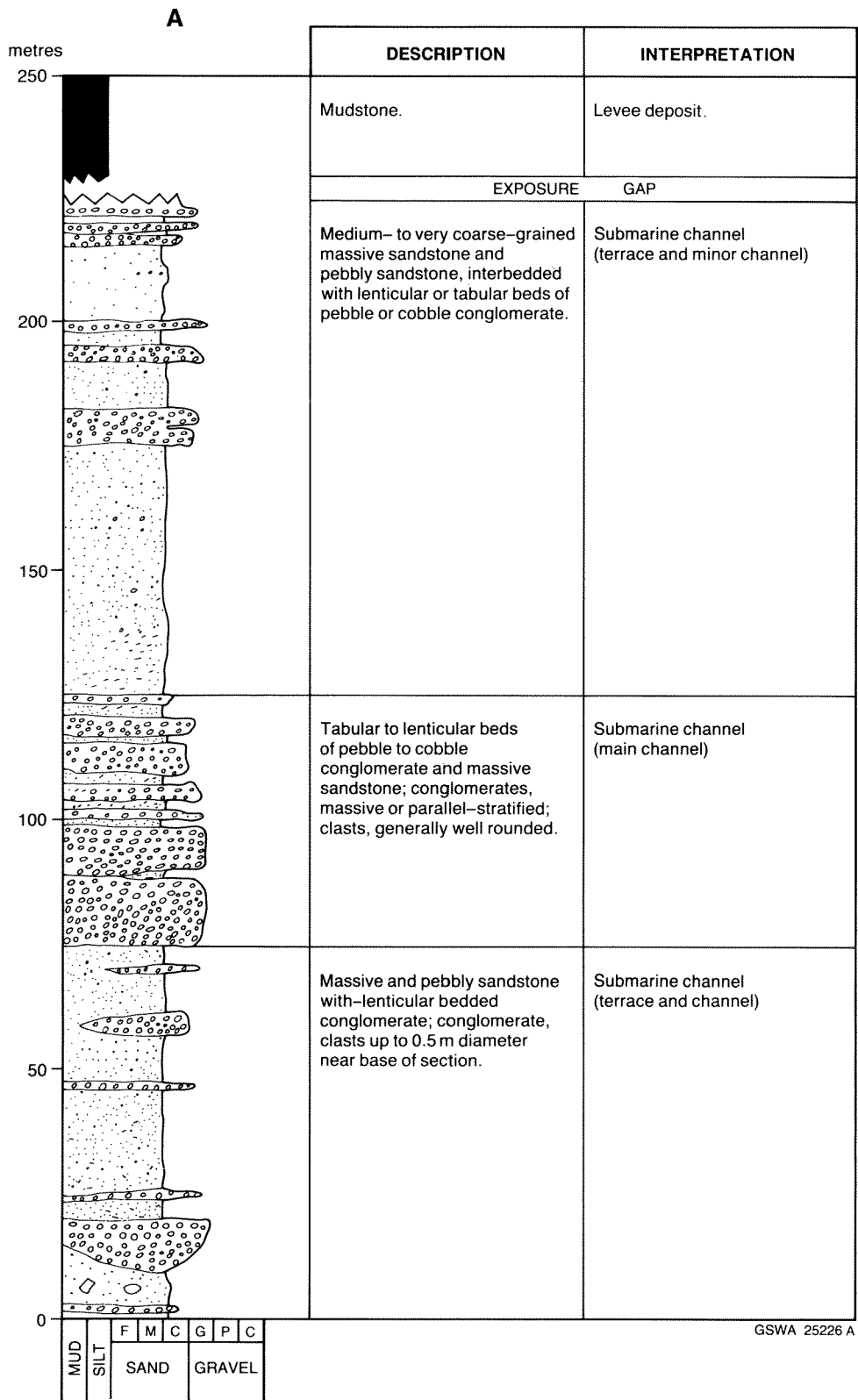
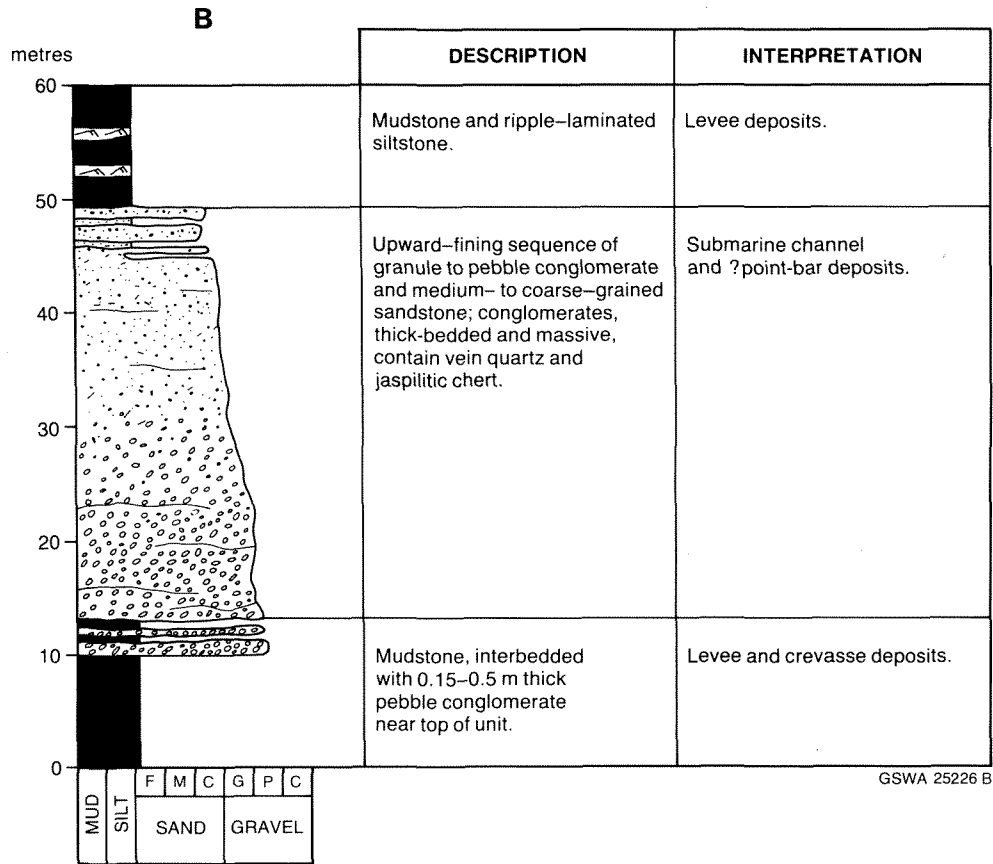


**Figure 60** Vertical profiles showing Type 1 sequences of the conglomerate–massive sandstone–mudstone association, summarizing major rock-types and internal structure. Ashburton Formation. A — at 22°22'05"S, 116°07'20"E. B (opposite) — at 23°33'10"S, 117°45'00". See text for discussion.



### Mudstone–thin-bedded sandstone–BIF and chert association

The mudstone–thin-bedded sandstone–BIF and chert association occurs in sequences ranging in thickness from a few tens to many hundreds of metres and is interlayered with both of the other major facies associations. Most sequences consist of thick intervals of mudstone and siltstone interbedded with minor, thin-bedded sandstone, BIF and chert. No systematic upward fining and thinning, or upward coarsening and thickening trends are apparent in the association.

### Interpretation

The lithofacies associations described above are considered to have been laid down in a deep-marine environment on the basis of the following evidence: presence of very large thicknesses of mudstone over a large area (>17 000 km<sup>2</sup>); abundant turbidite sandstones and massive sandstones; absence of wave-formed structures or other evidence of sustained sediment reworking; and the presence of pillow lavas within the succession.

Studies of both Holocene and ancient deep-sea clastic deposits — see reviews by Howell and Normark (1982), Rupke (1978), Stow (1986), and Walker (1978) — show that they often accumulate as submarine fans, a few to hundreds of kilometres across. Walker (1978) has shown

that many submarine fans show a broad threefold subdivision of depositional environments:

- (a) the upper fan, comprising the gravelly main feeder channel and adjacent muddy levees;
- (b) mid fan, where rapid sand deposition takes place in braided distributary channels and on associated terminal lobes; and
- (c) lower fan to basin plain, where unconfined turbidity currents deposit thick sequences of mudstone and thin-bedded sandstone.

The conglomerate–massive sandstone–mudstone association is interpreted as a major channel deposit. In a study of a well-exposed Cambro-Ordovician submarine channel system, Hein and Walker (1982) identified three important sub-environments within the main channel complex. These are the deep main channel and associated bars; channelled terraces adjacent to the main channel; and smooth terraces, further away from, and topographically higher than, the main channel. Type 1 sequences from the Ashburton Formation probably represent the depositional record of a migrating major channel system. Stacked beds of pebble and cobble conglomerate are equivalent to the main channel deposits of Hein and Walker (1982); whereas stratified pebble conglomerate, pebbly sandstone, and massive sandstone are similar to

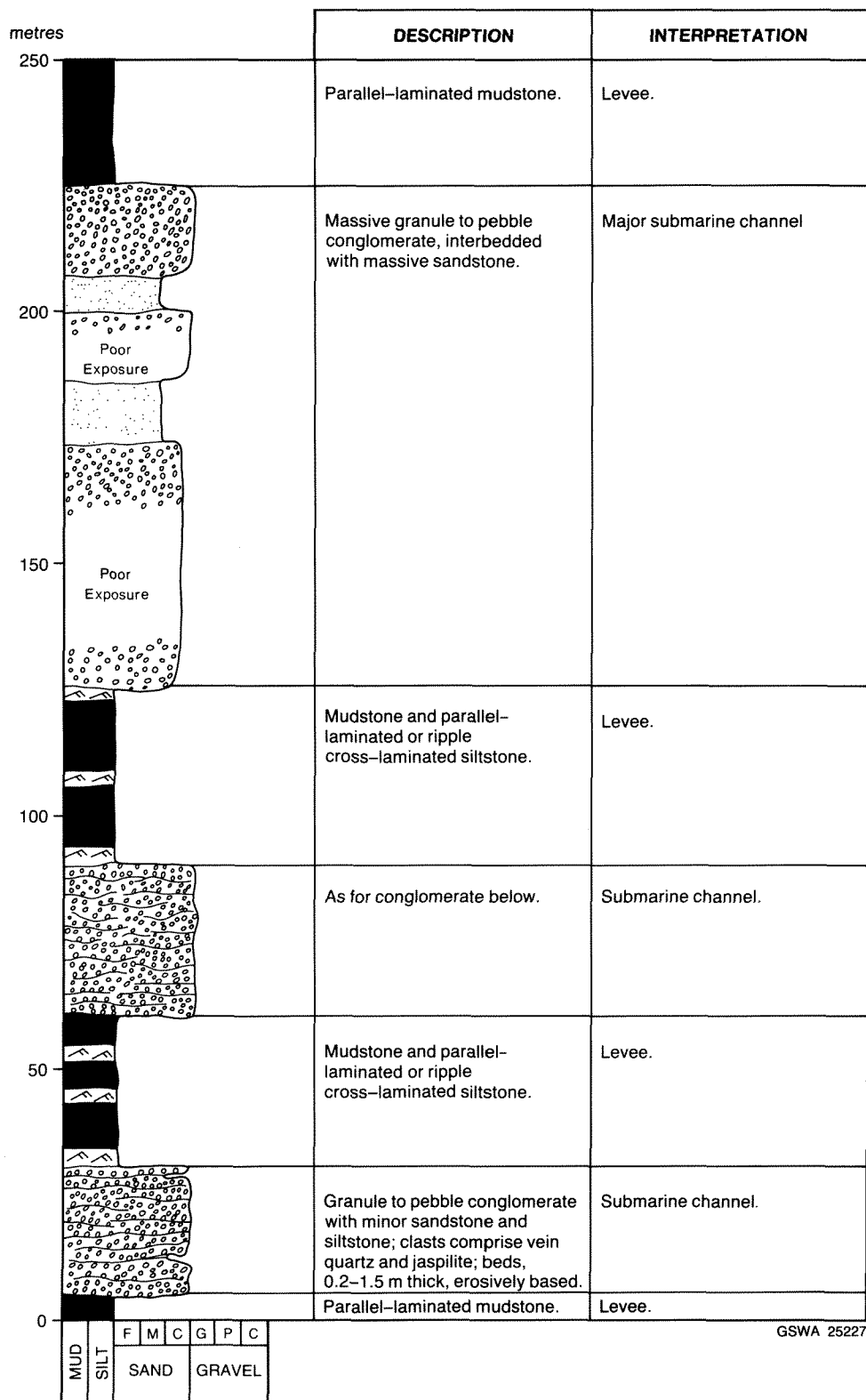
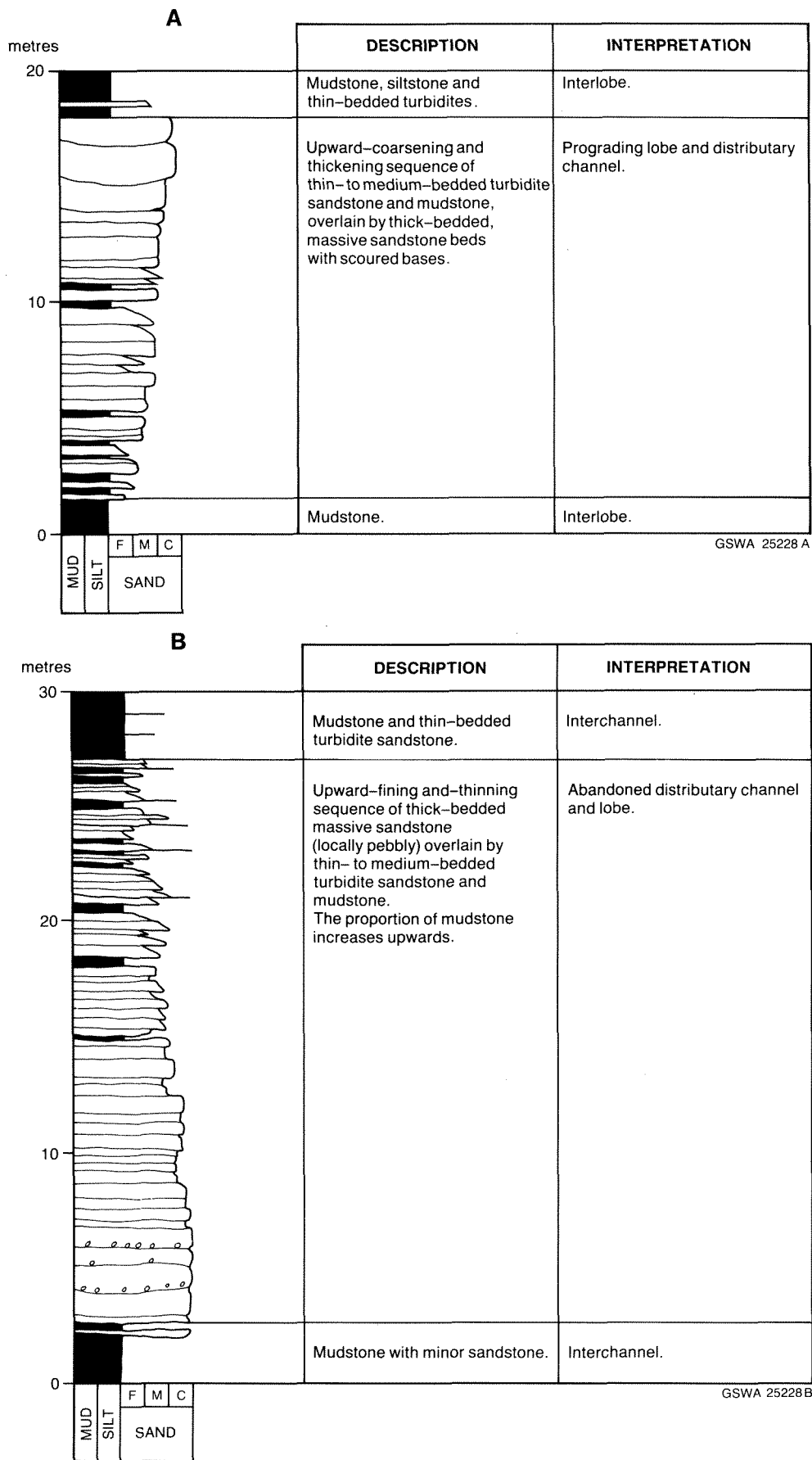


Figure 61 Vertical profile of a Type 2 sequence of the conglomerate-massive sandstone-mudstone association, summarizing major rock-types and internal structure. Ashburton Formation. See text for discussion.



**Figure 62** Sequence organization in the massive sandstone–thin- to medium-bedded sandstone–mudstone association of the Ashburton Formation. **A** — upward-coarsening and thickening. **B** — upward-thinning and fining.

the various terrace deposits laid down on either side of the main channel. The presence of isolated lenses of cobble conglomerate, up to 8 m thick, within terrace deposits of some type 1 sequences, suggests that the main channel split locally.

Upward-fining (type 1) sequences may have formed during the migration of a submarine channel–point-bar system in a manner analogous to that described for fluvial systems (Allen, 1965). If this interpretation is valid, the thickness of the channel–point-bar sequences (approximately 35 m) would roughly correspond with the depth of the former channel.

Type 2 sequences are also thought to have resulted from lateral migration of a submarine channel complex. The conglomerate units are interpreted as main channel deposits, whereas the interbedded mudstone and rippled siltstone are thought to represent levee deposits laid down from dilute turbidity currents overflowing from the main channel (Mutti, 1977). Thin, erosively based sandstones and conglomerates within the levee sequence represent deposition from more powerful currents that overflowed, or breached the levees.

The massive sandstone–thin- to medium-bedded sandstone–mudstone association is interpreted as the depositional record of a distributary channel and depositional lobe system similar to that present on the mid fan of Walker's (1978) model. Upward coarsening and thickening sequences are regarded as the product of sedimentary lobe progradation. Small-scale upward coarsening and thickening sequences composed of thin- to medium-bedded turbidite sandstone record deposition on the fringe of an advancing lobe away from the main distributary channel supply. Thicker sequences of this type, which are capped by scoured pebbly sandstones, formed when the main body of the lobe, and its associated channel, prograded over the lobe fringe deposits.

Upward fining and thinning sequences which incorporate a basal, scoured pebbly sandstone unit are interpreted as distributary channel deposits. Sequences of this type may have formed during lateral migration of a distributary channel; however, a more likely explanation is that they developed during progressive abandonment of one distributary channel as another developed. Thick (5–50 m) mudstone units, which occur interbedded with channel and lobe deposits, were probably laid down during long periods when channels were abandoned.

Many sandstone and mudstone sequences display neither upward coarsening and thickening nor upward fining and thinning trends. They are likely to have formed as a result of disordered stacking of deposits from adjacent lobes and distributary channels. Similar sequences could also be expected from a single distributary channel and lobe system which had a sustained history of deposition — without undergoing progradation — before abandonment (Collinson et al., 1978).

The mudstone–thin-bedded sandstone–BIF and chert association are thought to have been laid down in a vari-

ety of depositional settings within the deep basin. Very thick (hundreds of metres) sequences of mudstone and thin-bedded sandstone that are interlayered with the major channel facies are interpreted as channel–levee deposits. Normark et al., (1983), and Piper and Normark (1982, 1983), show that levees are important depositional features on modern submarine fan systems off the North American coast. In these Holocene examples, levee–channel systems commonly have widths of several tens of kilometres; the channel floor to levee crest relief may be as much as 1 km (Normark et al., 1983). The principal deposits of levees are thought to be mudstone, siltstone, and thin turbidite sandstone (Mutti, 1977; Winn, Jr and Dott Jr, 1979). Within the Ashburton Formation, sequences of mudstone and thin-bedded sandstone are also associated with the distributary channel and lobe deposits. Thin sequences were probably laid down on inactive parts of the fan during periods of channel and lobe abandonment. Thicker accumulations, such as occur above the Duck Creek Dolomite or June Hill volcanics, may represent basin-plain deposits.

## Distribution of lithofacies associations and palaeocurrent data

The distribution of lithofacies within the Ashburton Formation is shown in Plate 1. Because of structural complexity and locally poor outcrop, only a very broad-scale subdivision of the formation is attempted. To facilitate description, the outcrop of the Ashburton Formation is subdivided into (Fig. 55): a southeastern region, lying to the east of longitude 117°; a central region, bounded by latitude 23° 30' S and longitude 117° E; and a northwestern region to the north of latitude 22° 30' S.

### Southeastern region

In the southeastern region the Ashburton Formation rests with a gradational, conformable contact upon the Duck Creek Dolomite. At 23° 07' 10" S, 117° 04' 30" E and 23° 13' 00" S, 117° 24' 30" E, thin-bedded dolomite and dolomitic mudstone are interbedded with chloritic and ferruginous mudstone; the proportion of the latter increases up the section. These argillaceous rocks, interpreted as basin-plain deposits, dominate the lower 100–200 m of the Ashburton Formation. They are overlain by the massive sandstone–thin- to medium-bedded sandstone–mudstone association (distributary channel and lobe deposits).

The massive sandstone–thin- to medium-bedded sandstone–mudstone association crops out as a belt 2.5–10 km wide, which broadly parallels the outcrop of the Duck Creek Dolomite. Within it, the minimum thickness of the association is estimated to be approximately 2.4 km, a value obtained from a relatively unmetamorphosed succession 17 km southwest of Paraburdoo (23° 19' S, 117° 31' E). This association also crops out locally within the mudstone-dominated succession further to the southwest, e.g. Cherrybooka Creek (23° 46' 00" S, 118° 00' 00" E),

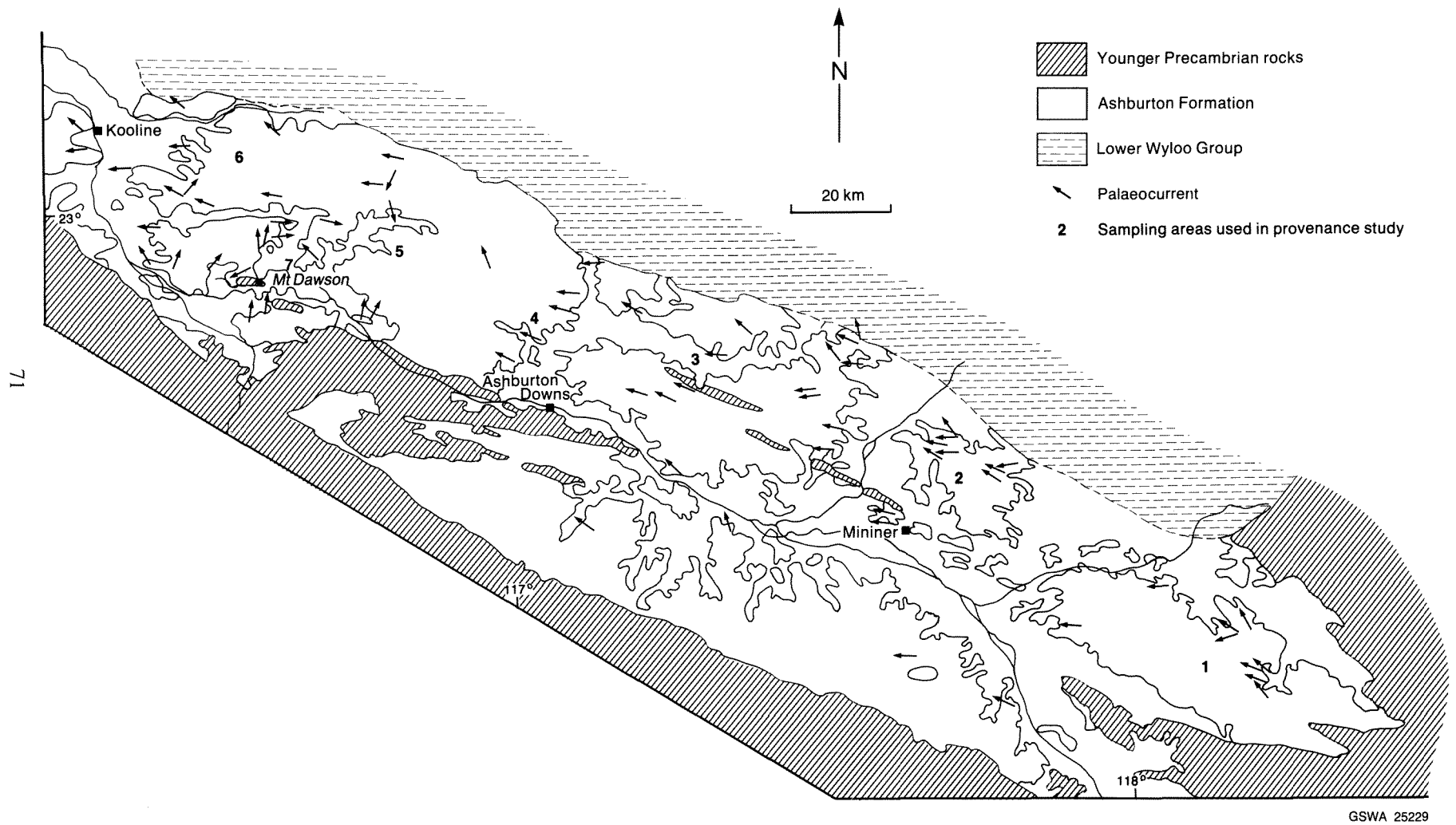


Figure 63 Outcrop map of the southeastern and central part of the Ashburton Basin showing palaeocurrent trends and sampling areas used in Ashburton Formation provenance study.



Fords Creek (23° 44' 00"S, 117° 17' 40"E), and north of Prismoid Hill (23° 29' S, 117° 17' E). In these areas, the sandstone sequences are generally 5–300 m thick.

The mudstone–thin-bedded sandstone–BIF and chert association crops out in a belt 20–50 km wide in the southwest of the Ashburton Basin; it has an estimated minimum thickness of approximately 2.0 km 30 km southwest of Parburdoo (23° 23'S, 117° 30'E) Most of the succession comprises mudstone (with siltstone) and thin-bedded sandstone. Thick (>150 m) deposits of BIF and chert are recorded from the vicinity of Mount Boggola (23° 45' 30"S, 117° 41' 00"E), where they overlie a sequence of mafic and intermediate volcanic rocks.

The conglomerate–massive sandstone–mudstone association occurs as localized sequences interbedded within the mudstone–thin-bedded sandstone–BIF and chert association, e.g. 30 km southwest of Parburdoo (23° 23'S, 117° 30'E); ) 5 km northeast of Mount Elephant (23° 30' 30"S, 117° 39' 00"E; and 30 km east of Mount Bresnahan (23° 52'S, 118° 14'E). Most sequences are 10–200 m thick.

#### Palaeocurrent data

Palaeocurrent data, recorded from flute structures on the bases of turbidite sandstones, are shown in Figures 63 and 64. The vector mean of 293° and low scatter (vector magnitude 0.87) indicate that sediment transport was from east-southeast to west-northwest, parallel to the principal structural trend in the Ashburton Basin.

#### Central region

In the central part of the Ashburton Basin, the Ashburton Formation has a conformable, gradational contact with the underlying Duck Creek Dolomite. Twenty-five kilometres southeast of Wyloo Homestead (22° 46'S, 116° 24'E) the lowest beds comprise 10 m of ferruginous mudstone. They are overlain by an unknown thickness of the massive sandstone–thin- to medium-bedded sandstone–mudstone association. In the southeast, these deposits crop out as a 4–6 km wide strip adjacent to the Duck Creek Dolomite, and also within large F<sub>2</sub> synclinal closures near Mount Dawson (23° 09' 10"S, 116° 32' 00"E). In the latter setting, this association is approximately 1 km thick. To the west, mixed sandstone–mudstone assemblages also crop out extensively in the area bounded by Kooline (22° 54' 30" S, 116° 17' 00"E) and Glen Florrie (22° 56' 00"S, 115° 58' 50"E) Homesteads and Hardey Junction (22° 44' S, 116° 07'E).

The mudstone–thin-bedded sandstone–BIF and chert association crops out over a large area southeast of Kooline Homestead. Between 23° 05'S, 116° 40'E and 23° 09'S, 116° 57'E) these deposits are interbedded with up to 100 m of the conglomerate–massive sandstone–mudstone association.

#### Palaeocurrent data

Over most of the region, the major palaeoflow is directed towards 295°, i.e. the same transport direction as in

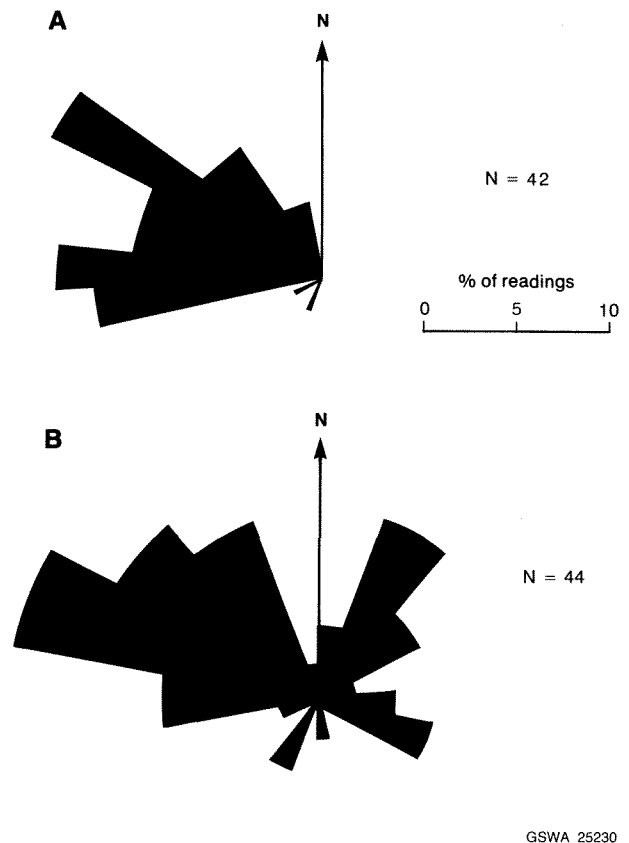


Figure 64 Ashburton Formation palaeocurrent data. A — southeastern Ashburton Basin. B — central Ashburton Basin.

the southeastern region. In addition, data from Mount Dawson area (recorded from upward-facing F<sub>2</sub> folds) shows a radial pattern with its axis directed towards 040° (Fig. 64B).

#### Northwestern region

North of Wyloo Dome, the Ashburton Formation disconformably overlies the June Hill Volcanics. The lowermost 100–500 m of the formation comprises mudstone, thin-bedded sandstone, BIF, and chert; the latter well developed in the vicinity of June Hill (22° 29' 28" S, 116° 16' E). These deposits are overlain by approximately 1 km of the massive sandstone–thin- to medium-bedded sandstone–mudstone association, which is succeeded by at least 2 km of mudstone and thin-bedded sandstone, with minor BIF and chert. The conglomerate–massive sandstone–mudstone association occurs in scattered exposures to the east and south of Mount Amy (22° 15'S, 115° 53'E), but is best developed to the northeast of Mulga Bore (22° 22' 00"S, 116° 07' 20"E).

#### Palaeocurrent data

No palaeocurrent data have been obtained from the northwest region.

## Summary of Ashburton Formation stratigraphy

Structural complexity and lack of continuous marker horizons make it impossible to provide a detailed stratigraphy for the Ashburton Formation. It is possible, however, to establish a very broad-scale stratigraphy based on distribution of the principal facies associations. Over most of the Ashburton Basin a threefold subdivision can be applied (Fig. 65). The lower levels of the formation consist of a few tens to several hundred metres of the mudstone–thin-bedded sandstone–BIF and chert association, which are interpreted as basin–plain deposits. These are overlain by 1–2.4 (minimum) km of the massive sandstone–thin- to medium-bedded sandstone–mudstone association (submarine distributary–channel and lobe deposits), which are succeeded by another mudstone–thin-bedded sandstone–BIF and chert unit which has an estimated minimum thickness of 2.5 km. This upper unit is interpreted as a sequence of submarine channel, levee, and interchannel deposits; it includes localized occurrences of the conglomerate–massive sandstone–mudstone association and the massive sandstone–thin- to medium-bedded sandstone–mudstone association.

Exceptions to this broad-scale stratigraphy occur in two areas: at the western closure of the Wyloo Dome, where the massive sandstone–thin- to medium-bedded sandstone–mudstone association occurs at the base of the formation; and near Mount Dawson, where a similar assemblage, 1 km thick, outcrops in the upper part of the formation.

### Sandstone composition

This section describes the composition of the Ashburton Formation sandstones, with a view to determining provenance. To gain maximum information about source-rock composition, a point-counting method based upon that of Dickinson (1970) was used. The main departure from

Dickinson's method concerns the category to which clasts of fine-grained, polycrystalline quartz are assigned. Using Dickinson's (1970) approach, these fragments would be recorded as polycrystalline quartz, and included with other quartz clasts, generally of igneous or metamorphic origin, on the sandstone composition diagrams. In the Ashburton formation sandstones, most of these clasts are chert and are therefore recorded as sedimentary lithic fragments.

One hundred and sixty thin-sections of sandstone were examined under the petrological microscope. Of these, 65 medium- to coarse-grained samples were point-counted, using 300 points per sample. Attempts to stain for K-feldspar, using cobaltinitrate solution, met with little success; however, it was found that K-feldspar could be readily distinguished on the basis of its cross-hatched twinning, characteristic exsolution pattern, weathering, and relative refractive index.

Sandstone data are supplemented by information from 25 conglomerate samples. It was found that conglomerate compositions generally reflect the greater resistance to abrasion of certain clasts, especially vein quartz and chert, and could not therefore be used to accurately reconstruct provenance.

To facilitate description, the Ashburton Basin is subdivided into southeast, central, and northwestern regions (Fig. 55).

### Southeast and central Ashburton Basin

#### Results

Point-count data from 52 Ashburton Formation sandstones taken from the southeast and central part of the Ashburton Basin are shown in Table 2 and Figures 66 and 67. In Table 2, samples from the same outcrop area (numbered 1–7 in Fig. 63) are grouped together, and the seven areas are listed in order of increasing distance from the eastern end of the Ashburton Basin. Areas 1–6 are charac-

ESTIMATED THICKNESS	LITHOFACIES ASSOCIATION	INTERPRETATION
2.5 – 6 km	Mudstone and thin-bedded sandstone with local BIF and chert; incorporates several conglomerate and sandstone units, generally 5 – 200 m thick.	Submarine – channel and levee system.
2.4 – 5 km	Massive sandstone; thin- to medium-bedded sandstone and mudstone with minor conglomerate and pebbly sandstone.	Submarine distributary channels and depositional lobes.
20 – 500 m	Mudstone and thin-bedded sandstone with local BIF and chert.	Deep marine basin–plain.
Duck Creek Dolomite or June Hill Volcanics		

GSWA 25231

Figure 65 Generalized stratigraphy for the Ashburton Formation.

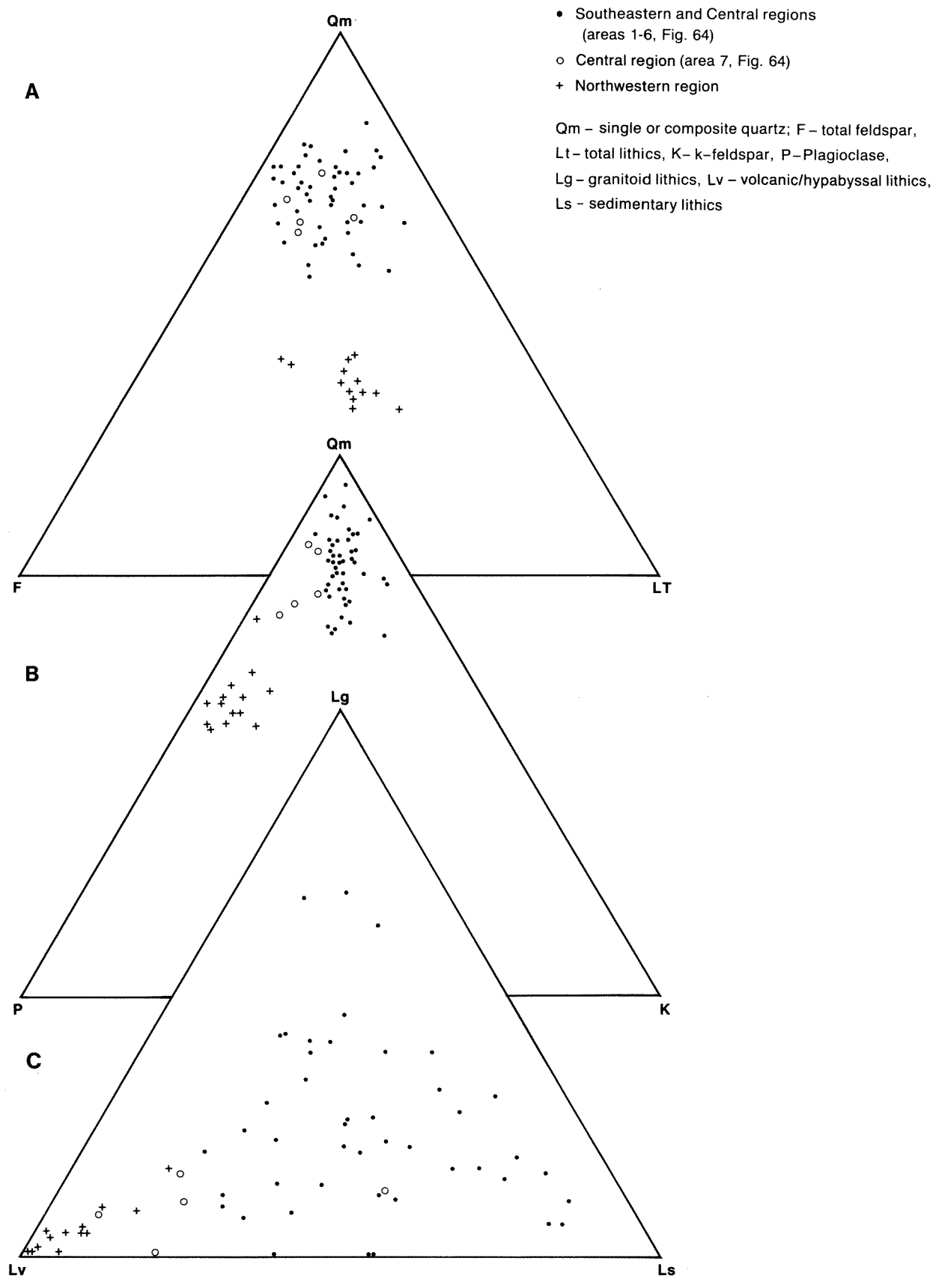
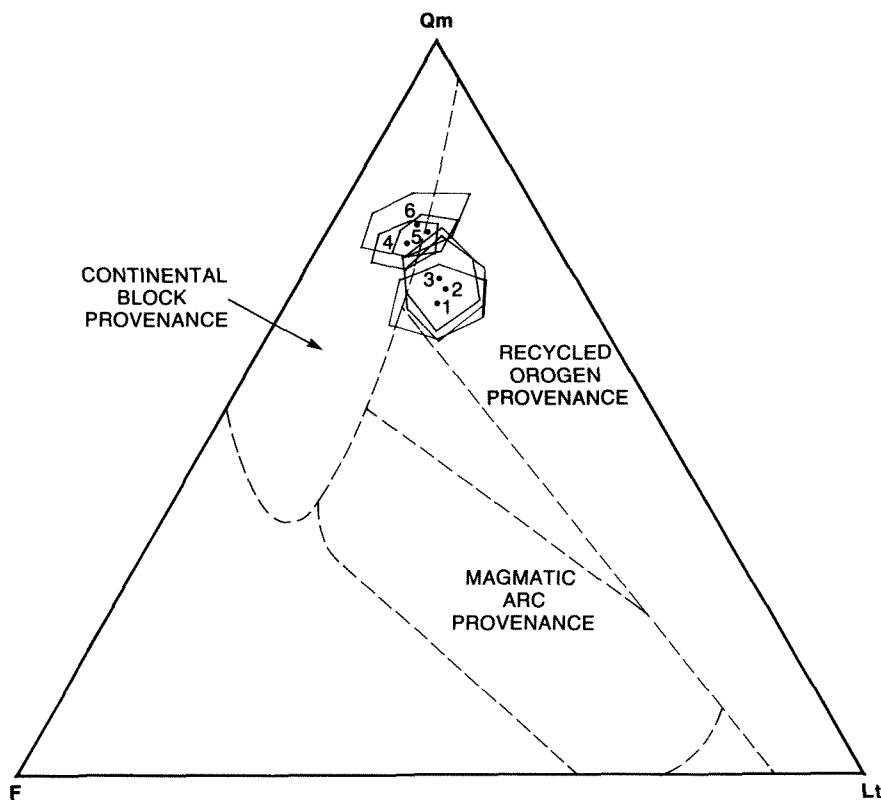


Figure 66 Composition diagrams for Ashburton Formation sandstones.



GSWA 25233

**Figure 67** Mean compositions and standard deviations of Ashburton Formation sandstones from areas 1–6 in the southeastern and central Ashburton Basin. Also shown are the tectonic provenance fields of Dickinson and Suczek (1979). See Figure 66 for key.

terized by a southeast to northwest palaeocurrent trend. Area 7, near Mount Dawson, has a northeasterly directed palaeoflow. For areas 1–6, the data are presented in order of inferred stratigraphic level.

The principal clasts recognized in the sandstones are :

- Quartz (Qm)–anhedral, single grains or polycrystalline fragments; some embayed crystals of volcanic quartz were identified; no recycled quartz was recognized.
- Plagioclase (P), K-feldspar (K), and total feldspar (F).
- Lithic fragments (Lt)–felsic volcanics, chert (often ferruginous), mudstone, sandstone, and granitoid.

In areas 1–6 quartz is the most abundant clast type; but there are lesser, often subequal, amounts of feldspar and lithic fragments (mean composition Qm 69 %, F 17%, Lt 14%). The feldspar component is made up of subequal proportions of plagioclase and K-feldspar, whereas the lithic category comprises sedimentary, felsic volcanic, and granitoid rock fragments in varied proportions. The results show a gradual southeast to northwest increase in quartz content (64%–75%), largely at the expense of the lithic fragments (18%–10%). This trend is summarized in Figure 67. No systematic variation in sandstone composition with inferred stratigraphic height is observed.

Conglomerate from areas 1–6 comprises fragments of vein quartz, with smaller amounts of jaspilitic chert, felsic volcanic rock, and silicified sandstone.

Sandstones from area 7 have abundant quartz, with lesser amounts of feldspar and lithics (mean composition - Qm 68%, F 21%, Lt 11%). Plagioclase is the dominant feldspar. The lithic category comprises felsic volcanic rock, with lesser amounts of granodiorite and sedimentary rock.

### Interpretation

#### *Southeasterly derived sandstone (areas 1–6)*

In areas 1–6, the high proportion of quartz, coupled with the significant quantities of plagioclase and K-feldspar, point to a major exposure of granitoid in the source area. The fact that plagioclase and K-feldspar are present in subequal amounts suggests that the granitoid was of monzogranite composition, a view supported by the mineralogy of many larger lithic fragments. The moderate to high degree of strain shown by the quartz and feldspar suggests that the monzogranite was somewhat tectonized. Fragments of chert, sandstone, and felsic volcanic rock suggest that sedimentary and volcanic rocks were also exposed in the source area.

Sandstone compositions and palaeocurrent data point to the Sylvania Inlier as being the most likely source area. Here, monzogranites and granodiorites, many of them

**TABLE 2 COMPOSITION OF ASHBURTON FORMATION SANDSTONES FROM THE SOUTHEAST AND CENTRAL ASHBURTON BASIN**

Sample No.	Qm	P	K	F	Lt	Lv	Ls	Lg	Lv (%)	Ls (%)	Lg (%)
<b>Area 1</b>											
77090	65	13	14	27	8	4	4	6	28	28	44
66146	57	11	15	26	17	10	7	11	36	25	39
77089	61	15	13	28	11	6	5	7	33	28	39
82809	65	3	4	7	28	2	24	2	10	80	10
82808	68	1	8	9	24	4	20	3	15	74	11
82806	69	4	17	21	18	2	16	2	10	80	10
82805	69	4	8	12	20	5	15	4	21	63	16
82802	74	3	10	13	13	2	11	3	13	69	18
77100	57	3	15	18	25	5	20	4	18	68	14
77097	64	10	11	21	15	5	10	8	18	45	37
<b>Area 2</b>											
66137	56	5	9	14	30	21	9	3	64	27	9
77087	70	10	10	20	10	5	5	3	38	38	24
77091	61	10	13	23	16	6	10	4	30	50	20
77084	75	5	9	14	12	2	10	5	12	59	29
77085	77	2	3	5	18	3	15	1	16	75	9
77088	63	8	9	17	20	5	15	7	19	55	26
77086	62	12	9	31	17	10	7	8	40	28	32
<b>Area 3</b>											
77061	61	10	12	22	17	12	5	5	54	23	23
77060	55	14	13	27	18	12	6	7	48	24	28
82865	68	8	9	17	15	10	5	1	62	31	7
77079	79	5	10	15	6	3	3	2	37	38	25
77080	74	5	5	10	16	7	9	2	39	50	11
77065	65	9	7	16	19	8	11	5	33	46	21
77064	65	9	5	14	21	10	11	5	38	43	19
<b>Area 4</b>											
77031	73	8	6	14	13	7	6	2	47	40	13
77058	76	5	2	7	17	12	5	2	63	26	11
77063	71	9	7	16	13	6	7	0	46	54	0
77062	71	12	9	21	8	4	4	2	40	40	20
77059	78	6	4	10	12	7	5	1	54	38	8
82848	68	8	12	20	11	7	4	3	50	29	21
<b>Area 5</b>											
77053	67	13	10	23	10	7	3	3	64	19	19
77051	72	10	13	23	5	2	3	7	15	25	60
77028	72	10	10	20	9	4	5	3	33	42	25
77027	77	9	8	17	6	4	2	4	40	20	40
77026	72	7	8	15	13	8	5	2	54	33	13
77056	74	7	5	12	14	4	10	3	24	59	17
77032	75	10	12	22	3	2	1	6	22	11	66
<b>Area 6</b>											
77021	73	2	2	4	24	11	13	0	46	54	0
51677	78	2	3	5	17	7	10	2	47	53	10
51692	83	2	2	4	13	8	5	0	61	39	0
51691	71	11	9	19	10	6	4	6	37	26	37
51674	68	16	10	26	7	2	5	3	20	50	30
51675	79	9	7	16	5	2	3	3	25	38	37
51689	75	14	5	19	6	3	3	3	33	33	33
51686	74	14	6	20	6	4	2	4	40	20	40
51678	75	13	10	23	2	1	1	4	17	17	66
<b>Area 7</b>											
82850	69	15	9	24	7	3	4	1	38	50	12
77020	66	10	5	15	19	14	4	0	79	21	0
82854	74	12	4	16	9	7	2	1	70	20	10
66124	66	18	6	24	10	8	2	2	68	16	16
82852	63	20	5	25	12	11	1	1	84	8	8

Single or composite crystals of quartz (Qm); plagioclase feldspar (P); K-feldspar (K); total feldspar (F); total lithic fragments (Lt); volcanic - hypabyssal lithics (Lv); sedimentary lithics (Ls), granitoid lithics (Lg). Granitoid lithics were recorded both as a clast and as the component mineral (Qm, P and K) during point counting.

tectonized, outcrop over approximately 7500 km<sup>2</sup>. Along the northern and southwestern margin of the inlier, these rocks are overlain by sedimentary and volcanic rocks of the Mount Bruce Supergroup. The possibility that other granitoid inliers within the Hamersley Basin acted as source areas is rejected on grounds of their small size and geographic location.

Similar sandstone compositions are recorded throughout the Ashburton Formation stratigraphy; they indicate that the granitoid terrane was exposed for the entire time that these rocks were being deposited.

The southeast to northwest increase in quartz content observed in this region parallels the main palaeocurrent trend. It is thought to reflect downcurrent increase in clast abrasion — the proportion of resistant quartz rising as less stable lithic fragments are broken down. Data in this study show that the proportion of quartz increases downcurrent at the rate of approximately 1% per 30 km.

Dickinson and Suczek (1979) recognized three groups of sandstone composition which they relate to the plate tectonic setting of the source area (Fig. 68). Sandstone data from areas 1–6 plot in the Recycled Orogen and Continental Block fields. Tectonic evolution of the southwestern Pilbara during deposition of the Wyloo Group is discussed in Chapter 12.

#### *Southwesterly derived sandstones (area 7)*

In area 7, the high proportion of quartz and plagioclase feldspar points to a major exposure of granodiorite in the source area. Clasts of chert and felsic volcanic rock suggest that a mixed sedimentary and volcanic sequence was also exposed. Composition data from sandstones in this area plot in the Continental Block and Recycled Orogen fields (Fig. 68) of Dickinson and Suczek (1979).

### **Northwestern region**

#### **Results**

Point-count data from fourteen samples collected from the area to the northwest of the Wyloo Dome are shown in Table 3 and are summarized in Fig. 66. Principal clast-types are:

- (a) Quartz (Qm) — anhedral single or composite grains. Embayed crystals of volcanic quartz are abundant.
- (b) Plagioclase (P), K-feldspar (K), and total feldspar (F).
- (c) Lithic fragments (Lt) — felsic volcanic rock (chiefly dacite), chert, BIF, sandstone, mudstone and granitoid

Most sandstones comprise subequal amounts of quartz, feldspar and lithic fragments (mean composition — Qm 36%, F 31%, Lt 33%). Plagioclase is considerably more abundant than K-feldspar in all samples. The lithic com-

ponent includes abundant dacite fragments and lesser amounts of sedimentary rock and granitoid detritus.

Conglomerates include fragments of dacite, basalt, quartz-filled amygdales, vein quartz, quartz sandstone, dolomite, chert, and BIF.

#### **Interpretation**

Sandstone and conglomerate data point to a source area composed of felsic volcanic and sedimentary rocks; many lithic fragments can be matched with rocks to the north and east of Wyloo Dome. Felsic volcanic clasts are closely similar to dacite in the Woongarra Volcanics (Hamersley Group), and the BIF and chert are thought also to be derived from the Hamersley Group. Basalts with quartz-filled amygdales are abundant in the Fortescue Group, and sandstone and dolomite form a major part of the Wyloo Group.

Sandstones plot in the Magmatic Arc Provenance field (Fig. 68) of Dickinson and Suczek (1979).

## **Depositional model and palaeogeographic reconstruction**

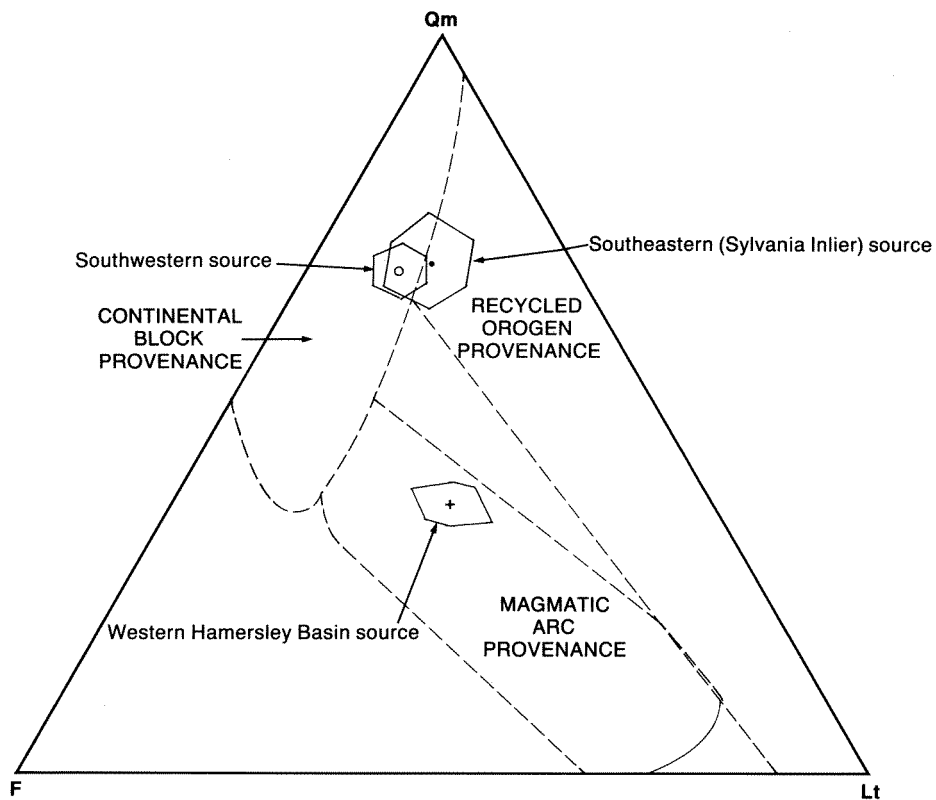
The following model for Ashburton Formation sedimentation is based on the nature and distribution of the lithofacies associations, combined with palaeocurrent and provenance data. Main features of the model are summarized in Figures 69 and 70. The principal tectonic controls at the start of Ashburton Formation deposition were:

- (a) A subsiding deep marine basin developed around the southern and western margin of the Hamersley Basin. This corresponds to the Ashburton Trough of Doust (1975) and Gee (1979a).
- (b) A tectonically active upland region of granitoid, sedimentary and felsic volcanic rock in the Sylvania Inlier.

Major uplift and erosion in the Sylvania Inlier resulted in granitic sand and mud being shed into the eastern end of the deep marine basin. This detritus was distributed westwards by an elongate system of braided distributary channels (with associated depositional lobes) which extended at least as far as Wyloo Dome. Subsequent decrease in sand supply led to development of a mud-dominated depositional system in which coarse-grained sediment was transported in a few major leveed channels separated by extensive areas of mudstone deposition.

Later in the evolution of southern Pilbara (Fig. 70), uplift took place southwest of the Ashburton Trough, and also in the western Hamersley Basin. Detritus from the southwestern upland supplied a submarine fan system south of Wyloo Dome, and sediment from the western Hamersley Basin was distributed to a third submarine fan complex lying to the northwest of Wyloo Dome.





GSWA 25234

**Figure 68** Mean compositions and standard deviations of Ashburton Formation sandstones from source areas in the Sylvania Inlier, Western Hamersley Basin, and southwest of the Ashburton Basin.

## Discussion

Evidence presented in this chapter indicates that the Sylvania Inlier underwent major uplift and erosion during deposition of the Ashburton Formation. Tyler (in press), and Tyler and Thorne (in press) recognize two major periods of Ophthalmian folding in the southeastern Hamersley Basin. The earliest took place during the interval between deposition of the Cheela Springs Basalt and the Mount McGrath Formation (see discussion, Chapter 4) and resulted in development of large, upright to steeply inclined folds in the vicinity of the Turee Creek Syncline. The second event produced overturned, north-facing folds and reverse faults in the extreme southeast Hamersley Basin, and caused major uplift along steep reverse faults and shear zones in the Sylvania Inlier. Provenance and palaeocurrent data indicate that folding and faulting associated with the major period of Sylvania Inlier uplift took place during deposition of the Ashburton Formation; that is, after the upright folds in the Turee Creek Syncline area were formed. The presence of abundant granitoid detritus in the lowest sandstones of the Ashburton Formation implies that the Sylvania Granitoid was at least partly exposed at the start of Ashburton Formation sedimentation. Exposure probably resulted from stripping of the cover during and immediately after the first deformation.

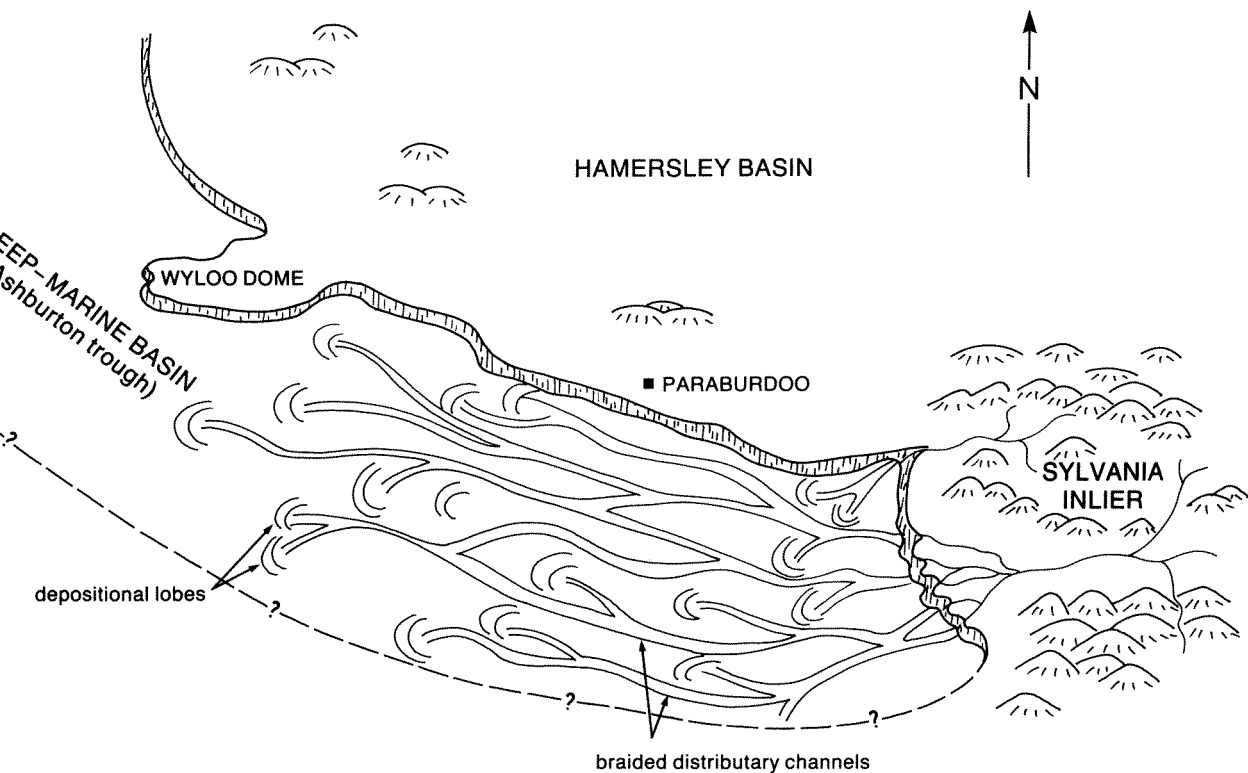
The Sylvania Inlier is the largest of the three source areas identified for the Ashburton Formation. Using pressure-temperature estimates from metamorphic mineral assemblages in amphibolite dykes within the inlier, Tyler (in press, a) calculated that 8–11 km of granitoid have been stripped off the inlier since uplift. This estimate, combined with the present-day outcrop area of the granitoid, suggests that the Sylvania Inlier could have supplied approximately 72 000 km<sup>3</sup> of sediment to the Ashburton Trough. Using a minimum value of 5 km for the Ashburton Formation thickness, and the present day outcrop width of 60 km, it is estimated that a minimum of 100 000 km<sup>3</sup> of sediment was deposited in the southeastern part of the Ashburton Trough. These estimates, although uncertain, suggest that the area of granitoid formerly exposed in the Sylvania region was larger than that seen today. It is thus likely that the Sylvania Inlier extends for perhaps 30 km to the south, beneath the Bangemall Group unconformity.

This study has identified two other source areas for the Ashburton Formation, one to the southwest of the Ashburton Trough, the other in the western Hamersley Basin. The exact location of the southwestern source region is unknown; provenance studies suggest that it was an upland composed largely of granodiorite. Granitoids of this composition are widespread in the northern Gascoyne

**TABLE 3 COMPOSITION OF ASHBURTON FORMATION SANDSTONES FROM THE NORTHWESTERN PART OF THE ASHBURTON BASIN**

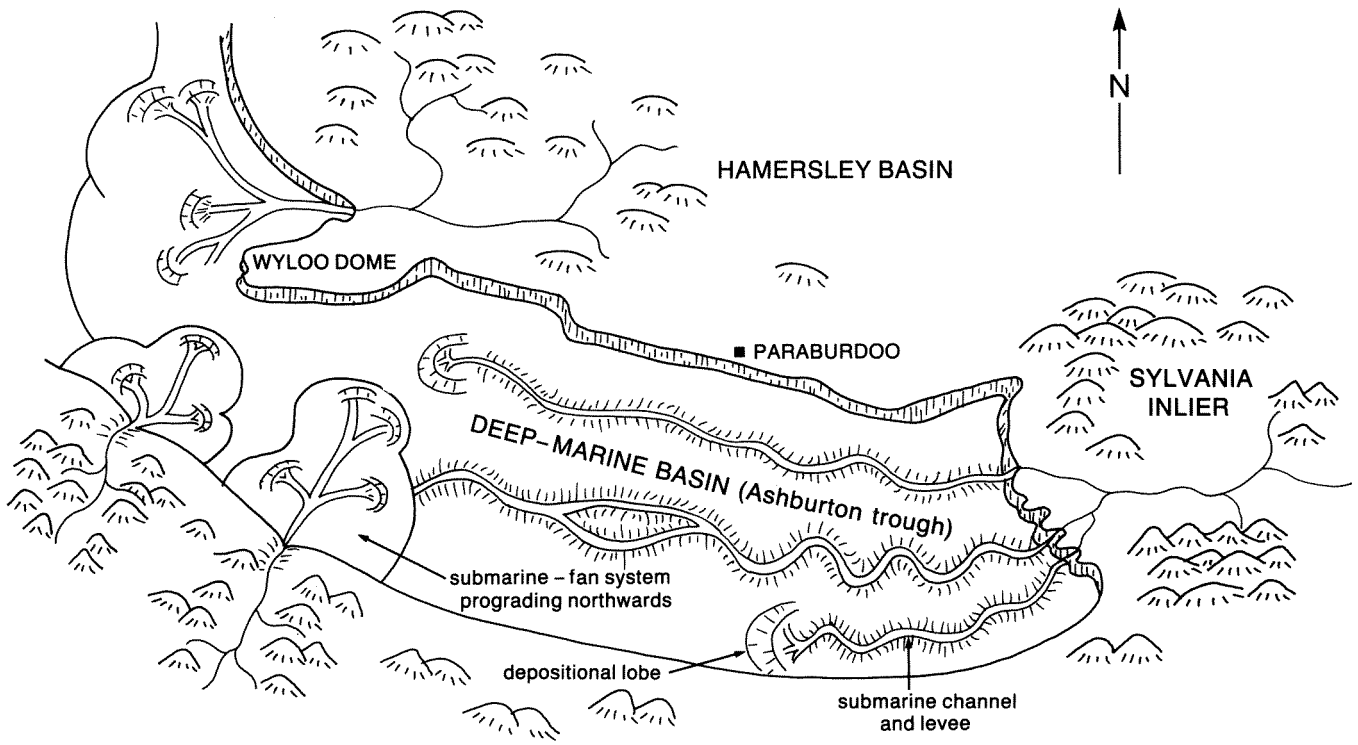
Sample No.	Qm	P	K	F	Lt	Lv	Ls	Lg	Lv (%)	Ls (%)	Lg (%)
51669	34	26	5	31	35	32	3	3	84	8	8
51642	39	29	9	38	23	23	0	0	100	0	0
51644	31	22	3	25	44	43	1	2	94	2	4
51746	35	23	4	27	38	37	1	1	94	3	3
51647	40	33	6	39	21	20	1	0	95	1	0
51629	41	22	5	27	32	32	0	0	100	0	0
51637	33	25	6	31	36	33	3	2	88	7	5
51651	35	24	5	29	34	29	5	3	78	14	8
51654	38	22	8	30	32	27	5	6	69	15	16
51656	34	26	3	29	36	33	3	2	88	8	4
51657	31	28	4	32	37	35	2	1	97	2	1
82863	36	29	2	31	33	32	1	0	97	3	0
69391	40	26	2	28	32	32	2	1	91	6	3
69385	33	30	3	33	36	33	3	2	88	7	5

Single or composite crystals of quartz (Qm); plagioclase feldspar (P); K-feldspar (K); total feldspar (F); total lithic fragments (Lt); volcanic - hypabyssal lithics (Lv); sedimentary lithics (Ls); granitoid lithics (Lg). Granitoid lithics were recorded both as a clast and as the component mineral (Qm, P and K) during point counting.



GSWA 25235

**Figure 69 Palaeogeographic reconstruction of the southwestern Pilbara during deposition of the lower Ashburton Formation.**



GSWA 25236

**Figure 70** Palaeogeographic reconstruction of the southwestern Pilbara during deposition of the upper Ashburton Formation.

Province but have an intrusive relationship with the Ashburton Formation (Seymour et al., 1988). Williams (1986) noted that granodiorite gneiss and migmatites of similar composition occur throughout the Gascoyne Complex. Although many of their features result from post - Wyloo Group tectonism, their presence — coupled with the sandstone composition data — suggests the former existence of a granodiorite basement which was uplifted during the latter part of Ashburton Formation deposition and tectonized during the Capricorn Orogeny.

There is little direct evidence for major tectonism in the western Hamersley Basin during deposition of the Ashburton Formation. The supply of sediment into the northwestern part of the Ashburton Trough is, therefore, thought to be the result of regional uplift of a previously folded terrane. The relatively large size of the submarine fan in this area suggests that sediment was supplied by a river system which drained most of the western Hamersley Basin. Over much of this area, gently folded rocks of the Hamersley Group are now eroded to the level of the Brockman Iron Formation. In view of the high proportion of dacite clasts (probably from the Woongarra Volcanics) in the submarine-fan deposits, it is likely that much of the erosion dates from the time that the Ashburton Formation was laid down.

Important differences exist between the submarine-fan model presented for the southeastern part of the Ashburton Trough and the submarine-fan model of Walker (1978). A central feature of Walker's (1978) model is that sediment is supplied from what is essentially a point source,

before being distributed over the fan by a radial system of braided channels. Facies distributions, combined with palaeocurrent and provenance data, suggest that much of the Ashburton Formation was deposited in an elongate system of submarine channels and depositional lobes.

The depositional model for the Ashburton Formation is analogous to the sediment dispersal system in the Bay of Bengal (Curry and Moore, 1971; Graham et al., 1975; Ingersoll and Suczek, 1979). Here, sediment from the Himalayas is fed by the Ganges-Brahmaputra river system into the Bay of Bengal, where much of it accumulates on a huge, elongate submarine fan — the Bengal Fan. This sediment body, up to 15 km thick, is characterized by a longitudinal system of leveed channels which extends over most of the fan's length.

The broad-scale stratigraphy of the Ashburton Formation, in which basin-plain mudstones are overlain by sandy-channel and lobe deposits, succeeded by major-channel and levee facies, is similar to the progradational sequence predicted by Walker's (1978) model. Anomalies exist with this interpretation however:

- (a) the upper part of the Ashburton Formation contains several major channel units of varying thickness and internal structure, and not one as would be required if Walker's (1978) model were strictly applied;
- (b) there is no southeast to northwest thickening of basin-plain facies at the base of the formation, as would be expected in a progradational succession; and

- (c) the fact that major channel deposits are recorded to the south of the Wyloo Dome requires the channelled upper fan to have prograded approximately 300 km along the length of the basin.

In the light of these observations the stratigraphy of the Ashburton Formation is interpreted, not as a single large-scale progradational event, but instead is thought to reflect change in the nature of sediment supply, which caused the 'fan' to evolve from sand-dominated to a mud-dominated depositional system.

Sandstone composition data, from each of the identified source areas, plot in three of the tectonic provenance fields recognized by Dickinson and Suczek (1979). Most of the sandstones derived from the Sylvania Dome can be assigned to the Recycled Orogen field (Fig. 68); those from the southwestern source area and western Hamersley Basin plot in the Continental Block and Magmatic Arc fields respectively. The fact that three different tectonic settings could be inferred for the southwestern Pilbara during deposition of the Ashburton Formation highlights some limitations of the provenance method. In particular, clast abrasion during transport and geology of the source areas have had a major influence on the composition of Ashburton Formation sandstones.

Even the most careful petrographic techniques cannot entirely compensate for the effects of clast abrasion during transport. In sandstones derived from the Sylvania Inlier the proportion of unstable lithic fragments decreases at a rate of approximately 1% per 30 km travelled. Over a

300 km distance abrasion has been sufficient to move the modal composition of these sandstones from the Recycled Orogen field into the Continental Block field. On this evidence the most reliable data for tectonic reconstruction should come from sandstones deposited relatively close to the source area.

Sandstones derived from the southwestern source area have a similar composition to the most mature sandstones eroded from the Sylvania Inlier; this suggests that the former may also have originated from a granitoid-cover rock sequence some distance from the final place of deposition. Similar compositions could, however, be expected from a nearby granitoid terrane that had only a thin sedimentary cover. Sand-sized detritus from a source area of this type would show a strong granitic component (quartz and feldspar) with a smaller amount of lithic fragments, originating mainly from the sedimentary sequence. Sandstones derived from a terrane of this type would be biased towards the Continental Block field, regardless of the tectonic regime controlling source area uplift.

Similarly, the composition of sandstones derived from the western Hamersley Basin probably does not reflect the tectonic regime at the time of Ashburton Formation deposition (see Chapter 11), but instead was determined by source rocks, formed earlier in the area's history. In this case, the high proportion of felsic volcanic detritus in the sandstones results from erosion of a pre-existing sequence, the Woongarra Volcanics, and not from a penecontemporaneous magmatic arc system.



## Chapter Seven

# Large allochthonous blocks and olistostromes within the Ashburton Formation

The Ashburton Formation comprises mudstone, siltstone, immature sandstone, conglomerate, banded iron-formation (BIF), chert, and volcanic rock. Locally, other lithologies (e.g. dolomite and quartz sandstone) occur within the Ashburton Formation. These additional rock-types, and some BIF and volcanic rock sequences, have been interpreted as large allochthonous blocks and olistostromes that had been transported into the Ashburton Trough during deposition of the Ashburton Formation (Horwitz, 1978, 1980, 1981; Horwitz and Smith, 1978; Lascelles, 1983). This chapter describes major occurrences of apparently exotic rock-types within the Ashburton Formation and discusses their possible origins. For descriptive purposes, the Ashburton Basin is subdivided into northwestern and southeastern regions, along the latitude of the southern Wyloo Dome.

### Northwestern region

In the northwestern part of the Ashburton Basin, several outcrops of felsic and mafic volcanic rock, dolomite, quartz sandstone, and BIF have been interpreted as olistoliths and olistostromes (Horwitz, 1981). Principal occurrences are near Mount Amy, Mount Stuart, Hardey Junction, and the western closure of Wyloo Dome (Fig. 71).

#### Mount Amy

Seven kilometres east of Mount Amy (Fig. 71, locality 1) a massive porphyritic dacite, approximately 500 m thick and 5 km long, occurs interbedded in a sequence of mudstone, turbidite sandstone, and conglomerate. The dacite contains approximately 40% oligoclase phenocrysts; these occur in two modes, large (2–5 mm) euhedral crystals, and smaller anhedral grains and fragments. The matrix is composed of very fine-grained quartz, feldspar, chlorite, small phenocrysts of opaque minerals and prominent secondary apatite. The boundary between dacite and underlying mudstone is irregular, and the thickness of the mudstone decreases from approximately 400 m to 120 m over two kilometres. The poorly exposed volcanic rock appears to lack a chilled margin, and no contact-metamorphic aureole is present in the finely laminated mudstone close to its lower contact.

Four kilometres to the northeast, and stratigraphically lower in the Ashburton Formation, a 1.5–5 m thick unit of

dolomite and quartz sandstone is interbedded in a thick succession of Ashburton Formation mudstone. This dolomite, which outcrops over a strike length of 800 m, is medium bedded and incorporates domical stromatolites and conglomerate. Sandstone beds are generally tabular, 0.2 m thick, and lack internal structure. No evidence of major disruption was observed in the enclosing mudstone.

Horwitz (1981, p.398) referred to an olistolith of “brecciated mixtures of dominantly basic igneous rocks resembling Fortescue Group assemblages” 15 km southwest of Mount Amy (Fig. 71, locality 2). The exposed sequence is 450 m thick and is conformable within sandstone and mudstone of the Ashburton Formation. It is a chaotic sequence of locally vesicular basalt, coarse basaltic agglomerate, and thin-bedded basaltic tuff.

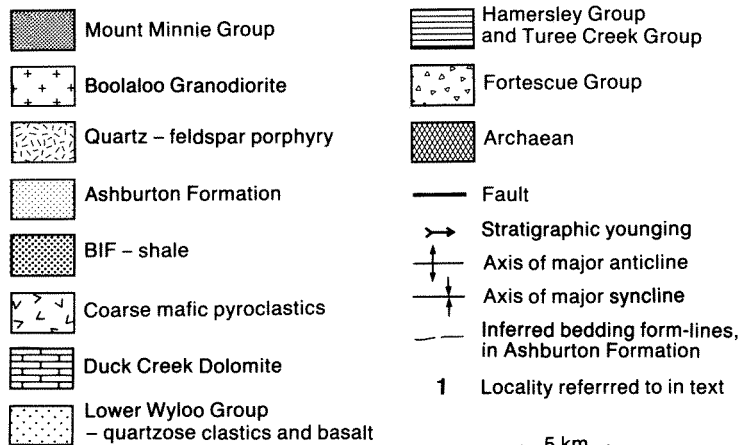
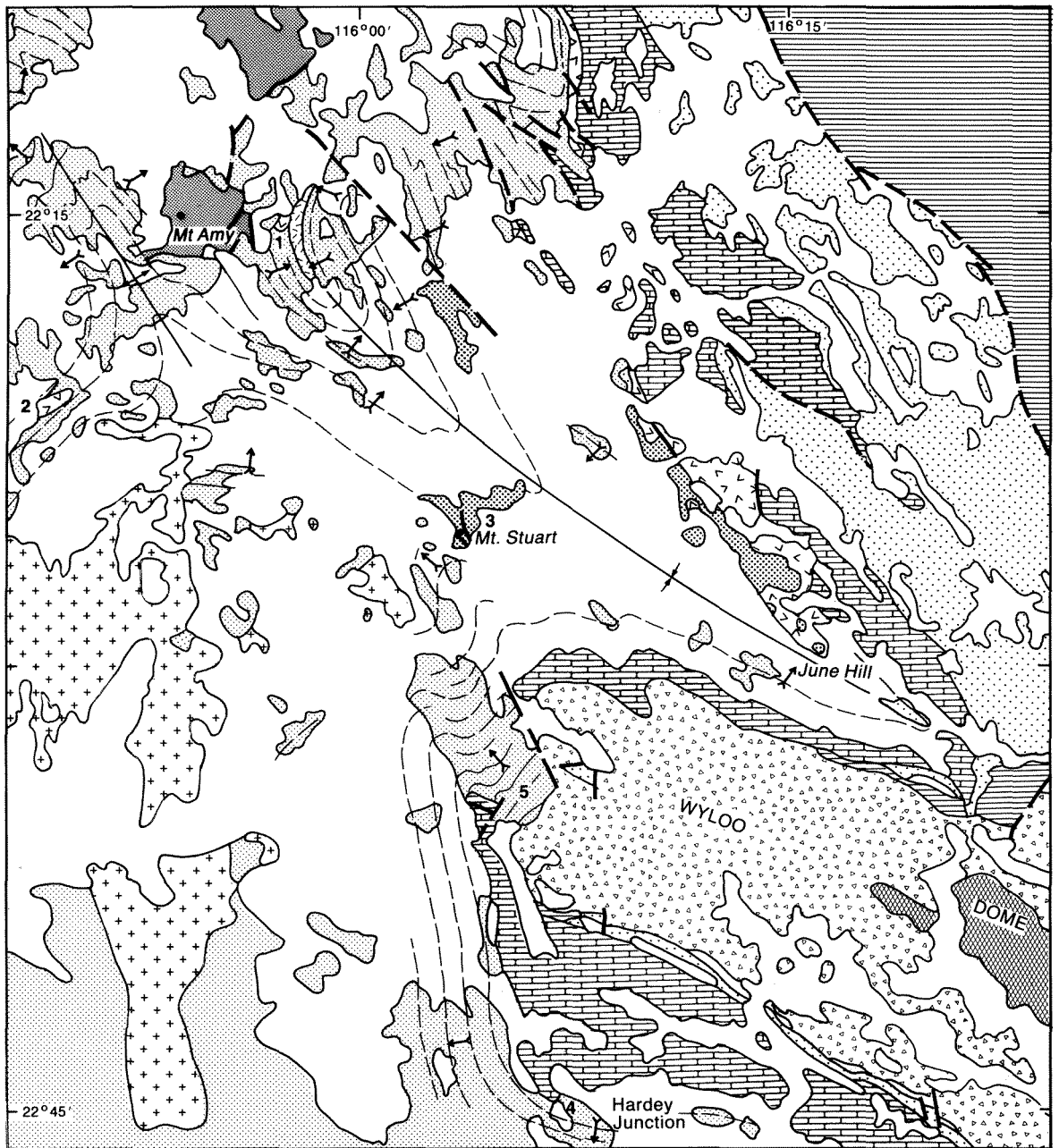
#### Mount Stuart

Horwitz (1981) reported two horizons of olistoliths and olistostromes at Mount Stuart (Fig. 71, locality 3). Here, a 375 m thick sequence of BIF, mudstone, siltstone, sandstone, and conglomerate is faulted against foliated meta-sandstones of the Ashburton Formation. The lower part of the succession, corresponding to the lower olistostrome horizon of Horwitz (1981), comprises a disorganized assemblage of sandstone and conglomerate that contains large clasts of dolomite, basalt, dolerite, and felsic volcanic rock. The conglomerate and sandstone unit becomes finer grained upwards, and is transitional into BIF alternating with tuffaceous mudstone and siltstone. Horwitz (1981) interpreted this upper sequence as a second olistolith horizon “resembling Hamersley Group assemblages”. The BIF features parallel lamination, soft-sediment creep folds, and boudinage structures; large folds are of tectonic origin and display an axial-planar cleavage. Unpublished company aeromagnetic data suggests that the Mount Stuart BIF is not connected to a similar BIF sequence which outcrops 12 km to the north.

#### Hardey Junction and the western closure of the Wyloo Dome

Two dolomite outcrops, the largest 400 m long and 70 m thick, occur within the Ashburton Formation at Hardey Junction (Fig. 71, locality 4; Fig. 72). The stratigraphy of the dolomite blocks is inverted relative to the enclosing turbidite sandstone, which shows southward younging





GSWA 25237

Figure 71 Geological map of the northwestern Ashburton Basin, showing localities mentioned in the text.

## Southeastern region

Horwitz (1980) and Lascelles (1983) recorded several large olistoliths and olistostromes from the southeastern Ashburton Basin, in the vicinity of Radio Hill Fault, Mount Elephant, and Mount Boggola (Fig.73).

### Radio Hill Fault

Lascelles (1983) describes two inliers of Hamersley Group BIF and shale in the Wyloo Group succession 10 km south of Paraburdoo (Fig. 73, locality 1), and suggests that they represent large olistostromes and olistoliths within the Ashburton Formation. The larger inlier is up to 100 m thick and 2 km long and consists of moderately fresh to strongly weathered BIF. It shows coarse mesobanding with local podding, and incorporates a 30 m thick chert-shale sequence along part of its southern boundary. The other inlier is about 1 km long and consists of angular blocks of BIF, jasper and chert, in a goethitic jasper matrix. In both inliers, strike of the bedding may differ from that of the overlying Wyloo Group, which dips south at 30–40°.

The sequence underlying the inliers is mudstone and siltstone interbedded with thin sandstone. These rocks are strongly contorted near the contact with the BIF (Lascelles, 1983; p.164). The strata overlying the inliers consist of coarse-grained sandstone with minor mudstone and siltstone. Despite offsets due to faulting, this sequence can be traced along strike for 5 km to the southeast, where it is contiguous with units belonging to the Mount McGrath Formation. These deposits are overlain by the Duck Creek Dolomite; the lowest beds of the Ashburton Formation are exposed some 5 km to the south.

### Mount Elephant

At Mount Elephant (Figs. 73, 74), a northwest-trending ridge of sandstone, siltstone, and minor stromatolitic dolomite, lies with angular unconformity upon the Ashburton Formation. The sequence above the unconformity forms a syncline, the southern margin of which is faulted along the southern flank of Mount Elephant. Bedding in a silicified sandstone, which crops out around the summit of Mount Elephant, is either horizontal or steeply overturned against the fault (Fig. 75). Away from the fault, the quartz sandstone conformably overlies the lower part of the post-Ashburton Formation stratigraphy. Horwitz (1980) interpreted this upper unit as an allochthonous mass of lower Wyloo Group rocks which slid into the basin during deposition of the Ashburton Formation, and was locally overturned along its leading edge during transport.

### Mount Boggola

The belt of intermediate to mafic volcanic rock outcropping to the north and west of Mount Boggola (Figs. 73, 76) was mapped as a dolerite dyke on the 1st

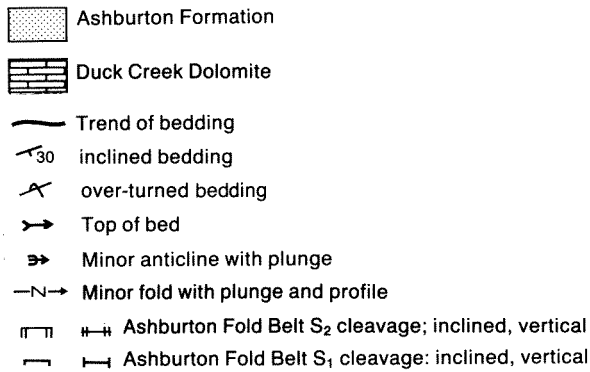
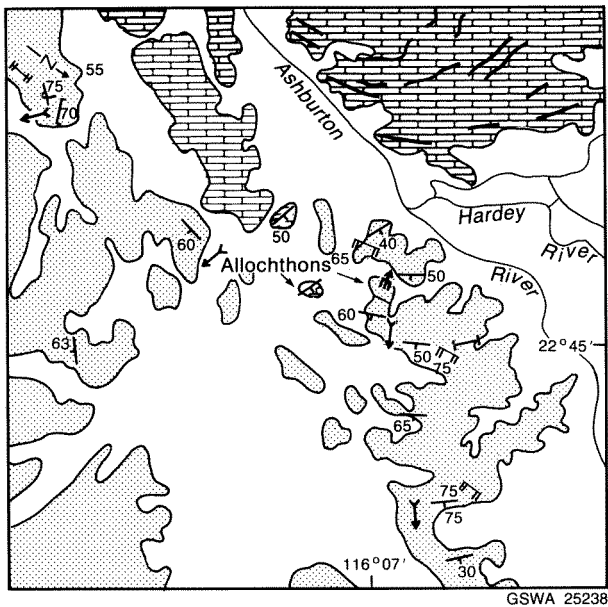
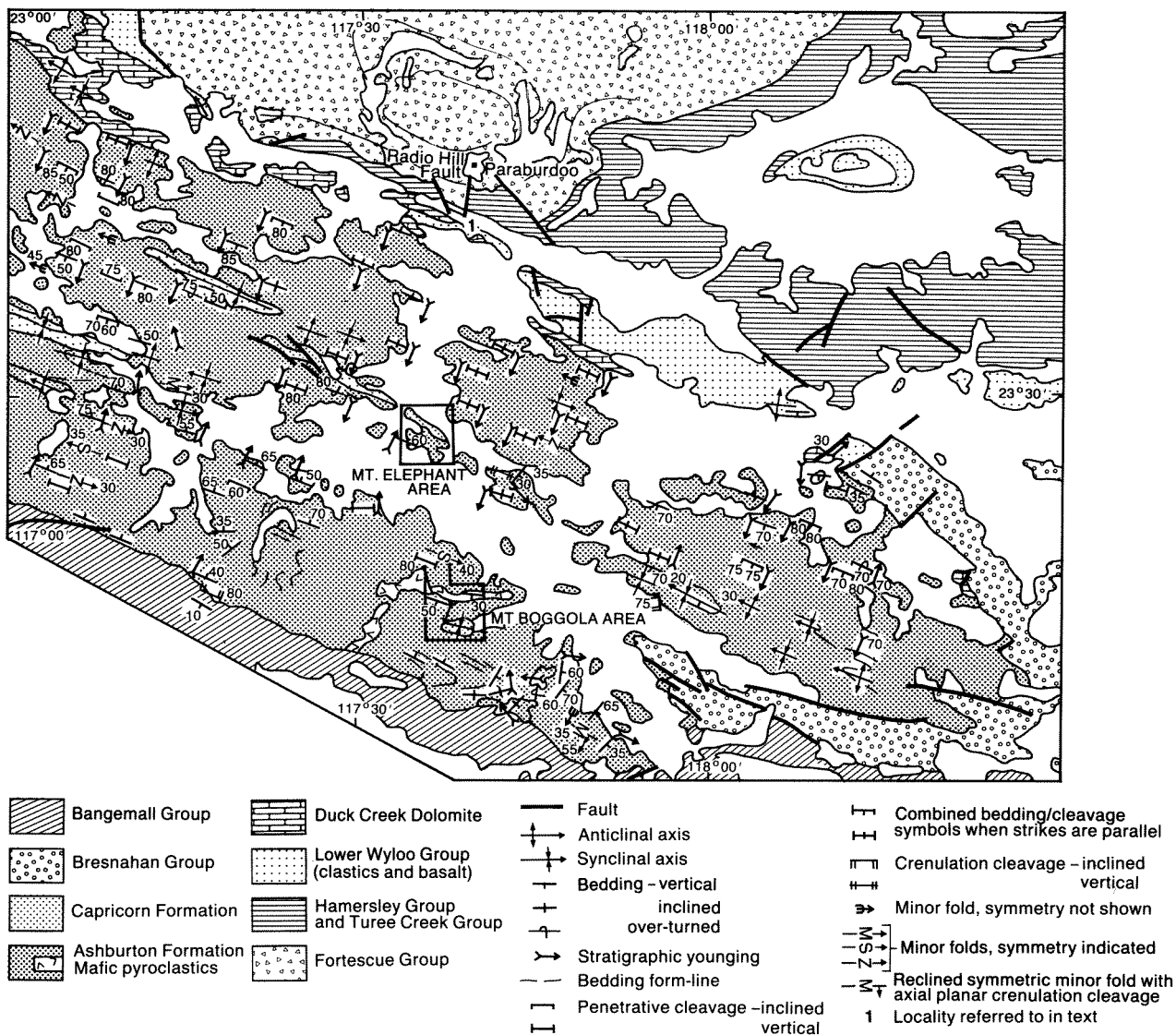


**Figure 72** Geological map of the Hardey Junction area, showing location of allochthonous dolomite units described in the text.

directions. Along its original base, the largest block shows tight soft-sediment folds, that are outlined by chert layers in the thin-bedded dolomite. The axial surfaces of these folds are normal to the top and bottom of the block, and do not relate to any local tectonic folds or cleavages. The original upper part of the largest block has thin mudstone layers interbedded with the dolomite.

Isolated blocks of dolomite crop out in the lower part of the Ashburton Formation at the western closure of the Wyloo Dome (Fig. 71, locality 5). The blocks are up to several tens of metres long and up to 15 m wide. They are composed of thin-bedded, parallel-laminated dolomite that is locally interbedded with 0.1–2 m thick slumped and brecciated layers. Some of the dolomites contain numerous laminae of quartz sandstone. No evidence of soft-sediment deformation was observed in the enclosing mudstones and turbidite sandstones.



GSWA 25239

Figure 73 Geological map of the southeastern Ashburton Basin, showing localities mentioned in the text.

edition of TUREE CREEK (Daniels, 1968). Horwitz (1980) recognized its extrusive character, and interpreted both this unit and the quartz sandstone which forms the summit of Mount Boggola as allochthonous sequences of lower Wyloo Group strata.

Northwest of Mount Boggola, the volcanic sequence comprises approximately 600 m of vesicular pillow lava, pillow breccia (fragments up to 2 m across), and coarse-grained volcanoclastics and laminated tuff. Near the top of the sequence, the pillows and pillow breccia are locally altered to jaspilitic chert. The lowermost volcanics are interbedded with mudstone and siltstone of the Ashburton Formation, and the top of the unit is conformably overlain by mudstone or BIF and chert. Two kilometres west-northwest of Mount Boggola, a thin and laterally restricted sequence of similar volcanic rocks is exposed on the southern limb of a complex, northwest-trending syncline (Fig. 76).

At Mount Boggola, a thick (200 m) succession of quartz sandstone and ferruginous sandstone and siltstone rests with angular unconformity on cleaved mudstones of the Ashburton Formation. The lower 50 m is thick-bedded, medium- to coarse-grained quartz sandstone whose internal structure consists of stacked sets of medium- to large-scale (up to 0.5 m thick) trough cross-strata with local lags of mudstone pebbles. The quartz sandstones are transitional upwards into a 54 m thick, upward-fining sequence of ferruginous siltstone and fine- to medium-grained sandstone. Thin-bedded siltstones and fine-grained sandstones are parallel-laminated or ripple cross-laminated; thicker bedded (up to 0.5 m) medium-grained sandstones display trough cross-stratification. Load structures are abundant throughout the unit. Approximately 100 m above the basal unconformity, the proportion of sandstone increases, and the uppermost 100 m of the succession is medium- to thick-bedded, medium- to coarse-grained quartz sandstone interbedded with small

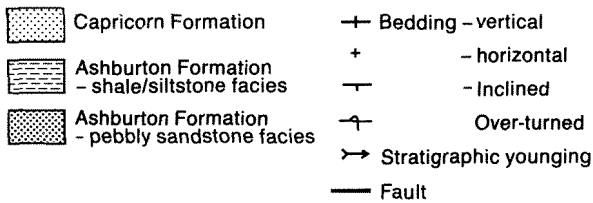
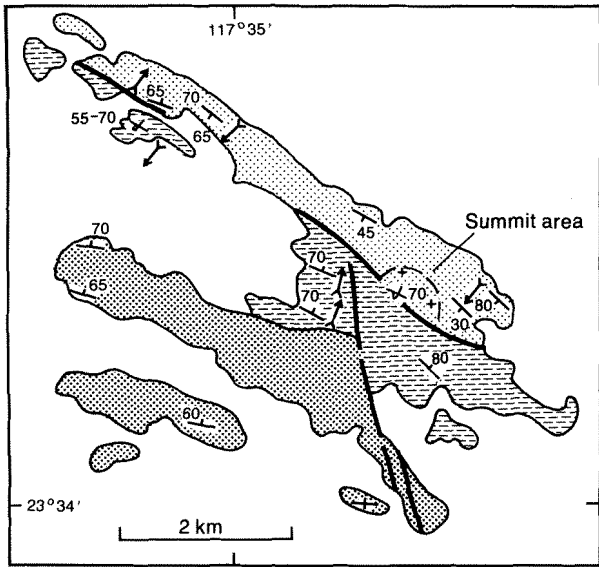
amounts of ferruginous siltstone. The quartz sandstone is dominated by stacked sets of trough cross-strata.

## Discussion

Most of the localized outcrops of sedimentary and volcanic rock, described above, have been interpreted as large olistoliths and olistostromes that were transported into the basin during deposition of the Ashburton Formation (Horwitz, 1978, 1980, 1981; Lascelles, 1983). For many of these occurrences, field relationships suggest that this is an unlikely explanation; for others, the evidence appears inconclusive. Only at three localities, all in the northwestern part of the Ashburton Basin, is there strong evidence of an allochthonous origin.

### Northwestern region

An allochthonous origin is considered likely for many of the unusual rock units reported from the northwestern Ashburton Basin. At Hardey Junction and the western closure of Wyloo Dome, isolated blocks of dolomite, ranging from 1–400 m across, are enclosed within the Ashburton Formation. Similar rock-types are abundant in the Duck Creek Dolomite, which outcrops within 5 km of these localities. Field relationships rule out the possibility that these carbonates are tectonic or erosional inliers of Duck Creek Dolomite, while the localized occurrence and geometry makes it unlikely that they are penecontemporaneous.



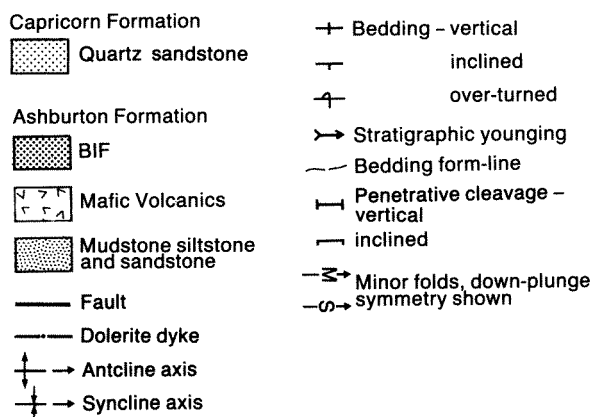
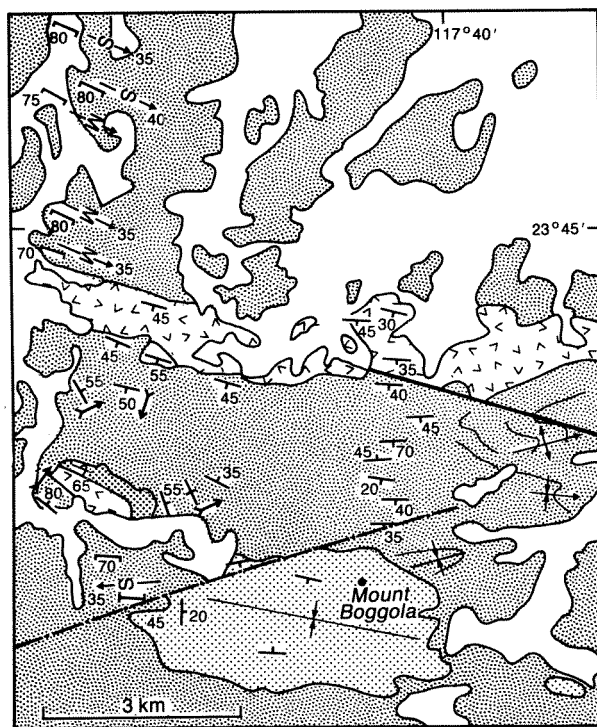
GSWA 25240

Figure 74 Geological map of the Mount Elephant area.



GSWA 25241

Figure 75 The northeastern slopes of Mount Elephant, viewed from the north, showing horizontal Capricorn Formation at the summit and overturned beds adjacent to a steeply dipping  $D_2$  fault (not seen in this view).



GSWA 25242

**Figure 76** Geological map of the Mount Boggola area showing principal outcrops of Ashburton Formation BIF and mafic volcanic rock, and Capricorn Formation sandstone.

neous carbonate deposits. It is therefore probable that the exotic rocks at Hardey Junction and the western closure of Wyloo Dome are of Duck Creek Dolomite transported into the deep marine basin during deposition of the Ashburton Formation. This interpretation was originally proposed by Horwitz (1978, 1981).

The 1.5–5 m thick dolomite and quartz sandstone unit that outcrops northeast of Mount Amy is also interpreted as an olistolith on the basis of its lithology, restricted lateral extent, and conformable relationship to the Ashburton Formation. Several carbonate and quartz sandstone sequences occur within the Wyloo Group and Mount Bruce Supergroup; however, the small thickness of the allochthonous deposit precludes correlation with any part of the underlying stratigraphy.

Horwitz (1981) interpreted the Mount Amy dacite as an olistolith “resembling facies in the Woongarra

Volcanics”. Support for this view comes from the geometry of the dacite, its limited lateral extent, conformable relationship to the Ashburton Formation, and the apparent lack of a metamorphic aureole. The possibility exists, however, that the dacite is a localized, post-Ashburton Formation intrusion which did not develop a significant contact aureole. Similar doubt concerns the origin of the basalt and basaltic agglomerate sequence that outcrops 15 km to the southwest of Mount Amy. Horwitz (1981) referred to this unit as an olistolith of “brecciated mixtures of dominantly basic igneous rocks resembling Fortescue Group assemblages”. There is little convincing evidence for large-scale transport, however, and they could equally well be the product of local pencontemporaneous volcanism.

The sandstone and conglomerate unit outcropping at the base of the Mount Stuart succession is interpreted as an olistostrome on the basis of its thickness, very poor sorting, disorganized internal structure, and variety of clasts. This supports the view of Horwitz (1981), although no evidence was found of the large (5 x 1 x 2.5 km) slab of allochthonous felsic volcanic rock shown as part of this unit in Figures 2 and 3 of Horwitz (1981).

Horwitz (1981) referred to the upper part of the Mount Stuart succession as an allochthonous BIF and shale sequence “resembling Hamersley Group assemblages”, which was still poorly consolidated at the time of emplacement, resulting in “convoluted and disharmonically folded slumps”. There is, however, little direct evidence for this interpretation. Firstly, the extent of soft-sediment folding is not as great as implied by Horwitz (1981): all medium- to large-scale folds examined during the present study have axial-plane cleavage, and are probably tectonic. Only small-scale asymmetric folds in chert mesobands, which lack an axial-plane cleavage, could be confidently interpreted as the result of soft-sediment deformation. Similar features, formed by post-depositional downslope creep, are abundant in BIF sequences in the Hamersley Group (Trendall and Blockley, 1970).

Attempts to relate the BIF succession at Mount Stuart to the rest of the Ashburton Formation are hampered by the faulted southern boundary and the poor exposure on the other three sides. Only on part of the western side of Mount Stuart is the stratigraphy well exposed. There the succession shows an upward transition from conglomerate and sandstone, rather than the abrupt change which might be expected if the sequence were allochthonous.

A third problem with the olistolith interpretation concerns the identity of the rock unit from which the Mount Stuart BIF was allegedly derived. The succession cannot, as originally implied by Horwitz (1981), be matched with any part of the Hamersley Group. Similar iron-rich deposits occur at the base of the Ashburton Formation, 10 km east of Mount Stuart but, to date, no detailed correlation has been put forward.

In the absence of convincing evidence for large-scale transport, the Mount Stuart BIF is considered to be an autochthonous part of the Ashburton Formation. It is interpreted as a sequence of chemical and hemipelagic de-

posits, laid down upon the sandstone and conglomerate olistostrome during a period of low terrigenous supply.

### Southeastern region

The sedimentary rock sequences at Mount Elephant and Mount Boggola lie with angular unconformity upon tectonically folded Ashburton Formation. This relationship casts considerable doubt upon the suggestion that they are allochthonous lower Wyloo Group sequences transported into the Ashburton Trough during deposition of the Ashburton Formation (Horwitz, 1980). Although the Mount Elephant and Mount Boggola successions have a superficial resemblance to parts of the Beasley River Quartzite and Mount McGrath Formation, they differ considerably in details of facies type and sequence organization, and cannot be matched with either formation. The successions are, however, closely similar to braided-fluvial and shallow-marine facies in the Capricorn Formation, which unconformably overlies the Ashburton Formation to the south and west of Ashburton Downs station (23° 23'S, 117° 01' 40"E). On the basis of this similarity, and their unconformable relationship to the Ashburton Formation, the Mount Elephant and Mount Boggola successions are considered part of the Capricorn Formation.

There is little evidence to support the view of Horwitz (1980) that the volcanic rocks outcropping north and west of Mount Boggola represent an allochthonous deposit that was derived from either the lower Wyloo Group to the north or from an unknown source to the south of the Ashburton Basin. The fact that the lowermost volcanics are conformable, and interbedded, with the Ashburton Formation suggests strongly that they were laid down as a result of penecontemporaneous submarine eruption, which took place close to the present day outcrop area. A further objection to the allochthonous interpretation is the difficulty of correlating this volcanic sequence with any in the lower Wyloo Group. Thick accumulations of pillow lava and pillow breccia have not been reported from the Cheela Springs Basalt. The only comparable sequence, the June Hill Volcanics, is much thinner (120 m) and outcrops 200 km to the northwest of Mount Boggola. Similarly, there is little likelihood that the volcanics were transported *en*

*masse* from the south, as no volcanic sequences of equivalent age, or older, outcrop to the south of Mount Boggola within a radius of 250 km.

Geological mapping by Daniels et al. (1967), Horwitz (1980), and the present authors does not support the view that the Radio Hill Fault inliers form part of the Ashburton Formation (Lascelles, 1983). Sandstones which immediately overlie the BIF pass along strike into upward-fining fluvio-deltaic deposits of the Mount McGrath Formation. These are overlain by the Duck Creek Dolomite, and the lowermost Ashburton Formation crops out approximately 5 km to the south.

To the southeast of Paraburdoo, the Mount McGrath Formation rests with strong erosional unconformity upon the Mount Bruce Supergroup and the lower Wyloo Group. At Stony Creek, 5 km to the northeast of the Radio Hill Fault sequence, the Mount McGrath Formation directly overlies the Weeli Wolli Formation of the Hamersley Group. This relationship, coupled with the disturbed contact at the base of the inliers, suggests that the BIF-sandstone sequence is a section of the Mount McGrath Formation-Hamersley Group unconformity, which has been exposed as a result of reverse faulting. Steep, west-northwest-trending reverse faults are responsible for stratigraphic repetition in the Mount Bruce Supergroup and Wyloo Group near Mount Maguire, 10 km to the southeast of the Radio Hill Fault Inliers (Chapter 9).

### Emplacement mechanisms

In the northwestern Ashburton Basin there is evidence to suggest that large blocks of dolomite, and dolomite and quartz sandstone were transported into the deep sea basin during deposition of the Ashburton Formation. For most, the nearest source rocks crop out 1–20 km from the site of deposition. This, coupled with the coherent nature of most of the allochthonous blocks, suggests that they were emplaced as large slides rather than as slumps or rockfalls (Stow, 1986). Chaotic beds of sandstone and conglomerate, such as occur at Mount Stuart, are more closely comparable to true olistostromes (Bates and Jackson, 1980) and were probably deposited from submarine debris flows.





## Chapter Eight

# Capricorn Formation, Mount Minnie Group and Bresnahan Group

The Capricorn Formation, the Mount Minnie Group and the Bresnahan Group are localized, pre-Bangemall Group rock units which unconformably overlie the Wyloo Group. The Capricorn Formation was deposited during the interval between two episodes ( $D_1$  and  $D_2$ ) of post-Wyloo Group–pre-Bresnahan deformation. The Boolaloo Granodiorite intruded the Wyloo Group during this break, but the timing of this event relative to deposition of the Capricorn Formation is uncertain. On such evidence, this rock unit has a maximum age of about 2000 Ma (the likely age of the Wyloo Group) and a minimum age of about 1680 Ma (the Rb–Sr age of the Boolaloo Granodiorite; Leggo et al., 1965).

The Mount Minnie Group post-dates early  $D_2$  folds in the Ashburton Basin, but is cut by late  $D_2$  wrench faults. These relationships indicate that the Mount Minnie Group is younger than the Boolaloo Granodiorite (1680 Ma) and the Capricorn Formation. The minimum age of about 1100 Ma is set by the inferred age of the Bangemall Group (Muhling and Brakel, 1985).

The Bresnahan Group, deposited after the  $D_2$  deformation event, is the youngest of the three post-Wyloo Group–pre-Bangemall Group rock units. As with the Mount Minnie Group, its maximum age is set by the Rb–Sr mineral isochron of 1680 Ma, obtained from the Boolaloo Granodiorite (Leggo et al.). Its minimum age, based upon data from the Bangemall Group, is about 1100 Ma (Muhling and Brakel, 1985).

## Capricorn Formation

The 800 m thick Capricorn Formation is the only stratigraphic unit within the Blair Basin (see Chapter 1). It rests with angular unconformity upon the Ashburton Formation in the central and southeastern Ashburton Basin (Fig. 77). This section describes and interprets principal facies associations of the Capricorn Formation. Most of this information was obtained from three stratigraphic sections (Fig. 77, localities 3, 4 and 5) and 1:40 000 scale mapping of adjacent outcrops.

The formation consists of sandstone, siltstone and mudstone, and minor amounts of conglomerate, dolomite and felsic volcanic rock. Three important facies associations are recognized: braided-fluvial, shallow-marine and fan-delta.

## Braided-fluvial facies association

### Description

This facies association consists of medium- to coarse-grained quartz sandstone (locally micaceous or ferruginous) and pebbly sandstone. Braided-fluvial sequences are generally 5–50 m thick, and are interbedded with the shallow-marine and fan-delta facies associations (Fig. 78A). They comprise stacked sets of medium- to large-scale (0.2–1.5 m) trough cross-strata. Lower set boundaries are sometimes marked by a mudstone pebble lag. Palaeocurrent data from locality 3 indicate that sediment transport was towards the west (Fig. 79). Sparse data from locality 2 suggest an easterly directed flow during deposition of the upper Capricorn Formation.

### Interpretation

Trough cross-stratified sandstones and pebbly sandstones are attributed to the downstream migration of medium- to large-scale dunes (Harms et al., 1982) in a braided-fluvial system.

## Shallow-marine facies association

### Description

The shallow-marine (or possibly lacustrine) facies association comprises mudstone, siltstone, fine- to medium-grained sandstone, dolomite, and felsic volcanic rock. These deposits form 5–70 m thick sequences, and are interbedded with the braided-fluvial and fan-delta facies associations.

Mudstone, siltstone, and fine- to medium-grained sandstone are generally ferruginous and micaceous. They outcrop in tabular beds, generally 0.01–5 m thick. Mudstones are either structureless or parallel-laminated. Siltstone and fine-grained sandstone are parallel-laminated (with local current lineations) or else display a variety of ripple profiles and bedforms. Straight-crested, bifurcated ripples, with symmetrical or asymmetrical profiles, are abundant. Linguoid ripples are less commonly observed, and generally occur on the upper surfaces of thin-bedded sandstones. Many ripples are deformed by sediment loading. Medium-grained sandstone exhibits medium- to large-scale trough cross-stratification. In many beds, internal

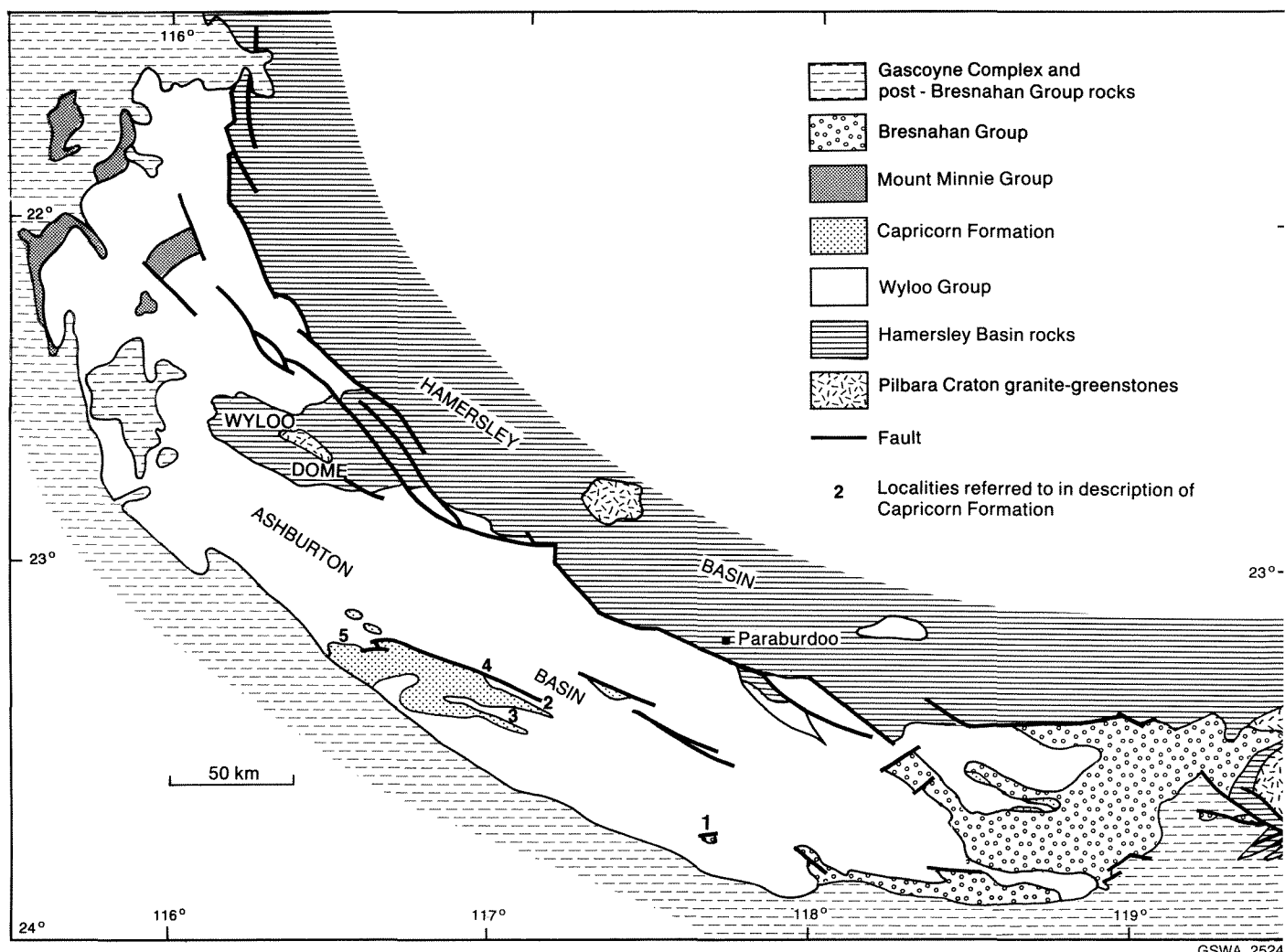


Figure 77 Geological map of the south and southwestern Pilbara showing principal outcrops of Capricorn Formation, Mount Minnie Group, and Bresnahan Group, and localities referred to in the text.

stratification is modified by ball-and-pillow structures (Fig. 80A).

Stromatolitic, ferroan dolomite and thin-bedded dolomite occur locally within this facies association (Fig. 80B). Stromatolitic dolomite is 0.1–0.5 m thick, and is characterized by small (10–20 mm wide), laterally linked columns with convex lamination. Columns may pass upwards into small, linked domes. The stromatolites are locally ridge-like in plan view and oriented parallel to the local palaeocurrent trend. Grey (1984) described a small branching-columnar stromatolite from Mount Elephant, but was unable to assign it to any previously described form. Thin-bedded dolomites outcrop as isolated beds, or form composite units up to 6 m thick. Internal structure consists of parallel or undulatory lamination.

A single rhyodacitic tuff unit, ranging from 4.5–15 m thick, is interbedded with shallow-marine shelf deposits at localities 3 and 4 (Fig. 77). The lower bounding surface is generally sharp, but the upper contact is transitional. The unit comprises 0.05–0.3 m thick tabular beds of

structureless tuff and parallel-stratified lapilli tuff. Some beds of ovoid to spherulitic lapilli (up to 10 mm diameter) show normal distribution grading; in others the coarsest fragments are in the middle of the bed.

### Interpretation

These lithofacies probably formed in a low- to moderately high-energy, shallow-marine (or possibly lacustrine) environment. The fine grain-size, parallel lamination and lack of scouring suggest that the mudstone was laid down from suspension during periods of low-energy sedimentation. The internal structure of the siltstone and fine-grained sandstone implies that they were laid down under the influence of wave and current processes. Bifurcated, straight-crested, symmetrical, and asymmetrical ripples are interpreted as wave ripples, formed under conditions of low to moderate sediment supply (de Raaf et al., 1977). Linguoid ripples, however, result from deposition under unidirectional flows of low to moderate velocity (Harms et al., 1982). Parallel-laminated siltstone and fine-grained sandstone which display current lineations record deposi-



GSWA 25244A

**Figure 78A** Lenticular coarse-grained sandstone (braided-fluvial facies association) interbedded with cleaved siltstone and fine-grained sandstone (shallow-marine facies association), Capricorn Formation, locality 3.

tion from moderate- to high-velocity currents. Similar lithologies which do not display current lineations are more difficult to interpret. They may have been deposited from high-energy traction currents or from slow-moving suspension clouds. Trough cross-stratified, medium-grained sandstone was deposited as a result of downcurrent migration of dunes under moderate current velocities (Harms et al., 1984). Ball-and-pillow structures are soft-sediment deformation features, caused by gravitational instability between sediment layers of contrasting grain-size (Allen, 1984, part 2).

The ridged form of the stromatolite bioherms resembles, albeit on a much smaller scale, the groove-and-spur morphology developed by Holocene stromatolites in the intertidal zone at Shark Bay. In this environment most stromatolite ridges are developed perpendicular to the shoreline, parallel to the direction of maximum wave and tidal scour (Hoffman, 1976). The trend of ridges and grooves in stromatolites of the Capricorn Formation is sub-perpendicular to the inferred southwestern margin of the sedimentary basin.

The rhyodacitic tuff is interpreted as a submarine pyroclastic fall deposit on the basis of the following evidence: its sharp, non-erosive base and transitional upper



GSWA 25244B

**Figure 78B** Small, laterally linked columnar stromatolites. The stromatolites are ridge-like or domical in plan view. Capricorn Formation, shallow-marine facies association, locality 3.

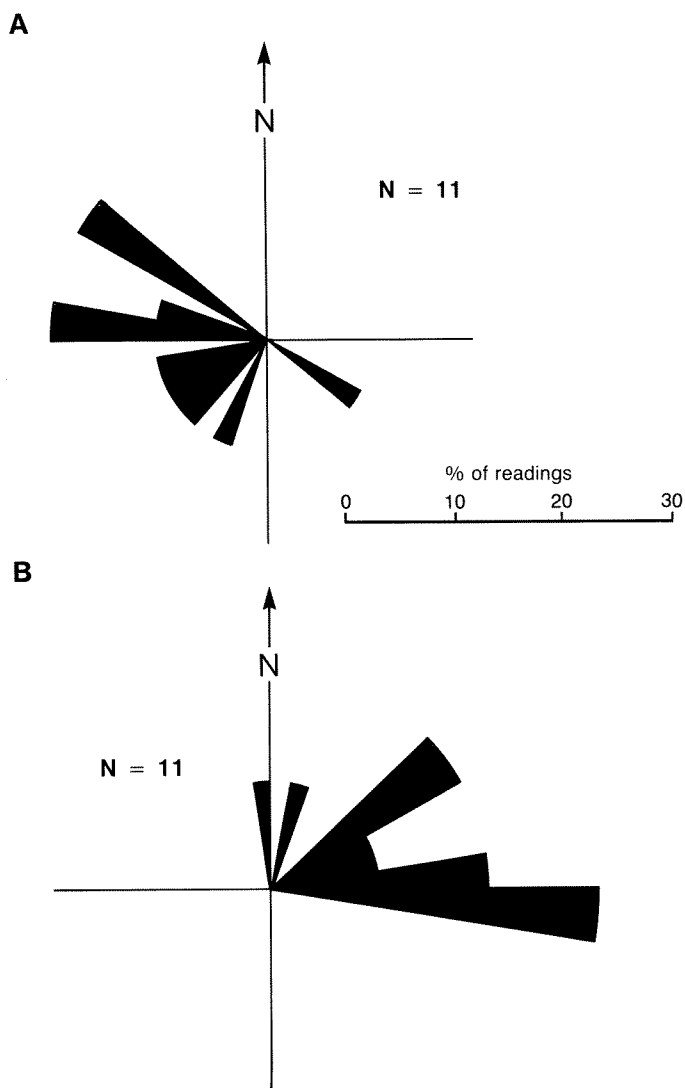


**Figure 79** Palaeocurrent data from the Capricorn Formation: **A** — braided-fluvial facies association, locality 2; **B** — fan-delta facies association, central Capricorn Range.

contact; the presence of parallel lamination and lack of cross-stratification or scouring; the normally graded and inverse to normally graded lapilli layers; and the nature of the associated rock types. The variation in the unit's thickness (4.5–15 m) between localities 3 and 4 may reflect differing amounts of marine reworking which took place during and after the eruption; however, there are no sedimentary structures to support this view. It is thought more likely that the variation results from primary differences in thickness of the fallout deposit.

### Fan-delta facies association

#### Description

The fan-delta facies association comprises medium- to very thick-bedded, matrix-supported conglomerate,

dolomitic and pebbly sandstone, and medium- to thick-bedded massive sandstone. These rock-types are interbedded with the shallow-marine facies association.

Medium- to very thick-bedded matrix-supported conglomerate units are 30–40 m thick; lower boundaries are either sharp or transitional, upper contacts are transitional. These deposits are structureless, apart from local trough cross-stratification in some of the medium-bedded conglomerates. Sorting is generally very poor and most clast diameters range from 5–200 mm (1200 mm maximum). Clasts are composed of dolomite, sandstone, chert, vein quartz, and mudstone. Most, apart from the dolomite fragments, are well-rounded.

Dolomitic, medium- to coarse-grained sandstone and pebbly sandstone occur in single beds, 0.1–0.4 m thick, or in medium- to thick-bedded units 0.5–20 m thick. Lower bedding surfaces are erosional, upper contacts are erosional or gradational. Many beds have a granule or pebble base, and fine upwards to medium-grained sandstone. Internal structure consists of single or stacked sets of medium-scale trough cross-strata (Fig. 80B), though the primary stratification is sometimes modified by soft-sediment deformation. Clasts comprise rounded quartz and subordinate lithic fragments (generally mudstone, chert, dolomite, and felsic volcanic rock).

Massive, medium- to coarse-grained sandstone and granule sandstone occurs in tabular to gently lenticular beds, generally 0.2–0.5 m thick. Lower boundaries are erosive; upper contacts are erosive, or sharply gradational into thin, fine- to medium-grained sandstone or dolomite. Massive sandstone lacks internal structure apart from rare horizontal layering. Locally, fine- to medium-grained sandstone displays ripple cross-lamination. Clasts include abundant lithic fragments (felsic to mafic volcanic rock, granite, sandstone, mudstone, and chert); and lesser amounts of quartz, feldspar, and vitric fragments.

#### Interpretation

The fan-delta facies association comprises both subaerial and subaqueous facies. Thick-bedded conglomerates are interpreted as debris-flow deposits, on the basis of their coarse grain-size and very poor sorting, matrix support, and lack of stratification. Those that are interbedded with dolomite or mudstone sequences are thought to represent subaqueous deposits. Others, that occur interlayered with trough cross-stratified sandstone and conglomerate, were probably laid down on the subaerial fan surface.

Cross-stratified sandstone, pebbly sandstone, and conglomerate, formed as a result of downcurrent migration of small to medium-sized dunes and gravel bars on the subaerial fan.

Massive sandstone is interpreted as a high-density turbidity current deposit. Lowe (1982) suggests that this type of bed forms under conditions of high suspended-load fallout, when there is insufficient time for development of either a bed-load layer or an organized traction carpet,





GSWA 25246A

**Figure 80A** Ball-and-pillow structures in interbedded coarse-grained sandstone and siltstone. Capricorn Formation, shallow-marine facies association, locality 3.



GSWA 24246B

**Figure 80B** Trough-cross stratified pebbly sandstone overlying parallel-laminated siltstone. Capricorn Formation, fan-delta facies association, locality 3.

and when deposition is by direct suspension. Thin beds of ripple-laminated sandstone, interbedded with the massive beds, represent fine-grained sediment deposited from the tail of the turbidity current.

## Distribution of facies associations

The vertical and lateral distribution of facies associations in the Capricorn Formation is summarized in Figure 81. In the vicinity of Irregully Creek the Capricorn Formation rests with angular unconformity upon the Ashburton Formation. The lower part of the formation is exposed southwest of Irregully Bore, at 23° 14' 30"S, 116° 28' 30"E. It consists of approximately 300 m of coarse-grained quartz sandstone and pebbly quartz sandstone, and an impersistent basal conglomerate. These rocks are assigned to the braided-fluvial facies association. Middle and upper levels of the formation, exposed north and east of Irregully Gorge (23° 19' 30"S, 116° 31' 30"E), comprise an estimated 450 m of parallel-laminated or ripple-laminated siltstone and mudstone, and minor amounts of fine- to coarse-grained sandstone (shallow-marine facies association).

Thirteen kilometres west of Ashburton Downs Homestead, the middle part of the Capricorn Formation is faulted against the Ashburton Formation. The Capricorn Formation consists of 120 m of siltstone, mudstone, and minor dolomite (shallow-marine facies association), interbedded with trough cross-stratified ferruginous sandstone (braided-fluvial facies association?). A 4.5 m thick felsic lapilli tuff occurs in the middle of the sequence. The upper part of the formation is exposed north of Koonong Pool (23° 21' 30"S, 116° 55' 30"E). It comprises 40 m of trough cross-stratified sandstone (braided-fluvial facies association) overlain by 20 m of mudstone and parallel-laminated dolomite (shallow-marine facies association). These are succeeded by 65 m of matrix-supported conglomerate and massive sandstone (fan-delta facies association).

Southwest of Ashburton Downs Homestead, at 23° 23' 30"S, 116° 55' 00"E, the Capricorn Formation lies with angular unconformity upon the Ashburton Formation, and has an estimated thickness of 700 m. The lowermost 100 m of the succession comprises mudstone and siltstone interbedded with thin- to thick-bedded immature sandstone (shallow-marine and fan-delta facies associations). These are overlain by 120 m of medium- to thick-bedded, cross-stratified sandstone (braided-fluvial facies association) which are succeeded by a further 140 m of mudstone, siltstone and immature sandstone (shallow-marine and fan-delta facies associations). Three hundred and sixty metres above the basal unconformity, a 15 m thick felsic lapilli tuff is interbedded with the mudstone and siltstone. The upper half of the succession comprises 270 m of mudstone, siltstone, dolomite, and fine- to medium-grained sandstone (shallow-marine facies association), interbedded with 20 m thick cross-stratified sandstone units. The uppermost of these sandstone bodies, which are assigned to the braided-fluvial facies association, is succeeded by 30 m of thick-bedded, matrix-supported conglomerate (fan-delta facies association).

The basal unconformity of the Capricorn Formation is exposed in a small, southward-draining creek, 800 m east of the Mount Blair road-cutting (23° 26' 40"S, 117° 08' 00"E). Ashburton Formation mudstone and sandstone dip south at 0 - 35° and are overlain by northward-dipping Capricorn Formation. The unconformity is marked by a thin stromatolitic dolomite succeeded by alternating mudstone, siltstone and immature cross-stratified sandstone (shallow-marine and fan-delta facies associations).

At Mount Boggola, the Capricorn Formation is about 200 m thick, and unconformably overlies the Ashburton Formation. It comprises lower and upper sequences of trough cross-stratified sandstone, 50 m and 100 m thick respectively, separated by 50 m of ferruginous siltstone and fine- to medium-grained sandstone. The lower and upper units are assigned to the braided-fluvial facies association, the middle division to the shallow-marine facies association.

## Depositional model

Deposition of the Capricorn Formation was initiated following D<sub>1</sub> deformation of the Wyloo Group. The principal controls at the start of Capricorn Formation sedimentation are (Fig. 82):

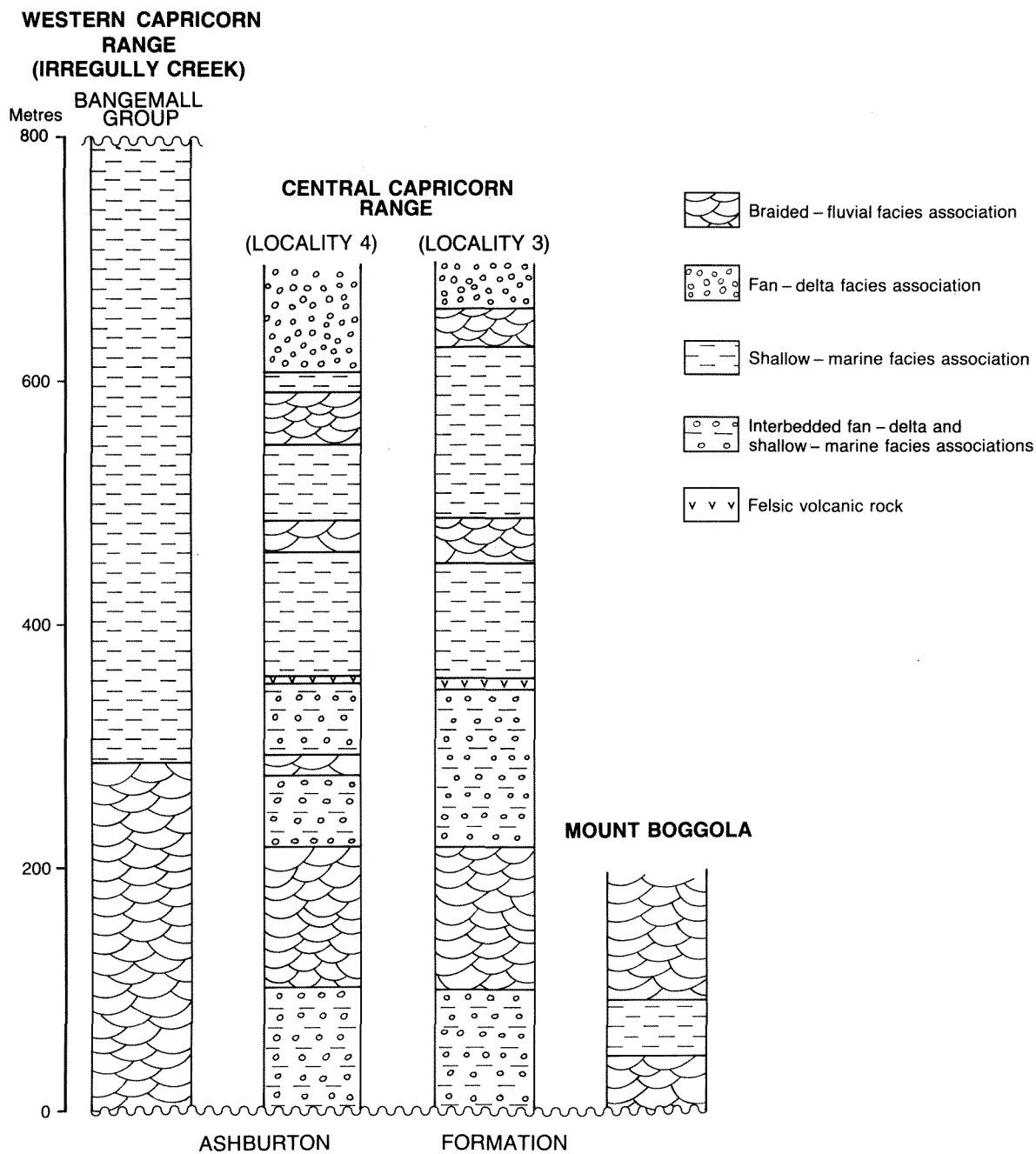
- (a) a tectonically active upland located to the east and southwest of the Ashburton Basin; and
- (b) a southeast-trending sedimentary basin developed along the faulted northeastern margin of the upland.

Braided streams, which drained the upland, deposited quartz-rich sand and gravel in eastern and western parts of the basin. Near the present-day central Capricorn Range, distal fluvial channels entered a shallow marine (or lacustrine) body, and resulted in an interfingering of fine- to coarse-grained siliciclastic and carbonate sediments. Additional sandy detritus, much of it volcanic in origin, was supplied from distal alluvial fan channels which entered the water body along its southwestern margin.

Deposition of the middle Capricorn Formation was influenced by a relative rise in sea or lake level, such that subaqueous facies were deposited over much of basin. This drowning was terminated by uplift of the source area and progradation of the braided fluvial systems. During the final stage of basin filling, proximal alluvial fan deposits, with a high proportion of carbonate and volcanic detritus, were introduced from the south and west.

## Discussion

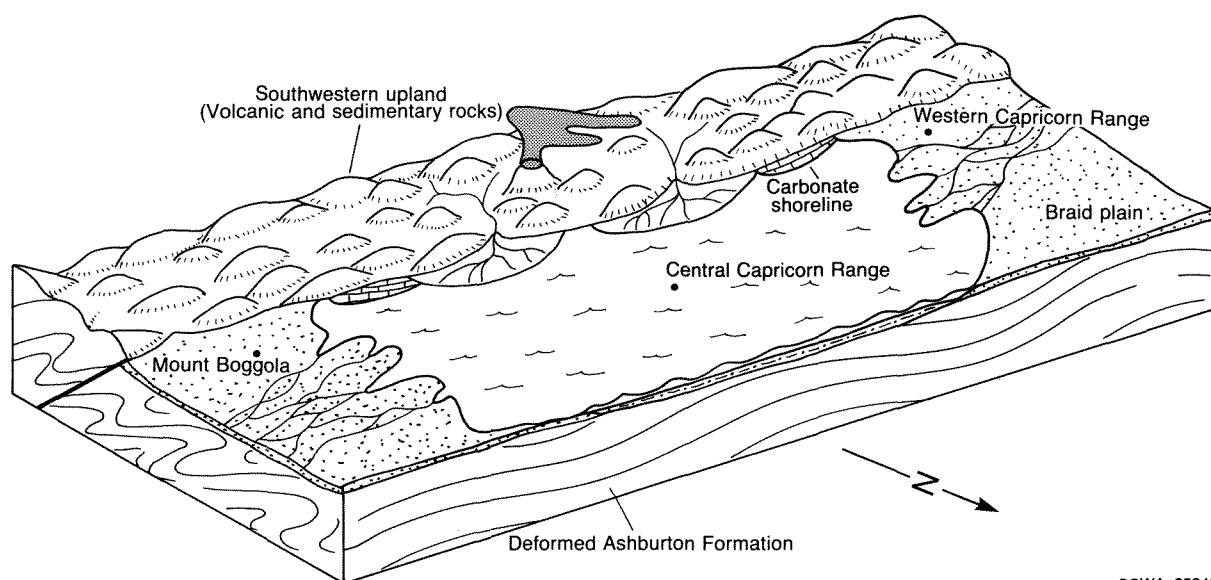
Sandstone and conglomerate compositions, and facies distributions, suggest three major source areas for the Capricorn Formation. Braided-fluvial sandstones were introduced from source terrains located east and west of the present day outcrop area. They are compositionally more mature than sandstones in the fan-delta or shallow-marine facies associations, and were probably derived from a distant source of granitoid and sedimentary rocks. Quartz



GSWA 25247

Figure 81 Generalized stratigraphic profiles summarizing the vertical and lateral distribution of facies within the Capricorn Formation.





GSWA 25248

**Figure 82** Deposition model for the lower Capricorn Formation. See text for discussion.

sandstones derived from the east are generally more ferruginous than those from the west, and may have originated from granite–greenstone and BIF sequences near the Sylvania Inlier.

Immature lithic sandstone and conglomerate were derived from a sedimentary–volcanic–granitoid source, which probably lay close to the southwestern margin of the Ashburton Basin. Today, this area consists of high-grade metamorphic rocks and granitoids (Gascoyne Complex), covered by younger Bangemall Group rocks. Metamorphic overprinting relationships in the northeastern Gascoyne Complex and Ashburton Basin (Chapter 10) suggest that peak regional metamorphism in this area was coeval with post-Wyloo Group  $D_1$  deformation, whereas granitoid intrusion and deposition of the Capricorn Formation both took place in the interval between  $D_1$  and  $D_2$ . High-grade metamorphic rock fragments are scarce in the Capricorn Formation, suggesting that metamorphics of the Gascoyne Complex were not exposed (at least not in the immediate vicinity of the Capricorn Range) during the time that these rocks were being deposited. Granitoid clasts, found in some fan-delta sandstones, are not sufficiently distinctive to allow identification of their source; they could be derived either from post- $D_1$  intrusions or from pre-existing granitic basement.

## Mount Minnie Group

The Mount Minnie Group (incorporating the Tanpool Beds of Williams, 1968) unconformably overlies the Ashburton Formation, and forms a series of outliers, occupying a total area of approximately 350 km<sup>2</sup>, in the northwestern part of the Ashburton Basin (Plate 1). It has a maximum thickness of about 2400 m and is unconformably overlain by the Bangemall Group and the Cretaceous Nanutarra Formation. Williams (1968) and

Daniels (1970) provided the first detailed descriptions of the group, and these were summarized by Daniels (1975) and Goode (1981). Further discussion is presented by Seymour et al. (1988). The following account is based largely on these works.

Williams (1968) and Daniels (1970) subdivide the Mount Minnie Group into three formations: Brodagee Sandstone, Wabco Shale, and Warramboe Sandstone.

### Brodagee Sandstone

#### Description

The Brodagee Sandstone, including the Katanga Conglomerate of Williams (1968) is the lowest formation of the Mount Minnie Group. It ranges in thickness from 150–750 m and comprises quartz sandstone, pebbly quartz sandstone, and conglomerate.

Medium- to coarse-grained quartz sandstones and pebbly quartz sandstones generally outcrop in silicified, thick-bedded units. Internal structure consists of stacked sets (0.1–0.5 m thick) of trough cross-strata and local parallel stratification. Sparse palaeocurrent data from the Mount Minnie area suggests that sediment transport was towards the northwest.

Thick-bedded, clast- and matrix-supported conglomerate forms a laterally impersistent unit, up to 600 m thick, at the base of the Brodagee Sandstone. The conglomerate contains rounded clasts of vein quartz, silicified sandstone, jaspilite, and chert, together with angular fragments of cleaved mudstone and meta-sandstone. The matrix is composed of quartz sandstone. Several irregular lenses of quartz sandstone occur interbedded with the conglomerate in the vicinity of Katanga Bore (21° 45' 20"S, 115° 48' 30"E).

## Interpretation

The Brodagee Sandstone is interpreted as an alluvial-fan deposit. Thick-bedded conglomerates represent debris flow and fluvial-channel sediments laid down on proximal parts of the fan. Stacked sequences of trough cross-stratified sandstone and pebbly sandstone formed as a result of dune migration in braided channels on the middle and outer fan surface. Palaeocurrent data point to a source area southeast of the present outcrop.

## Wabco Shale

### Description

The Wabco Shale conformably overlies the Brodagee Sandstone and has a thickness of 30–500 m. It consists of brown-weathering mudstone and siltstone, and thin beds of quartz sandstone. The former are parallel-laminated or ripple cross-laminated, and locally show slump and load structures; the latter are generally cross-stratified. Williams (1968) records northerly directed palaeocurrents from sandstones outcropping south of Katanga Bore.

### Interpretation

The Wabco Shale is interpreted as a shallow-marine shelf deposit. Thick mudstone and siltstone sequences were deposited from suspension or weak currents. Thin, trough cross-stratified sandstones are of uncertain origin. They may represent small sand bodies formed as a result of wave or tidal currents, or distal-fan channel deposits. The former explanation is more likely in view of the palaeocurrent trend.

## Warramboe Sandstone

### Description

The Warramboe Sandstone rests conformably on the Wabco Shale in the Mount Minnie and Katanga Bore areas, but directly overlies the Brodagee Sandstone in the Parry Range. The formation has a maximum thickness of 600 m and comprises thin- to thick-bedded quartz sandstone, and minor siltstone and mudstone. Sandstones display cross-stratification, ripple marks, and slump structures.

### Interpretation

On the basis of lithology and conformable relationship to the Wabco Shale and the Brodagee Sandstone, the Warramboe Sandstone is interpreted as a shoreline and distal alluvial-fan deposit.

## Lithofacies distribution

Immediately south of Katanga Bore, the Brodagee Sandstone is represented by 150 m of conglomerate (the Katanga Conglomerate of Williams, 1968). It is conform-

ably overlain by up to 30 m of Wabco Shale, which is transitional upwards into 600 m of Warramboe Sandstone. In the Mount Minnie area, the Brodagee Sandstone comprises 750 m of sandstone, pebbly sandstone, and minor conglomerate. It is overlain by 500 m of Wabco Shale, which is in turn, succeeded by an estimated 400 m of Warramboe Sandstone. In the Parry Range, the Brodagee Sandstone is approximately 750 m thick and consists of sandstone and pebbly sandstone with local conglomerate; the Wabco Shale is absent and the Brodagee Sandstone is conformably overlain by 400 m of Warramboe Sandstone.

The thick (> 600 m) conglomerate and pebbly sandstone unit outcropping immediately to the west of Red Hill (Daniels, 1970), and the pebbly quartz sandstones exposed on the southeastern side of Mount Amy, are correlated with the Brodagee Sandstone.

## Depositional model

The following model for Mount Minnie Group sedimentation is based upon the vertical and lateral distribution of lithofacies within the Brodagee Sandstone, Wabco Shale, and Warramboe Sandstone.

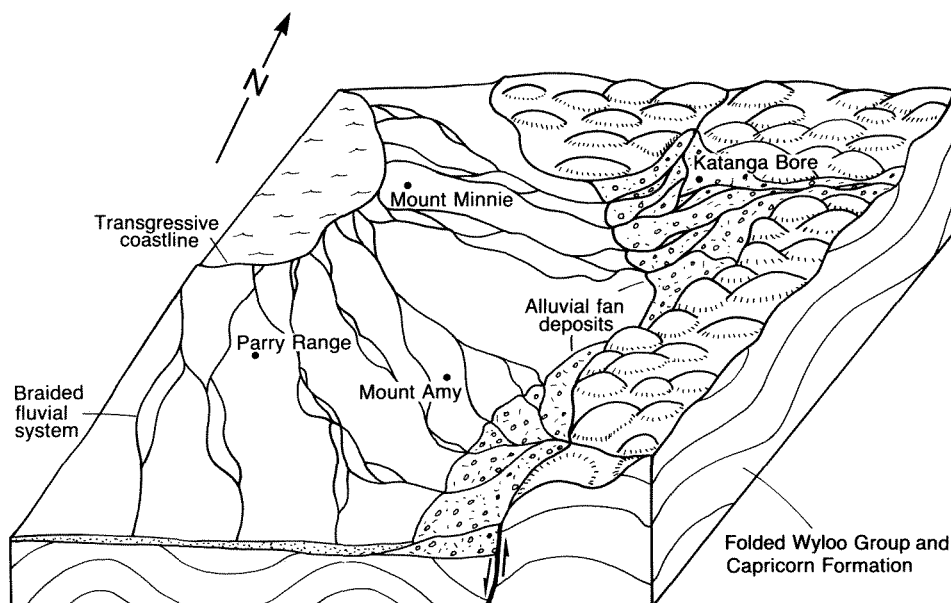
Deposition of the Mount Minnie Group was initiated during the early stages of  $D_2$  deformation. The principal sediment sources at the start of Mount Minnie Group deposition were upland areas of Wyloo Group rocks immediately north of Katanga Bore, and southeast of Mount Amy (Fig. 83). Detritus from these source areas accumulated as thick alluvial fans (Brodagee Sandstone) in a fault-bounded sedimentary basin to the south and east of Mount Minnie. Later basin subsidence resulted in marine incursion and deposition of coastal to offshore facies (Wabco Shale) in the Katanga Bore and Mount Minnie areas, and shoreline and distal alluvial fan sediments in the Parry Range (Warramboe Sandstone). During the latter part of Mount Minnie Group sedimentation, regressive shoreline and alluvial fan deposits built out into the northern part of the basin.

## Discussion

Daniels (1975, p.146) tentatively correlated the Mount Minnie Group and the Bresnahan Group on the basis of their stratigraphic position and inferred environment of deposition. On present evidence, however, such a correlation appears unlikely, because the Bresnahan Group was deposited after the  $D_2$  deformation event (Chapter 9) which was responsible for folding and faulting in the Mount Minnie Basin. In addition, the two successions are dissimilar in thickness, lithostratigraphy and source terrains.

## Bresnahan Group

The Bresnahan Group (Daniels and MacLeod, 1965), the only stratigraphic unit of the Bresnahan Basin, lies with marked angular unconformity upon the Mount Bruce



GSWA 25249

**Figure 83** Depositional model for the Mount Minnie Group during the transition from Brodagee Sandstone to Wabco Shale. See text for discussion.

Supergroup, Wyloo Group, and the Capricorn Formation (Fig. 84). It is unconformably overlain by the Bangemall Group. The Bresnahan Group has a maximum measured thickness of 4000 m. It was first described by Talbot (1926), and was mapped by Halligan and Daniels (1964), Daniels and MacLeod (1965), and Daniels (1968). A summary of Bresnahan Group geology is given by Daniels (1975) and Goode (1981); Ewers and Ferguson (1985) described a prospective uranium deposit near the basal unconformity. The most complete study of the Bresnahan Group to date is that of Hunter (1990). The following account is based upon work and a reconnaissance study by the author.

The Bresnahan Group comprises conglomerate, sandstone, siltstone and mudstone. The twofold division of the stratigraphy into the Cherrybooka Conglomerate and the Kunderong Sandstone, proposed by Daniels and MacLeod (1965), is not employed here as there is no distinct horizon marking the boundary between the formations; rather there is gradual, vertical and lateral transition from conglomerate to sandstone dominated lithofacies. As a result the two divisions are not clearly mappable units.

Three major facies associations are recognized within the Bresnahan Group: valley-fill, alluvial-fan channel, and lacustrine.

### Valley-fill facies association

#### Description

At the base of the Bresnahan Group, accumulations of conglomerate, sandstone, and small amounts of siltstone and mudstone, fill small palaeo-valleys and hollows on

the underlying surface. Locally, this buried topography has a relief of at least 30 m.

Most conglomerate units (Fig. 85) contain well-rounded, subspherical clasts of sandstone, pebbly sandstone, chert, vein quartz (generally tourmaline-bearing), and jaspilite. The conglomerates are often thick bedded (1–10 m), very poorly sorted, unstratified, and show a mixture of clast and matrix support. Maximum clast-size is up to 1.5 m and the matrix consists of purple, poorly sorted, micaceous granule sandstone. Very thick-bedded conglomerates may incorporate lenticular horizons of very coarse-grained sandstone, up to several metres thick.

Conglomeratic units are locally underlain by, or interbedded with, up to several metres of purple mudstone and siltstone and thin- to medium-bedded sandstone. Mudstones are parallel-laminated; siltstones and fine-grained sandstones display parallel-lamination or ripple cross-lamination. Coarse-grained sandstone forms erosively based lenticular beds which generally lack internal stratification.

#### Interpretation

The thickness and coarse grain-size of the conglomerates, their lack of stratification, and the mixture of clast and matrix support, suggest that they were deposited from a debris flow (Enos, 1977; Lowe, 1982). Many of the clasts are well rounded, implying that they were subject to turbulent streamflow transport prior to incorporation in the debris-flow deposit. Lenticular sandstones, which occur within some thick-bedded conglomerate units, are thought to represent fluvial-channel sediments, laid down in intervals between debris-flow events.

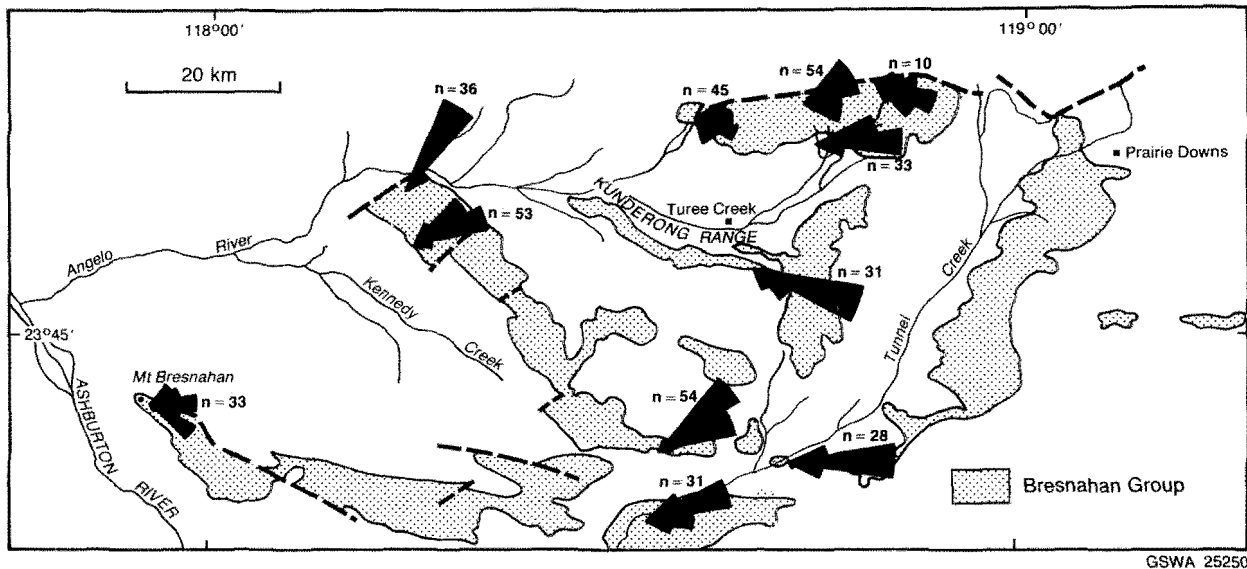


Figure 84 Palaeocurrent data from the alluvial-fan channel facies association, Bresnahan Group (data from W.M. Hunter, written communication, 1987).



GSWA 25251

Figure 85 Unconformable contact between the Capricorn Formation and the Bresnahan Group. The uppermost Capricorn Formation (exposed below 1.5 m staff) consists of lenticular-bedded quartz sandstone. The overlying Bresnahan Group is represented by very thick-bedded cobble- to boulder-conglomerate. Mount Bresnahan.

Mudstone, siltstone, and thin-bedded sandstone are interpreted as localized lacustrine deposits, laid down in hollows on the pre-Bresnahan Group surface.

### Alluvial-fan channel facies association

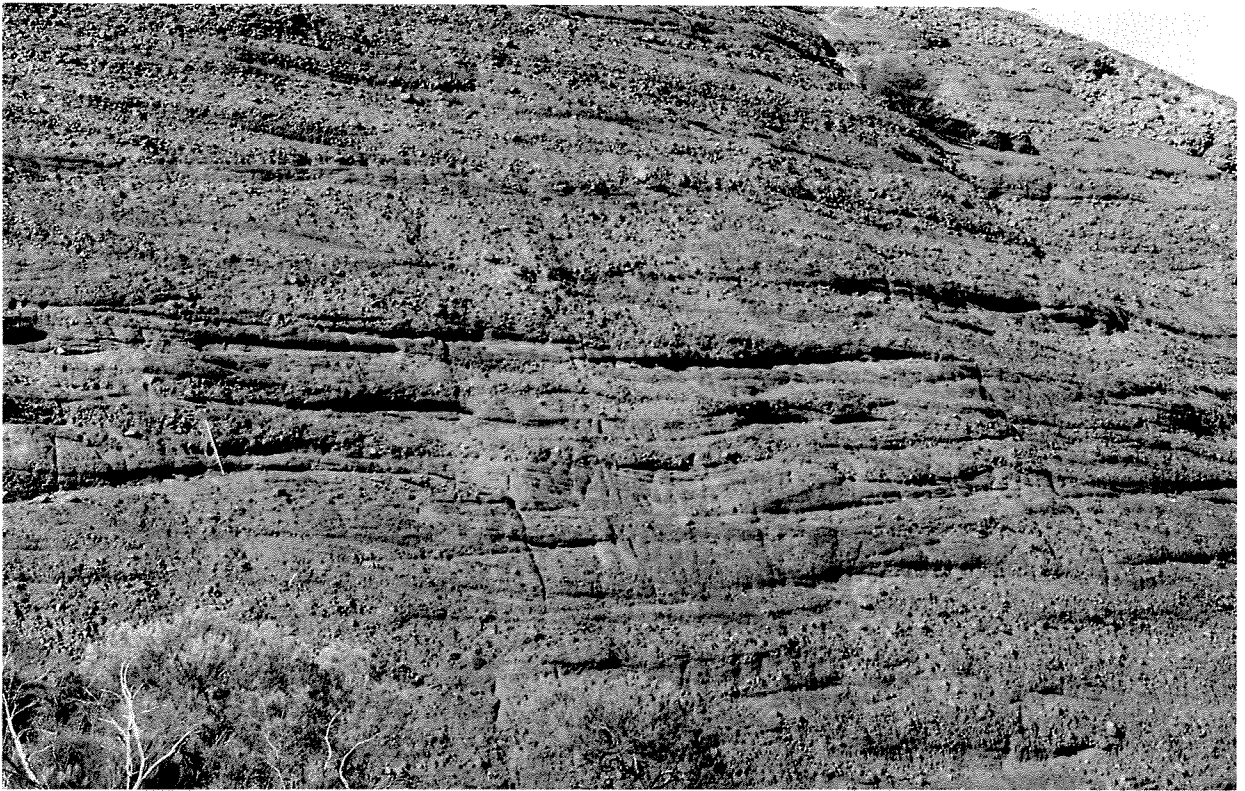
#### Description

The alluvial-fan channel facies association (Fig. 86 A,B) comprises sandstone (generally very coarse-grained to granular) and pebbly sandstone, locally interbedded with conglomerate. Pebble, cobble and boulder compositions are as described for the valley-fill facies association.

Sandstone and pebbly sandstone form a lenticular-bedded sequence (tabular bedded parallel to the paleocurrent trend), up to 4 km thick. Individual beds are generally 0.2–2.0 m thick, and, in many cases, include a pebble or cobble lag above the basal scour surface. Internal structure is dominated by single or stacked sets of medium- to large-scale trough cross-stratification. Paleocurrent data (written communication, W.M. Hunter, 1987) are strongly unidirectional for any locality, and record an easterly directed palaeoflow (Fig. 84).

Sandstones are composed of quartz and lithic fragments with various amounts of feldspar and mica. Accumulations of heavy minerals (including iron and titanium oxides, tourmaline, and apatite) occur throughout the sandstone, but are particularly abundant in the central northern outcrops where they occur in laminated bands up to 0.1 m thick. Elsewhere they occur at the asymptotes and bases of the trough cross-strata.

Pebble, cobble, and boulder conglomerates are lenticular-bedded (generally tens of metres wide and several metres deep) normal to the local palaeoflow, and tabular-



GSWA 25252A

**Figure 86A** Lenticular bedding and large-scale trough cross-stratification in Bresnahan Group alluvial-fan channel facies association, Mount Bresnahan. Staff in left centre of photograph is 1.5 m long.



GSWA 25252B

**Figure 86B** Trough cross-stratification in alluvial-fan channel pebbly sandstone. Current flow was left to right, scale-bar is in centimetres. Bresnahan Group, south of Horrigan Pool. Photograph by W.M. Hunter.





GSWA 25252C

**Figure 86C** Cross-laminated medium-grained sandstone interbedded with parallel-laminated siltstone and mudstone. Bresnahan Group, lacustrine facies association, central Kunderong Range. Photograph by W.M. Hunter.

bedded parallel to this direction. They are clast-supported, with a sandy matrix, and lack internal stratification.

### Interpretation

Lenticular beds of trough cross-stratified sandstone and pebbly sandstone are considered to have formed as a result of downstream migration of medium to large dunes in braided fan channels. Unidirectional palaeocurrents, and tabular bed profiles parallel to the palaeoflow, imply a channel system of low sinuosity.

Clast-supported conglomerates are interpreted as high-energy, braided-fluvial channel deposits. Highly competent flows are indicated by the large clast-sizes in many beds.

## Lacustrine facies association

### Description

The lacustrine facies association consists of mudstone and siltstone, interlayered with thin- to medium-bedded sandstone (Fig. 86C). Mudstone and siltstone are generally parallel-laminated and micaceous. Fine- to medium-grained sandstone occurs in tabular to lenticular beds. The thickest sandstone beds display trough cross-stratification; thin beds are generally parallel-laminated and show locally developed current lineations, ripples, and flute markings. Ball-and-pillow structures are abundant.

### Interpretation

These rocks were laid down in a subaqueous environment where deposition from suspension and weak currents (mudstone and siltstone) alternated with periods of higher energy (sandstone) sedimentation. The precise depositional setting is uncertain; however, lack of evidence for wave and tidal reworking suggests a lacustrine rather than open-marine environment. Lenticular, trough cross-stratified sandstones are interpreted as distal fluvial-channel deposits, whereas tabular bedded sandstones — which display parallel lamination, current lineations and flute-marked bases — may be turbidites or flash-flood deposits laid down near the shallow margins of the lake.

### Distribution of facies associations

On the southwestern slopes of Mount Bresnahan (23° 49' 30"S, 117° 54' 30"E) the group lies with marked angular unconformity upon lenticular-bedded quartz sandstones of the Capricorn Formation. The lowermost 30–50 m of strata comprises thick-bedded conglomerate (valley-fill facies association) with a maximum clast size of 1.5 m. These are overlain by 200 m of pebble- and boulder-conglomerate, and large-scale, trough cross-stratified pebbly sandstones (alluvial-fan channel facies association).

Close to the northern boundary of the Bresnahan Group, between the Angelo River and Tunnel Creek, some outcrops contain exotic blocks of quartz sandstone up to 10

m across and 2–3 m thick. The angular blocks are underlain by conglomerate which contains rounded cobbles and boulders of similar quartz sandstone. This part of the sequence is enclosed in coarse-grained pebbly sandstones, typical of the alluvial-fan channel facies association. The horizon of exotic blocks is interpreted as a rockfall of Beasley River Quartzite fragments (Hunter, 1990).

Eight kilometres south of Horrigan Pool (23° 32' 30"S, 118° 15' 00"E) the lowermost 65 m of strata comprises massive conglomerate and sandy conglomerate (valley-fill and alluvial-fan channel facies association) with clasts up to 0.5 m in diameter. These are overlain by 4000 m of cross-stratified sandstone and pebbly sandstone (alluvial-fan channel facies association). At Tunnel Creek, and along most of the Kunderong Range, the basal conglomerate is thin and impersistent. An exception is in the central Kunderong Range, where 50 m of massive conglomerate, similar to that at Mount Bresnahan, underlies coarse-grained sandstone.

East of Nalgomia Creek, the Bresnahan Group consists of mudstone and siltstone, interbedded with medium-grained sandstone (lacustrine facies association). To the south and southwest of Prairie Downs Homestead (23° 33' 00"S, 119° 09' 00"E) these deposits are overlain by coarse-grained sandstone and pebbly sandstone.

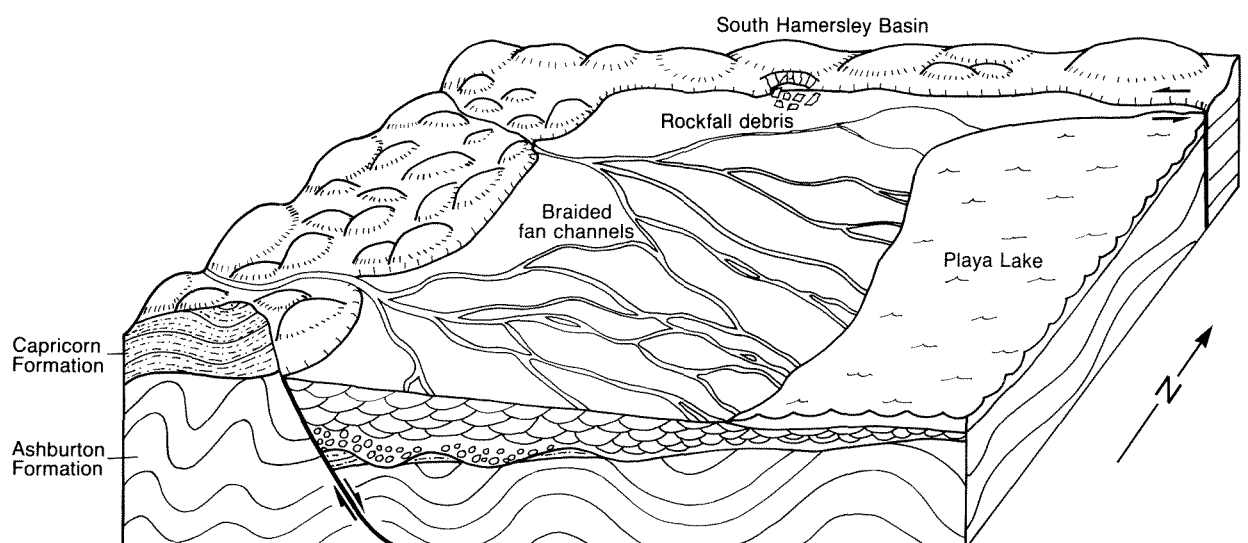
## Depositional model and palaeogeographic reconstruction

The following model for Bresnahan Group sedimentation is adapted from Hunter (1990), and the main features are summarized in Figures 87 and 88. Deposition of the Bresnahan Group began in response to post-D<sub>2</sub>, southeasterly directed extension along the southern Pilbara margin. The principal tectonic controls at the start of Bresnahan Group deposition were:

- (a) An extensional fault system, comprising east-north-east-trending normal faults (southeast side downthrown) and west-northwest-trending transfer faults, bounding the southern margin of the Hamersley Basin. This system delineates the northern and western margin of a small sedimentary basin south and southwest of Prairie Downs Homestead.
- b) An upland, formed of Capricorn Formation, Wyloo Group, and granitoid rocks, lying to the west (upthrow) of the normal fault.

High-gradient rivers entered the basin from the upland area and built an alluvial-fan complex on the eroded surface of Capricorn Formation and upper Wyloo Group rocks. Close to the faulted western margin of the basin, debris-flow conglomerates and thin, laterally restricted lacustrine sequences were deposited in small valleys and hollows on the pre-Bresnahan Group surface. Middle parts of the alluvial-fan system were characterized by gravelly braided, fluvial channels. These passed downslope into a number of sandy braided channels, which merged into a playa lake complex in distal (eastern) parts of the basin. Intermittent uplift along the associated transfer fault was responsible for localized rock-fall and debris-flow sedimentation along the basin's northern margin.

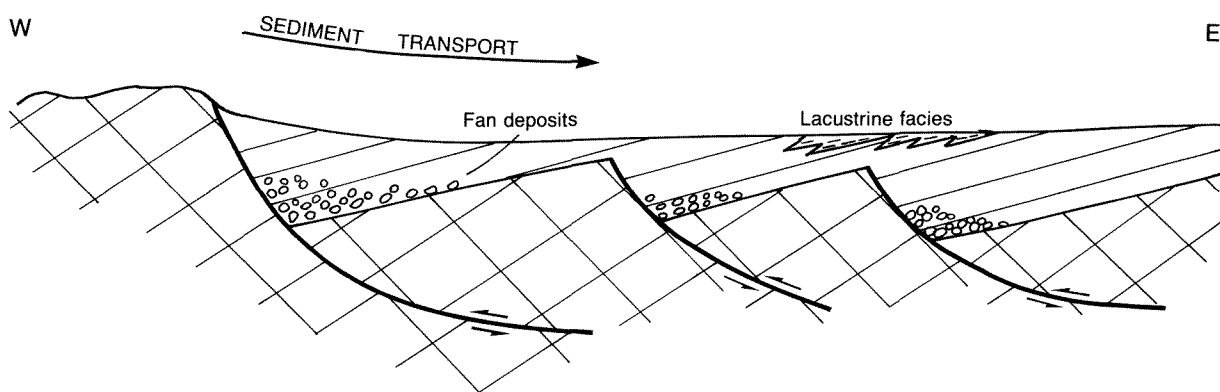
Evolution of the Bresnahan Basin was controlled by east-west crustal extension, which initiated northeast-trending normal faulting at the eastern end of the Kunderong Range. Block subsidence on the eastern side of this fault caused backstepping of the western margin of the original sedimentary basin, and development of a new alluvial fan system west of the initial fan body. Distribution of sedimentary facies in the second fan system followed the same pattern as before; debris-flow and stream-flow conglomerates were deposited close to the faulted western boundary, and successively finer sediments accumulated in braided channels on mid to outer parts of



GSWA 25253

Figure 87 Depositional model for the Bresnahan Group. See text for discussion.





GSWA 25254

Figure 88 Cross-section showing the evolution of the Bresnahan Basin by repeated back-stepping of its western margin.

the fan. Continued southeasterly directed extension resulted in northwestward propagation of the normal fault system, further backstepping of the western margin of the Bresnahan Basin, and westerly migration of proximal alluvial fan facies.

## Discussion

Tyler et al., (in press) identify a system of east-north-east-trending normal faults, and east-southeast-trending transfer faults (part of the Mount Whaleback Fault system), at the northern margin of the Bresnahan Basin. Movement along this fault system post-dates uplift of the Sylvania Inlier,  $D_2$  folding in the Ashburton Fold Belt, and deposition of the Bresnahan Group, but pre-dates deposition of the Bangemall Group. The character, thickness, and distribution of sedimentary facies outlined in this section provides evidence for early fault movements that are contemporaneous with Bresnahan Group sedimentation.

Alluvial-fan successions, built up as a result of back-faulting of the basin margin, are commonly developed in extensional tectonic regimes, particularly those associated with strike-slip fault systems (see review by Mitchell and Reading, 1986). A widespread feature of such tectonic settings is the accumulation of geographically extensive, coarse-grained alluvial-fan successions, which dip towards the backfaulting i.e. towards the source area (Fig. 88). Bedding in the Bresnahan group dips generally towards the east, north, or south, rather than the west; this is attributed to post-depositional tilting and folding of the alluvial fan succession (Tyler et al., in press)

Although the total stratigraphic thickness that may accumulate in a backstepped basin is often great, the thickness deposited and preserved on any downthrown

block is notably less (Heward, 1978b). Such a relationship accounts for the anomalous thickness measurements published for the Bresnahan Group. For example, Hunter (1990) records approximately 4 km of sandstone in the western Kunderong Range, whereas Daniels and Macleod (1965) estimated a minimum thickness for the Group of 11.9 km in the eastern part of the Bresnahan Basin.

Palaeocurrent data, sandstone and conglomerate composition, and stratigraphic relationships between the Bresnahan Group and the underlying rock units, demonstrate that the principal source rocks were the Capricorn Formation and granitoids of the Gascoyne Province that outcrop west of the Bresnahan Basin (Hunter, 1990). This interpretation differs from that of Daniels (1975) and Goode (1981), who thought that sedimentary rock fragments present in the Bresnahan Group were derived from outcrops of Beasley River Quartzite north of the Bresnahan Basin; and that much of the granitic component originated from the Sylvania Inlier. Many of the sedimentary rock clasts are of quartz conglomerate and pebbly quartz sandstone — lithologies which are much more abundant in the Capricorn Formation than in the Beasley River Quartzite. Strong evidence that the Capricorn Formation was the major source of sedimentary rock fragments is provided by the easterly directed palaeocurrents and by the presence of eroded Capricorn Formation rocks beneath the Bresnahan Group unconformity. The only clasts recorded from the Bresnahan Group which can be confidently matched with the Beasley River Quartzite form part of a localized rockfall deposit, 32 km northeast of Turee Creek Homestead. Palaeocurrent data suggests that the Gascoyne Complex, rather than the Sylvania Inlier, was the source of most granitic detritus. Daniels (1975) proposed a minor sediment supply from this area, citing as evidence, the presence of distinctive tourmaline-rich clasts in Bresnahan Group conglomerate.



## Chapter Nine

# Structure and metamorphism

## Structure

The Ashburton, Blair, and Mount Minnie Basins, form the major part of the Ashburton Fold Belt, a region of open to tight folding and pervasive slaty cleavage in the northern part of the Capricorn Orogen (Gee, 1979a). The northeastern part of the Ashburton Basin also forms part of the Ophthalmia Fold Belt (Halligan and Daniels, 1964; Gee, 1979a); this structural unit developed before the Ashburton Fold Belt, during the earliest stages of the Capricorn Orogeny (Tyler and Thorne, in press).

Two subsequent deformation events, referred to as the Newmanian and Edmundian fold periods by Halligan and Daniels (1964), post-date the Capricorn Orogeny. They were responsible for open to tight folding and faulting in the Bresnahan, Mount Minnie and Ashburton Basins.

Major Capricorn Orogen and post-Capricorn Orogen structures in the southwestern Pilbara are shown in Plates 1 and 2.

## Capricorn Orogen structures

### Ophthalmia Fold Belt

Ophthalmia Fold Belt structures affect the Hamersley Basin and the northeastern Ashburton Basin (Fig. 89). Two groups of structures are recognized, pre-Wyloo Group and syn-Wyloo Group:

#### *Pre-Wyloo Group structures*

Large-scale dome and basin structures predate the Wyloo Group in the southwestern Ophthalmia Fold Belt. This relationship is clearly displayed in the Hardey Syncline (22° 53'S, 117° 00'E), where a westerly plunging syncline of Turee Creek Group rocks is truncated by the unconformity at the base of the Beasley River Quartzite (Trendall, 1979; Seymour et al., 1988). The Wyloo Dome was also initiated during this early folding event. Although much of its present day form is the result of later deformation, the large concentric fold which forms the southeastern closure is cross-cut by the angular unconformity at the base of the Wyloo Group.

Pre-Wyloo Group folds have not been identified in the southeastern part of the Ophthalmia Fold Belt. Here, the

Beasley River Quartzite lies disconformably upon different stratigraphic levels within the Mount Bruce Supergroup. Southwest of Paraburdoo, southeast of Mount Maguire (23° 20' 00"S, 117° 44' 30"E), and 5 km southeast of Divide Well (23° 28' 30"S, 118° 28' 30"E) the basal unconformity overlies Weeli Wolli Formation, lowermost Turee Creek Group, and Woongarra Volcanics, respectively. No angular discordance between the Wyloo Group and Mount Bruce Supergroup has been observed at any of these localities; this suggests that deformation took the form of gentle tilting, possibly accompanied by block faulting.

#### *Syn-Wyloo Group structures*

The major Ophthalmia Fold Belt structures on TUREE CREEK are coeval with Wyloo Group sedimentation. Folds of this generation (e.g. Turee Creek Syncline) post-date the Beasley River Quartzite and Cheela Springs Basalt, but are cut by a set of dykes which predate formation of the iron-ore deposit at Paraburdoo. The fact that pebbles of mature hematite ore occur in the basal Mount McGrath Formation (Morris, 1980) limits the timing of deformation to post-Cheela Springs Basalt, pre-Mount McGrath Formation.

The earliest structures associated with syn-Wyloo Group deformation are localized, small-scale, tight to isoclinal, layer-parallel folds (Tyler and Thorne, in press). They occur within the middle BIF unit of the Woongarra Volcanics where it crops out along the southern margin of the Turee Creek Syncline, southeast of Koothano Pool (23° 17' 00"S, 118° 16' 30"E). Folds typically have tectonic cleavage and are locally associated with mylonitic fabrics.

The principal syn-Wyloo Group structures are upright to steeply inclined, north-facing buckle-type folds (Tyler and Thorne, in press). They are close to tight, parallel to flattened-parallel, and often conjugate. Hinge lines are non-cylindrical and folds on all scales die out vertically and laterally. Axial-plane cleavage may be present in the northeastern part of TUREE CREEK, but is weak to absent further west. Most fold axes trend west-northwest to northwest. East-trending folds are restricted to the core of the Turee Creek Syncline and the southeastern part of the Ophthalmia Fold Belt (e.g. Wanmunna Anticline, 118° 45'S, 23° 04'E). Some reorientation of fold trends, most noticeably in the Turee Creek Syncline, has resulted from

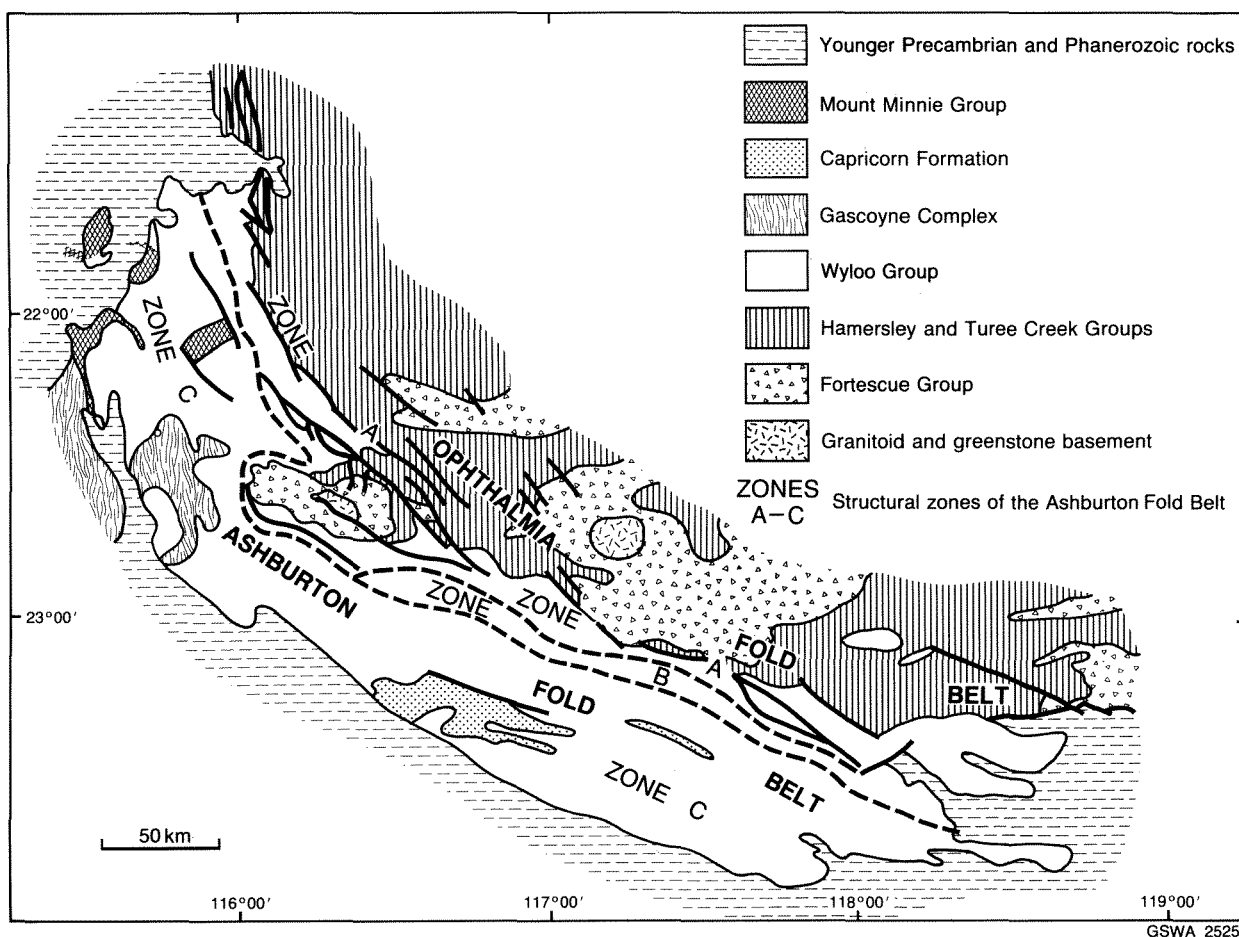


Figure 89 Geological map showing the principal structural divisions of the southwest Pilbara.

post-Wyloo Group dextral wrench faulting (Tyler, in press a).

Evidence of syn-Wyloo Group folding is less abundant in the southwestern part of the Ophthalmia Fold Belt. On the southern flank of Wyloo Dome, a gentle angular unconformity locally separates Woolly Dolomite and Cheela Springs Basalt from the overlying Mount McGrath Formation. In addition, lower formations in the Wyloo Group, up to and including the Mount McGrath Formation, thin westwards along the southern and northern margins of the dome. This thinning probably reflects intermittent basement uplift during lower Wyloo Group deposition (Horwitz, 1978).

#### *Interpretation of Ophthalmia Fold Belt structures*

The *en echelon*, dome-and-basin style of folding which characterizes the southwestern Ophthalmia Fold Belt was formerly considered to result from interference between two sets of folds: the Ophthalmian, with west- to north-west-trending axes; and the Rocklean, with northeast- to north-northeast-trending axes (MacLeod et al., 1963; Halligan and Daniels, 1964; MacLeod, 1966; Horwitz and

Smith, 1978). There is, however, little evidence of north-east-trending minor folds or cleavages to support the cross-folding interpretation. Gee (1979) favoured the view that the dome-and-basin pattern formed in response to vertical movement of basement blocks, and that the northeasterly "cross-fold" directions are simply deflections of fold axes around basement highs.

Tyler (in press) believes deformation in both basement and cover to be linked, and the structures of the Ophthalmia Fold Belt to represent the frontal part of a regional foreland fold-and-thrust belt. Pre-Wyloo Group folding in the southwest Hamersley Basin was accompanied by tilting and uplift further east, and reflects basement instability during the initial stages of north-south crustal shortening. Further north-south compression, in the interval following deposition of the Cheela Springs Basalt, caused reverse movement on basement faults and deformation of the supracrustal sequence in the southeast Hamersley Basin. Small-scale folds parallel to bedding may have formed in response to gravity sliding during early stages of deformation. Subsequently, medium- to large-scale, north-facing folds were generated east of Paraburdoo. Near the Sylvania Inlier, folding was accompanied by northerly directed thrusting (Tyler, in press).

## Ashburton Fold Belt structures

Ashburton Fold Belt structures formed as a result of post-Wyloo Group–pre-Bresnahan Group deformation. During this event, Wyloo Group, Capricorn Formation, Mount Minnie Group, and Mount Bruce Supergroup rocks, were subjected to open to isoclinal folding and normal, reverse and strike-slip faulting. Two generations of structure ( $D_1$  and  $D_2$ ) are recognized.  $D_1$  structures post-date the Wyloo Group and pre-date the Capricorn Formation and Mount Minnie Group.  $D_2$  structures are broadly coeval with Mount Minnie Group deposition; they post-date the Capricorn Formation but predate the Bresnahan Group.

### $D_1$ structures

$D_1$  structures affect the Ashburton Formation but have not been observed in underlying parts of the Wyloo Group. Much of the evidence for this deformation comes from the widespread occurrence of an  $S_1$  foliation, which is crenulated by  $S_2$ , and from the presence of large-scale fold-interference patterns.

In the northwestern Ashburton Fold Belt,  $S_1$  foliation is mainly restricted to the area northwest of a line joining Red Hill (22° 06' 00"S, 116° 02' 00"E) with the Boolaloo Granodiorite. In this region, it is a well-developed penetrative cleavage which dips in the same direction as, but more steeply than, the bedding. Bedding -  $S_1$  intersections are horizontal to gently plunging lineations ( $L_1$ ). In southeastern WYLOO, the  $S_1$  foliation is well developed in the area west of a line joining Hardey Junction (22° 44' 00"S, 116° 07' 00"E) to the 116° longitude on the southern boundary of the map sheet. Westward from this line, with increase in metamorphic grade, it develops into a metamorphic schistosity sub-parallel with bedding.

On EDMUND and TUREE CREEK, recognition of the  $S_1$  foliation is generally difficult in northern parts of the fold belt because of its coaxial (and often coplanar) relationship to  $S_2$ . The  $S_1$  foliation is more clearly evident in the area south of the Ashburton River. In the eastern Capricorn Range, mudstone and sandstone of the Ashburton Formation show a well-developed  $S_1$  penetrative cleavage not present in the overlying Capricorn Formation. At Mount Blair, the basal unconformity of the Capricorn Formation dips north at 50° as a result of  $D_2$  folding. The  $S_1$  cleavage in the underlying Ashburton Formation dips 15–45° south, while bedding dips (and youngs) southward at 0–30°. Rotation of bedding and  $S_1$  to their pre- $D_2$  orientation indicates that the tight  $F_1$  fold was characterized by a steeply southward-dipping axial surface.

Beneath the Bangemall Group unconformity at Fords Creek (22° 45' 00"S, 117° 17' 00"E)  $S_1$  is a penetrative cleavage which consistently dips northeast at a slightly shallower angle than bedding (younging to the southwest). Both are cut by a steep, northeasterly dipping  $S_2$  crenulation cleavage. The two foliations are coaxial in the most southerly outcrops but may diverge by up to 60° locally. Three kilometres northeast of the Bangemall Group unconformity, on the northeastern limb of a medium-

scale  $F_2$  anticline,  $S_1$  dips more steeply than bedding (younging to the northeast). Here,  $S_2$  is sub-vertical and approximately coaxial with  $S_1$ . These relationships suggest the presence of a large-scale, tight, southwesterly facing  $F_1$  fold, which has been refolded during  $D_2$ .

Further evidence for  $F_1$  folding on TUREE CREEK is seen southeast of Mount Boggola (Plates 1 and 2). Here, a large-scale southward facing  $F_1$  anticline has been coaxially refolded by the  $D_2$  event.

### $D_2$ structures

The most prominent structures in the Ashburton Fold Belt were formed during the  $D_2$  deformation event. They affect the Wyloo Group, Capricorn Formation, Mount Minnie Group, Mount Bruce Supergroup, and granitoid–greenstone basement. Three structural zones are recognized within the Ashburton Fold Belt (Fig. 89): Zone A, flanking the Ophthalmia Fold Belt; Zone B, forming the central part of the Ashburton Fold Belt on TUREE CREEK and EDMUND; and Zone C forming the southern and western part of the fold belt.

#### Zone A

Zone A forms the northern and eastern part of the Ashburton Fold Belt, adjacent to the Ophthalmia Fold Belt, and is dominated by large-scale open to tight folds and dextral wrench faults. It covers the most southerly part of the Hamersley Basin, and extends southward to include outcrop of the Duck Creek Dolomite outcrop. Separation of Ashburton and Ophthalmia Fold Belt structures in the northern part of the zone can be difficult, because the later deformation tightened pre-existing folds and reactivated earlier faults.

An extensive system of northwest-oriented dextral wrench faults outcrops in the area between Bukardi Creek (23° 33' 00"S, 118° 13' 00"E) and Cairn Hill Well (23° 09' 20"S, 117° 18' 30"E) on TUREE CREEK. Offsets on individual faults may be up to 7.5 km. Southwest of Snowy Mountain a major wrench fault cross-cuts an *en echelon* suite of east-west trending  $F_2$  folds in Mount McGrath Formation. The northwesterly continuation of this fault system passes to the north of Mount Maguire and intersects the main part of the Hamersley Basin near the Paraburdoo minesite. Small north- and northwest-trending faults near Radio Hill have sinistral and dextral senses of movement respectively, and represent antithetic and synthetic faults associated with the main strike-slip fracture (Wilcox et al., 1973). A second large wrench fault bounds the western margin of the Wyloo Group–Mount Bruce Supergroup outcrop at Mount Maguire. Steeply dipping, west-northwest-trending reverse faults cause local stratigraphic repetition of the Wyloo Group and Mount Bruce Supergroup immediately east of Mount Maguire and south of Radio Hill; they probably formed in response to north-northeasterly directed compression within the strike-slip system.

In the eastern part of the Ashburton Fold Belt,  $F_2$  folds are characteristically open, large-scale, and non-cylindri-

cal, and have upright or steeply southward-dipping axial-plane cleavages. Fold trends are generally between east and northwest.

A major dextral wrench-fault system forms the northeastern and eastern margin of the Ashburton Fold Belt on WYLOO and YARRALOOA. Wyloo Dome has been displaced about 11 km along a series of northwest- to north-northwest-trending faults which extend from the Beasley River to Duck Creek homestead and continue along the western edge of the Hamersley Basin to Deepdale. These faults cross-cut west-northwest- to northwest-trending fold axes in the Hamersley Basin, and give rise to localized lenticular outcrop patterns in the adjacent Wyloo Group (e.g. between Duck Creek Gorge and Urandy Creek Outcamp). North of Wyloo Dome, faults bounding the Hamersley Basin step the rocks downward towards the southwest, away from the craton. Further west, they locally step rocks down towards the craton, (e.g. at Duck Creek Gorge) and cause stratigraphic repetition of the generally westward-dipping Wyloo Group. Gentle  $D_2$  folds occur between Red Hill Creek and the Wyloo Dome. These are generally open and upright and trend between west and north-northwest.

The Wyloo Dome shows some structural affinity with the Ophthalmia Fold Belt; however, most of its present form post-dates the Wyloo Group and is considered to result from the  $D_2$  deformation event. Ophthalmia Fold Belt structures are evident northeast and east of the Metawandy Granite; they comprise open-concentric to flattened-concentric easterly plunging folds with weak axial-plane cleavage. In contrast, southern and western parts of the dome are characterized by tight, upright to northeast-facing folds plunging northwest or southeast. These are associated with strong west-northwest- to northwest-trending axial-plane cleavage which parallels the  $S_2$  crenulation cleavage in the adjacent Ashburton Formation. West-northwest- to north-northeast-trending synthetic and antithetic faults cut the northeastern and southern margin of the dome. Fault planes are subvertical, and have linear to sigmoidal surface traces. Steep, northwest-trending reverse faults cause outcrop repetition of the Duck Creek Dolomite on the southwestern flank of the dome (R. C. Horwitz, personal communication, 1985).

### Zone B

Zone B occupies the northeastern part of the Ashburton Formation outcrop on TUREE CREEK, EDMUND, and the southeastern part of WYLOO (Fig. 89). It is characterized by tight to isoclinal, non-cylindrical folds, with wavelengths of 5–200 m. Folds trend west to northwest and are associated with a pronounced axial-plane cleavage ( $S_2$ ) which generally dips 60–90° to the southwest.

Along the northern margin of the zone, high-angle reverse faults, oriented parallel or sub-parallel to the  $F_2$  fold axes, cause local repetition of outcrop of the Duck Creek Dolomite–Ashburton Formation contact. Within the main body of Ashburton Formation the faults are generally associated with sub-parallel quartz veins and are frequently observed to cut out all or part of the north-

ern limb of the  $F_2$  folds. This fact, coupled with lack of marker horizons in the Ashburton Formation, and the tight to isoclinal folding, creates an impression of simple stratigraphy and southwesterly dipping beds throughout much of Zone B. In such cases, evidence for  $F_2$  folding comes from local reversals in younging direction and the presence of isolated  $F_2$  fold closures within the otherwise uniformly dipping Ashburton Formation.

### Zone C

Zone C occupies the remainder of the Ashburton Fold Belt (Fig. 89). It is distinguished from Zone B by the presence of large-scale  $F_2$  folds. Southeast of Wyloo Dome,  $F_2$  folds are large (100–6000 m wavelength), non-cylindrical, and trend west to northwest. Most plunge 10–40° (up to 80° locally) to the southeast or northwest. Axial planes dip steeply to the southwest or northeast. In the eastern and central Capricorn Range,  $F_2$  folds in Capricorn Formation trend west-northwest but swing southwest and then west-northwest again near Irregularly Creek. Close to the northern margin of Zone C, folds are open to tight (or locally isoclinal), but are generally more open in central and southwestern parts of the fold belt (Fig. 90A). Downward-facing structures, which result from the refolding of  $F_1$  folds, are present near the head of Fords Creek and between Cherrybooka Creek and Kennedy Creek.

Between Glen Florrie and Kooline Homesteads,  $F_2$  folds are steeply plunging, tight to upright, and show east-trending axial surfaces.  $S_2$  is a penetrative slaty cleavage in the more easterly outcrops, but is present as a crenulation cleavage further west (Fig. 90B). Around 22° 55'S, 116° 12'E and the Mount Clement prospect, interference between  $F_1$  and  $F_2$  folds has created a complex dome-and-basin pattern.

At the eastern margin of the Mount Danvers Granodiorite, around 22° 46' 30"S, 115° 55' 00"E, hinge lines of minor  $D_2$  folds trend at high angle to the granitoid margin. Fold tightness and amplitude decrease towards the pluton. This suggests that country rocks adjacent to the granitoid were in a strain shadow during the  $D_2$  deformation. A poorly developed  $S_2$  cleavage occurs within the outer part of the granitoid, and indicates that the  $D_2$  deformation event post-dates granitoid intrusion. Timing of granitoid intrusion into the Wyloo Group is discussed in the section describing metamorphism of the Wyloo Group.

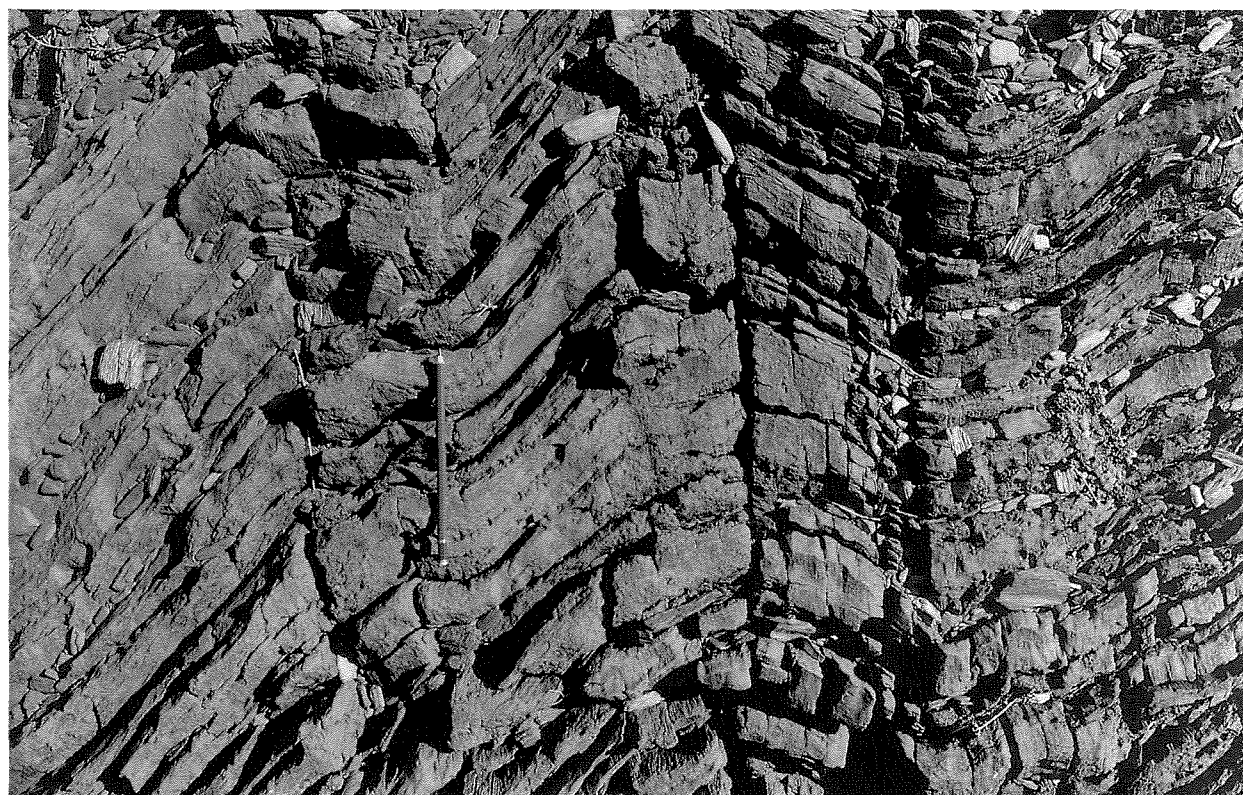
North of Wyloo Dome, large-scale  $F_2$  folds are present south of latitude 22°S. Here, large, open to tight  $F_2$  folds (Plates 1, 2) are second-order structures distributed about a first-order, northwest-plunging syncline. Second-order  $F_2$  folds have steep or vertical axial surfaces and moderately to steeply plunging hinge lines (40–65°) of northwesterly trend. Wavelengths range from 7–15 km. Immediately north of Wyloo Dome, where  $S_1$  is weak or absent,  $S_2$  is a penetrative slaty cleavage. North and west of Mount Amy, an  $S_1$  penetrative cleavage or metamorphic schistosity is generally present, and  $S_2$  takes the form of an axial-planar crenulation cleavage. In such cases most





GSWA 25256A

**Figure 90A** Open,  $F_2$  folds in Ashburton Formation sandstone. Note the strong axial-planar cleavage. Zone C, Ashburton River, east of Mount Dawson.



GSWA 25256B

**Figure 90B**  $F_2$  folds in Ashburton Formation metapelites. The steeply dipping  $S_2$  foliation has crenulated a bedding-parallel  $S_1$  fabric. The resultant crenulation lineation, plunging toward the camera, can be seen at the bottom centre of the photograph. Zone C, west of Glen Florrie Homestead.



$F_2$  minor folds are straight limbed and have narrow to angular closures.

Numerous west-northwest- to north-northwest-trending wrench faults parallel the  $F_2$  fold axes or cross-cut them at a shallow angle. Locally, a dextral displacement of up to 3 km can be measured. In general, however, lack of marker horizons within the Ashburton Formation makes it difficult to assess accurately the amount of relative movement. The northern margin of the Capricorn Range is marked by a steep, southward-dipping fracture. Outliers of Capricorn Formation, between Six Mile Creek and Mount Elephant are partly or completely fault-bounded. Locally this results in a distinctive rhomboidal outcrop geometry, e.g. 20 km west-northwest of Mount Elephant.

North of Wyloo Dome, near Cardo Outcamp (22° 14' 40"S, 116° 08' 00"E), north-northwest-trending faults have a major component of reverse movement and cause repetition of outcrop of the Duck Creek Dolomite and June Hill Volcanics.

Many faults are marked by a line of *en echelon* quartz veins, dipping 30–90° northeast or southwest. Locally they are associated with a second suite of steeply dipping veins that trend between north-northwest and north-northeast. Most consist of equant to prismatic, subhedral to anhedral quartz with irregular goethite vugs (after sulphide). Locally, quartz crystals are kinked as a result of progressive fault movement. Most copper, gold, lead, and silver mineralization, discovered to date in the Ashburton Fold Belt, is associated with  $D_2$  faults and quartz veins (Chapter 10).

### Interpretation of Ashburton Fold Belt structures

Widespread development of  $S_1$  and  $S_2$  foliations, coupled with local occurrence of refolded  $F_1$  folds, provides evidence for two deformation events ( $D_1$  and  $D_2$ ) in the Ashburton Fold Belt. At present little is known regarding the shape or orientation of  $F_1$  folds. On TUREE CREEK, EDMUND and southeast WYLOO,  $S_1$  is generally coaxial with  $S_2$ , suggesting a west-northwest to northwest trend for  $F_1$  fold axes. Resolving the shape of  $F_1$  folds from  $S_1$  bedding, and younging relationships at Fords Creek, Mount Boggola, and Mount Blair, suggests that they were large-scale, tight structures which faced southwest and northeast in southern and central parts of the fold belt respectively. This change in vergence may result from fanning of  $F_1$  folds over a thrust ramp in the underlying supracrustal succession (Tyler and Thorne, in press).  $S_1$  is absent from the northern and eastern margin of the fold belt; this probably reflects a decrease in intensity of  $F_1$  folding towards the craton.

Most obvious folding and faulting in the Ashburton Fold Belt results from the second post-Wyloo Group deformation ( $D_2$ ). It can be related to a major dextral wrenching event which post-dates deposition of the Capricorn Formation and intrusion of the Boolaloo Granodiorite, but pre-dates the Bresnahan Group.

The dextral wrench-fault system parallels the present-day margin of the Pilbara Craton and may be partly con-

trolled by pre-existing basement fractures. Although measured offsets on individual faults commonly range from 0.5 to 5 km, these may be minimum values since they take no account of strain taken up by folding within the wrench system. This observation, and the fact that it is not usually possible to determine the amount of offset within the Ashburton Formation, means that no estimate can be given of the total amount of strike-slip movement within the Ashburton Fold Belt.

North- and northwest-trending faults near Radio Hill, Paraburdoo, were interpreted as pre-Wyloo Group structures by Bourne and Jackson (1979). Although these fractures clearly displace the Mount Bruce Supergroup, there is little evidence to support the view that they pre-date the Beasley River Quartzite. Instead, their orientation and sense of movement suggest that they are synthetic and antithetic faults (Wilcox et al., 1973), associated with a major post-Wyloo Group dextral wrench fault which extends from south of Dublin Hill to the Paraburdoo minesite.

Most of the northwest- to northeast-trending faults which occur in the vicinity of the Wyloo Dome are also interpreted as conjugate fractures related to the strike-slip system. Five kilometres north-northwest of Miningee Well (22° 50'30"S, 116° 38' 30"E) synthetic and antithetic faults cause southeasterly displacement of the lower Wyloo Group. On the northeastern flank of the Wyloo Dome, north-northeast-trending antithetic fractures cut the Mount Bruce Supergroup and Beasley River Quartzite. Their left-handed sigmoidal trace is characteristic of antithetic faults which have become rotated as a result of continued movement along the strike-slip system (Wilcox et al., 1973). Antithetic fractures which have been rotated to an orientation almost normal to the principal strike-slip faults generally result in little or no displacement of country rock, e.g. Aerial and Silent Sisters lead mines (Plate 1).

North of Wyloo Dome, at 22° 23'S, 116° 16'E, a lenticular horst of Cheela Springs Basalt (15 x 3.5 km) has been uplifted as a result of local compression between two sigmoidal strike-slip faults. Small, fault-bounded rhombic outcrops of Mount McGrath Formation near the northern end of the inlier reflect normal faulting at right angles to the principal extension direction in the strike-slip system.

Open to tight and isoclinal, *en echelon*  $F_2$  folds were formed as a result of plastic deformation during initial stages of dextral strike-slip movement. Wilcox et al. (1973) noted that, as displacement on the wrench zone increases, initial folds are broken, first by fractures and then by faults. In later stages of strike-slip movement, fold axes on either side of the wrench fault may be offset; this sequence of deformation accounts for the late-stage relationship of wrench faulting to  $F_2$  folding in the Ashburton Fold Belt.

$F_2$  fold axes are generally oriented 5–30° to the trend of the principal wrench faults. This relatively acute angle is characteristic of wrench-fault systems in which strike-slip movement is accompanied by horizontal shortening across the fault plane (Sanderson and Marchini, 1984). Significant horizontal compression is also indicated by

the numerous steeply dipping reverse faults which parallel the  $F_2$  fold axes, and by the clockwise rotation of synthetic and antithetic faults. Much of the horizontal shortening within the southeastern part of the Ashburton Fold Belt has been accommodated by tight to isoclinal, generally upright folding and reverse faulting in Zone B. Less horizontal shortening in Zones A and C is indicated by the more open  $F_2$  folds, and by less widespread reverse faulting and greater angular separation between  $F_2$  fold axes and wrench faults in these areas. In the western Capricorn Range,  $F_2$  fold axes are oriented at 60–70° to the line of wrench faults which forms the northern margin of the Capricorn Formation outcrop. Here, large angular discordance is indicative of a wrench system in which there is lateral offset of the shear zone (Sanderson and Marchini, 1984).

Northwest-trending, small to large  $F_2$  folds in the western part of Wyloo Dome are also related to the  $D_2$  dextral wrenching event. Fold axes trend 25–35° to the line of wrench faults which cuts the northern margin of the dome; this orientation is normal to the direction of maximum horizontal compression within the strike-slip system. The northwest-trending reverse fault — responsible for outcrop repetition of the Duck Creek Dolomite and lowermost Ashburton Formation on the southwestern limb of the dome — also formed as a result of northeasterly directed compression. Within the dome, most shortening in the Mount Bruce Supergroup–Wyloo Group cover sequence has taken place west and south of the Archaean granitoid–greenstone core. Comparatively little  $D_2$  deformation is observed in equivalent rocks on the northeastern limb and eastern closure, where generally eastward-trending, Ophthalmian structures predominate. This decrease in intensity of  $D_2$  deformation across Wyloo Dome is attributed to a strain-shadow effect; the northeastern and eastern margin were sheltered from the effects of northeastward-directed compression by rigid Archaean basement in the core of the dome.

Folding and minor thrusting, associated with  $D_2$  dextral wrenching, has occurred on the northwest limb of the Turee Creek Syncline (Tyler, in press). Here, an anticline of Brockman Iron Formation has been thrust onto Marra Mamba Iron Formation. Tyler (in press) believes that the rhombohedral shape of the Turee Creek Syncline reflects the imposition of dextral rotation upon a pre-existing, east-trending syncline.

### Late $D_2$ structures in the Mount Minnie Basin

In the Deep Well–Peedamullah area, large-scale, open to tight, upright folds in the Mount Minnie Group plunge gently to the east-northeast. Fold axes are aligned about 60° to the trend of most  $F_2$  folds in the northern Ashburton Fold Belt. Similarly, they do not correspond to fold trends in the western Bangemall Basin, which are oriented north to north-northwest. Seven kilometres north of Red Hill, southeastward-dipping Mount Minnie Group unconformably overlies a large-scale northwesterly-plunging  $F_2$  fold in the Ashburton Formation (Plates 1, 2). Northeastern and southwestern margins of the Red Hill outlier are, however, cut by northwest trending  $D_2$  wrench faults.

The relationships outlined above suggest that the Mount Minnie Group was deposited and deformed during the  $D_2$  event. Northwest-trending  $F_2$  folds, oriented 25–40° to the major faults, formed in the Ashburton Basin in response to cover shortening during the early stages of dextral wrenching (Wilcox et al., 1973). The Mount Minnie Group was subsequently deposited in a strike-slip basin floored by deformed Ashburton Formation. Progressive movement on the wrench system initially resulted in folding, then faulting, of the Mount Minnie Group. The large angle between late  $F_2$  fold axes and wrench faults is characteristic of deformation in the offset sector between *en echelon* strike-slip faults (Ramsay and Huber, 1987, p.528). In addition, some clockwise rotation of fold axes has occurred in the Yarraloola–Deep Well area, where  $F_2$  folds in Ashburton Formation trend north to northeast.

### Post-Capricorn Orogen structures

The Bresnahan Group post-dates all  $D_2$  structures in the Ashburton Fold Belt. It has been subjected to pre-Bangemall Group deformation, which caused open folding about southeast and south-southeast-plunging axes (Tyler et al., in press). No cleavage was formed during this event, which corresponds to the Newmanian Fold Period of Halligan and Daniels (1964). Folds are cross-cut by northeast-trending normal faults (downthrown to the southeast) and east-southeast-trending sinistral transfer faults. These form part of the Mount Whaleback Fault system of Tyler et al. (in press) and were probably active during Bresnahan Group deposition.

Steep, northeast-trending faults, which cut the Mount Bruce Supergroup and lower part of the Wyloo Group in the vicinity of Mount Maguire and Mount Channar, have an orientation and apparent sense of movement which suggest that they are part of the post-Bresnahan fault system. They are also similar to  $D_2$  antithetic faults that formed during the Capricorn Orogeny, and may represent reactivation of earlier structures.

Post-Bangemall Group deformation — the Edmundian Fold Period of Halligan and Daniels (1964) — has affected the Ashburton Formation and Mount Minnie Group on western WYLOO. Here, folds in the Bangemall Basin are generally upright, open to tight, and trend north to northwest. East of the Parry Range, at 22° 23'S, 115° 34'E, the Ashburton Formation and Mount Minnie Group outcrop in the core of a large, southward-plunging anticline. The western limb of this fold has been cut out by a northward-trending reverse fault which forms the eastern boundary of the Parry Range. North of Cane River Station (22° 05'S, 115° 37'E) the Mount Minnie Group outcrops around the closure of a broad, north-northwesterly plunging anticline of inferred post-Bangemall age.

### Metamorphism

Rocks of the Ashburton Basin were subjected to regional metamorphism of generally low grade during the Capricorn Orogeny. In southwest WYLOO, the Boolaloo

and Mount Danvers Granodiorites were intruded into Ashburton Formation following peak regional metamorphism, and caused local development of contact metamorphic aureoles.

## Regional metamorphism

Throughout most of the Ashburton Basin, metamorphic grade is low; there is, however, general increase in grade and schistosity towards the west and southwest, where the Ashburton Basin merges into the Gascoyne Complex. Within the Gascoyne Complex the presumed metamorphic equivalents of the Ashburton Formation are referred to as the Morrissey Metamorphic Suite (Williams, 1986). Northeast of the Bangemall Group unconformity the nature of the transition is such that it suggests that many metapsammities and metapelites represent metamorphosed Wyloo Group rocks. Southwest of this line, however, higher metamorphic grade and lack of stratigraphic continuity make the origin of many schists, gneisses and migmatites uncertain. For this reason, rocks of the Gascoyne Complex to the southwest of the Bangemall Group are excluded from the following discussion.

Much of the Ashburton Basin is characterized by the mineral assemblage quartz–chlorite–muscovite (sericite), in pelitic and psammitic rocks; but Smith et al. (1982) recorded pumpellyite–epidote–actinolite from mafic Wyloo Group rocks outcropping west of Paraburdoo. Upper greenschist facies rocks with quartz–chlorite–muscovite–biotite–andalusite, and quartz–chlorite–muscovite–biotite–garnet assemblages occur at Fords Creek near the southern margin of the basin. Textures indicate that porphyroblastic minerals (garnet, biotite and andalusite) grew during and after the  $D_1$  deformation event, overgrowing a quartz, muscovite, and chlorite groundmass. Lower grade metamorphism accompanied  $D_2$  and caused the regression of biotite to chlorite and andalusite to sericite.

On southwest WYLOO, medium-grade metamorphic rocks within the Ashburton Basin are shown on Plate 1 by an overprint on the *Wa* colour and by the symbol *lm*. The boundary between *lm* and the Ashburton Formation represents the first appearance of quartz–mica schist, as opposed to cleaved mudstone and sandstone. The metamorphic schistosity ( $S_1$ ) is typically deformed by  $F_2$  folds and crenulation cleavage. Cordierite and andalusite schists, occur to the northeast of the abandoned Meilga Homestead ( $22^\circ 44'S$ ,  $115^\circ 47'E$ ) and almandine–andalusite–biotite–quartz–muscovite schists are present at  $22^\circ 39' 30''S$ ,  $15^\circ 55' 30''E$ ; together they indicate medium-grade metamorphic conditions. These assemblages show partial regression in the form of sericitization of andalusite and growth of chlorite and porphyroblastic muscovite.

On the basis of structural and stratigraphic relationships, Tyler (in press) has demonstrated that regional metamorphism in the Ashburton Basin post-dates burial metamorphism in the Hamersley Basin (Smith et al., 1982). Burial metamorphism must have reached a peak during deposition of the uppermost Turee Creek Group, because subsequent (pre-Wyloo Group) deformation resulted in significant uplift and erosion of the Mount Bruce Supergroup. Tyler (in press) argues that peak regional metamorphism in the Ashburton Basin results from structural thickening of the supracrustal succession during  $D_1$  deformation. Retrogressive mineral assemblages formed during the higher level  $D_2$  event. Pumpellyite–epidote–actinolite assemblages reported from Wyloo Group rocks by Smith et al. (1982) record either the syn- $D_2$  retrogression, or burial metamorphism during Wyloo Group sedimentation.

## Contact metamorphism

The contact metamorphic aureole around the Boolaloo Granodiorite is very narrow, except along its eastern margin between Middle Bore ( $22^\circ 32'S$ ,  $115^\circ 57'E$ ) and Mount Elizabeth ( $22^\circ 41'S$ ,  $115^\circ 56'E$ ) where it is several kilometres wide. Within a few metres of the granitoid contact at  $22^\circ 25'S$ ,  $115^\circ 46'E$ , regionally metamorphosed, quartz–chlorite–muscovite schists have been spotted by growth of chloritoid porphyroblasts. These are syn- to late-tectonic relative to  $S_1$  foliation but are cross-cut by  $S_2$  crenulation cleavage and indicate that the Boolaloo Granodiorite was intruded before  $D_2$  deformation.

Hornfels in the eastern contact aureole are characterized by a granoblastic, interlobate texture which overprints the regional  $S_1$  foliation. Immediately north of Mount Elizabeth the rocks contain the assemblages: andalusite–biotite–muscovite–quartz(–tourmaline); and garnet–sillimanite (incipient)–andalusite–biotite–muscovite–quartz. These assemblages are consistent with metamorphic temperatures of 600–650°C at low to intermediate pressure (2–4 MPa). Partial retrogression to chlorite and white mica assemblages took place during  $D_2$ .

In the northeastern part of the aureole, near Middle Bore, assemblages include: cordierite, K-feldspar, biotite, quartz, and, optionally, oligoclase, sillimanite, and garnet (almandine). Muscovite was rarely seen in these rocks, except where retrograde alteration produced fine white mica aggregates. In some samples sillimanite occurs as well-formed bladed crystals, suggesting that it was stable at the peak of metamorphism. This fact, coupled with the general lack of muscovite, constrains the P - T field to about 650 - 680°C at, or less than, 4 MPa.

No contact metamorphic aureole has been observed around the Mount Danvers Granodiorite.

## Chapter Ten

# Economic geology

In terms of Department of Mines administration and statistical records the Ashburton Basin is divided between three mineral fields: Ashburton, West Pilbara, and Peak Hill. The locations of principal mineral occurrences described in the text are shown on Plate 1.

## Gold

Gold was first recorded from the Ashburton Basin in 1890 (Woodward, 1891); total production reported to the Mines Department to the end of 1986 stood at 478 kg (Table 4). This figure does not take into account much of the gold removed during the latter part of the 19th and early part of the 20th centuries. Jones and Telford (1939) estimated that prior to 1938, gold production, mostly from alluvial workings, was probably more than 595 kg; however, production reported to the Mines Department amounted to only 20 kg.

**TABLE 4 GOLD PRODUCTION FROM ASHBURTON BASIN TO 31 DECEMBER 1986**

<i>Mining centre</i>	<i>Alluvial</i>	<i>Dollied</i>	<i>Ore</i>	<i>Gold</i>	<i>Total gold</i>
	(kg)	(kg)	(t)	(kg)	(kg)
Belvedere	0.6	0.3	1 585	13.6	14.3
Dead Finish	20.6	0.4	1 832	34.8	55.8
Melrose	29.1	0.7	3 318	34.4	64.2
Mount Mortimer	38.9	11.1	846	5.5	55.6
Sundry parcels and deposits at Perth Mint (a)	282.4	5.8	..	..	288.4
<b>Total</b>	<b>371.6</b>	<b>18.3</b>	<b>7 581</b>	<b>88.3</b>	<b>478.3</b>

(a) Undifferentiated Ashburton Goldfield

Gold deposits in the Ashburton Basin are classified into four principal types:

- Post-Wyloo Group quartz veins in Wyloo Dome.
- Quartz veins in Ashburton Formation.
- Cainozoic alluvial-colluvial deposits.
- Syngenetic mineralization in Ashburton Formation.

## Post-Wyloo Group quartz veins in Wyloo Dome

### Paulsen (Melrose Group)

Paulsen Mine is located 24 km southeast of Mount Stuart Homestead at 22° 34' 30"S, 116° 14' 20"E. Descriptions of the workings were given by Forman (1938), Finucane (1939), Marston (1979), and Blight (1985). The mine had produced 64.2 kg of gold to the end of 1985.

Auriferous quartz veins strike approximately 310°, and dip northeast at 20 - 30°. They cut across basalt and sandstone of the Mount Jope Volcanics (Fortescue Group), close to the contact with the underlying Hardey Sandstone, and can be traced on the surface for approximately 60 m. Finucane (1939) noted that the deposit shows evidence of secondary enrichment: there are lower average grades and significant amounts of pyrite below a depth of about 17 m. Small amounts of gold were reported from other north-westerly trending quartz veins, north, east, and south of the main prospect (Finucane, 1939).

### Belvedere Group

Belvedere Group is located 6.5 km southeast of the Paulsen Mine, at 22° 36' 50" S, 116° 17' 20"E. Descriptions of the workings were given by Forman (1938), Finucane (1939), Blockley (1971), Marston (1978) and Blight (1985). Gold production to the end of 1986 amounted to 14.4 kg.

Gold, copper, lead, and silver mineralization occur in two sets of quartz veins. One, the No. 1 reef of Finucane, (1939), strikes north and dips west at approximately 45°; the other, the No. 2 reef, strikes 215° and dips northwest at 75-85°. The No. 2 reef parallels a northeast-trending fault that displaces the No. 1 reef 3-4 m to the northeast. In addition, there are a number of barren veins striking at 310°. Country rocks include mafic and felsic volcanic rock, and sandstone of the Mount Roe Basalt (Fortescue Group). Lead isotope ratios reported by Richards et al. (1981) indicate that mineralization may be late Proterozoic, but the data are poor, and this conclusion is equivocal.

### Monster Lode

A small gold deposit, the Monster Lode, occurs 1.6 km southeast of Wyloo Homestead, at 22° 41' 30"S, 116°

14° 20'E (Talbot, 1926; Finucane, 1939). No production figures are available for the mine, although grades were estimated during operation at approximately 5 g/t ore (Talbot, 1926).

The lode consists of quartz veins within the Marra Mamba Iron Formation (Hamersley Group), but close to the unconformity with the Mount McGrath Formation. Veins strike 305°, are parallel to bedding, and may be traced over a strike length of 600 m. Talbot (1926) noted that gold was present in vugs of oxidized arsenopyrite within the quartz veins.

## Quartz veins in Ashburton Formation

Significant gold mineralization is locally associated with late D<sub>2</sub> quartz veins in the Ashburton Formation, especially in the central part of the Ashburton Basin. The gold is usually obtained from the upper, more weathered parts of veins, which generally carry a considerable amount of goethite; a little galena may accompany the gold (Simpson, 1926). Most ore was extracted from shallow workings and small shafts at Top Camp, Soldiers Secret, Dead Finish, The Gorge, and Mount Mortimer.

### Top Camp

Wright (1897) estimated that approximately 20 kg of gold had been obtained from a single shaft in the Top Camp area (23° 44' 40"S, 117° 16' 30"E to 23° 42' 30"S, 117° 16' 00"E) to the end of 1892. In addition, an unknown quantity was extracted from shallow surface workings. No production had been reported to the Mines Department before 1986.

Most surface workings follow the margins of a north-west-trending quartz dolerite dyke that cuts the Ashburton Formation and the overlying Bangemall Group. Country rocks, mudstone and siltstone, dip steeply north-northeast or south-southwest. Most auriferous quartz veins dip steeply and strike between southwest and northwest (Jones and Telford, 1939, Plate 3).

### Soldiers Secret

Soldiers Secret is located east of Wandarray Creek, at 23° 36' 00"S, 117° 05' 00"E. Although much alluvial gold has been found, most quartz veins are barren (Simpson, 1926). There is no official record of production.

### Dead Finish

Dead Finish refers to the area on EDMUND which includes Star of the West (Mckenzie's Find), Star of the East (Greggs Find), and a number of alluvial workings. The principal deposits have been described by Woodward (1891), Maitland (1909), Talbot (1926), Simpson (1926), and Jones and Telford (1939); there is also a brief summary by Johnston (1983). Mines Department records show that 34.8 kg of gold (excluding alluvial) was produced from this area before 1986.

### Star of the West

Star of the West workings are 1 km north of the Ashburton Downs–Kooline road, at 22° 16' 40"S, 116° 53' 00"E. Although most of the extracted gold was alluvial, Jones and Telford (1939) noted that a quartz vein, 35 m long and trending 020°, had been worked to a depth of 20 m. The country rock is tightly folded mudstone, siltstone, and minor sandstone, that strikes approximately 120°.

### Star of the East

Star of the East is approximately 10 km northeast of Star of the West workings, at 22° 16' 30"S, 116° 58' 00"E. The mine was described by Jones and Telford (1939). No production figures have been supplied to the Mines Department.

During 1984, mining efforts were centered on three quartz veins, (striking 150° and dipping northeast at 25°), which cross-cut chloritic siltstone and mudstone. Small amounts of gold have been recovered from these seams; however, the most extensive gold mineralization (5 to 6 g/t Au) is in country rock, close to where veins are cut by two fractures, that strike 100°, and dip 65° south and 60° north respectively. Here, the mudstone and siltstone are strongly bleached and contain numerous cubic goethite pseudomorphs (faces up to 10 mm) after pyrite.

### Hearns Find (O'Grady's)

Simpson (1926) and Wright (1897) stated that Hearns Find was located on a tributary of the west branch of O'Grady's Creek (The Deep), about 8 miles (13 km) south of Hardey River. An unspecified amount of gold was recovered from a 0.3 m wide ferruginous quartz vein in siltstone and mudstone.

### Northwest of Dead Finish

Jones and Telford (1939) recorded several auriferous quartz veins that extend approximately 8 km southeast from a conspicuous quartz ridge at 23° 10'S, 116° 48'E. Country rocks are open to tightly folded (axes trend 120°) mudstone, siltstone, and sandstone. Most of the prominent fissures strike slightly south of 120°, thereby cutting fold axes at an acute angle. In addition, numerous smaller veins strike north-northwest to north-northeast. The most significant mineralization (6 g/t from a vein 0.15 m wide) was found at the western end of the belt (Jones and Telford, 1939).

### The Gorge

Simpson (1926) referred to The Gorge as being ten miles (16 km) southeast of Mount Mortimer (Mount Dawson). This placed the mined area within the Capricorn Formation outcrop; however, descriptions of prospect geology (Wright, 1897) are more consistent with Ashburton Formation. Jones and Telford (1939, Plate 1) marked the track to the workings further to the southeast, and it is more likely that The Gorge was situated near the headwa-

ters of Gorge Creek (23° 21'S, 116 ° 40'E), where there are still a number of small spoil heaps.

Wright (1897) and Simpson (1926) noted that the area has numerous quartz outcrops, many auriferous. Although most veins are only weakly mineralized, Simpson (1926) recorded a value of 400 g/t Au from one ore sample. Traces of copper, silver, and lead occur with the gold. Unpublished lead-isotope data from a galena and gold specimen give a model age of about 1600 Ma (I. Fletcher, written comm., 1987), based on the Model III curve of Cumming and Richards (1975).

### Mount Mortimer

Mount Mortimer diggings are located approximately 10 km southeast of Mount Dawson (Mount Mortimer), at 23° 13' 30"S, 116° 36' 00"E. Country rocks comprise tightly folded mudstone, siltstone and sandstone. Most of the gold was recovered from alluvial deposits; however, east-striking, auriferous quartz veins have also been worked (Woodward, 1891; Wright, 1897; Maitland, 1909; Simpson, 1926; Jones and Telford, 1939). Most veins have been mined only to shallow depth. Small amounts of galena occur locally with the gold (Maitland, 1909).

### Cainozoic alluvial and colluvial deposits

Most gold recovered from the Ashburton Basin was from alluvial and colluvial deposits overlying the Ashburton Formation (Woodward, 1891; Jones and Telford, 1939; unpublished Mines Department records). Five localities have been worked intermittently since the 1890s: Top Camp, Soldiers Secret, Dead Finish, The Gorge, and Mount Mortimer. In all, the source of gold appears to be quartz veins, which post-date  $D_2$  folds in the Ashburton Formation.

Woodward (1891) reported that approximately 250–280 kg of alluvial gold had been obtained from the Top Camp area by the end of 1890. Although much gold was fine-grained, Simpson (1926) recorded that a 2.36 kg nugget was found in 1893.

Approximately 43 kg of gold is thought to have been removed from the Soldiers Secret area during 1890 (Woodward, 1891). The largest nugget weighed approximately 0.28 kg (Simpson, 1926).

Alluvial gold production from the Dead Finish area probably amounted to about 30 kg during the early 1890s (Woodward, 1891), and a further 20.5 kg was reported to the Mines Department between 1983 and 1986. The largest nugget, weighing approximately 0.8 kg, was discovered at Hearn's Find (Wright, 1897).

Mines Department records show that 39 kg of gold was extracted from Mount Mortimer prior to 1987; however, this figure does not include the amount removed during the latter part of the 19th century. Two large nuggets, one weighing 1.87 kg and the other, 1.74 kg, were

discovered during the 1890s (Woodward, 1891; Wright, 1897).

No production figures are available for The Gorge.

### Syngenetic mineralization in Ashburton Formation

Mount Clement prospect is a stratiform, syngenetic gold and silver deposit (accompanied by As, Cu, Bi, Sb, and Pb), situated 20 km southwest of Wyloo homestead and 8.5 km south-southeast of the topographic feature of Mount Clement. Prospect geology has been described by Doust (1984) and by Davy et al. (in press). The following account is summarized from Davy et al. (in press).

There are two prospects at Mount Clement: the Main Prospect, located at 22° 50'S, 116° 07'E; and the Eastern Prospect, which is 2 km southeast of the Main Prospect. Mineralized rocks occur within distributary-lobe and interdistributary-lobe facies of the Ashburton Formation. Principal rock types are thin- to thick-bedded sandstone, siltstone, and mudstone.

The Ashburton Formation has undergone two phases of deformation ( $D_1$  and  $D_2$ , see Chapter 9); this has resulted in large-scale dome-and-basin fold geometry in the prospect area. The mineralized sequence in the Main Prospect crops out as a lenticular body in the core of one of the domes, whereas the Eastern Prospect occurs on the southeastern flank of this dome. Bedding in the enclosing Ashburton Formation dips steeply ( $>45^\circ$ ), and is commonly vertical. Host rocks were subject to lower greenschist metamorphism prior to  $D_2$ . The Mount Clement succession is cut by two northeast trending dolerite dykes which post-date  $D_2$ .

### Main prospect

The mineralized sequence is about 450 m thick, and extends along strike (east–west) for 1.2 km. Its surface expression is marked by a silicified, ferruginous caprock. The base of the sequence is marked by a siliceous–ferruginous breccia (which conformably overlies unmineralized siltstone), whereas the upper boundary is defined by a brecciated, siliceous siltstone. The intervening sequence can be divided into lower and upper parts. Cherty iron-formation (hematite- or magnetite-bearing), ferruginous chert breccia, talc-bearing rocks, and gossans, are restricted to the lower part, which contains most of the significant mineralization.

Substantial sulphide mineralization (arsenopyrite and tetrahedrite–tennantite) has been encountered in only one drill hole; the intersection was from 99.5 to 102.5 m. Throughout most of the mineralized sequence, sulphide is present as sparsely disseminated arsenopyrite, rarely accompanied by pyrite and/or pyrrhotite, in chert, dolomite, siltstone and talc-rock. Locally, sulphides occur in fracture veins.

Up to 4.2 ppm of gold is recorded in the massive sulphide; however, most economically significant miner-



alization is in the oxide zone, and is associated with a diverse assemblage of generally green-colored, As–Ag–Cu–Fe compounds (see Davy et al., in press; Appendix A). The highest gold values occur in gossans (generally 1–42 ppm), chert breccia (1–7.7 ppm), talc rock (0.1–4.5 ppm) and non-banded, ferruginous chert (0.1–2.8 ppm). Gold is free, and generally fine-grained (<0.03 mm); however, elongate grains up to 0.25 mm long occur in some gossans.

### Eastern prospect

Significant sulphide mineralization has been encountered in a quartz vein, 3 m wide, and trending 260°, which cuts across sandstone and siltstone. Sulphides and sulphosalts present include (in decreasing order of abundance): pyrite, pyrrothite, arsenopyrite, boulangerite, chalcopyrite, galena, and ullmanite. There appears to be negligible gold.

### Discussion

Davy et al. (in press) interpreted the mineralized sequence in the Main Prospect as a hot-spring deposit on the following evidence:

- The deposit is stratabound.
- Cryptocrystalline and microcrystalline scorodite in veins and colloform linings, and syngenetic tourmaline and talc are indicative of hydrothermal alteration.
- Deuterium isotope ratios ( $\delta^2\text{H}$ )<sup>\*</sup> of -63 ‰ to -83 ‰ obtained from talc suggest that the mineral formed when hydrothermal brines reacted at 300–400°C with dolomitic sediment.
- Size and shape of the deposit is consistent with Holocene subaerial hot-spring deposits. In addition, chert breccias occurring at the base of the mineralized sequence, are closely comparable with hydraulic breccia deposits, reported from Holocene hot-spring environments.
- Lack of evidence for alternative mineralization models.

The geometry of the mineralized sequence, and the distribution of chert breccia, suggests that there may have been several vents, connected to the primary conduit and active at different times. Precious and base metals were probably deposited from fluids at 350–400°C, whereas iron, silica, manganese, and arsenic, were deposited when temperatures fell below about 250°C. Primary magnetite and hematite were precipitated together with sulphides, suggesting that the oxygen fugacity ( $\log f\text{O}_2$ ) was about -35 to -40. Although mineralization was essentially syngenetic, epigenetic deposits (generally rich in scorodite) resulted when primary minerals reacted with the fluid phase.

\*  $\delta^2\text{H} = R_{\text{(sample)}} - R_{\text{(SMOW)}} \times 1000$  Where  $R = \text{H}/\text{H}$ , and  
 $R_{\text{(SMOW)}}$  SMOW = Standard Mean Ocean Water

## Copper

Total copper production (Table 5) from copper ore and cupreous ore amounts to 160 t. This was extracted from 739 t of ore, indicating an average grade of 21.5% Cu. The true grade is likely to be lower than this, however, as much early production was from concentrates. Principal occurrences were described by Maitland (1909, 1919), Blatchford (1913), Jones (1939), Low (1963), Marston (1979), Doust (1984), and Blight (1985).

TABLE 5 COPPER PRODUCTION FROM ASHBURTON BASIN TO 31 DECEMBER 1986

Mine or group	Copper ore and concentrate (t)	Cupreous ore and concentrate (t)	Average grade (%)	Contained copper (t)
Yarraloola	..	2.8	14.6	0.4
Red Hill	178.0	..	19.0	34.0
Cane Hill	..	47.0	15.0	7.0
Paulsen	223.0	..	34.4	76.7
Belvedere	8.4	..	16.6	1.4
Windy Ridge	..	1.3	14.4	0.2
Goobaroo Pool	..	20.4	17.7	3.6
Ashburton Downs	..	(a)115.4	17.7	20.4
Total	..	3.3	15.9	0.5
	1.8	..	23.8	0.4
	..	(a)140.3	11.0	15.4
	<b>432.9</b>	<b>308.8</b>	(b)21.5	160.0

(a) Cupreous ore. (b) Overall weighted average for copper and cupreous ore and concentrate.

Copper deposits in the Ashburton Basin can be classified into four categories:

- Post-Wyloo Group quartz veins in Wyloo Dome.
- Quartz veins in Duck Creek Dolomite.
- Quartz veins and shears in Ashburton Formation and Capricorn Formation.
- Volcanogenic deposits in Ashburton Formation.

### Post-Wyloo Group quartz veins in Wyloo Dome

Copper minerals accompany gold-bearing quartz veins at the Paulsen and Belvedere mines (see description of gold deposits). Small quantities of ore were produced in 1916, 1939 and 1949 (Marston, 1979).

### Quartz veins in Duck Creek Dolomite

A number of small deposits, associated with quartz veins, occur in Duck Creek Dolomite in the northwestern part of the Ashburton Basin. They have been described by Maitland (1909, 1919), Blatchford (1913), Jones (1939), Low (1963) and Marston (1979).

Red Hill Mine is 12.5 km north-northeast of Red Hill Homestead, (21° 52' 00"S, 116° 05' 20"E). Country rocks are partly silicified dolomite, that dips west at 30° to 40°. Although mineralization occurs in several east-striking veins, only one — a 0.3 to 2.0 m wide and 130 m long laminated quartzite — has been worked to any extent. Marston (1979) records that the vein is vertical at its centre, dips steeply northwards at its western end and steeply southwards at its eastern end. Shafts have been sunk on pods rich in malachite and cuprite at the hill summit. Jones (1939) and Low (1963) noted that one ore seam occurs where the quartz vein cuts a 7.5 m wide, north-trending dolerite dyke.

Red Hill South Mine is 1 km south of Red Hill Mine, where the dolomite succession dips south-southwest at 25°. Marston (1979) stated that the prospect was a subvertical cupriferous limonite-quartz vein, up to 0.4 m thick, occurring within a small northeast-striking fault. Copper mineralization (malachite and chrysocolla) appears most abundant where a dolerite sill intrudes the sequence. Production apparently took place in 1907 (about 8 t of 50% picked ore) and in 1937 (about 40 t of 50% copper ore), but there are no official records of this.

Rundles Hill prospect is 7.5 km southeast of Red Hill (22° 10'S, 116° 04' E). The prospect is in a fault-bounded outlier of Duck Creek Dolomite which dips northeast at 25°. Small amounts of malachite, cuprite and chalcocopyrite are present in a vertical quartz vein, 400 m long and up to 1 m wide, striking 300° (Jones, 1939). A few tonnes of copper ore were raised early this century (Marston, 1979), but there is no official record of production.

## Quartz veins and shears in Ashburton Formation and Capricorn Formation

Small amounts of copper have been extracted from veins and shears in Ashburton Formation and Capricorn Formation. Mining activity has focussed on two districts, Red Hill and Ashburton Downs.

### Red Hill district

Cane Hill Mine (Maitland, 1909, 1919; Jones, 1939; Low, 1963; Marston, 1979) is 5 km south of Red Hill, at 22° 09' 30"S, 116° 02' 20"E. Ashburton Formation country rocks comprise lithic and feldspathic turbidite sandstone, siltstone, mudstone, and minor chert and dolomite. Bedding, and a sub-parallel axial-plane cleavage, strike 320° and dip steeply towards the southwest. Mining efforts have centred upon a mineralized quartz vein, 400 m long and up to 2.4 m wide, which strikes parallel to bedding and dips southwest at 75–80°. Jones (1939) and Low (1963) report that veins and lenses of malachite, cuprite, chalcocopyrite, chalcocite, and iron oxides, were up to 0.75 m thick. Great Boulder Mines Ltd. reported a maximum intersection of 1.52 m of 1.74% Cu from three shallow percussion drill holes (Marston, 1979).

Lockes (Whynot) Mine (22° 07' 10"S, 116° 00' 50"E) is within Ashburton Formation (cleaved mudstone and

dolomite). Maitland (1909) reported a cupriferous (malachite, chalcocite, and cuprite) quartz vein, 30 m long, trending in a northeasterly direction. Mine workings, which previously extended to a depth of 8.5 m, are now filled in. Big Blow prospect is about 600 m west of Lockes Mine, and includes several north-northwest-trending mineralized quartz veins up to 2.4 m wide.

### Ashburton Downs district

Windy Ridge (Tropic) Mine is 24 km east-southeast of Ashburton Downs Homestead (23° 27' 10"S, 117° 15' 10"E). Descriptions of the deposit are given by Low (1963) and Marston (1979). Malachite, chrysocolla, chalcocite, and cuprite occur in impersistent limonitic chert veins and pods, up to 0.5 m thick, in Ashburton Formation chloritic mudstone. Bedding strikes generally about 280° and dips steeply north or south; a strong slaty cleavage strikes 290°, and dips 5–10° northwards. Some veins are parallel to bedding, others are vertical and cross-cutting (Marston, 1979). A ferruginous gossan, up to 1 m thick, is reported to have capped the deposit (Low, 1963); it has since been removed.

Marston (1979) describes a cupriferous, limonitic quartz vein at the Goobaroo Pool prospect (23° 29' 00"S, 117° 17' 36"E). The vein is parallel to bedding in the Ashburton Formation, and dips 30° to the northeast.

Mount Blair South prospect (23° 29' S, 117° 08' E) is 4.5 km south of Mount Blair in open-folded Ashburton Formation mudstone (Marston, 1979). Bedding strikes about 280° and dips 10–70° north. Malachite–limonite veins strike 295° and dip steeply south, parallel to a curving, slaty cleavage. Fine-grained specularite occurs in some veins.

Station Creek prospect (c. 23° 26' 12"S, 117° 01' 48"E) is reported to be 5.6 km south of Ashburton Downs homestead (Blockley, 1971). A narrow, mineralized (low-grade copper, lead, and silver minerals) shear strikes 290° in Ashburton Formation mudstone and conglomerate.

Soldiers Creek Northeast (Donnelly) copper-gold occurrences (23° 35' 30" S, 117° 06' 00"E) comprise malachite-, chrysocolla-, limonite-, and gold-bearing veins, emplaced along bedding, cleavage, and fracture planes. Country rocks are cleaved mudstone, striking east, with moderate to vertical dips. The area was investigated by Australian Anglo American Services Ltd in 1973. Geochemically anomalous zones, 200–400 m long and 30–40 m wide, were defined and costeamed. Average assay values of samples from the costeams were 0.43% Cu and 0.37 ppm Au (Marston, 1979).

The Anticline, Bali High East, Casleys, Ledge, and Stockyard Creek prospects are about 13 km southwest of Ashburton Downs Homestead. Most deposits are in shear planes at, or close to, the unconformable base of the Capricorn Formation. They are described by Low (1963), Blockley (1971), and Marston (1979).

Casleys (Bali Low, Bali Lo) prospect (23° 23' 50"S, 116° 55' 10"E) is in a shear-zone close to the hinge of a

major west-northwest-trending anticline. Small pods (up to 1 m long by 0.5 m wide) of limonite with disseminated malachite, azurite, chrysocolla, and various copper arsenates occur in a 240 m long by 1–3 m wide brecciated zone that dips steeply southward (Bridge and Pryce, 1978; Marston, 1979). Metazeunerite (a uraniferous copper arsenate) occurs as fracture coatings within the Capricorn Formation. Diamond drilling near the eastern end of the prospect intersected the mineralized zone at a depth of 60 m, and assayed 1.2% Cu over a drilled width of 1.2 m. Assays of up to 50 ppm Pb, 460 ppm Au, and 370 ppm Ni were also obtained (Marston, 1979).

Anticline (Bali High, Bali Hi) prospect (23° 24' 00" S, 116° 56' 00" E) is located 1.2 km east-southeast of the Casleys deposit. The shear zone, which dips south at about 50°, is 1–2 m wide and sporadically mineralized for 700 m (Marston, 1979). A fracture cleavage is associated with the shear. The mineralized zone was encountered in a shaft sunk by Pickands Mather and Co. International (PMI), and consisted of about 12 m of disseminated pyrite, galena, chalcocopyrite, bornite, digenite, covellite, tetrahedrite, skutterudite (CoAs<sub>3</sub>), and a copper–antimony sulphide (Marston, 1979). Diamond drilling by PMI encountered mainly pyrrhotite at 76 m vertical depth, assaying up to 300 ppm Cu, 530 ppm Pb, and 2600 ppm Zn, over a true width of 3.9 m. Surface sampling has also revealed anomalous Bi (150 ppm), U (200 ppm U<sub>3</sub>O<sub>8</sub>), Ag (270 ppm), and As (4.8%).

Bali High East prospect (23° 24' 20"S, 116° 57' 00"E) is 2.8 km southeast of the Casleys workings. The mineralized portion of the shear cuts Ashburton Formation; it is about 280 m long and 1–2 m wide, and contains malachite, azurite, chrysocolla and traces of chalcocite. Surface material may assay up to 27% Cu, and give anomalous levels of Pb, Zn, Bi, As, Ag and U (Marston, 1979).

Ledge prospect (23° 23' 40"S, 116° 53' 40"E) is 2.8 km west of the Casleys deposit. Country rocks comprise Capricorn Formation mudstone, siltstone, and fine- to coarse-grained sandstone. These rocks strike 285° and dip north at about 55°. Mineralization is in a 1–2 m wide siliceous shear zone that strikes 285° and dips 80° south. Pods of malachite, chrysocolla, chalcocite, tenorite, cuprite, cerussite, limonite, and quartz, occur as breccia matrix in the shear zone (Marston, 1979).

Stockyard Creek prospect (23° 25' 40"S, 116° 55' 10"E) is about 5 km southeast of Casleys prospect. A little malachite occurs as staining and fracture coatings in Ashburton Formation sandstone, mudstone and conglomerate. Marston (1979) suggests that this may reflect the redistribution of syngenetic copper from the Capricorn Formation by meteoric water.

## Volcanogenic deposits in Ashburton Formation

Yarraloola prospect (21° 35' 40"S, 115° 55' 50"E) is 6.9 km southeast of Yarraloola Homestead. The deposit has been described by Maitland (1909, 1919), Jones (1939), Low (1963), Marston (1979), and Doust (1984). The pros-

pect comprises two, 1–5 m wide zones of silicified ferruginous caprock striking 020° and dipping northwest at 40–80°. Pyrite casts are present in this caprock, which has developed over siliceous, disseminated-to-massive iron sulphides (Marston, 1979). There is little copper staining in the outcrop. Country rock is pyritic, quartz–feldspar–mica–chlorite schist that contains lenses and small veins of quartz. Thin horizons of metamorphosed basalt, dolerite, quartz–feldspar porphyry, and dacite, have been reported from drill core (Marston, 1979).

Exploratory drilling by Great Boulder Mines Pty., between 1970 and 1973, indicated the presence of a mineralized body 100 m long and up to 13 m wide, to a depth of 250 m (Marston, 1979). Principal minerals are cobalt-bearing pyrite, and smaller amounts of chalcocopyrite, galena and iron-bearing sphalerite. Gangue consists of quartz, variably silicified schist, and carbonate. The richest mineralized intersection had a drilled width of 23.8 m, and assayed 0.75% Cu, 0.51% Pb, 0.41% Zn, and 20.1 g/t Ag; however, average grades were much lower.

Marston, (1979) considered it likely that the original mineralization formed in a distal volcanogenic setting, in a sedimentary (partly volcanoclastic) sequence of chert, basalt and felsic pyroclastic intercalations. Isotope data from a sample of galena give a Pb model age of about 2000 Ma (J. R. Richards, written communication., 1983), based on the Model III curve of Cumming and Richards (1975).

## Lead and silver

Since 1901, 2897 t of lead and 868 kg of silver have been mined from the Ashburton Basin (Table 6). Most has come from the Kooline centre, but smaller amounts have come from the Wyloo Dome and adjacent area. Lead–silver prospects have been described by Maitland (1909), Forman (1938), Ellis (1951), Simpson (1951), Daniels (1966, 1969), and Blockley (1971).

TABLE 6 LEAD AND SILVER PRODUCTION FROM ASHBURTON BASIN TO 31 DECEMBER 1986

Mine or Group	Lead ore and concentrate (t)	Lead (t)	Silver (kg)
Belvedere	4.0	1.8	2.5
Aerial	155.0	100.0	27.1
Silent Sisters	162.0	116.0	13.8
Kooline	3 638.0	2 679.0	868.4
<b>Total</b>	<b>3 959.0</b>	<b>2 896.8</b>	<b>911.8</b>

Lead–silver deposits in the Ashburton Basin can be grouped into three categories:

- Post-Wyloo Group quartz veins in the Wyloo Dome.
- Quartz veins in the Duck Creek Dolomite.

(c) Quartz veins and shears in the Ashburton and Capricorn Formations.

## Post-Wyloo Group quartz veins in the Wyloo Dome

In 1949, 1.8 t of lead and 2.5 kg of silver were extracted from the Belvedere Mine (see description of gold deposits). Principal lead minerals were galena, cerussite, beudantite, and plumbojarosite (Blockley, 1971).

## Quartz veins in the Duck Creek Dolomite

Between 1949 and 1953, 216 tonnes of lead and 41 kg of silver were mined from quartz veins within the Duck Creek Dolomite. The largest producers were the Silent Sisters and Aerial mines.

### Silent Sisters Mine

Silent Sisters Mine (22° 52' 40"S, 116° 27' 30"E) is 24.1 km southeast of Wyloo Homestead. It has been described by Ellis (1951) and Blockley (1971). Five lead-bearing quartz veins, trending northeast to northwest and dipping steeply to the east and west, cut across the Duck Creek Dolomite bedding. Ore comprises galena and sphalerite in a gangue of quartz, silicified dolomite, barite, and calcite. Blockley (1971) noted that most deposits are tension-gash fillings. Isotope data from a galena sample gave a Pb model age of about 1700 ± 150 Ma (Riley, quoted in Leggo et al., 1965).

### Aerial Mine

Aerial Mine (22° 53'S, 116° 37'E) is 16 km east of the Silent Sisters Mine. Most ore was extracted from a 15 m wide, northeast-trending fault zone cutting across the upper part of the Duck Creek Dolomite. Lead occurs as galena and cerussite pods in a quartz-kaolin-silicified dolomite gangue. A little copper is associated with the ore (Blockley, 1971). Unpublished isotope data from a sample of galena give a Pb model age of about 1550 Ma (J.R. Richards, written communication, 1987), based on the Model III curve of Cumming and Richards (1975).

## Quartz veins and shears in Ashburton Formation and Capricorn Formation

Most lead and silver from the Ashburton Basin has come from quartz veins and shears in the Ashburton Formation and, to a much lesser extent, from the Capricorn Formation. Principal areas of mineralization are the Kooline and Ashburton Downs centres, Gorge Creek, and smaller occurrences on WYLOO.

### Kooline centre

Kooline centre (23° 06'S, 116° 26'E) includes an area 7.2 km long by 2.4 km wide, 25.7 km southeast of Kooline Homestead. Blockley (1971) listed 17 mines (or groups)

and 10 miscellaneous deposits which produced 2679 t of lead and 825 kg of silver between 1948 and 1959. About 65% of production came from the Gift, June Audrey, and Bilrose Mines.

With the exception of Big Chief Mine, galena-bearing veins occur within Ashburton Formation mudstone, siltstone, and sandstone, on the northern limb of a large, upward facing D<sub>2</sub> syncline. Axes of medium- to large-scale D<sub>2</sub> folds trend about 280°, and axial-plane cleavages are generally vertical or dip steeply southwards. Most mineralized veins are parallel to the axial-plane cleavage, although some smaller fissures cut it at high angle. Within the Kooline centre, there appears to be no correlation between mineralization and the type of country rock.

Galena-bearing veins range from a few centimetres to 1.2 m thick and are up to 60 m long. Often, several veins are distributed *en echelon*. Principal minerals are galena, quartz, cerussite, malachite, calcite, and barite. Ore minerals may be disseminated through quartz, or restricted to narrow seams of massive sulphide or carbonate. The grade of ore mined was 10–12% Pb, and 31.1–46.6 g/t Ag (Blockley, 1971).

Big Chief Mine (23° 11' 30"S, 116° 35' 15"E) is 16 km southeast of the main group of Kooline deposits. The mineralized zone is 12 m long, strikes 285°, and dips 60° south, parallel to bedding in the host Capricorn Formation. The richest galena and cerussite ore is in a narrow bed of sheared mudstone and siltstone occurring beneath a massive quartz sandstone and above a 0.6 m thick lithic sandstone. Some disseminated cerussite occurs in the footwall and in the hanging wall.

Lead-isotope data from 34 galena samples collected from the Kooline centre give an average Pb model age of about 1550 Ma (J.R. Richards, written comm., 1987, based upon the Model III curve of Cumming and Richards, 1975).

### Ashburton Downs district

Small amounts of lead and copper occur in sheared rocks of the Ashburton and Capricorn Formations in the Ashburton Downs centre (see section describing copper mineralization). There has been no commercial production of lead from these prospects.

### Gorge Creek

Samples of auriferous lead ore have been reported from a gorge (probably Gorge Creek), 32.1 km southeast of Mount Dawson (Blockley, 1971). The vein, up to 1.8 m wide, contains cerussite and galena in a quartz gangue.

### Wyloo occurrences

Simpson (1951) and Blockley (1971) listed several small lead occurrences within Ashburton Formation rocks on WYLOO, but there are no production figures for these prospects.

A narrow leader of lead ore occurs near Cane River Mine (see copper section). It is too small to be payable.

Blockley (1971) notes that a specimen of galena, reported to have come from the Hardey River 16 km south of Mount de Courcy, contained 249 g/t Ag. A subsequent Pb-isotope determination from this specimen gave a Pb model age of 1100 Ma, closely comparable to data obtained from galenas from the Bangemall Group. It is possible, therefore, that the location of the sample has been misreported (J. Blockley, written communication, 1988)

A 9 m deep shaft has been sunk on a lode containing carbonates of lead and copper at 22° 25' 40"S, 116° 02' 00"E, 2.4 km on a bearing of 235° from Mount Stuart trigonometrical station (Maitland, 1909; Simpson, 1951; Blockley, 1971). The mineralized zone follows an east-trending bed of sheared Ashburton Formation conglomerate. A sample from the dump assayed 35.7% Pb, 0.01% Zn, 4.76% Cu, and 84 g/t Ag (Blockley, 1971).

South Hardey River prospect (22° 58'S, 116° 36'E) is 10 km south-southwest of the Aerial Mine. The deposit is in tightly folded Ashburton Formation mudstone, siltstone and sandstone. D<sub>2</sub> fold axes trend 280° and axial-plane cleavage dips south at about 80°. Several lenses of galena, cerussite, and copper minerals occur on shears parallel to bedding. Quartz veins near the deposits contain cubic pseudomorphs after pyrite (Blockley, 1971).

## Iron

Several small hematite deposits occur within braided-fluvial facies of the Mount McGrath Formation and basin plain deposits of the Ashburton Formation. There is no record of production from any of them.

## Mount McGrath Formation

The Barrett-Lennard ore body (22° 33' 40"S, 116° 20' 20"E) is about 19 km north of Wyloo Homestead. A 6.5 m thick mineralized conglomerate, derived from Hamersley Group BIF, occurs at the top of an upward-coarsening and thickening deltaic sequence, in the middle of the formation. The highest grade ore is dense and massive, assays more than 65% iron, and has a low phosphorous content (MacLeod, 1966).

Conglomeratic hematite deposits, most less than 10 m thick, have been described from the Paraburdoo area by Bourn and Jackson (1979) and Morris (1980, 1986). They occur within braided-fluvial facies at, or near, the base of the Mount McGrath Formation where it unconformably overlies the Mount Bruce Supergroup and lower part of the Wyloo Group. MacLeod (1966) and Bourn and Jackson (1979) considered the mineralization to post-date deposition of conglomerate in both the Paraburdoo and Barrett-Lennard occurrences. This view has been challenged by Morris (1980, 1986), who demonstrated that the conglomerates contain fragments of hematite derived from pre-existing ore bodies.

## Ashburton Formation

A small hematite deposit occurs near the base of the Ashburton Formation (22° 26' 10"S, 116° 14' 10"E) 21 km east of Mount Stuart Homestead. Mineralized BIF and ferruginous mudstone overlie coarse basaltic agglomerate of the June Hill Volcanics. Hematite enrichment appears to be greatest near a small normal fault that trends 125°, and marks the southwestern margin of the agglomerate body.

## Uranium

Most arenaceous sequences of the Ashburton Basin have been examined for sandstone-hosted uranium mineralization, but results have not been encouraging (Carter, 1981; unpublished Mines Dept. Open-file records). An investigation of the Beasley River Quartzite on TUREE CREEK was terminated, following a disappointing airborne radiometric survey. Most radioactive anomalies within the Capricorn Formation in the Mount Elephant and Ashburton Downs districts were found to be thorium-based. Maximum U<sub>3</sub>O<sub>8</sub> assays from these localities were 112 ppm and 353 ppm respectively. Localized radiometric anomalies are associated with heavy-mineral layers (containing uraniferous monazite, zircon, and ilmenite) in Bresnahan Group sandstone. However, numerous airborne and ground-based radiometric surveys have failed to record significant uranium mineralization.

Turee Creek (Angelo River) uranium prospect (23°34' 30"S, 118° 14' 00"E) is a fault-related deposit 37.5 km northeast of Mount Bresnahan. Mineralization occurs along a northeast-trending normal fault, which separates the upper part of the Mount McGrath Formation from the Bresnahan Group. Host rocks in the fault zone are brecciated hematitic or carbonaceous shale, sandstone breccia, chert breccia, dolomitic shale, and clay. Petrological, geochemical, and stable-isotope studies of these rocks (Ewers and Ferguson, 1985) indicate that uranium has been syngenetically enriched in the Mount McGrath Formation. Extensive fracturing along the fault zone resulted in these syngenetically enriched rocks being mixed with fragments of Bresnahan Group sandstone. Acid, fluorine-bearing groundwaters circulated through the brecciated zone, leaching uranium from the syngenetically enriched rocks. Further enrichment has taken place through solution-wall-rock reactions which promoted deposition of secondary uranium phosphate minerals in late-stage fractures (Ewers and Ferguson, 1985).

## Marble

A small quantity of marble was produced from two mines on WYLOO (22° 48' 00" S, 116° 21' 30" E and 22° 54' 30" S, 116° 46' 00" E) during the late 1970s and early 1980s. In both, a brecciated marble in the upper part of the Duck Creek Dolomite (slope and basin facies) was quarried for ornamental and facing stone. It is thought that both operations closed because the marble is cut by a strong penetrative cleavage which limited the size of some

quarried blocks, and because of the high cost of transporting the marble to market.

## Amethyst

A small amethyst deposit occurs within the Duck Creek Dolomite at 22° 47' 30"S, 116° 21' 40"E. The mineral is a late-stage cavity fill in faulted, slope-facies breccia. Mines Department records show that 18.8 t of amethyst, mostly of poor quality, was produced to the end of 1978.

## Discussion

### Age and distribution of mineralization

Most Au, Cu, Ag, Pb, and U mineralization reported from the Ashburton Basin occurs in west-northwest-, north-northwest-, and northeast-trending quartz veins and faults. Stratigraphic and structural evidence indicates that these fractures were formed relatively late in the tectonic evolution of the area, after deposition of the Capricorn Formation and intrusion of the Boolaloo Granodiorite. Two episodes of post-Wyloo Group mineralization are recognized: the earlier is associated with pre-Bresnahan Group ( $D_2$ ) dextral wrenching, but the later event is linked to post-Bresnahan Group normal faulting (Chapter 9)

West-northwest- and north-northwest-trending  $D_2$  faults and quartz veins host much of the Au, Ag, Cu, and Pb mineralization in the Ashburton Basin. They cut across  $F_2$  folds and are aligned parallel to, or at an acute angle to, the trend of the principal wrench faults which bound the northeastern margin of the Ashburton Basin. In addition, several small deposits occur in north- to northeast-trending fissures in the Mount Bruce Supergroup and lower Wyloo Group, e.g. at Aerial, Belvedere and Silent Sisters Mines. The orientation and sense of movement across the fractures suggests that they are synthetic and antithetic faults, formed during the  $D_2$  dextral wrenching event.

The only reported occurrence of post-Bresnahan Group mineralization is at the Turee Creek prospect. Here, a small uranium deposit is associated with a northeast-trending normal fault, which juxtaposes Mount McGrath Formation and Bresnahan Group. The younger age limit for mineralization is unknown, since faults of this type also cut the Bangemall Group on NEWMAN.

Geochronological studies support the concept of late-stage mineralization in the Ashburton Basin. Isotope data from west-northwest trending,  $D_2$  fractures the Kooline centre and the Gorge prospect give Pb model ages of about 1550 Ma (I. Fletcher, written comm., 1987; J.R. Richards, written comm., 1987). Similar studies, carried out for north to northeast trending  $D_2$  faults and veins in the Wyloo Dome and Duck Creek Dolomite, also show that mineralization took place about 1550 Ma. (Richards et al., 1981; I. Fletcher, written comm., 1987).

Blockley (1971) considered that mineralization the Kooline centre may have been related to intrusion of the Boolaloo Granodiorite. This is now thought to be unlikely, as the granitoid was intruded into the Wyloo Group during the interval between the  $D_1$  and  $D_2$  deformations, about 1700 Ma ago (Leggo et al., 1965).

It is uncertain to what extent host rocks and/or geographic location may have influenced the type of vein-related mineralization. Most gold deposits occur within veins and faults in the Ashburton Formation; though in the Wyloo Dome they are associated with Fortescue Group volcanic rocks and the Mount McGrath Formation–Hamersley Group unconformity. Similarly, copper mineralization occurs within Duck Creek Dolomite and Ashburton Formation in the northwestern part of the basin, and Ashburton Formation and Capricorn Formation in the Ashburton Downs district. Significant lead deposits are confined to the central part of the basin, where they are hosted by Ashburton Formation and Duck Creek Dolomite. The most extensive lead mineralization is in the Kooline centre, within a suite of submarine fan deposits derived from an area which lay to the south of the Ashburton Basin.

### Exploration targets in the Ashburton Basin

The known association of Au, Ag, Cu, and Pb mineralization with  $D_2$  wrench faulting suggests that these fractures could be targets for future mineral exploration. Major west-northwest to north-northwest-trending wrench faults and associated synthetic, antithetic and reverse faults are abundant along the northeastern margin of the Ashburton Basin (Plates 1 and 2). Faults which cut carbonate units (lower and upper parts of the Mount McGrath Formation and Duck Creek Dolomite) are prospective targets for uranium mineralization. Ewers and Ferguson (1985) proposed that uranium may be transported along fault planes in acid, fluorine-bearing solutions. Deposition occurs when such solutions are neutralized and buffered through wall-rock reactions, particularly with dolomite. Lead- and silver-bearing veins (Aerial and Silent Sisters prospects) are present in the upper part of the Duck Creek Dolomite on WYLOO, suggesting that other metals besides uranium may be deposited in this type of setting.

Most of the recovered gold originated from faults and quartz veins in the central and southern Ashburton Basin. Goethite pseudomorphs after pyrite and arsenopyrite occur locally within auriferous veins and adjacent country rock, and may be useful indicators of gold mineralization. In many of the reported occurrences, supergene gold enrichment is present to a maximum depth of about 20 m. As most veins are narrow (generally < 2.0 m), deposits are likely to be small in all except the major fracture zones.

The surface expression of the Mount Clement gold–silver deposit is marked by a distinctive ferruginous gossan containing a variety of copper–arsenic minerals. Absence of gold nuggets around the prospect suggests that the discovery of further examples of this style of mineralization may depend upon recognition of other gossanous

outcrops, coupled with sampling for appropriate tracer elements. Davy et al. (in press) note that arsenic is a general indicator of mineralization at Mount Clement and elsewhere in the Ashburton Basin (e.g. Ashburton Downs copper prospects), but is not specific to gold. Anomalous levels of Bi, Cu, Pb, and Sb are also recorded at Mount Clement, but it is not known whether their presence has regional significance (Davy et al., in press).

Geological and geochronological data suggest that the Yarraloola prospect represents a volcanogenic copper deposit within the Ashburton Formation (Marston, 1979). Other volcanic sequences occur north of the Wyloo Dome (June Hill Volcanics), 15 km southwest of Mount Amy, and north and west of Mount Boggola (see chapters 5, 7, 8). These occurrences may also be prospective for base-metal and gold mineralization.

### **Formation of iron ore in the Hamersley Basin**

Clasts of microplaty hematite ore occur in Mount McGrath Formation conglomerate, but have not been recorded from similar rocks in the Beasley River Quartzite. This observation coupled with evidence for supergene enrichment in many Pilbara iron-ore bodies, suggests that a major episode of iron-ore formation took place in the Hamersley Basin during deposition of the lower part of the Wyloo Group (Morris, 1980, 1985, 1986). Absence of ore fragments in Beasley River Quartzite conglomerate may simply reflect lack of a suitable ore-body in the source area (eastern Wyloo Dome). However, the concept of early Proterozoic ore formation is further supported by structural and intrusive relationships in the Paraburdoo district (Tyler and Thorne, in press). There, folded Beasley River Quartzite and Cheela Springs Basalt are cut by a suite of west-northwest-trending dolerite dykes that pre-

date ore formation. Because fragments of microplaty hematite ore are found in the lower part of the Mount McGrath Formation, mineralization must post-date the Cheela Springs Basalt and pre-date the Mount McGrath Formation.

Morris (1985) proposed that goethite (formed during supergene enrichment of BIF) was converted to microplaty hematite by burial at depths sufficient to raise the ore temperature to about 100°C. For this reason, Morris (1985) favoured the view that supergene-enriched orebodies in the Hamersley Basin post-date the Beasley River Quartzite, but were subsequently buried by the Cheela Springs Basalt. If the sequence of events proposed by Tyler and Thorne (in press) is correct, it implies either that supergene ore was buried by a stratigraphic unit no longer preserved, or that burial is not essential for the formation of microplaty hematite.

In addition to subaerial exposure, the presence of folded and faulted BIF, with good groundwater circulation, is an important prerequisite for supergene iron-ore formation (Morris, 1985). Structural and stratigraphic data from the Hamersley and Ashburton Basins point to two episodes of post-Hamersley Group - pre-Mount McGrath Formation deformation. The first, which produced large open folds in the Wyloo Dome-Hardey Syncline area, occurred during and immediately after Turee Creek Group deposition. The second took place following Cheela Springs Basalt deposition, and was responsible for large, upright folds in the southeastern Hamersley Basin (Tyler et al., in press). Most of the large, pre-Mount McGrath Formation iron-ore bodies discovered so far (e.g. Paraburdoo, Mount Channar) appear to be associated with the latter event. On structural and stratigraphic grounds alone, however, pre-Wyloo Group folds in the southwestern Hamersley Basin might also be expected to contain sizable ore deposits of this type.



## Chapter Eleven

# Tectonic evolution

### Introduction

The Ashburton Basin forms the northern part of the Capricorn Orogen, a major orogenic zone between the Pilbara and Yilgarn Cratons (Gee, 1979a). Previous tectonic models for the Capricorn Orogen (e.g. Horwitz and Smith, 1978; Gee, 1979a; Kroner, 1983) are based on the concept that the Pilbara and Yilgarn Cratons were once part of a single Archaean continent that underwent rifting during the early Proterozoic. Sedimentary cover sequences of the Ashburton and Naberu Basins were subsequently deposited on the downfaulted margins of the Pilbara and Yilgarn respectively; later convergence caused orogenic activity which produced the Gascoyne Complex mobile belt.

Gee (1979a), Drummond (1979, 1983), and Drummond et al. (1981) list important differences between the Pilbara and Yilgarn Cratons which challenge the view that they formed a single continent during the Archaean:

- (a) The western Yilgarn Craton has large areas of high-grade Archaean gneiss; no similar rocks have been found in the Pilbara Craton.
- (b) Granitoids are abundant in both Pilbara and Yilgarn Cratons; reliable dates for those of the Pilbara are greater than 3000 Ma, whereas most of those from the Yilgarn fall in the range 2600 to 2700 Ma.
- (c) The 2750 to 2500 Ma Fortescue Group and Hamersley Group sequences in the Pilbara have no counterparts in the Yilgarn Craton.
- (d) Clastic sequences within Pilbara greenstone belts are more mature than those of the Yilgarn Craton.
- (e) Pilbara granitoid batholiths are nearly circular in plan, but those of the Yilgarn Craton have a linear trend.
- (f) The Pilbara crust is 28–33 km thick, but that of the Yilgarn is more than 50 km thick in the north and more than 40 km thick in the south.
- (g) Excluding rocks of the Hamersley Basin, the Pilbara crust is two layered, whereas three layers are present in the Yilgarn Craton.

A further point of difference, to be added to the above, is that lower Proterozoic cover sequences of the Pilbara Craton and northern Yilgarn Craton (Wyloo and Glen-

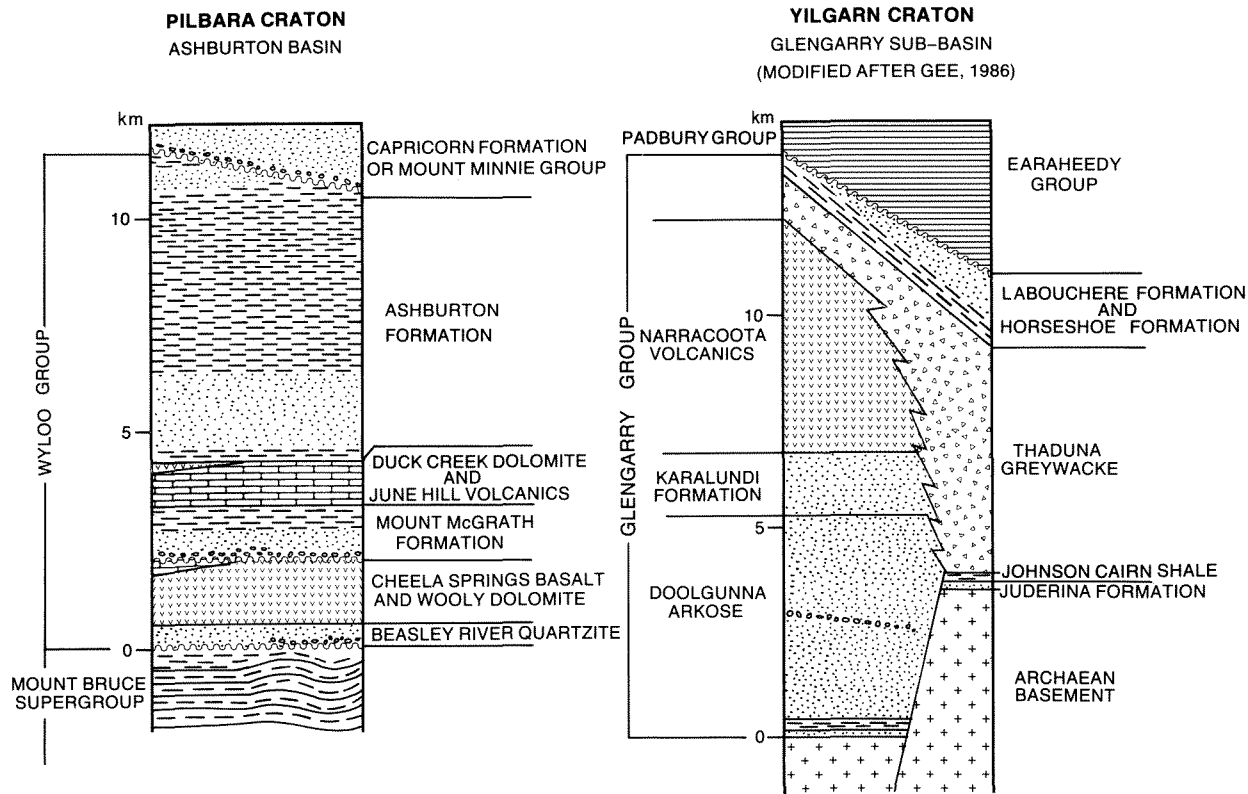
garry Groups respectively) differ considerably in details of stratigraphy (Fig. 91).

The base of the Wyloo Group is marked by a shallow-marine quartz sandstone (Beasley River Quartzite). This is overlain by: subaerial and shallow-marine mafic volcanics (Cheela Springs Basalt, 1 to 2 km thick); deltaic siliciclastics (Mount McGrath Formation, 1.3 km); deep- and shallow-marine shelf carbonates (Duck Creek Dolomite, 1.0 km); and deep-marine siliciclastics (Ashburton Formation, 5–10 km).

The Glengarry Group also has a quartz sandstone, the Juderina Formation, at its base; but the overlying stratigraphy (Gee, 1986) differs markedly from the Wyloo Group. It consists of: outer shelf mudstone (Johnson Cairn Shale, 0.25 km); fluvial to deep-marine arkosic sandstone (Dolgunna Formation, > 5 km); fluvial to shallow-marine sandstone (Karalundi Formation, 1.5 km); tholeiitic basalt (Narracoota Volcanics, 6 km); volcanic-derived turbidite (Thaduna Greywacke, 5 km); and deep- to shallow- marine iron-formation, mudstone, and sandstone (Horseshoe Formation, 0.5 km; and Labouchere Formation, > 0.3 km). These differences in stratigraphy reflect fundamental differences between the tectonic evolution of the Pilbara Craton and northern Yilgarn Craton. The Wyloo Group records large-scale subsidence of the Pilbara shelf, accompanied by initial waning, then increase, in terrigenous supply. In contrast, the Glengarry Group was deposited in a generally more active tectonic environment, in which basement uplift was accompanied by significant mafic volcanism.

Dissimilarities between the Pilbara and Yilgarn Cratons make the conventional rift, or rift followed by A-subduction, models for the Capricorn Orogen unacceptable. Geological mapping in the Ashburton Basin (presented here), and in the Sylvania Inlier and southern Hamersley Basin (Tyler, in press) shows that the tectonic evolution of the northern margin of the Capricorn Orogen has many parallels with that of foreland regions of Phanerozoic continent–continent collision zones (see Allen and Homewood, 1986; Coward and Ries, 1986). This chapter presents a plate tectonic model for the geological evolution of the southern Pilbara during the interval between Fortescue Group deposition and post-Bresnahan Group faulting. Five stages are recognized:

- (a) Continental rifting and breakup of the Pilbara Craton (low to middle Fortescue Group);



GSWA 25257

Figure 91 Comparative stratigraphies of the Ashburton Basin and Glengarry Sub-Basin.

- (b) Passive margin (upper Fortescue Group to Hamersley Group);
- (c) Active margin (Turee Creek Group to lower Wyloo Group);
- (d) Continental crustal collision (middle Wyloo Group to D<sub>2</sub> dextral wrench faulting); and
- (e) Post-collision (Bresnahan Group to post-Bresnahan Group faulting).

## Pilbara Craton rifting

The Pilbara Craton comprises a 3500–2900 Ma granite–greenstone terrane, unconformably overlain by the 2750–2490 Ma Mount Bruce Supergroup. Sedimentological, structural and stratigraphic data point to major rifting of the granite–greenstone terrane during deposition of the Fortescue Group — the lowermost stratigraphic unit of the Mount Bruce Supergroup (Blake, 1984 a,b; Blake and Groves 1987). Blake and Groves (1987) recognized three tectonic phases which controlled Fortescue Group evolution. The initial phase, interpreted as a pre-rifting volcanic event, was characterized by formation of a thick (locally up to 2.5 km) succession of dominantly subaerial tholeiitic basalts, locally underlain by fluvial clastic deposits. The second phase reflects ma-

yor east-west extension, and was dominated by alluvial fan, fluvial, and lacustrine sedimentation, accompanied by both mafic and felsic volcanism. Sedimentation occurred in linear, mainly north-northeast-trending belts, at least 100 km long (Blake, 1984 b), which were bounded locally by growth faults with throws up to 1500 m. The third phase was regional subsidence, associated with extensive mafic volcanism. Subaerial lavas, including flood basalts, typified the northern craton, whereas subaqueous volcanism, including minor komatiitic lavas, predominated in the southwest.

Blake and Groves (1987) believed that the east–west extensional phase was associated with the generation of a major north-northeast-trending rift, located either east or west of the present craton; but that the regional subsidence phase reflected later rifting (Fig. 92A) along the approximate line of the present day southern Pilbara margin. East-trending fault scarps, which were an important control on lower Fortescue Group deposition in the southern Pilbara (Blight, 1985), were probably generated during the early stages of north–south extension.

## Passive continental margin phase

Syn-Fortescue Group rifting resulted in formation of an expanding ocean basin south of the Pilbara Craton. The Jeerinah Formation — the uppermost stratigraphic unit of

the Fortescue Group — and the overlying Hamersley Group were deposited in a passive margin environment, on subsiding southern Pilbara crust (Fig. 92B).

The Jeerinah Formation and Hamersley Group comprise finely laminated BIF, chert, mudstone, siltstone, and sandstone (commonly tuffaceous), dolomite, and felsic and mafic volcanic rocks. The predominance of suspension, chemical, and turbidite deposits, coupled with lack of evidence for wave and current reworking, points to deposition in a relatively deep (below storm-wave base) outer shelf environment. Palaeocurrent and turbidite thickness data from the Wittenoom Dolomite indicate that a shallow-marine shelf existed north and east of the Hamersley Basin (B. M. Simonson, written comm., 1986). Support for this interpretation comes from evaporite (halite?) pseudomorphs and wave ripples in the Carawine Dolomite — the likely equivalent of the Wittenoom Dolomite, in the northeastern Hamersley Basin (B.M.Simonson, written communication, 1986).

## Active continental margin phase

Transition from passive to active continental margin took place following deposition of the Hamersley Group. This change in tectonic regime resulted from gradual closing of the ocean basin south of the Pilbara Craton. Closure was accommodated by subduction of oceanic crust beneath a northward-moving continent, unrelated to Pilbara Craton rifting — the Yilgarn Craton. Compression, associated with plate convergence, was responsible for reverse movement on pre-existing extensional faults in the Pilbara Craton, (cf. Cohen, 1982). This caused shortening of the southern Pilbara crust, which in turn caused uplift and local folding of the overlying passive margin succession (Fig. 92C). Final stages of active-margin tectonism were characterized by crustal extension that resulted from arching of continental lithosphere as adjacent ocean floor was depressed by the approaching Yilgarn Craton. (cf. Jordan, 1981; Dewey, 1982).

The stratigraphy of the Turee Creek Group reflects shallowing, and local uplift, of the southern Pilbara shelf during the initial phase of ocean-basin closure. In the southwest (Hardey Syncline), the lower part of the Group comprises “deep water” facies, overlain by tidal shoreline and possible glacial deposits (Trendall, 1976; Seymour et al., in press). They are succeeded by a second suite of marine-shelf deposits that grade upwards into predominantly sandy and conglomeratic deltaic facies. Fragments of Hamersley Group present in the upper part of the stratigraphy point to uplift and erosion of the former passive margin succession in this area. Coarse-grained deltaic facies are not recorded in the southeastern Pilbara. Instead, the succession comprises an upward-shallowing sequence of shelf mudstone and sandstone, overlain by stromatolitic carbonate and shallow-marine sandstone.

Further crustal shortening, in the interval which followed Turee Creek Group sedimentation, was responsible for widespread uplift and erosion of the Mount Bruce

Supergroup. In the southeastern Pilbara, lack of angular discordance between the Mount Bruce Supergroup and the overlying Wyloo Group points to only minor deformation of the sedimentary cover sequence in this area. Further to the southwest, movement along basement faults was greater, and gave rise locally to more intense folding. This instability is reflected in the angular unconformity between the Mount Bruce Supergroup and the overlying Wyloo Group in the Hardey Syncline–Wyloo Dome area.

Beasley River Quartzite sedimentation took place on a tidally influenced, shallow-marine shelf which extended over most of the southern Pilbara. In the tectonically stable southeast, sandy detritus was introduced from a distal braided-fluvial system located northeast of Turee Creek Syncline. Additional gravel and sand was supplied from a fan-delta complex near the eastern closure of Wyloo Dome; this sediment source reflects further, intermittent movement on basement faults.

The Cheela Springs Basalt comprises terrestrial and shallow-marine basalt; basaltic tuff and agglomerate; and sedimentary rock. It was deposited during the final stages of ocean-basin closure, when load-induced crustal arching caused extension along the northern margin of the Ashburton Basin.

## Continental crustal collision

### Post-Cheela Springs Basalt to Duck Creek Dolomite

The Pilbara and Yilgarn Cratons collided soon after the Cheela Springs Basalt was deposited. As a result of oblique closure and the shape of the opposing craton margin, collision began in the east and migrated westward. Geophysical data (Drummond, 1979, 1983; Drummond et al., 1981) indicate that the suture between the Pilbara and Yilgarn Cratons now lies approximately 80 km south of Newman. A foreland fold and thrust belt was established in the southeastern Hamersley Basin; the Sylvania Inlier represents slices of Pilbara granite–greenstone basement, collected from the edge of the craton and thrust back into the Hamersley Basin cover (Tyler, 1990a). Initial folding and thrusting in the southeastern Hamersley Basin was followed by further flexural uplift as thrust-sheet stacking caused subsidence of the Pilbara Craton margin. Northward migration of the crustal flexure took place in response to further craton convergence, and resulted initially in uplift, then subsidence, of the southern Pilbara Crust.

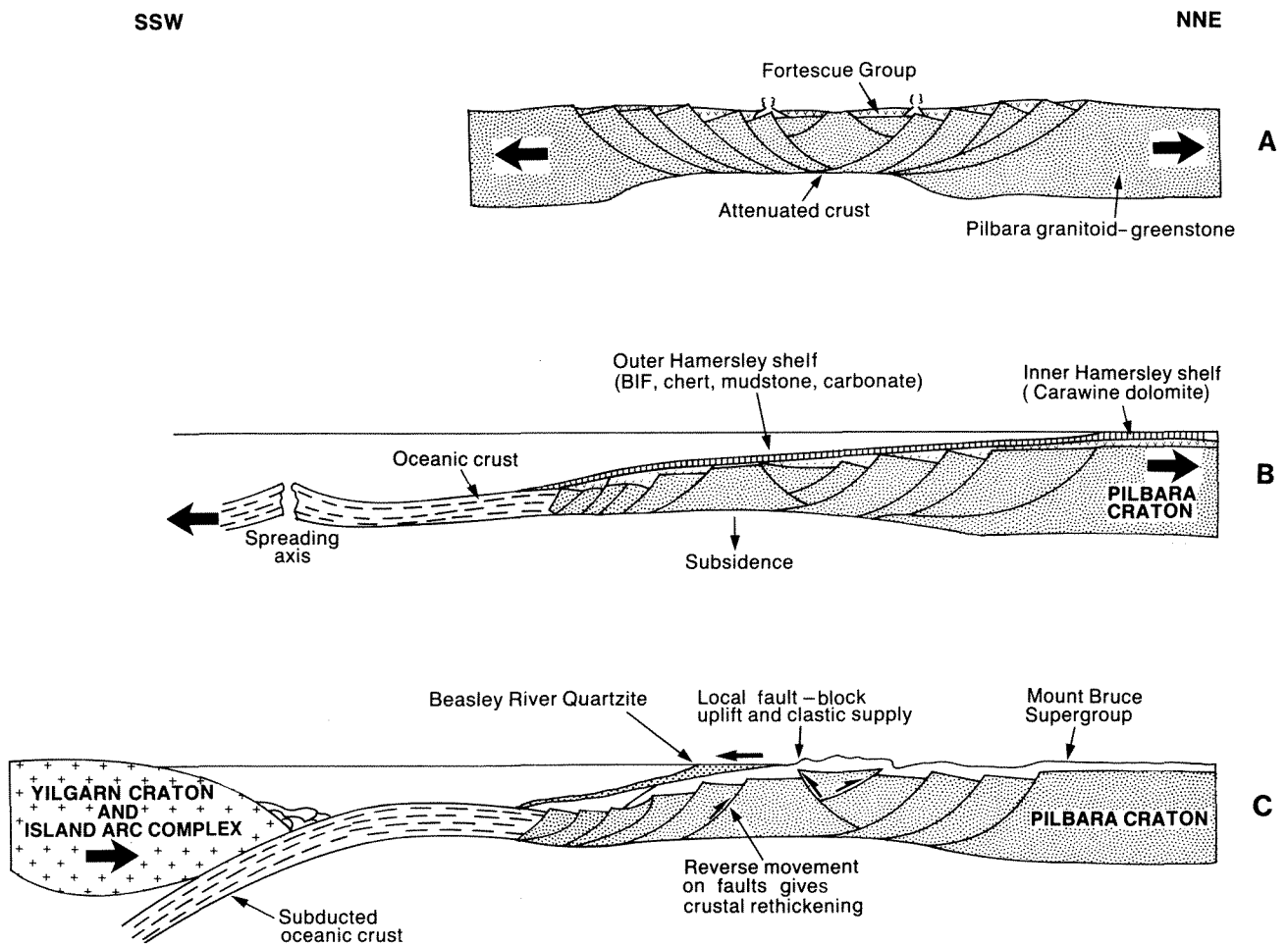
Flexural arching was responsible for post-folding uplift and extension in the southern Hamersley Basin. During this time a west-northwest-trending suite of dolerite dykes was emplaced along the southern margin of the Hamersley Basin (Tyler, 1990b). Subaerial exposure resulted in formation of iron-ore at Paraburdoo, and was accompanied by widespread erosion of the Mount Bruce Supergroup and low to middle Wyloo Group in the southern Hamersley Basin. Coarse-grained detritus from this

source area was supplied to a fluvial-dominated delta system (Mount McGrath Formation) which fringed the southern Hamersley Basin (Fig. 92D).

Mount McGrath Formation stratigraphy records the gradual subsidence of the southern Pilbara crust as the flexural bulge migrated northwards. In the southeastern Ashburton Basin, the lowermost 450 m of the succession comprises seven major deltaic cycles, each capped by conglomeratic delta-plain deposits. Subaerial and shallow-marine facies decrease in abundance up the succession; this decline is accompanied by increase in the proportion of deeper water, prodelta facies. Middle and upper levels of the formation consist largely of deep water mudstone and siltstone, and local carbonate. A similar deepening trend, accompanied by declining siliciclastic input, is also evident in the western Ashburton Basin.

There, the presence of only one or two deltaic cycles at the base of the succession reflects small initial uplift in this area.

The decline in the supply of terrigenous material that accompanied crustal downwarp culminated in widespread deposition of carbonate facies (Duck Creek Dolomite; Fig. 92E). The stratigraphy of this formation is broadly similar throughout the south and west Pilbara. Apart from 200 m of shallow-marine shelf deposits in the middle of the succession it consists mainly of slope and basin facies. Numerous debris flows and slump folds in lower and upper parts of the Duck Creek Dolomite reflect oversteepening, or downfaulting, of the shelf slope with increased basin subsidence. North of Wyloo Dome, this was accompanied by limited mafic volcanism (June Hill Volcanics).

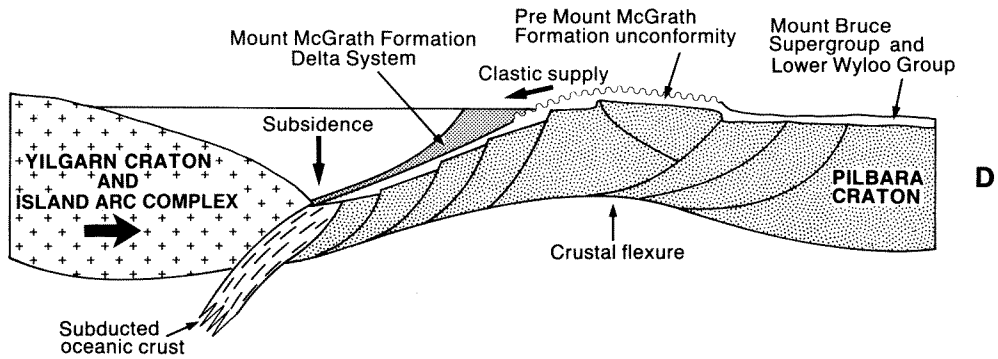


GSWA 25258A

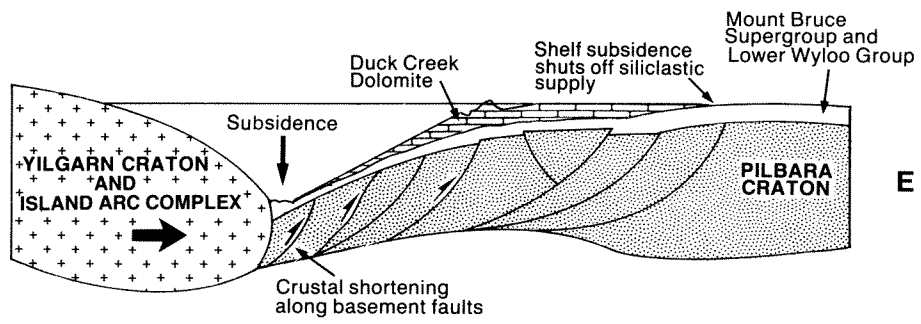
**Figure 92** Tectonic model showing the evolution of the southern margin during the interval 2700 to 2000 Ma. **A** — rifting of the Pilbara Craton and deposition of the Fortescue Group; **B** — Hamersley Group sedimentation on a passive continental margin; **C** — Beasley River Quartzite deposition on an active (convergent) continental margin; **D** — continental crustal collision and deposition of the Mount McGrath Formation; **E** — crustal loading and foreland basin subsidence leading to deposition of the Duck Creek Dolomite; **F** — infill of the foreland basin by Ashburton Formation; **G** — deposition of the Capricorn Formation during the interval between  $D_1$  and  $D_2$ .

SSW

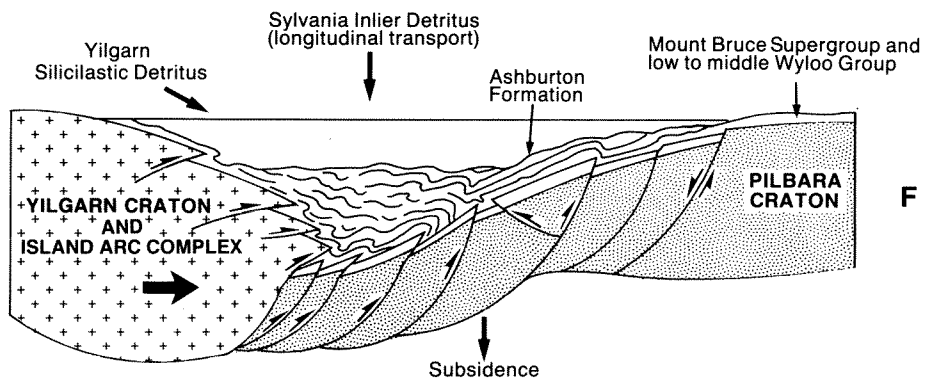
NNE



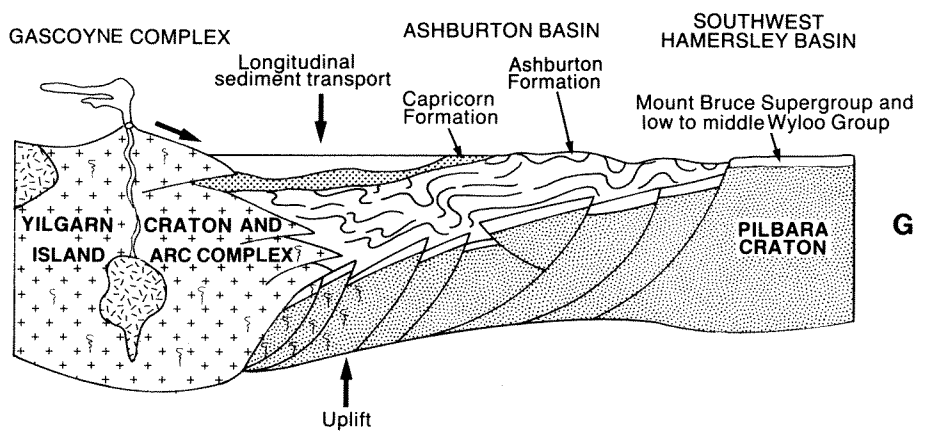
D



E



F



G

GSWA 25258 B

## Ashburton Formation–D<sub>1</sub> deformation–Capricorn Formation

Further major thrusting in the Pilbara foreland was responsible for granite–greenstone uplift in the Sylvania Inlier, and open to tight folding in the adjacent Hamersley Basin (Tyler, 1990a; Tyler et al., in press). In the west, continued thrust stacking at the edge of the Pilbara Craton maintained subsidence and created a deep-water foreland basin — the Ashburton Trough.

Granite–greenstone detritus, eroded from the Sylvania Inlier, was shed into the eastern end of the Ashburton Trough and transported westwards by means of an elongate submarine fan system (Ashburton Formation, Fig. 92F). The presence of abundant granitoid detritus in lower levels of the Ashburton Formation implies that most of the Mount Bruce Supergroup and lower Wyloo Group cover had been removed from the Sylvania Inlier during post-Cheela Springs Basalt–pre-Mount McGrath Formation uplift. In the early history of Ashburton Formation deposition, abundant sand detritus was deposited in braided submarine distributary channels and depositional lobes. Subsequent increase in the proportion of fine-grained sediment led to development of a mud-dominated fan system, in which coarse-grained material was transported in a few major channels flanked by extensive levees. Palaeocurrent and provenance data indicate that both braided and leveed sediment dispersal systems extended at least as far as the Wyloo Dome, 300 km west-northwest of the Sylvania Inlier.

With increased convergence, continent–continent collision took place further west; the major suture between Pilbara and Yilgarn cratons was located in the Gascoyne Complex. North to northeasterly directed thrusting, north and northeast of the suture, had a twofold effect. Firstly, it caused basement uplift in the northern Gascoyne Complex; and secondly, loading induced by thrust-sheet stacking maintained subsidence in the foreland basin further to the north.

Granitoid detritus from the newly uplifted basement was incorporated into a second submarine-fan system which prograded north-northeastwards into the Ashburton Basin, over the easterly derived sediment prism. Penecontemporaneous uplift in the western Hamersley Basin gave rise to a third submarine-fan complex in the northwestern Ashburton Basin. There, sediment derived from the Mount Bruce Supergroup, and low to middle Wyloo Group, was distributed by a feeder channel located to the north of the Wyloo Dome.

Large-scale, tight, northeast-facing F<sub>1</sub> folds formed in response to north and northeasterly directed thrusting in the southern and eastern Ashburton Basin. Large-scale southwest-facing F<sub>1</sub> folds, which occur in the central-southern part of basin, may reflect fanning of D<sub>1</sub> structures over a thrust ramp in the underlying supracrustal succession. Along the southern and western margin of the Ashburton Basin, thrust-sheet stacking resulted in considerable thickening of the foreland basin succession. Increased P–T conditions beneath the overthrust terrain were

responsible for low to upper greenschist-facies metamorphism in the Ashburton Formation. In the southwest, partial melting of the thickened Pilbara crust (and possibly the supracrustal sedimentary pile) generated granitoid batholiths.

Continued north- to northeasterly directed thrusting resulted in major uplift and erosion of the structurally thickened Ashburton Formation. Along the southern and western margin of the basin, this was accompanied by tectonic emplacement of allochthonous sequences, comprising metamorphosed and unmetamorphosed shelf deposits, felsic and mafic volcanic rocks, and granitoid (Fig. 92G). Sediment derived from these upland areas was deposited in a fluvial-dominated delta and fan-delta complex (Capricorn Formation) on the eroded surface of the Ashburton Formation. Capricorn Formation sedimentation was accompanied by some felsic volcanism in the source area.

## D<sub>2</sub> deformation–Mount Minnie Group

Final stages of the collision were characterized by widespread dextral wrenching in the Pilbara Craton and supracrustal sequence. Open to tight, F<sub>2</sub> folds with steep, south- to southwest-dipping axial surfaces formed in the cover as a result of plastic deformation in the early stages of strike-slip movement. Further displacement across the wrench zone was accommodated firstly by fracturing, and then by faulting in the supracrustal rocks. The Wyloo Dome was translated 10–12 km to the northwest, along steeply dipping wrench faults which bound the southwestern Hamersley Basin.

Fan-delta deposits of the Mount Minnie Group were deposited in a small, fault-bounded basin, formed as a result of localized crustal extension during dextral wrenching.

Major strike-slip faults, and their associated veins and fissures, were the principal depositional sites for silver, gold, copper, and lead mineralization during the latter part of the D<sub>2</sub> event.

## Post-collision (Bresnahan Group) sedimentation

Northeast-trending normal faults, and associated northwest-trending transfer faults, were formed in response to southeasterly directed crustal extension in the eastern Hamersley and Ashburton Basins. Sand and gravel, derived principally from the Capricorn Formation, Wyloo Group, and Gascoyne Complex, accumulated in thick, stream-dominated alluvial fans (Bresnahan Group) on the downthrown side of the faults. Northwestward propagation of the fault system accompanied further crustal extension, and resulted in the western boundary of the Bresnahan Basin being backstepped to the vicinity of Mount Bresnahan. Post-Bresnahan Group deformation was accompanied by localized, fault-related uranium enrichment in the Angelo River district.

## Discussion

### Precambrian plate tectonics

The foregoing model is based upon the Wilson cycle of ocean basin opening and closure (Wilson, 1968; Dewey and Burke, 1974).

Although the Wilson cycle concept has been successfully applied to numerous Phanerozoic and Upper Proterozoic orogenic belts, many geologists have been reluctant to apply it to Precambrian terranes older than about 1000 Ma (see discussions by Kroner, 1981, 1983; Windley, 1984). Principal arguments put forward against this type of model are:

- (a) Cratons on either side of Precambrian orogenic belts are apparently closely similar.
- (b) Precambrian orogenic belts lack subduction- or collision-related volcanism.
- (c) No convincing ophiolites or glaucophane schists have been reported from orogenic belts older than about 1000 Ma.
- (d) Palaeomagnetic evidence does not support the hypothesis of large-scale ocean-basin opening and closure during the early to middle Precambrian.
- (e) The duration of Precambrian Wilson cycles is apparently very large in comparison to the time-scale of Phanerozoic ocean-basin formation and destruction.

These objections, as they relate to the Capricorn Orogen, will now be addressed.

### Comparisons between the Pilbara and Yilgarn Cratons

The first argument, which relates to alleged similarities between the Pilbara and Yilgarn Cratons, and their respective lower Proterozoic cover sequences (Horwitz and Smith, 1978; Gee, 1979a; Kroner, 1983), is rejected for reasons listed in the introduction to this chapter.

### Subduction-related volcanism

The collision model presented here invokes subduction of oceanic crust beneath the northern Yilgarn Craton during ocean basin closure; evidence of subduction-related volcanism would therefore be expected on the northern margin of the Yilgarn Craton.

The Narracoota Volcanics (Gee, 1986) are a thick (4–6 km) sequence of mafic and ultramafic lavas and breccias within the pre-1800 Ma Glengarry Group, on the northern Yilgarn Craton. Geochemistry of these volcanics strongly suggests a subduction-related origin (Hynes and Gee, 1986). Basalt, basaltic andesite, andesite, and related ultramafics, from northern Glengarry Sub-basin are characteristically very low in titanium and zirconium; they have more similarities to the boninite association of fore-arc regions of the western Pacific than to any other mod-

ern association. Similarly, tholeiitic basalts from the southern Glengarry Sub-basin closely resemble low-K tholeiites formed during rifting of modern island arcs (Hynes and Gee, 1986).

The Narracoota Volcanics interfinger with, and are overlain by, the Thaduna Greywacke, a 5 km thick turbidite sequence containing abundant basalt fragments and calcic plagioclase (Gee, 1986). These are probable forearc, intra-arc, or backarc basin deposits, derived from a relatively undissected magmatic arc complex (Dickinson and Suczek, 1979). Sandstones that contain a significant proportion of alkali feldspar and quartz, in addition to volcanic detritus, occur to the east of the Thaduna area (Gee, 1986), and may indicate erosional unroofing of arc-related plutons.

### Ophiolites and glaucophane schists

No ophiolites or glaucophane schists have yet been reported from the Capricorn Orogen. This is not unexpected, however, given that erosion has removed most of the higher structural levels. Windley (1984) notes that on the 2700 km long Indus–Yarlung Zangbo suture of the Himalayas, glaucophane-bearing rocks crop out at only five localities (about 0.3 % of the suture zone) while ophiolites occupy less than 1 % of the suture length. With time, and only a few more kilometres of uplift, these occurrences would be removed by erosion.

Recognition of former oceanic crust or trench sediments in the Gascoyne Complex is likely to be difficult, because of strong deformation and metamorphism. Pillow lavas, gabbros, and basic dykes, would have been converted to banded and foliated amphibolites. Similarly, low-temperature glaucophane will have recrystallized to higher temperature hornblende during uplift (England and Richardson, 1977).

### Palaeomagnetic data

Palaeomagnetic data suggest that there was little relative motion between the Pilbara and Yilgarn Cratons during the lower to middle Proterozoic (McElhinny and Embleton, 1976; McElhinny and McWilliams, 1977; Embleton, 1978). Problems arising from use of these and other data from the Precambrian are discussed by McWilliams (1981) and Windley (1984). Of major concern are: the lack of palaeo-longitudinal control, poor data coverage, and inadequacy of isotopic age constraints. These limitations make it difficult to infer a static model for the Pilbara and Yilgarn Cratons with any confidence. McWilliams (1981) has shown that a displacement of 1000–2000 km could have separated the Pilbara and Yilgarn Cratons, prior to 1800 Ma. On this basis, available paleomagnetic evidence neither proves, nor disproves, a collision model for the Capricorn Orogen.

### Geochronological data

Geochronological data for the base of the Fortescue Group (Trendall, 1983) suggest that Pilbara craton rifting started about 2750 Ma; whereas most age determinations for Capricorn Orogeny lie within the range 1600–1900



Ma (Leggo et al., 1965; de Laeter, 1976; Williams et al., 1978; Libby and de Laeter, 1985; Libby et al., 1986). At face value, these data suggest a time span of 850–1150 Ma between opening and closing stages of the Pilbara Wilson cycle, compared with approximately 300, 150, and 350 Ma respectively for equivalent cycles in the Caledonian–Appalachian and Alpine–Himalayan fold belts (Windley, 1984), and the Late Precambrian Hoggar Shield, North Africa (Caby et al., 1981).

The apparent longevity of the Pilbara Wilson cycle largely reflects the use of unsuitable Rb–Sr data in fixing the age of collision. Blake and McNaughton (1984) noted that Rb–Sr determinations for the Pilbara and Gascoyne Province generally record post-orogenic events, such as cooling or hydrothermal or metamorphic alteration; in most cases, such ages are about 200–400 Ma younger than those obtained from more robust isotopic systems (e.g. U–Pb, Pb–Pb, Sm–Nd). Sm–Nd model ages for Gascoyne Province gneiss and granitoid (Fletcher et al., 1983) support this view, and indicate that collision probably occurred between 2400 and 2000 Ma. On this basis, a 350–750 Ma time-span for the Pilbara Wilson cycle is likely; the lower part of this range is of comparable duration to Phanerozoic and Late Precambrian ocean basin cycles.

Most arguments put forward against a plate-tectonic interpretation for the Capricorn Orogen are, therefore, unconvincing. Conversely, there is abundant geophysical, petrological, stratigraphic, sedimentological, and structural data to suggest that the southern Pilbara evolved from a rifted continental margin, to an active margin, before undergoing continent–continent collision with the Yilgarn Craton between 2400 and 2000 Ma. In view of the high structural levels now exposed in the suture zone (Gascoyne Complex), the apparent lack of ophiolites and

glauco-phane schists is insufficient reason to abandon the Wilson cycle model in favour of an ensialic one.

### **Active margin and foreland-basin volcanism**

Limited mafic volcanism accompanied the active margin and collision stages of Pilbara crustal evolution. The 0–2 km thick Cheela Springs Basalt was extruded during the active margin stage, when flexuring (because of Yilgarn Craton loading) resulted in intermittent extension in the Pilbara Crust. The sequence is comparable to the 150 m to >1200 m thick mafic lavas, of Cretaceous age, that outcrop in the Caribbean mountain system (Maresch, 1974). Cohen (1982) noted that these volcanics were deposited when an island arc–trench system moved south relative to the Venezuelan continental margin. During convergence, crustal flexure on the active edge of the continent was accompanied by basaltic volcanism, developed along an east-west trend.

The 0–120 m thick June Hill Volcanics were deposited during the early stages of continent - continent collision. They outcrop in a north-northwest-trending belt sub-parallel to the Ashburton Basin axis, and may reflect localized extension associated with foreland basin subsidence.

Mafic lava and agglomerate, up to 600 m thick, occur locally within the upper part (Ashburton Formation) of the foreland basin succession. A Cainozoic analogy occurs in the Taiwan Strait. There, a foreland basin has developed on the continental margin of southeast China, where it is being obliquely overridden by the foreland fold-and-thrust belt of Taiwan (Davis et al., 1983). Foreland basin magmatism has taken the form of 320 m of basaltic lava of early Pleistocene or Pliocene age, which underlie the Penghu Islands, in the central Taiwan Strait.

## References

- ALLEN, J. R. L., 1965, Fining upwards cycles in alluvial successions: *Geological Journal*, v. 4, p. 229–246.
- ALLEN, J. R. L., 1984, Sedimentary structures, their character and physical basis, parts 1 and 2: Amsterdam, Elsevier, 593 and 663 p.
- ALLEN, P. A. and HOMEWOOD, P. (editors), 1986, Foreland Basins: International Association of Sedimentologists, Special Publication 8, 453 p.
- ASSERETO, R. L. A. M. and KENDALL, C. G. St. C., 1977, Nature, origin and classification of peritidal tepee structures and related breccias: *Sedimentology*, v. 24, p. 153–210.
- BARTLETT, W. M., 1986, Western Australian Yearbook: Perth, Australian Bureau of Statistics, West Australian Office.
- BATES, R. L. and JACKSON, J. A., 1980, Glossary of geology, 2nd edition: Falls Church, American Geological Institute, 749 p.
- BEARD, J. S., 1975, The vegetation of the Pilbara area: Explanatory notes to Sheet 5, Vegetation Survey of Western Australia: Nedlands, University of Western Australia Press.
- BLAKE, T. S., 1984a, The Lower Fortescue Group of the northern Pilbara Craton: Stratigraphy, and palaeogeography, in *Archaean and Proterozoic basins of the Pilbara, evolution and mineralization potential*, edited by J. R. Muhling, D. I. Groves, and T. S. Blake: University of Western Australia, Geology Department and University Extension, Publication 9, p. 123–143.
- BLAKE, T. S., 1984b, Evidence for stabilization of the Pilbara Block, Western Australia: *Nature*, v. 307, p. 721–723.
- BLAKE, T. S., and GROVES, D. I., 1987, Continental rifting and the Archaean–Proterozoic transition: *Geology*, v. 15, p. 229–232.
- BLAKE, T. S., and McNAUGHTON, N.J., 1984, A geochronological framework for the Pilbara region, in *Archaean and Proterozoic basins of the Pilbara*, Western Australia: Evolution and mineralization potential, edited by J. R. Muhling, D.I. Groves, and T. S. Blake: Perth, University of Western Australia, Geology Department and University Extension, Publication 9 p. 1–22.
- BLATCHFORD, T., 1913, Mineral resources of the Northwest Division, Western Australia: Western Australia, Geological Survey, Bulletin 52.
- BIIGHT, D. F., 1985, Economic potential of the lower Fortescue Group and adjacent units in the southern Hamersley Basin — A study of depositional environments: Western Australia, Geological Survey, Report 13.
- BLOCKLEY, J. G., 1971, The lead, zinc and silver deposits of Western Australia: Western Australia, Geological Survey, Mineral Resources Bulletin 9, 234 p.
- BLOCKLEY, J. G., 1980, The tin deposits of Western Australia: Western Australia, Geological Survey, Mineral Resources Bulletin 12, p. 184.
- BOURN, R., and JACKSON, D. G., 1979, A generalized account of the Paraburdoo iron ore bodies: Australasian Institute of Mining and Metallurgy Conference, Perth, Western Australia, p. 187–201.
- BRIDGE, P. J., and PRYCE, M. W., 1978, Copper deposits from Bali Lo copper mine, Ashburton Downs, Western Australia: *Australian Mineralogist*, 14, p. 69–70.
- BULL, W.B., 1972, Recognition of alluvial fan deposits in the stratigraphic record, in *Recognition of ancient sedimentary environments*, edited by I. K. Rigby and W. K. Hamblin: Society of Economic Palaeontologists and Mineralogists, Special Publication 16, p. 63–83.
- BUNTING, J. A., 1986, Geology of the eastern part of the Nabberu Basin, Western Australia: Western Australia, Geological Survey, Bulletin 131.
- CABY, R., BERTRAND, J. M. L., and BLACK, R., 1981, Pan-African ocean closure and continental collision in the Hoggar–Iforas segment, central Sahara, in *Precambrian plate tectonics*, edited by A. Kroner: Amsterdam, Elsevier, p. 407–434.

- CANT, D. J., 1982, Fluvial facies models and their application, *in* Sandstone depositional environments, *edited by* P.A. Scholle and D. Spearing: American Association of Petroleum Geologists, Memoir 31, p. 115–137.
- CARTER, J. D., 1981, Uranium exploration in Western Australia: Western Australia, Geological Survey, Record, 1981/6, 29 p.
- COHEN, C. R., 1982, Model for a passive to active continental transition: Implications for hydrocarbon exploration: American Association of Petroleum Geologists, Bulletin, v. 66, p. 708–718.
- COLEMAN, J. M. and PRIOR, D.B., 1982, Deltaic environments of deposition, *in* Sandstone depositional environments, *edited by* P. A. Scholle and D. Spearing: American Association of Petroleum Geologists, Memoir 31, p. 139–178.
- COLEMAN, J.M., SUHAYDA, J.N., WHELAN, T. and WRIGHT, L.D., 1974, Mass movement of Mississippi River delta sediments: Gulf- Coast Association Geological Society, Transactions, v.24, p. 49–68.
- COLLINSON, J. D., 1978a, Vertical sequence and sand-body shape in alluvial sequences, *in* Fluvial sedimentology, *edited by* A. D. Miall: Canadian Society of Petroleum Geologists, Memoir 5, p. 577–586.
- COLLINSON, J. D., 1978b, Alluvial sediments, *in* Sedimentary environments and facies (1st edition), *edited by* H.G. Reading: Oxford, Blackwell Scientific Publication, p. 15–60.
- COLLINSON, J. D., ELLIOTT, T., and READING, H. G., 1978, Environments and facies of sand bodies: Oxford, Sedimentary Research Associates, 212p.
- COMPSTON, W. and ARRIENS, P. A., 1968, The Precambrian geochronology of Australia: Canadian Journal of Earth Science, v. 5, p. 561–583.
- COMPSTON, W., WILLIAMS, I. S., McCULLOCH, M. T., FOSTER, J. J., ARRIENS, P. A., and TRENDALL, A. F., 1981, A revised age for the Hamersley Group: Geological Society of Australia, 5th Annual Convention, Perth, Abstracts, 3, p. 40.
- COWARD, M. P. and RIES, A. C.(editors), 1986, Collision tectonics: Geological Society of London, Special Publication 19, 415 p.
- CUMMING, G. L., and RICHARDS, J. R., 1975, Ore lead isotope ratios in a continuously changing Earth: Earth and Planetary Science Letters, 1, 259–269.
- CURRAY, J. R. and MOORE, D. G., 1971, Growth of the Bengal deep-sea fan and denudation in the Himalayas: Geological Society of America, Bulletin, v. 82, p. 563–572.
- DANIELS, J. L., 1966, Southern part of the Kooline lead field: Western Australia, Geological Survey, Annual Report, 1965, p. 72–73.
- DANIELS, J. L., 1968, Turee Creek, W.A.: Western Australia, Geological Survey, 1:250 000 Geological Series — Explanatory Notes.
- DANIELS, J. L., 1969, Edmund, W.A.: Western Australia, Geological Survey, 1:250 000 Geological Series — Explanatory Notes
- DANIELS, J. L., 1970, Wyloo, W. A.: Western Australia, Geological Survey, 1:250 000 Geological Series — Explanatory Notes.
- DANIELS, J. L., 1975, Palaeogeographic development of Western Australia: Precambrian, *in* Geology of Western Australia: Western Australia, Geological Survey, Memoir 2, p.437–450.
- DANIELS, J. L. and MacLEOD, W. N., 1965, Newman, W.A.: Western Australia, Geological Survey, 1:250 000 Geological Series — Explanatory Notes.
- DANIELS, J. D., HALLIGAN, R., and JONES, W. R., 1967, Turee Creek (1st edition): Western Australia, Geological Survey, 1:250 000 Geological Series - Map.
- DAVIS, D., SUPPE, J., and DAHLEN, F. A., 1983, Mechanics of fold-and-thrust belts and accretionary wedges: Journal of Geophysical Research, v. 88, p. 1153–1172.
- DAVY, R., CLARKE, R., THORNE, A.M., and SEYMOUR, D.B., *in press*, Geology, mineralization and origins of the Mount Clement gold and lead prospects, Ashburton Basin *in* Professional Papers: Western Australia, Geological Survey, Report 30.
- de LAETER, J. R., 1976, Rb–Sr whole-rock and mineral ages from the Gascoyne Province: Western Australia, Geological Survey, Annual Report, 1975, p. 126–130.
- de la HUNTY, L. E., 1965, Mount Bruce, W.A.: Western Australia, Geological Survey, 1:250 000 Geological Series — Explanatory Notes.
- de RAAF, J.F.M., and BOERSMA, J.R., 1971, Tidal deposits and their sedimentary structures: Geologie Mijnbouw, v. 50, p. 479–504.
- de RAAF, J.F.M., BOERSMA, J.R., and van GELDER, A., 1977, Wave generated structures and sequences from a shallow marine succession. Lower Carboniferous, County Cork, Ireland: Sedimentology, v. 24, p. 1–52.
- DEWEY, J.F., 1982, Plate tectonics and the evolution of the British Isles: Geological Society of London, Journal, v. 139, p. 371–412.

- DEWEY, J. F. and BURKE, K. C. A., 1974, Hot spots and continental breakup: Implications for collisional orogeny: *Geology*, v. 3, p. 422–424.
- DICKINSON, W. R., 1970, Interpreting detrital modes of graywacke and arkose: *Journal of Sedimentary Petrology*, v. 40, p. 695–707.
- DICKINSON, W. R. and SUCZEK, C. A., 1979, Plate tectonics and sandstone compositions: *American Association of Petroleum Geologists, Bulletin*, v. 63, p. 2164–2182.
- DOUST, G., 1975, Economic implications of the Duck Creek syncline, Ashburton: *Geological Society of Australia, First Australian Geological Convention Abstracts*, p. 77.
- DOUST, G., 1984, Stratiform polymetallic sulphide mineralization: An exploration perspective for the Ashburton Basin, W.A.: James Cook University of North Queensland, M.Sc. Thesis (unpublished), 185 p.
- DOTT, R. H. Jr, 1974, Palaeocurrent analysis of severely deformed flysch-type strata — A case study from South Georgia Island: *Journal of Sedimentary Petrology*, v. 44, p. 1166–1173.
- DRUMMOND, B. J., 1979, A crustal profile across the Archean Pilbara and northern Yilgarn Cratons, northwest Australia: *BMR Journal of Geology and Geophysics*, v. 4, p. 171–180.
- DRUMMOND, B. J., 1983, Detailed seismic velocity/depth models of the upper lithosphere of the Pilbara craton, northwest Australia: *BMR Journal of Geology and Geophysics*, v. 8, p. 35–51.
- DRUMMOND, B. J., SMITH, R.E., and HORWITZ, R. C., 1981, Crustal structure in the Pilbara and northern Yilgarn Blocks from deep seismic sounding, *in* *Archean Geology, Second International Archean Symposium*, edited by J. E. Glover and D. I. Groves: *Geological Society of Australia Special Publication*, 7, p. 33–41.
- EDGEELL, H. S., 1964, Precambrian fossils from the Hamersley Range, Western Australia and their use in stratigraphic correlation: *Geological Society of Australia, Journal*, v. 10, p. 235–262.
- ELLIOTT, T., 1974, Interdistributary bay sequences and their genesis: *Sedimentology*, v. 21, p. 611–622.
- ELLIOTT, T., 1986, *Deltas, in Sedimentary environments and facies (2nd edition)*, edited by H. G. Reading: Oxford, Blackwell Scientific Publications, p. 113–154.
- ELLIS, H. A., 1951, Report on a reconnaissance examination of the Kooline lead field: *Western Australia, Geological Survey, Annual Report 1949*, p. 9–15.
- EMBLETON, B. J., 1978, The palaeomagnetism of the 2400 m.y. old rocks from the Australian Pilbara Craton and its relation to Archean - Proterozoic tectonics: *Precambrian Research*, v. 6, p. 275–291.
- ENGLAND, P. C. and RICHARDSON, S. W., 1977, The influence of erosion upon the mineral facies of rocks from different tectonic environments: *Geological Society of London, Journal*, v. 134, p. 201–213.
- ENOS, P., 1977, Flow regimes in debris flow: *Sedimentology*, v. 24, p. 133–142.
- EWERS, G. R. and FERGUSON, J., 1985, Unconformity-related uranium deposits — Turee Creek uranium prospect, Western Australia: *Australia, Bureau of Mineral Resources, Annual Report, 1985*, p. 35–37.
- EWERS, W.E., 1983, Chemical factors in the deposition and diagenesis of banded iron-formation, *in* *Iron formation facts and problems*, edited by A.F. Trendall and R.C. Morris: Amsterdam, Elsevier, *Developments in Precambrian Geology*, 6, p. 491–512.
- FAVENC, E., 1888, The history of Australian exploration from 1788 to 1888: Sydney, Turner and Henderson, 474 p.
- FLETCHER, I. R., WILLIAMS, S. J., GEE, R. D., and ROSMAN, K. J. R., 1983, Sm–Nd model ages across the margins of the Yilgarn Block, Western Australia: Northwest transect into the Proterozoic Gascoyne Province: *Geological Society of Australia, Journal*, v. 30 p. 167–174.
- FINUCANE, K. J., 1939, The Black Hills area, Ashburton Goldfield: Aerial Geological and Geophysical Survey of Northern Australia, Western Australia, Report 60, p. 1–9.
- FOLK, R. L., 1974, *Petrology of Sedimentary Rocks*: Austin, Hemphill, 182 p.
- FORMAN, F. G., 1938, The Melrose and Belvedere gold mines and vicinity, Mount Stuart Station, Ashburton Goldfield: *Western Australia, Geological Survey, Annual Report, 1937*, p. 4–5.
- GEBELEIN, C.D., 1976, Open marine subtidal and intertidal stromatolites (Florida, the Bahamas and Bermuda), *in* *Stromatolites*, edited by M.R. Walter: Amsterdam, Elsevier, p. 381–389.
- GEE, R. D., 1979a, Structure and tectonic style of Western Australia: *Tectonophysics*, v. 58, p. 327–369.
- GEE, R. D., 1979b, *Geological map of Western Australia at 1:2 500 000 scale*: Western Australia, Geological Survey.
- GEE, R. D., 1980, Summary of the Precambrian stratigraphy of Western Australia: *Western Australia, Geological Survey, Annual Report 1979*, p. 85–90.

- GEE, R. D., 1986, Explanatory notes on the Peak Hill 1:250 000 geological sheet, Western Australia, Second Edition: Western Australia, Geological Survey, Record 1986/11.
- GOODE, A. D. T., 1981, Proterozoic Geology of Western Australia, in *Precambrian of the Southern Hemisphere*, edited by D. R. Hunter: Amsterdam, Elsevier, p. 105–203.
- GRAHAM, S. A., DICKINSON, W. R. and INGERSOLL, R. V., 1975, Himalayan - Bengal model for flysch dispersal in the Appalachian-Ouachita system: Geological Society of America, Bulletin, v. 86. p. 273–286.
- GREGORY, A. C. and GREGORY, F. T., 1884, *Journal of Australian Explorations*: Brisbane, 184 p.
- GREY, K., 1979, Preliminary results of biostratigraphic studies of Proterozoic stromatolites in Western Australia: Western Australia, Geological Survey, Record 1979/2.
- GREY, K., 1981a, *Patomia* f. indet. from an un-named carbonate unit (Early Proterozoic) Newman 1:250 000 Sheet: Western Australia, Geological Survey, Palaeontology Report 51/81 (unpublished).
- GREY, K., 1981b, A new digitate stromatolite from the Kunderong Range, Turee Creek 1:250 000 Sheet: Western Australia, Geological Survey, Palaeontology Report 53/81 (unpublished).
- GREY, K., 1982, Aspects of Proterozoic biostratigraphy in Western Australia: *Precambrian Research*, v. 18, p. 347–365.
- GREY, K., 1984, Stromatolitic limestone from the Duck Creek Dolomite, near Kennedy Creek (Turee Creek Sheet), and a re-assessment of the occurrence of *Patomia* f. indet. at the same locality: Western Australia, Geological Survey, Palaeontology Report 8/84 (unpublished).
- GREY, K., 1985, Stromatolites in the Proterozoic Duck Creek Dolomite, Western Australia, in *Professional Papers for 1983*: Western Australia, Geological Survey, Report 14, p. 94–103.
- GREY, K. and THORNE, A. M., 1985, Biostratigraphic significance of stromatolites in upward-shallowing sequences of the Early Proterozoic Duck Creek Dolomite, Western Australia: *Precambrian Research*, v. 29, p. 183–206.
- GROTZINGER, J. P., 1986, Cyclicality and palaeoenvironmental dynamics, Rocknest platform, northwest Canada: Geological Society of America, Bulletin, v. 97, p. 1208–1231.
- HALLIGAN, R. and DANIELS, J. L., 1964, Precambrian geology of the Ashburton valley region, North-West Division: Western Australia, Geological Survey, Annual Report, 1963, p.38–46.
- HARMS, J. C. and FAHNESTOCK, R. K., 1965, Stratification, bed forms, and flow phenomena (with an example from the Rio Grande), in *Primary sedimentary structures and their hydrodynamic interpretation*, edited by G. V. Middleton: Society of Economic Palaeontologists and Mineralogists, Special Publication, 12, p. 84–115.
- HARMS, J. C., SOUTHARD, J. B. and WALKER, R. G., 1982, Structures and sequences in clastic rocks: Society of Economic Palaeontologists and Mineralogists, Short Course No. 9, Lecture Notes.
- HAYES, M. O. and MICHEL, J., 1982, Shoreline sedimentation within a forearc embayment, Lower Cook Inlet, Alaska: *Journal of Sedimentary Petrology*, v. 52, p. 351–264.
- HEIN, F. J. and WALKER, R. G., 1977, Bar evolution and development of stratification in the gravelly, braided, Kicking Horse River, British Columbia: *Canadian Journal of Earth Sciences*, v. 14, p. 562–570.
- HEIN, F. J. and WALKER, R. G., 1982, The Cambro-Ordovician Cap Enrage Formation, Quebec, Canada: Conglomerate deposits of a braided submarine channel with terraces: *Sedimentology*, v. 29, p. 309–329.
- HEWARD, A. P., 1978a, Alluvial fan sequence and mega sequence models: with examples from the Westphalian D–Stephanian B coalfields, Northern Spain, in *Fluvial Sedimentology*, edited by A..D. Miall: Canadian Society of Petroleum Geologists, Memoir 5, p. 669–702.
- HEWARD, A. P., 1978b, Alluvial fan and lacustrine sediments from the Stephanian A and B (La Magdaleria, Cinera - Matallaria and Sabero) coalfields, northern Spain: *Sedimentology*, v. 25, p. 451–488.
- HICKMAN, A. H., 1983, Geology of the Pilbara Block and its environs: Western Australia, Geological Survey, Bulletin 127.
- HOFFMAN, P., 1976, Stromatolite morphologies in Shark Bay, Western Australia, in *Stromatolites*, edited by M. R. Walter: Amsterdam, Elsevier, p. 261–272.
- HOFMANN, H. J., and SCHOPF J. W., 1983, Early Proterozoic microfossils in Earth's Earliest Biosphere: Its Origin and Evolution, edited by J. W. Schopf: Princeton, Princeton University Press, p. 321–359.
- HOWELL, D. G. and NORMARK, W. R., 1982, Sedimentology of submarine fans, in *Sandstone depositional environments*, edited by P. A. Scholle

- and D. Spearing: American Association of Petroleum Geologists, Memoir 31, p. 365–404.
- HORWITZ, R. C., 1978, The Lower Proterozoic of the Wyloo Anticline: Australia, Commonwealth Scientific and Industrial Research Organization, Division of Mineralogy, Report FP20.
- HORWITZ, R. C., 1980, The Lower Proterozoic succession south of the Hamersley Iron Province between the Angelo and Beasley Rivers: Australia, Commonwealth Scientific and Industrial Research Organization, Division of Mineralogy, Report FP22.
- HORWITZ, R. C., 1981, Large scale slumping in the Ashburton Trough of Western Australia: Precambrian Research, v. 14, p. 389–401.
- HORWITZ, R. C., 1982, Geological history of the early Proterozoic Paraburdoo Hinge Zone, Western Australia: Precambrian Research, v. 19, p. 191–200.
- HORWITZ, R. C., 1983, Paleogeographic evolution of the Paraburdoo Hinge Zone: A summary of events: Australia Commonwealth Scientific and Industrial Research Organization, Division of Mineralogy, Research Review 1983, p.77–79.
- HORWITZ, R. C. and SMITH, R. E., 1978, Bridging the Yilgarn and Pilbara blocks, Western Australia: Precambrian Research, v. 6, p. 293–322.
- HUGHES, C. J., 1982, Igneous petrology: Amsterdam, Elsevier, 551 p.
- HUNTER, W. M., 1990, Bresnahan Basin, *in* Geology and Mineral Resources of Western Australia: Western Australia, Geological Survey, Memoir 3, p. 304–308.
- HYNES, A. and GEE, R. D., 1986, Geological setting and petrochemistry of the Narracoota Volcanics, Capricorn Orogen, Western Australia: Precambrian Research, v. 31, p. 107–132.
- INGERSOLL, R. V. and SUCZEK, C. A., 1979, Petrology and provenance of Neogene sand from the Nicobar and Bengal Fans, DSDP sites 211 and 218: Journal of Sedimentary Petrology, v. 49, p. 1217–1228.
- JAMES, N. P., 1984, Shallowing-upward sequences in carbonates, *in* Facies models (second edition), *edited by* R. G. Walker: Geoscience Canada, Reprint Series, 1, p. 213–228.
- JOHNSON, H. D., 1975, Tide- and wave-dominated inshore and shoreline sequences from the late Precambrian, Finnmark, north Norway: Sedimentology, v. 22, p. 45–73.
- JOHNSON, H. D. and BALDWIN, C. T., 1986, Shallow siliciclastic seas, *in* Sedimentary environments and facies, *edited by* H. G. Reading: Oxford, Blackwell Scientific Publications, p. 155 - 188.
- JOHNSTON, T. E., 1983, Gold: A guide to alluvial gold and dryblowing patches in the Ashburton, Pilbara and Kimberley regions of Western Australia: Perth, Johnston, 54 p.
- JONES, F. H., 1939, The Red Hill and Yarraloola copper fields, Ashburton District: Aerial Geological and Geophysical Survey Northern Australia, Western Australia, Report 63, p. 9–14.
- JONES, F. H., and TELFORD, R. J., 1939, The Dead Finish, Mount Mortimer, Top Camp and Soldiers Secret mining centres, Ashburton Goldfield: Aerial Geological and Geophysical Survey Northern Australia, Western Australia, Report 61, p. 11–16.
- JORDAN, T. E., 1981, Thrust loads and foreland basin evolution, Cretaceous, western United States: American Association of Petroleum Geologists, Bulletin, v. 65, p. 2506–2520.
- KINSMAN, D. J. J. and PARK, R. K. 1976, Algal belt and coastal sabkha evolution, *in* Stromatolites, *edited by* M. R. Walter: Amsterdam, Elsevier, p. 421–433.
- KLEIN, G. de V., 1970a, Deposition and dispersal dynamics of intertidal sandbars: Journal of Sedimentary Petrology, v. 40, p. 1095–1127.
- KLEIN, J. de V., 1970b, Tidal origin of a Precambrian quartzite — The lower fine-grained quartzite (Middle Dalradian) of Islay, Scotland: Journal of Sedimentary Petrology, v. 40, p. 973–985.
- KLEIN, J. de V., 1971, A sedimentary model for determining palaeotidal range: Geological Society of America, Bulletin, v. 82, p. 2585–2592.
- KNOLL, A. H. and BARGHOORN, E. S., 1976, A Gunflint-type microbiota from the Duck Creek Dolomite, Western Australia: Origins of Life, v. 7, p. 417–423.
- KNOLL, A. H., STROTHER, P. K., and ROSS, S., 1988, Distribution and diagenesis of microfossils from the Lower Proterozoic Duck Creek Dolomite, Western Australia: Precambrian Research, v. 38, p. 257–279.
- KRONER, A., 1981, Precambrian plate tectonics, *in* Precambrian plate tectonics, *edited by* A. Kroner: Amsterdam, Elsevier, p. 57–90.
- KRONER, A., 1983, Proterozoic mobile belts compatible with the plate tectonics concept, *in* Proterozoic Geology: Selected papers from an International Proterozoic Symposium, *edited by* G. M. Medaris, C. W. Byers, D. M. Mikelson, and W. G. Shanks: Geological Society of America, Memoir, v. 161, p. 59–74.

- LASCELLES, D. F., 1983, Inliers of banded iron-formation in the Proterozoic Wyloo Group sediments near Paraburdoo, Western Australia: Geological Society of Australia, Journal, v. 30, p. 161–165.
- LEGGO, P. J., COMPSTON, W. and TRENDALL A. F., 1965, Radiometric ages of some Precambrian rocks from the Northwest Division of Western Australia: Geological Society of Australia, Journal, v. 12, p. 53–65.
- LEVELL, B. K., 1980, A late Precambrian tidal shelf deposit, the Lower Sandfjord Formation, Finnmark, North Norway: Sedimentology, v. 27, p. 539–557.
- LEWIS, D. R., 1981, Practical sedimentology: Christchurch, Apteryx Books, 262p.
- LIBBY, W. G. and de LAETER, J. R., 1985, Rubidium–strontium biotite dates in the Gascoyne Province, Western Australia: Western Australia, Geological Survey, Report 14.
- LIBBY, W. G., de LAETER, J. R., and MYERS, J. M., Geochronology of the Gascoyne Province: Western Australia, Geological Survey, Report 20.
- LOW, G. H., 1963, Copper deposits of Western Australia: Western Australia, Geological Survey, Mineral Resources Bulletin 8, 201 p.
- LOWE, D. R., 1982, Sediment gravity flows: II, depositional models with special reference to the deposits of high-density turbidity currents: Journal of Sedimentary Petrology, v. 52, p. 279–297.
- MacLEOD, W. N., 1966, The geology and iron deposits of the Hamersley Range area, Western Australia: Western Australia, Geological Survey, Bulletin 117.
- MacLEOD, W. N., de la HUNTY, L. E., JONES, W. R. and HALLIGAN, R., 1963, A preliminary report on the Hamersley Iron Province, North-West Division: Western Australia, Geological Survey, Annual Report, 1962, p. 44–54.
- MAITLAND, A. G., 1909, The country lying between 21° 30' and 25° S. Lat. and 113° 30' and 118° 30' E. Long., embracing parts of the Gascoyne, Ashburton and Pilbara Goldfields: Western Australia, Geological Survey, Bulletin 33.
- MAITLAND, A. G., 1919, Copper deposits of Western Australia, in Mining handbook of Western Australia: Western Australia, Geological Survey, Memoir 1, Chapter 2.
- MANN, A. W. and HORWITZ, R. C., 1979, Groundwater calcrete deposits in Australia: Some observations from Western Australia: Geological Society of Australia, Journal, v. 26, p. 293–303.
- MARESCH, W. V., 1974, Plate tectonics origin of the Caribbean mountain system of northern South America: Discussion and proposal: Geological Society of America, Bulletin, v. 85, p. 669–682.
- MARSTON, R. J., 1979, Copper mineralization in Western Australia: Western Australia, Geological Survey, Mineral Resources, Bulletin 13.
- McCONCHIE, D., 1984, A depositional environment for the Hamersley Group, in Archean and Proterozoic basins of the Pilbara, Western Australia: Evolution and mineralization potential, *edited by* J. R. Muhling, D. I. Groves and T. S. Blake: University of Western Australia, Geology Department and University Extension Publication, 9, p. 144–190.
- McELHINNY, M. W. and EMBLETON, B. J. J., 1976, Precambrian and early Palaeozoic magnetism in Australia: Royal Society of London, Philosophical Transactions, Series A, 280, p. 417–431.
- McELHINNY, M. W. and McWILLIAMS, M. O., 1977, Precambrian geodynamics — A palaeomagnetic view: Tectonophysics, v. 40, p. 41–54.
- McGOWEN, J. H., 1970, Gum Hollow fan delta, Nueces Bay, Texas: Texas Bureau of Economic Geology, Report of Investigations 72, 52 p.
- McWILLIAMS, M. O., 1981, Palaeomagnetism and Precambrian tectonic evolution of Gondwana, in Precambrian plate tectonics, *edited by* A. Kroner: Amsterdam, Elsevier, p. 649–687.
- MIALL, A. D., 1977, A review of the braided-river depositional environment: Earth-Science Review, v. 13, p. 1–62.
- MIALL, A. D. (editor), 1978, Fluvial sedimentology: Canadian Society of Petroleum Geologists, Memoir 5, 859 p.
- MITCHELL, A. H. G. and READING, H. G., 1986, Sedimentation and tectonics, in Sedimentary environments and facies, *edited by* H. G. Reading: Oxford, Blackwell Scientific Publications, p. 471–519.
- MORRIS, R. C., 1980, A textural and mineralogical study of the relationship of iron ore to banded iron-formation in the Hamersley Iron Province of Western Australia: Economic Geology, 75, p. 184–209.
- MORRIS, R. C., 1985, Genesis of iron ore in banded iron-formation by supergene and supergene-metamorphic processes — A conceptual model, in Handbook of strata-bound and stratiform ore deposits, v. 13, *edited by* K. H. Wolf: Amsterdam, Elsevier, p. 73–235.
- MORRIS, R. C., 1986, A review of geological research on the iron ores of the Hamersley Iron Province, in Publication of the 12th Council of Mining and Metallurgy Institutions Congress, *edited by* J.T. Woodcock: Parkville, Victoria, p. 191–200.



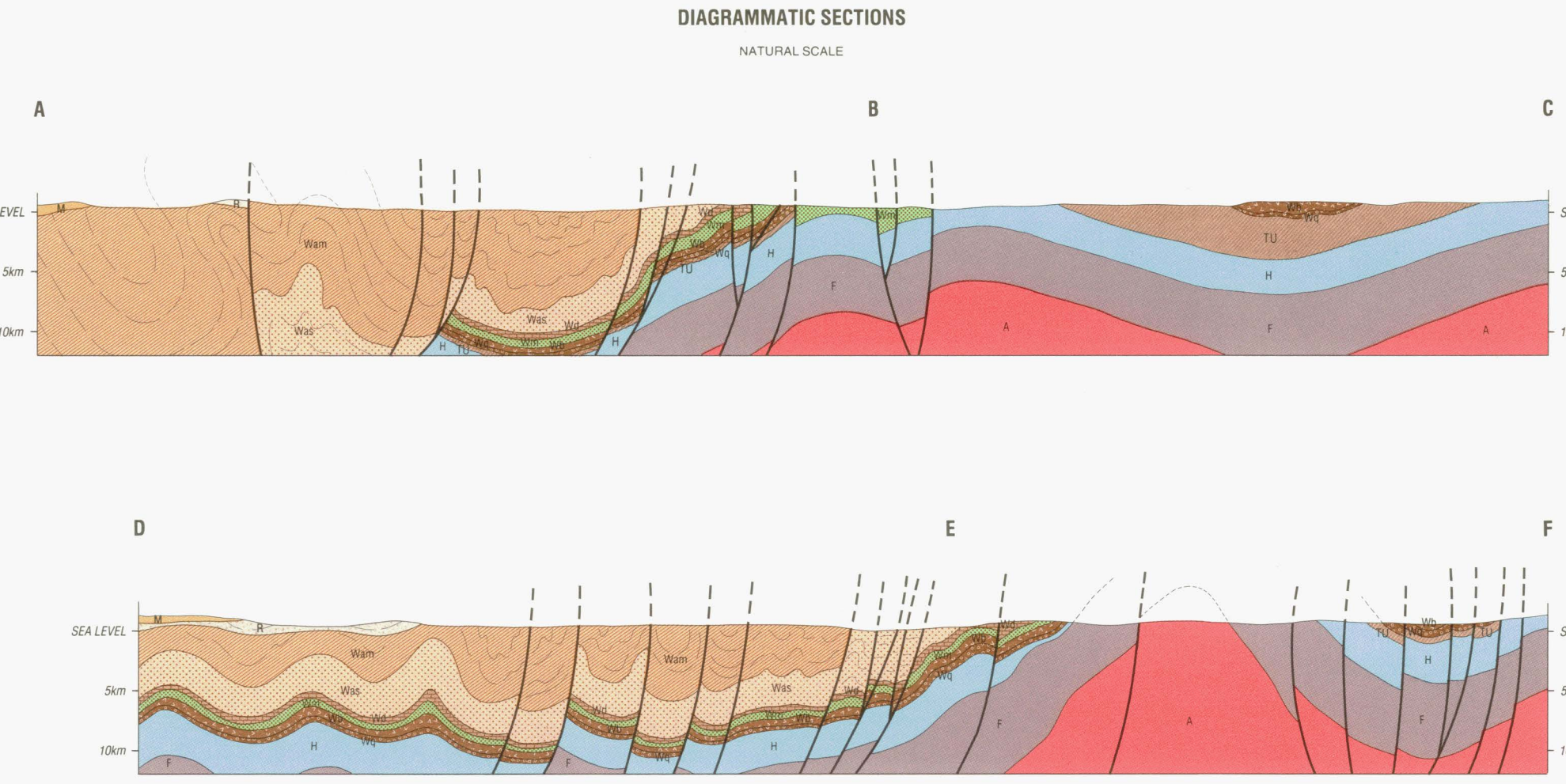
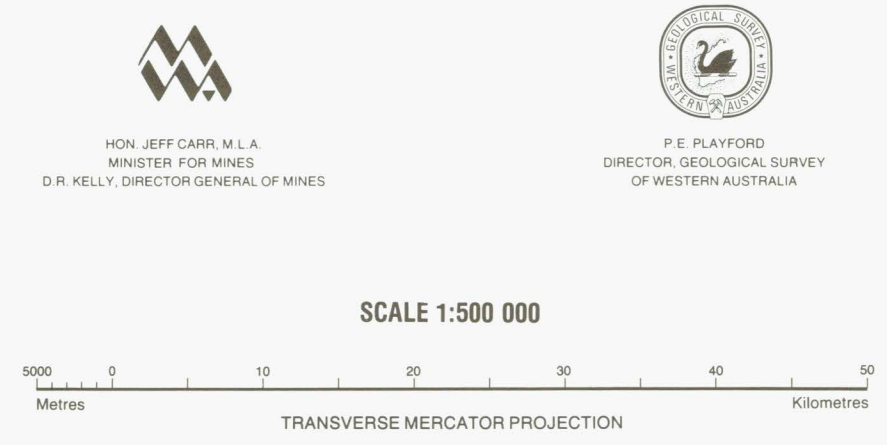
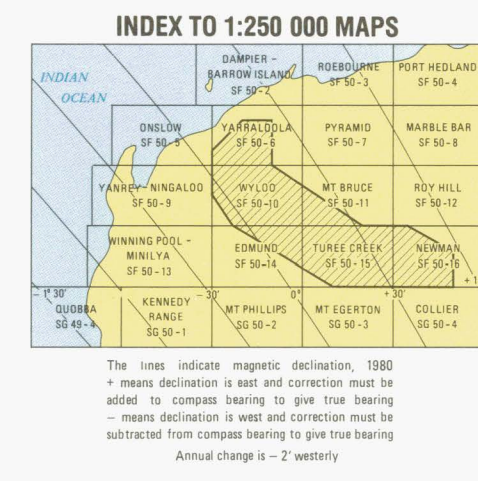
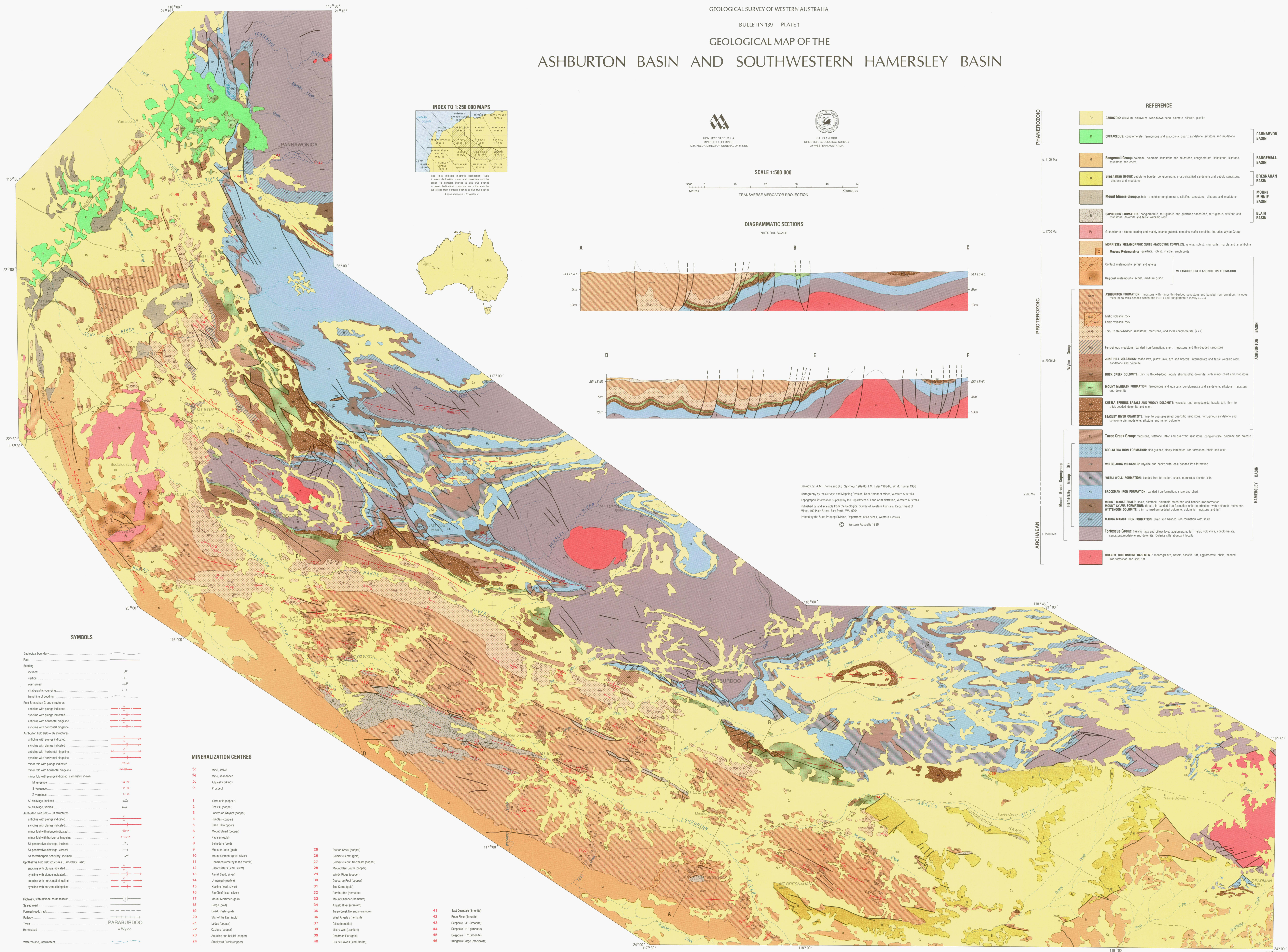
- MORRIS, R.C. and HORWITZ, R.C., 1983, The origin of the iron-formation-rich Hamersley Group of Western Australia — Deposition on a platform: *Precambrian Research*, v. 21, 273–297.
- MUHLING, P. C., and BRAKEL, A. T., 1985, Geology of the Bangemall Basin — The evolution of an intracratonic Proterozoic basin: Western Australia, Geological Survey, Bulletin 128.
- MUTTI, E., 1977, Distinctive thin-bedded turbidite facies and related depositional environments in the Eocene Hecho Group (South-central Pyrenees, Spain): *Sedimentology*, v. 24, p. 107 - 132.
- NORMARK, W. R., PIPER, D. J. and STOW, D.A.V., 1983, Quaternary development of channels, levees and lobes on middle Laurentian fan: *American Association of Petroleum Geologists Bulletin*, v. 67, p. 1400–1409.
- PARK, R. K., 1976, A note on the significance of lamination in stromatolites: *Sedimentology*, v. 23, p. 379–393.
- PARK, R.K., 1977, The preservation potential of some Recent stromatolites: *Sedimentology*, v. 24, p. 485–506.
- PIPER, D. J. W. and NORMARK, W. R., 1982, Acoustic interpretation of Quaternary sedimentation and erosion on the channelled upper part of the Laurentian Fan, Atlantic margin of Canada: *Canadian Journal of Earth Sciences*, v. 19, p. 1974–1984.
- PIPER, D. J. W. and NORMARK, W. R., 1983, Turbidite depositional patterns and flow characteristics, Navy Submarine Fan, California Borderland: *Sedimentology*, v. 30, p. 681–694.
- PLAYFORD, P. E. and COCKBAIN, A. E., 1976, Modern algal stromatolites at Hamelin Pool, a hypersaline barred basin in Shark Bay, Western Australia, *in* *Stromatolites*, edited by M.R. Walter: Amsterdam, Elsevier, p. 389–413.
- PURSER, B. H., 1973, The Persian Gulf: Holocene carbonate sedimentation and diagenesis in a shallow epicontinental sea: Berlin, Springer-Verlag, 471 p.
- PREISS, W. V., 1977, The biostratigraphic potential of Precambrian stromatolites: *Precambrian Research*, v. 5, p. 207–209.
- RAMSAY, J. G. and HUBER, M. I., 1987, The techniques of modern structural geology, volume 2: Folds and fractures: London, Academic Press, 700 p.
- READ, J. F., 1985, Carbonate platform facies models: *American Association of Petroleum Geologists, Bulletin*, v. 69, p.1–21.
- RICHARDS, J. R., FLETCHER, I. R., and BLOCKLEY, J. G., 1981, Pilbara galenas: Precise isotopic assay of the oldest Australian leads; Model ages and growth curve implications: *Mineralium Deposita*, v. 16, p. 7–30.
- ROBERTSON-HANDFORD, C., LOUCKS, R.G., and DAVIES, G. R., (editors), 1982, Depositional and diagenetic spectra of evaporites: *Society of Economic Palaeontologists and Mineralogists, Core Workshop Number 3*, 395 p.
- RUPKE, N. A., 1978, Deep Clastic Seas, *in* *Sedimentary environments and facies* (1st edition), edited by H. G. Reading: Oxford, Blackwell Scientific Publications, p. 372–415.
- RUST, B. R., 1979, Coarse alluvial deposits, *in* *Facies Models* (1st edition), edited by R. G. Walker: Geoscience Canada, Reprint Series, p.9–21.
- SANDERSON, D. J. and MARCHINI, W. R. D., 1984, Transpression: *Journal of Structural Geology*, v. 6, p. 449–458.
- SEYMOUR, D. B., THORNE, A. M., and BLIGHT, D. F., 1988, Wyloo Western Australia (2nd edition): Western Australia, Geological Survey, 1:250 000 Geological Series — Explanatory Notes.
- SHEARMAN, D. J., 1980, Sebkha facies evaporites, *in* *Evaporite deposits*: Paris, Imprimerie Louis-Jean, p. 19.
- SIMPSON, E. S., 1926, Minerals of the Ashburton and Gascoyne valleys (Appendix): Western Australia, Geological Survey, Bulletin 85.
- SIMPSON, E. S., 1951, Minerals of Western Australia Vol. II: Perth, Government Printer, 675 p.
- SMITH, R. E., PERDRIX, J. L. and PARKS, J. R., 1982, Burial metamorphism in the Hamersley Basin, Western Australia: *Journal of Petrology*, v. 23, p. 75–102.
- STAINES, H. R. E., 1985, Field geologist's guide to lithostratigraphic nomenclature in Australia: *Australian Journal of Earth Sciences*, v. 32, p. 83–106.
- STEEL, R. J., and THOMPSON, D. B., 1983, Structures and textures in Triassic braided stream conglomerates ('Bunter' Pebble Beds) in the Sherwood Sandstone Group, North Staffordshire, England: *Sedimentology*, v. 30, p. 341–367.
- STEIGER, R. H. and JAGER, E., 1977, Subcommission on geochronology — Convention on the use of decay constants in geo- and cosmochronology: *Earth and Planetary Science Letters*, v. 36, p. 559–62.
- STOW, D. A. V., 1986, Deep clastic seas, *in* *Sedimentary environments and facies* (2nd edition), edited by H.

- G. Reading: Oxford, Blackwell Scientific Publication, p.399–444.
- TALBOT, H. W. B., 1926, A geological reconnaissance of part of the Ashburton drainage area, with notes on the country southwards to Meekatharra: Western Australia, Geological Survey, Bulletin, 85.
- THORNE, A. M., 1985, Upward-shallowing sequences in the Precambrian Duck Creek Dolomite, Western Australia, *in* Professional Papers for 1983: Western Australia, Geological Survey, Report 14, p. 81–93.
- THORNE, A. M., 1986, Depositional history of the 2.0 Ga Wyloo Group, southern Pilbara, Western Australia: Geological Society of Australia, 8th Annual Convention, Adelaide, p. 189.
- THORNE, A. M. and SEYMOUR, D. B., 1986, The sedimentology of a tide-influenced fan-delta system in the Early Proterozoic Wyloo Group, on the southern margin of the Pilbara Craton, Western Australia, *in* Professional Papers for 1984: Western Australia, Geological Survey, Report 19, p. 70–82.
- TILL, R., 1978, Arid shorelines and evaporites, *in* Sedimentary environments and facies (1st edition), *edited by* H. G. Reading, Oxford, Blackwell Scientific Publications, p. 178–206.
- TRENDALL, A. F., 1975, Hamersley Basin, *in* Geology of Western Australia: Western Australia, Geological Survey, Memoir 2, p. 119–143.
- TRENDALL, A. F., 1976, Striated and faceted boulders from the Turee Creek Formation — Evidence for a possible Huronian glaciation on the Australian continent: Western Australia, Geological Survey Annual Report, 1975, p. 88–92.
- TRENDALL, A. F., 1979, A revision of the Mount Bruce Supergroup: Western Australia, Geological Survey, Annual Report, 1978, p. 63–71.
- TRENDALL, A. F., 1983, The Hamersley Basin, *in* Iron-formation: Facts and problems *edited by* A. F. Trendall and R. C. Morris: Amsterdam, Elsevier, p. 69–129.
- TRENDALL, A. F., 1990, The Hamersley Basin, *in* Geology and Mineral Resources of Western Australia: Western Australia, Geological Survey, Memoir 3, p. 163–191.
- TRENDALL, A. F. and BLOCKLEY, J. G., 1970, The iron formations of the Precambrian Hamersley Group, Western Australia, with special reference to the associated crocidolite: Western Australia, Geological Survey, Bulletin 119.
- TWIDALE, C. R., HORWITZ, R. C. and CAMPBELL, E. M., 1985, Hamersley landscapes of the north-west of Western Australia: *Revue de Geologie et de Geographie Physique*, vol. 26, p. 173–186.
- TYLER, I. M., 1990a, Inliers of granite–greenstone terrane, *in* Geology and Mineral Resources of Western Australia: Western Australia, Geological Survey, Memoir 3, p. 158–163.
- TYLER, I. M., 1990b, Mafic dyke swarms, *in* Chapter 2 - Cratons, Geology and Mineral Resources of Western Australia: Western Australia, Geological Survey, Memoir 3, p. 191–194.
- TYLER, I. M., *in press*, Geology of Sylvania Inlier and southeastern Hamersley Basin: Western Australia, Geological Survey Bulletin.
- TYLER, I. M., and THORNE, A. M., *in press*, The northern margin of the Capricorn Orogen, Western Australia — An example of an Early Proterozoic collision zone: *Journal of Structural Geology*.
- TYLER, I. M., HUNTER, W. M., and WILLIAMS, I. R., *in press*, Newman, Western Australia (2nd edition): Western Australia, Geological Survey, 1:250 000 Geological Series — Explanatory Notes.
- VOS, R. G., 1977, Sedimentology of an upper Palaeozoic river, wave and tide-influenced delta system in Southern Morocco: *Journal of Sedimentary Petrology*, v. 47, p. 1242–1260.
- WALKER, R. G., 1967, Turbidite sedimentary structures and their relationship to proximal and distal depositional environments: *Journal of Sedimentary Petrology*, v. 37, p. 25–43.
- WALKER, R. G., 1970, Review of the geometry and facies organization of turbidites and turbidite-bearing basins, *in* Flysch sedimentology in North America, *edited by* J. Lajoie: Geological Association of Canada, Special Publication, 7, p. 219–251.
- WALKER, R. G., 1975, Conglomerate: Sedimentary structures and facies models, *in* Depositional environments as interpreted from primary sedimentary structures and stratification sequences, *edited by* J.C. Harms, J.B. Southard, D.R. Spearing, and R.G. Walker: Society of Economic Palaeontologists and Mineralogists Short Course no. 2, p. 133–161.
- WALKER, R. G., 1978, Deep-water sandstone facies and ancient submarine fans: Models for exploration for stratigraphic traps: *American Association of Petroleum Geologists, Bulletin*, v. 62, p. 932–966.
- WALTER, M. R., 1972, Stromatolites and the biostratigraphy of the Australian Precambrian and Cambrian: *Palaeontological Association of London, Special Paper 11*, 190 p.
- WASSON, R. J., 1977, Late glacial alluvial fan sedimentation in the lower Derwent Valley, Tasmania: *Sedimentology*, v. 24, p. 781 - 799.

- WEIMER, R. J., HOWARD, J. D. and LINDSAY, D. R., 1982, Tidal flats, *in* Sandstone depositional environments, *edited by* P. A. Scholle and D. Spearing: American Association of Petroleum Geologists, Memoir 31, p. 191–245.
- WESCOTT W. A. and ETHERIDGE, F. G., 1980, Fan delta sedimentology and tectonic setting — Yallahs fan delta, southeast Jamaica: American Association of Petroleum Geologists, Bulletin, v. 64, p. 374–399.
- WHITE, B., 1981, Shallowing upwards cycles in the Middle Proterozoic Altyn Formation: *Nature*, v. 294, p. 157–158.
- WILCOX, R. E., HARDING, T. P. and SEELY, D. R., 1973, Basic wrench tectonics: American Association of Petroleum Geologists, Bulletin, v. 57, p. 74–96.
- WINDLEY, B. F., 1984, *The evolving continents* (second edition): Chichester, Wiley, 399 p.
- WILLIAMS, I. R., 1968, Yarraloola, W. A.: Western Australia, Geological Survey, 1:250 000 Geological Series — Explanatory Notes.
- WILLIAMS, S. J., 1986, Geology of the Gascoyne Province of Western Australia: Western Australia, Geological Survey, Report 15, 85 p.
- WILLIAMS, S. J., ELIAS, M., and de LAETER, J. R., 1978, Geochronology and evolution of the eastern Gascoyne Province and adjacent Yilgarn Block, Western Australia Geological Survey, Annual Report, 1977, p. 50–56.
- WILLIAMS, H. and McBIRNEY, A. R., 1979, *Volcanology*: San Francisco, Freeman Cooper and Company, 397 p.
- WILSON, J. T., 1968, Static or mobile earth: The current scientific revolution, *in* Gondwanaland Revisited: New evidence for continental drift: American Philosophical Society, Proceedings, p. 309–320.
- WINN, R. D. W. Jr., and DOTT, R. H. Jr., 1979, Deep-water fan-channel conglomerates of Late Cretaceous age, southern Chile: *Sedimentology*, v. 26, p. 203–228.
- WOODWARD, H. P., 1891, Annual general report of the Government Geologist, 1890, Western Australia Geological Survey, p. 20–22.
- WOODWARD, H. P., 1910, The country between Roebourne and Peak Hill: Western Australia, Geological Survey, Annual Report 1909, p. 21–23.
- WOODWARD, H. P., 1912, Notes to accompany the geological sketch map of the country at the heads of the Ashburton and Gascoyne Rivers: Western Australia, Geological Survey, Bulletin, 48.
- WRIGHT, H. G., 1897, Wardens report on the Ashburton Goldfield for 1897: Western Australia, Mines Department, Annual Report 1897.



# GEOLOGICAL MAP OF THE ASHBURTON BASIN AND SOUTHWESTERN HAMERSLEY BASIN



REFERENCE	
Cz	CANGZIC: alluvium, colluvium, wind-blown sand, calcareous siltstone, psiltite
K	CRINACEOUS: conglomerate, ferruginous and glauconitic quartz sandstone, siltstone and mudstone
M	Bangemall Group: coarsite, dolomitic sandstone and mudstone, conglomerate, sandstone, siltstone, mudstone and chert
B	Bresnanhan Group: cobble to boulder conglomerate, cross-stratified sandstone and pebbly sandstone, siltstone and mudstone
I	Mount Minnie Group: cobble to cobble conglomerate, silicified sandstone, siltstone and mudstone
Ca	CAPRICORN FORMATION: conglomerate, ferruginous and quartzitic sandstone, ferruginous siltstone and mudstone, dolomite and felsic volcanic rock
Pt	Granoblastic: bottle-bearing and mainly coarse-grained, contains mafic xenoliths, intrudes Wyloo Group
G	MORRISSEY METAMORPHIC SUITE (GASCOYNE COMPLEX): gneiss, schist, migmatite, marble and amphibolite
H	Mudong Metamorphics: quartzite, schist, marble, amphibolite
Co	Contact metamorphic schist and gneiss
Me	Regional metamorphic schist, medium grade
Am	ASHBURTON FORMATION: mudstone with minor thin-bedded sandstone and banded iron-formation; includes medium to thick-bedded sandstone (+) and conglomerate locally (+ +)
Wm	Mafic volcanic rock
Fv	Felsic volcanic rock
Wm	Thin to thick-bedded sandstone, mudstone, and local conglomerate (+ + +)
Wm	Ferruginous mudstone, banded iron-formation, chert, mudstone and thin-bedded sandstone
Jv	JUNE HILL VOLCANICS: mafic lava, pillow lava, tuff and breccia, intermediate and felsic volcanic rock, sandstone and dolomite
Dc	DUCK CREEK DOLOMITE: thin to thick-bedded, locally chromite-bearing dolomite, with minor chert and mudstone
Md	MOUNT MUGBATH FORMATION: ferruginous and quartzitic conglomerate and sandstone, siltstone, mudstone and dolomite
Os	OSHELLA SPRINGS BASALT AND WOOLLY DOLOMITE: vesicular and amygdaloidal basalt, tuff, thin to thick-bedded dolomite and chert
Rq	REARLEY RIVER QUARTZITE: fine to coarse-grained quartzitic sandstone, ferruginous sandstone and conglomerate, mudstone, siltstone and minor dolomite
Tc	TURNE CREEK GROUP: mudstone, siltstone, siliceous and quartzitic sandstone, conglomerate, dolomite and dolerite
Ii	IRRAWADDI IRON FORMATION: fine-grained, finely laminated iron-formation, shale and chert
Wv	WONGARRA VOLCANICS: rhyolite and dacite with local banded iron-formation
Wf	WELLI WELLI FORMATION: banded iron-formation, shale, numerous dolerite sills
Br	BROCKMAN IRON FORMATION: banded iron-formation, shale and chert
Mm	MOUNT MURRAE SHALE: shale, siltstone, dolomitic mudstone and banded iron-formation
St	STURTON STYLA FORMATION: three thin banded iron-formation units interbedded with dolomitic mudstone
It	INTERIOR DOLOMITE: thin to medium-bedded dolomite, dolomitic mudstone and tuff
Mh	MARKA HANBA IRON FORMATION: chert and banded iron-formation with shale
Fg	FORTESCUE GROUP: basaltic lava and pillow lava, agglomerate, tuff, felsic volcanics, conglomerate, sandstone, mudstone and dolomite. Dolomite sills abundant locally
A	GRANITE-GREENSTONE BASEMENT: monzonitic, basalt, basaltic tuff, agglomerate, shale, banded iron-formation and acid tuff

Geology by A.M. Thorne and D.B. Seymour 1982-85, I.M. Tyler 1983-85, W.M. Hunter 1986  
 Cartography by the Surveys and Mapping Division, Department of Mines, Western Australia  
 Topographic information supplied by the Department of Land Administration, Western Australia  
 Published by and available from the Geological Survey of Western Australia, Department of Mines, 100 Park Street, East Perth, WA 6004  
 Printed by the State Printing Division, Department of Services, Western Australia  
 © Western Australia 1989

### SYMBOLS

Geological boundary	—
Fault	—
Striking	—
Inclined	—
Vertical	—
Overturned	—
Stratigraphic pinching	—
Trace line of bedding	—
Post-Bresnanhan Group structures	—
anticline with plunge indicated	—
syncline with plunge indicated	—
anticline with horizontal hinge-line	—
syncline with horizontal hinge-line	—
Ashburton Fold Belt - O2 structures	—
anticline with plunge indicated	—
syncline with plunge indicated	—
anticline with horizontal hinge-line	—
syncline with horizontal hinge-line	—
minor fold with plunge indicated	—
minor fold with horizontal hinge-line	—
minor fold with plunge indicated, symmetry shown	—
W vergence	—
S vergence	—
Z vergence	—
O2 cleavage, inclined	—
O2 cleavage, vertical	—
Ashburton Fold Belt - O1 structures	—
anticline with plunge indicated	—
syncline with plunge indicated	—
anticline with horizontal hinge-line	—
syncline with horizontal hinge-line	—
minor fold with plunge indicated	—
minor fold with horizontal hinge-line	—
S1 penetrative cleavage, inclined	—
S1 penetrative cleavage, vertical	—
S1 metamorphic schistosity, inclined	—
Optimatum Fold Belt structures (Hamersley Basin)	—
anticline with plunge indicated	—
syncline with plunge indicated	—
anticline with horizontal hinge-line	—
syncline with horizontal hinge-line	—
anticline with horizontal hinge-line	—
syncline with horizontal hinge-line	—
Highway, with national road marker	—
Sealed road	—
Formed road, track	—
Railway	—
Town	—
Homestead	—
Watercourse, intermittent	—

### MINERALIZATION CENTRES

1	Yarrabook (copper)
2	Red Hill (copper)
3	Lickess or Wharf (copper)
4	Mudflats (copper)
5	Care Hill (copper)
6	Mount Stuart (copper)
7	Puritan (gold)
8	Belvedere (gold)
9	Monster Lode (gold)
10	Mount Cement (gold, silver)
11	Unnamed (antimony and molybdenum)
12	Silver Silvers (lead, silver)
13	Aural (lead, silver)
14	Unnamed (marble)
15	Kookie (lead, silver)
16	Big Chief (lead, silver)
17	Mount Mariner (gold)
18	Gorge (gold)
19	Dead Fish (gold)
20	Star of the East (gold)
21	Large (copper)
22	Colony (copper)
23	Archie and Bull (copper)
24	Stockyard Creek (copper)
25	Station Creek (copper)
26	Soldiers Secret (gold)
27	Soldiers Secret Northwest (copper)
28	Mount Bar South (copper)
29	Windy Ridge (copper)
30	Coobaroo Pool (copper)
31	Top Camp (gold)
32	Paraburdee (hematite)
33	Mount Channer (hematite)
34	Angelo River (uranium)
35	Turce Creek Noranda (uranium)
36	West Angles (hematite)
37	Gies (hematite)
38	Jenny Well (uranium)
39	Deadman Flat (gold)
40	Prarie Downs (lead, barite)
41	East Deepdale (ironoxide)
42	Ride River (ironoxide)
43	Goodwin "I" (ironoxide)
44	Deepdale "H" (ironoxide)
45	Deepdale "F" (ironoxide)
46	Kangaroo Gorge (crocotholite)



GEOLOGICAL SURVEY OF WESTERN AUSTRALIA

BULLETIN 139 PLATE 2

# STRUCTURAL INTERPRETATION OF THE ASHBURTON BASIN AND SOUTHWESTERN HAMERSLEY BASIN

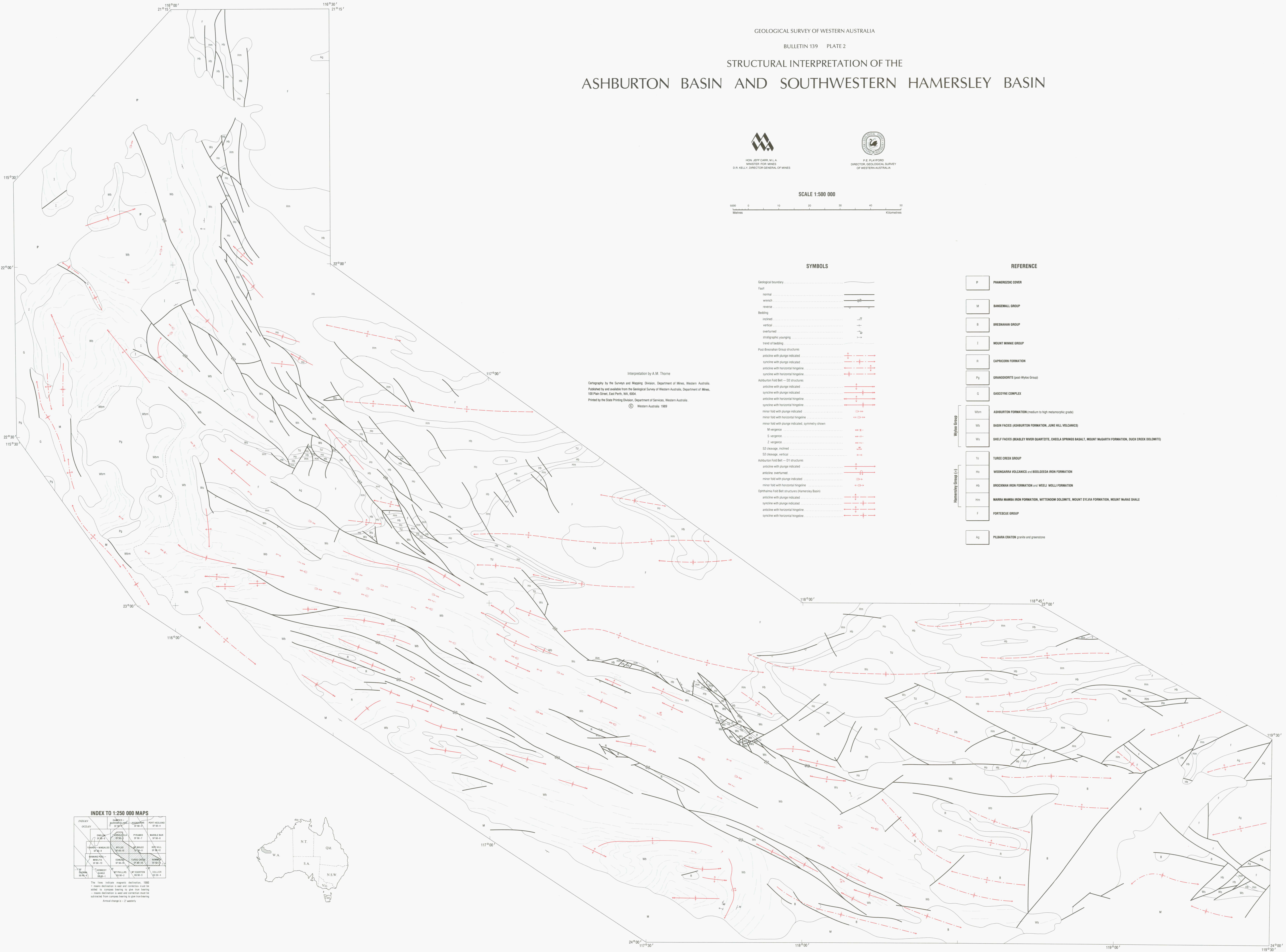


HON. JEFF CARL, M.L.A.  
MINISTER FOR MINES  
D.R. KELLY, DIRECTOR GENERAL OF MINES



R.E. PLAYFORD  
DIRECTOR, GEOLOGICAL SURVEY  
OF WESTERN AUSTRALIA

SCALE 1:500 000



Interpretation by A.M. Thorne  
Cartography by the Survey and Mapping Division, Department of Mines, Western Australia.  
Published by and available from the Geological Survey of Western Australia, Department of Mines,  
100 Plain Street, East Perth, W.A. 6004.  
Printed by the State Printing Division, Department of Services, Western Australia  
© Western Australia 1989

### SYMBOLS

Geological boundary	-----
Fault	-----
normal	-----
wrench	-----
reverse	-----
blending	-----
inclined	-----
vertical	-----
overturned	-----
stratigraphic younging	-----
trace of bedding	-----
Post-Breathra Group structures	-----
anticline with plunge indicated	-----
syncline with plunge indicated	-----
anticline with horizontal hinge line	-----
syncline with horizontal hinge line	-----
Ashburton Fold Belt - D2 structures	-----
anticline with plunge indicated	-----
syncline with plunge indicated	-----
anticline with horizontal hinge line	-----
syncline with horizontal hinge line	-----
minor fold with plunge indicated	-----
minor fold with horizontal hinge line	-----
W vergence	-----
E vergence	-----
S vergence	-----
N vergence	-----
D2 cleavage, inclined	-----
D2 cleavage, vertical	-----
Ashburton fold belt - D1 structures	-----
anticline with plunge indicated	-----
anticline overturned	-----
minor fold with plunge indicated	-----
minor fold with horizontal hinge line	-----
Continental fold belt structures (Hamersley Basin)	-----
anticline with plunge indicated	-----
syncline with plunge indicated	-----
anticline with horizontal hinge line	-----
syncline with horizontal hinge line	-----

### REFERENCE

P	PHANEROZOIC COVER
M	MANGAMALL GROUP
B	BRENNAN GROUP
I	MOUNT MINNIE GROUP
R	CAPRICORN FORMATION
Pg	GRANODIORITE (east Wyloo Group)
G	GASCOYNE COMPLEX
Wm	ASHBURTON FORMATION (medium to high metamorphic grade)
Wb	BASH FACIES (ASHBURTON FORMATION, JUNE HILL VOLCANICS)
Ws	SHELF FACIES (BEALEY RIVER QUARTZITE, CHEELA SPRINGS BASALT, MOUNT MEGARTH FORMATION, DUCK CREEK DOLOMITE)
Tu	TURE CREEK GROUP
Ho	WIDONGARRA VOLCANICS and BOOLEDEA IRON FORMATION
Hb	BROCKMAN IRON FORMATION and WELLI WOLLI FORMATION
Hm	MARBA NAMBIA IRON FORMATION, WITTENBOM DOLOMITE, MOUNT SYLVIA FORMATION, MOUNT MURRAY SHALES
F	FORTESCUE GROUP
Aq	PILBARA CRATON (granite and gneiss)

### INDEX TO 1:250 000 MAPS

INDIAN OCEAN	INDIAN OCEAN	INDIAN OCEAN	INDIAN OCEAN
INDIAN OCEAN	INDIAN OCEAN	INDIAN OCEAN	INDIAN OCEAN
INDIAN OCEAN	INDIAN OCEAN	INDIAN OCEAN	INDIAN OCEAN
INDIAN OCEAN	INDIAN OCEAN	INDIAN OCEAN	INDIAN OCEAN

